Survival and Migration Dynamics of Juvenile Chinook Salmon (*Oncorhynchus tshawytscha*) in the Sacramento-San Joaquin River Delta

Russell W. Perry

A dissertation
submitted in partial fulfillment of the
requirements for the degree of

Doctor of Philosophy

University of Washington

2010

Program Authorized to Offer Degree:
School of Aquatic and Fishery Sciences

University of Washington
Graduate School

This is to certify that I have examined this copy of a doctoral dissertation by

Russell W. Perry

and have found that it is complete and satisfactory in all respects,
and that any and all revisions required by the final
examining committee have been made.
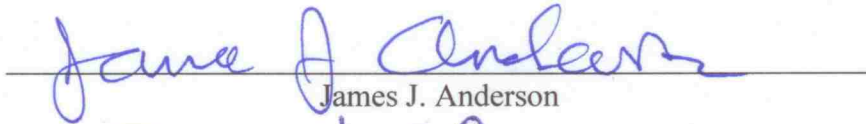
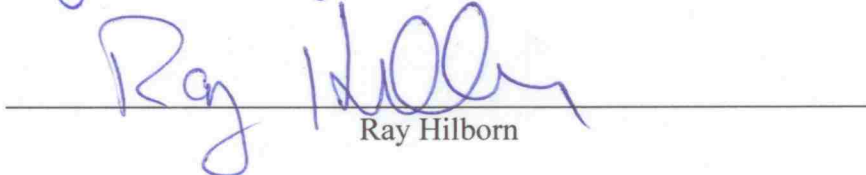Chair of the Supervisory Committee:

_____

John R. Skalski

Reading Committee:

_____

John R. Skalski

_____

James J. Anderson

_____

Ray Hilborn

Date:_____

University of Washington

Abstract

Survival and migration dynamics of juvenile Chinook salmon (*Oncorhynchus tshawytscha*) in the Sacramento-San Joaquin River Delta

Russell W. Perry

Chair of the Supervisory Committee:
Professor John R. Skalski
School of Aquatic and Fishery Sciences

Juvenile Chinook salmon (*Oncorhynchus tshawytscha*) emigrating from natal tributaries of the Sacramento River must negotiate the Sacramento–San Joaquin River Delta, a complex network of natural and man-made channels linking the Sacramento River with San Francisco Bay. Natural processes and water management actions affect the fraction of the population using different migration routes through the Delta and survival within those routes. In this dissertation, my goals were to 1) develop a mark-recapture model to explicitly estimate survival and migration route probabilities for each of four migration routes through the Delta, 2) link these route-specific probabilities to population-level survival, and 3) apply this model to the first available acoustic telemetry data of smolt migration through the Delta, and 4) quantify the effect of river flow and tides on movement and survival.

I found that survival of juvenile salmon migrating through the interior Delta, where water pumping stations are located, was consistently less than for fish that migrated via the Sacramento River. Thus, movement of fish among migration routes in the Delta will influence population-level survival. To examine factors affecting

migration routing, I used a multinomial model to quantify the effect of river flow, tides, and operation of a water diversion gate (the Delta Cross Channel) on entrainment of fish into the interior Delta. I found that the closing the Delta Cross Channel gate increased Sacramento River flow by about 30% but was expected to decrease entrainment into the interior Delta by only about 15%. I also found that river inflow affected entrainment by a similar magnitude as operation of the Delta Cross Channel gates. Flood tides causing upstream flow into the river junction increased the probability of fish entering the interior Delta, but increasing river flow dampens tidal fluctuations, thereby reducing entrainment probabilities. My study shows how movements among, and survival within, migration routes interact to influence population-level survival through the Delta. Models developed in this dissertation are critical for understanding how water management actions influence migration routing and population survival of juvenile salmon in the Sacramento–San Joaquin River Delta.

TABLE OF CONTENTS

LIST OF FIGURES

LIST OF TABLES

ACKNOWLEDGEMENTS

DEDICATION

For my best friend Kari and my beautiful daughter Lilah

INTRODUCTION

1.1 Historical Background

1.1.1 The Central Valley and its Chinook salmon

Chinook salmon populations in the Central Valley of California once numbered up to two million spawning adults (Fisher, 1994) and represent the southern-most extant population of Chinook salmon in the Pacific Ocean (Moyle, 2002). Historical accounts attest to such great abundance, "The year 1878 was the year of the immense gathering of salmon in the McCloud", a tributary to the Sacramento River, "…I have never seen anything like it anywhere, not even on the tributaries of the Columbia…" (Stone, 1897 as quoted in Yoshiyama et al., 2001). Such historical abundance should come as little surprise given that the Central Valley of California drains 40% of California's landmass and discharges 47% of its water (Figure 1.1; Healy, 2008). The Central Valley watershed is comprised of the Sacramento River to north and San Joaquin River to the south, both of which converge in the Sacramento-San Joaquin River Delta (hereafter, "the Delta") to empty their fresh waters into San Francisco Bay (Figure 1.1). These two major rivers are fed by numerous tributaries with headwaters originating in the Sierra-Nevada and southern Cascade mountain ranges, and most of these tributaries once harbored populations of anadromous salmonids (Figure 1.1).

Four runs of salmon have evolved distinct life histories to capitalize on the diversity of habitat available in Central Valley rivers and streams. As is common in other areas of the northwest, the runs are named according the season in which the adults return to fresh water: winter, spring, fall, and late-fall. Each run's life history capitalizes on a spatiotemporal niche formed by temperature, elevation, and timing of life-history events (Moyle, 2002). Water temperatures in the lower watershed and Delta can often reach lethal limits for salmon during late spring and summer (Baker et al., 1995; Myrick and Cech , 2004), and life histories have
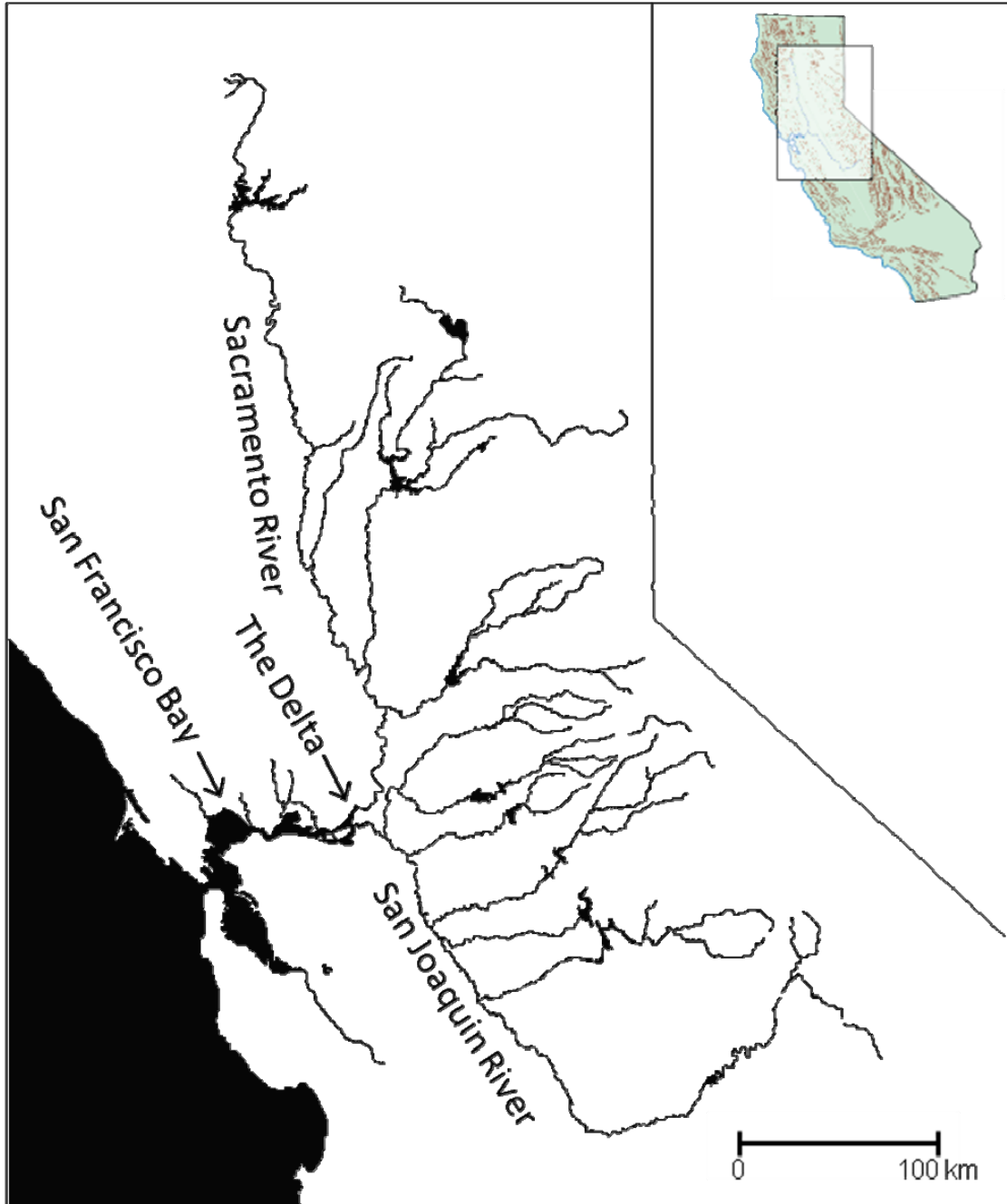
Figure 1.1. The Central Valley watershed of California.

evolved to avoid these locations during these seasons (Williams, 2006). In general, timing of adult returns is such that winter and spring runs spawn at higher elevations of the watershed, whereas fall and late-fall runs use the lowest reaches of the watershed for spawning. Spring-run adults arrive March through May, ascend the upper most-reaches and highest elevations of Central Valley rivers when spring run-off allows access, and remain in the stream until spawning in late summer (Moyle, 2002). Winter run arrive December through March, use lower elevations than the spring run, and consequently, spawn earlier than spring-run Chinook (May and June) when these reaches attain optimal spawning temperature (Moyle, 2002). Fall and late-fall run return in September – October and November – December destined for the lowest-elevation reaches and spawn soon after arriving at spawning grounds.

Such diversity in run timing, spawning, and habitat use dictates similar diversity in the life history patterns of juvenile Chinook salmon. Both ocean-type and stream-type forms are observed, with some runs exhibiting a mixture of both life history types (Moyle, 2002). Most spring-run juveniles exhibit the classic stream-type life history, but have shown considerable plasticity, with the in-stream rearing period ranging from 3 to 15 months (Moyle, 2002; Williams, 2006). Winter Chinook juveniles begin their migration shortly after emergence, but apparently rear extensively in the river for 5-10 months, as they are not observed in the Delta until they attain larger size (Moyle, 2002; Williams, 2006). Fall-run Chinook salmon exhibit both stream-type and ocean-type life history forms, with most juveniles entering and rearing in the Delta as fry and parr and some rearing in the river to emigrate as yearling smolts (Williams et al., 2006). Finally, juveniles of late-fall Chinook salmon typically emerge in the spring, rear in the stream during the summer, and then emigrate during the fall or winter. Although juveniles exhibit high life-history variation within and among runs, their common link is complete absence from lower-elevation rivers and the Delta between June and late September during periods of high water temperature (Williams, 2006).

Similar to many large West Coast rivers, salmon populations have declined substantially since the mid-1800s (Yoshiyama, 2001). All four runs of Chinook salmon in the Central Valley have been listed as either endangered (winter run), as threatened (spring run), or as a species of concern (fall/late-fall run) under federal and state endangered species legislation (Myers, 1998; Lindley, 2004). The winter run is the most imperiled, declining from an average

of 86,509 spawners during the 1960s to only 191 spawners in 1991 (Fisher, 1994; Black, 1995). Returns have since increased to around 10,000 fish during the early 2000s (Williams, 2006). Spring-run salmon were completely extirpated from the San Joaquin River and now exist only in the mainstem Sacramento River and three of its tributaries. Both spring and winter run are particularly sensitive to catastrophic events due to a very restricted age-at-maturity distribution: 90% of adults return as 3-year old spawners (Fisher, 1994). The late-fall run has also been extirpated from the San Joaquin River, with the sole population now occurring in the mainstem Sacramento River. The fall run remains the healthiest population due to its reliance on lower-elevation mainstem rivers and tributaries, which were least affected by human alterations to the watershed. Annual escapement of the other runs now rarely exceeds 20,000 but fall-run escapement typically exceeds 100,000. A record 725,000 fall-run spawners returned in 2002, but returns in 2007 and 2008 dropped below conservation targets, spurring management concern for the once healthiest of Central Valley Chinook salmon populations (NOAA, 2008; Lindley et al., 2009). Most runs are now supported largely by hatcheries, instituted as mitigative and recovery measures when stocks began to decline due to human impacts (Moyle, 2002; Williams, 2006).

The decline of salmon populations began early in the settlement of the Central Valley. Hydraulic gold mining from the mid 1800s to 1884 completely eliminated salmon populations from many large tributaries of the Sacramento and San Joaquin rivers (Black, 1995; Yoshiyama, 2001). Extensive habitat loss occurred between 1900 and 1950 when hydroelectric and irrigation development rapidly transformed the watershed from a naturally functioning, snow-melt driven hydrologic cycle to a highly regulated water delivery system. Large dams completely eliminated all spawning habitat for the winter run, which now exists owing to cold-water releases from Keswick Dam, the upstream boundary of access to anadromous fish on the Sacramento River (Fisher, 1994; Yoshiyama, 2001). Eighty percent of the 6000 stream miles of former spawning habitat has been blocked from access to the spring run (Fisher, 1994). Dams were also responsible for complete elimination of spring and late-fall runs in the San Joaquin River (Yoshiyama, 2001). Commercial fisheries also contributed to the decline and major gill net fisheries targeting winter and spring runs operated through the late 1870s (Black, 1995). Following decline of these runs, much of the commercial fishery shifted

to the ocean. However, the ocean fishery in southern Oregon and California was halted during 2008 and 2009 due to the collapse of the fall run (NOAA, 2008; Lindley et al., 2009). Because of its Mediterranean climate and variable rainfall, many irrigation canals were built to divert and reduce natural flows of Central Valley rivers for agricultural and municipal uses. Furthermore, with all water from the Sacramento River in the north and the San Joaquin River in the south funneling through the Delta, the Delta became the hub of the largest water delivery system in the world.

1.1.2 The Sacramento-San Joaquin River Delta

The Sacramento-San Joaquin River Delta is the largest wetland on the West Coast of the United States (Healy, 2008). Historically, the extensive freshwater and tidal wetlands once covered 2200 km^2 surrounding the confluence of the Sacramento and San Joaquin Rivers and upper San Francisco Bay (Nichols, 1986). As upland rivers entered the Delta, their flows dispersed through marshes, wetlands, and 700 miles of interconnected river channels, waterways, and sloughs (Figure 1.2). So unique is the Delta that it is home to a number of endemic fish species such as the Delta smelt (*Hypomesus transpacificus*). The Delta also provided a migration corridor for yearling Chinook smolts and critical habitat for subyearling Chinook salmon rearing in the shallow, productive wetlands and side channels of the Delta. The Delta played a critical role in the historical productivity of Chinook salmon populations of the Central Valley (Williams, 2006).

Degradation of the Delta occurred simultaneously with that of headwater tributaries as sediments from hydraulic mining washed downstream and settled in the slower water velocities of the Delta and San Francisco Bay. The Sacramento River's bed rose by six to seven feet at Sacramento (Black, 1995) and by over three feet in many bays (Nichols, 1986). Although mining ceased by 1884, not until the late 1920s did the river bed return to its pre-mining elevation (Nichols, 1986). Sedimentation of the Delta and San Francisco Bay reduced its capacity and substantially altered tidal and water circulation patterns on which the estuary ecosystem had evolved (Nichols, 1986). As the human population began to increase in the early 20th century, wetlands were filled and diked for agriculture, rivers were leveed for flood control, and channels were dredged for navigation. Only 125 km^2 of 2200 km^2 of wetlands
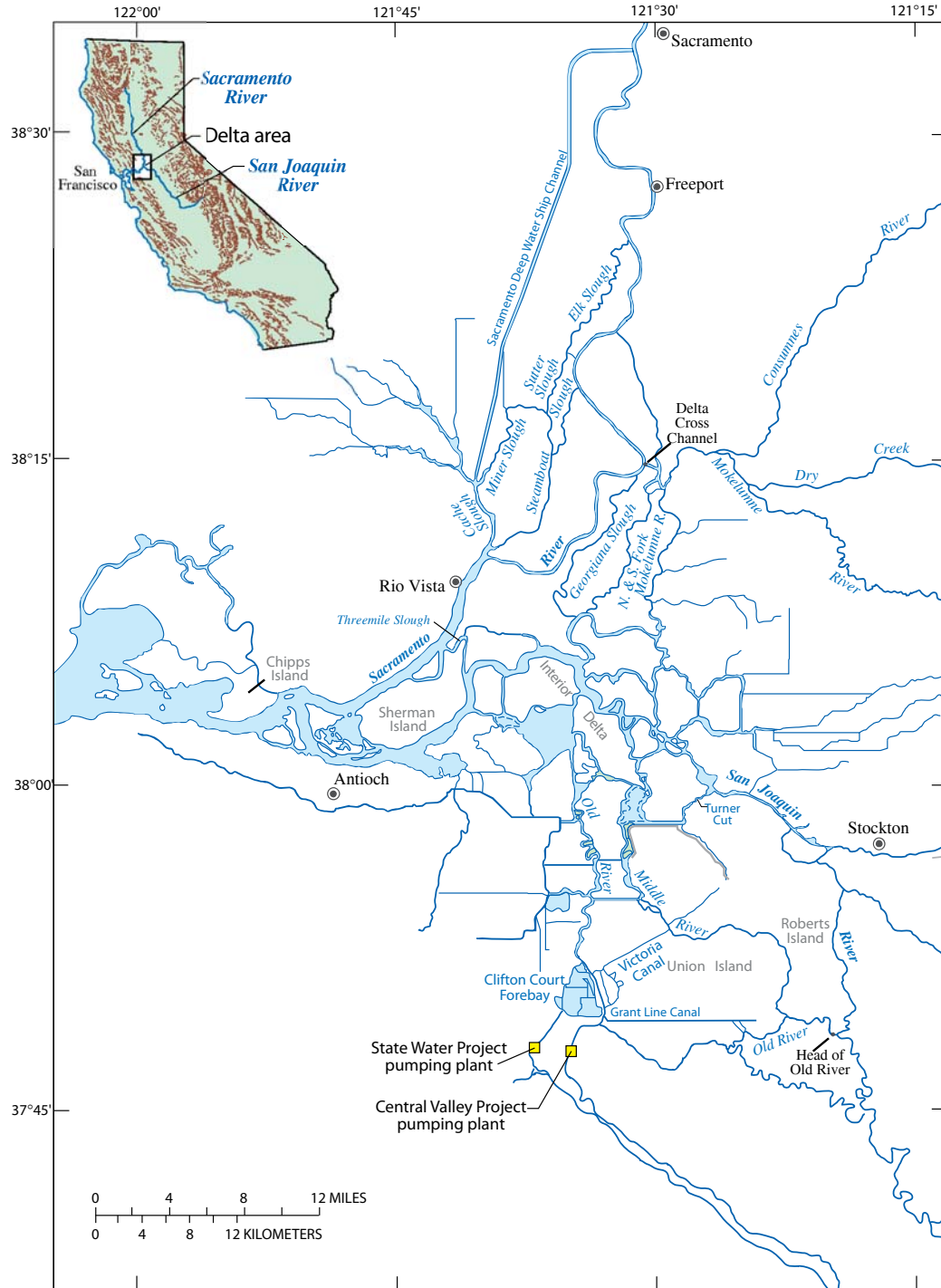
Figure 1.2. The Sacramento-San Joaquin River Delta.

(5.7%) remain intact today (Nichols, 1986). Changes in the structure of aquatic communities accompanied changes in the physical structure of the Delta. Due to both intentional and accidental introductions, over 130 invasive species have become established in the Delta (Healy et al. 2008). Invasive fish species now dominate both total biomass and abundance (Feyrer and Healy, 2003; Brown and Michniuk, 2007). However, the defining human alteration to today's Central Valley is the Central Valley Project and the State Water Project.

The Central Valley Project (CVP) and State Water Project (SWP) together form the world's largest water delivery system. Both projects form a system of reservoirs, pumping stations, and canals designed to move water from northern California, where most of the precipitation falls, to southern California which is much drier. The CVP is comprised of 20 dams and reservoirs, 11 powerplants, and 500 miles of canals (http://www.usbr.gov/dataweb/html/cvp.html; accessed May 2009). The SWP includes 34 storage facilities, 20 pumping plants, 5 hydroelectric generating plants, and over 700 miles of canals (http://www.water.ca.gov/swp/index.cfm; accessed May 2009). Since all water flowing into the Central Valley is funneled through the Delta, the Delta plays a prominent role as the hub of California's water delivery system. Both the CVP and the SWP pump large volumes of the water (termed "water exports") from two pumping stations located at the southern end of the Delta (Figure 1.2). Associated with these pumping stations is the Delta Cross Channel located on the Sacramento River in the northern Delta (Figure 1.2). The Delta Cross Channel is a man-made gated canal that diverts water from the mainstem Sacramento River into the central and southern Delta (hereafter, the "interior Delta"). Its purpose is to reduce salinities in the interior Delta to improve water quality at the pumping stations. This extensive water delivery system is critically important to state, national, and global economy, providing water to over 20 million Californians and to the world's fifth largest supplier of food and agricultural commodities (Culberson, 2008). Balancing human demands for water with maintenance of a functioning ecosystem capable of supporting healthy salmon populations has become a central challenge facing natural resource managers in the 21st century (Healy, 2008).

The influence of exporting water from the Delta on migrating juvenile salmon is profound. At times, the CVP and SWP can export up to 60% of the total inflow to the Delta, drawing water to the south and competing with flows heading towards the outlet of the Delta at

Chipps Island (Figure 1.2). Furthermore, when exports exceed inflow from the San Joaquin River, the net direction of flow is towards the pumps, rather than towards San Francisco Bay (Brandes and McLain, 2001). Thus, juvenile salmon emigrating from the San Joaquin and Sacramento rivers often become drawn towards the pumping stations rather the ocean (Brandes and McClain, 2001). This process increases their migration times and they become susceptible to entrainment into the intakes at the water pumping stations. Once at the pumping stations, predation rates are high and fish may be entrained into irrigation canals (Gringas, 1997; Kimmerer, 2008; Kimmerer and Nobriga, 2008; Clark et al., 2009). The role of the Delta on population-level survival has been recognized as critical to recovery of endangered salmon populations (CVPIA, 1992; Kimmerer et al., 2008; Lindley, 2009). Thus much research has focused on understanding the influence of exports and operation of the Delta Cross Channel on survival of endangered juvenile salmon migrating through the Delta.

1.2 Juvenile Salmon Survival in the Delta

1.2.1 State of Knowledge

The vast majority of research to quantify survival of juvenile salmon migrating through the Delta has been conducted by the U.S. Fish and Wildlife Service in Stockton, CA (http://www.fws.gov/Stockton; accessed May 2009). Studies since the 1970s through 2006 have focused on both the Sacramento and San Joaquin rivers and have employed mark-recapture methods using coded wire tags to estimate survival of subyearling fry and yearling smolts of Chinook salmon. In general, this methodology involves marking tens of thousands of fish, releasing them at various locations in the Delta, recapturing them using a mid-water trawl at the outlet of the Delta at Chipps Island (Figure 1.2), and recapturing them as adults in the commercial ocean fishery. Different release locations have served as reference points for comparing the relative probability of surviving through different migration routes. A variety of statistical methods have been used, ranging from analysis of survival "indices" based on expansion of trawl counts to sophisticated Bayesian hierarchical models that account for the multinomial structure of recapture data and for multiple sources of variation.

Early analyses of fry and smolt recaptures suggested that survival 1) differed among alternative migration routes through the Delta, 2) was affected by water exports, 3) depended on whether Delta Cross Channel gates were open or closed (Sacramento River), and 4) was influenced by presence or absence of a barrier blocking a migration pathway to the pumping stations (San Joaquin River). Fall-run fry releases occurred only in the Sacramento River through the 1980s and were recovered only in ocean fisheries (Brandes and McClain, 2001). Insights from these studies suggested that survival during dry years was higher for fish remaining in the Sacramento River relative to fish entering the interior Delta (Figure 2.1), but that survival was similar among migration routes during wet years. Brandes and McClain (2001) attributed this observation to the high inflows from rivers in wet years relative the amount of water exported at the pumping stations (the "export:inflow ratio").

The vast majority of mark-recapture studies have employed the use of fall-run and late-fall-run smolts, which can be captured by mid-water trawls at the outlet of the Delta. On the San Joaquin River, recovery rates of smolts migrating through the mainstem were higher than for smolts migrating through Old River, which took fish towards the pumping stations (Figure 1.2). In some years, a rock barrier was installed at the head of Old River to prevent smolts from entering this migration route, and recovery rates were compared with and without the barrier. Results from these experiments were statistically inconclusive, although Brandes and McClain (2001) presented several lines of supporting evidence that survival should increase with the rock barrier in place. Brandes and McClain (2001) also used the ratio of recovery rates of fish released into the upper San Joaquin River relative lower San Joaquin River near the terminus of the Delta to examine the relation between San Joaquin river flow and survival. The recovery ratio increased with flow, suggesting higher relative survival of the upstream release group as flows increased. Kjelson (1981) observed that coded-wire tag fish recovered at the pumping stations ("salvaged" fish) tended to increase with exports. Furthermore, Brandes and McClain (2001) noted that recovery rates of fish released into the San Joaquin River were much greater than that of fish released into the northern Delta, suggesting populations in the San Joaquin River were more susceptible to direct mortality at the pumping stations than populations from the Sacramento River.

For juvenile salmon smolts emigrating from the Sacramento River, studies with coded wire tags showed that river flow, water temperature, and migration routes through the interior Delta influenced survival (Kjelson et al., 1989; Brandes and McClain, 2001). First, recovery rates were positively related to river discharge of the Sacramento River and inversely related to temperatures. Second, for fish released upstream of the Delta Cross Channel, recovery rates were inversely correlated with the proportion of flow diverted into the interior Delta through the Delta Cross Channel and Georgiana Slough, suggesting diversion into the interior Delta reduced overall survival. Third, for paired releases into the interior Delta via Georgiana Slough or into the Sacramento River, fish entering the interior Delta survived at a lower rate. Finally, Brandes and McClain (2001) showed an inverse relationship between exports and recovery rates of fish released into the interior Delta. Taken together, this set of studies suggested a substantial negative effect of the Delta Cross Channel and water exports on survival of juvenile salmon.

Due to the implications of their findings, the statistical analyses of these studies (Kjelson et al., 1989; Brandes and McClain, 2001) were scrutinized and criticized on a number of counts (Williams, 2006; Brown and Kimmerer, 2006):

- Survival "indices", either based on recapture rates or ratios of recaptures between locations, failed to account for the underlying variance structure in each point estimate. That is, each observation received equal weight in regression analysis even though the variance of each point estimate differed.

- Multiple linear regression assuming normally distributed errors was used to analyze the effect of covariates, even though the data arise from the multinomial distribution.

- Recapture counts in ocean fisheries were expanded to an estimate of total recaptures in the fisheries based on sampling rates at various ports, but the error associated with such expansion was not accounted for in analyses.

- Recapture counts at the Chipps Island trawl were expanded to an estimate of the flux of fish passing Chipps Island using the fraction of time sampled and the fraction of water volume sample. This approach involved a number of untenable

assumptions such as a uniform distribution of fish through space and time passing Chipps Island.

To address these concerns, K. B. Newman published a series of papers that directly modeled recaptures or ratios of recaptures using appropriate statistical models that explicitly accounted for the multinomial structure of the data (Newman and Rice, 2002; Newman, 2003; Newman, 2008; Newman and Brandes, 2010). These studies analyzed both paired and unpaired releases, but recognized that paired releases provided stronger inferences about survival. With unpaired releases, observed recaptures arise due to the joint probability of survival and capture and these processes are confounded. For paired releases (e.g., simultaneous releases into the interior Delta and the Sacramento River), the ratio of recovery rates yields the ratio of survival probabilities under the assumption of equal capture probabilities and equal post-Delta survival for the two release groups. Newman's earlier papers largely confirmed the findings of the Kjelson's and Brandes' studies conducted in the Sacramento River and showed a positive effect of river flow, a negative effect of water temperature (also found by Baker et al. 1995), a negative effect of an open Delta Cross Channel gate, and a negative but sometimes nonsignificant effect of exports on survival (Newman and Rice, 2002; Newman, 2003). His most recent analyses used paired releases within a Bayesian hierarchical framework to evaluate and summarize the major coded-wire tag experiments occurring in the Delta (Newman, 2008; Newman and Brandes, 2010). He found modest evidence that closure of the Delta Cross Channel gate improved survival, and estimated that mean survival of fish migrating through the interior Delta was only 35-44% that of fish remaining within the Sacramento River. Newman and Brandes (2010) found a high probability of a negative export effect on survival, but when compared against models with and without an export effect, other models explained the observed data just as well. The conclusions from Newman's series of papers support the initial findings from the earlier analyses, but do so using statistical models appropriate to the data structure of the mark-recapture studies.

These studies represent the bulk of research to estimate survival of juvenile salmon in the Delta and have provided important information about the effects of water management actions. Generalities that arise include:

1) Survival of fish migrating through the interior Delta, where pumping stations are located, is less than that of fish that remain in the Sacramento River.

2) Survival with the Delta Cross Channel open is less than when the Delta Cross Channel is closed, presumably because a larger fraction of the population remains within the Sacramento River when the Delta Cross Channel is closed.

3) Exports may have a negative effect on survival, but high unexplained natural variability muddles the underlying signal.

While thirty years of coded wire tag studies have certainly shed light on factors influencing survival of migrating salmon through the Delta, much remains to be learned.

1.2.2 Gaps in Knowledge

To better understand natural and anthropogenic factors influencing population-level survival of juvenile salmon migrating through the Delta, consider the underlying processes acting on the population as they migrate through the Delta. As the juvenile salmon population enters the Delta from mainstem rivers, it disperses among the Delta's complex channel network. The dispersal process will be driven by the relative quantities of discharge entering each channel, the horizontal distribution of fish as they pass a channel junction (a main channel splitting into two or more channels), and by tidal cycles that alter flow patterns at river junctions. Once fish enter a given channel, they are subject to channel-specific processes that affect their rate of migration, vulnerability to predation, feeding success, growth rates, and ultimately, survival. Eventually, alternative migration routes converge at the exit of the Delta and the population once again comes together to migrate through San Francisco Bay. This dispersal and migration process suggests that population-level survival of juvenile salmon migrating through the Delta will be driven by 1) the survival rates arising from the biotic and abiotic processes unique to each migration route, and 2) the proportion of the population using each migration route. In turn, natural and human-imposed variation in discharge and water distribution will affect population dispersal and survival rates within each channel, driving population-level survival through the Delta. It is this process that is the focus of my dissertation.

From this perspective, mark-recapture studies conducted thus far have provided insight into individual components of the dispersal-survival process, but many gaps remain to be filled. Some migration routes may be critical to population survival, yet have not been studied. For example, Sutter and Steamboat sloughs, upstream of the Delta Cross Channel, may be an important migration route because fish taking either of these routes do not encounter the Delta Cross Channel (Figure 1.2). However, migration through Sutter and Steamboat sloughs will increase population survival only if survival through these routes is higher than alternative routes. Considering all major migration routes is therefore crucial for understanding how each route affects population survival. Yet the single most important missing piece to this puzzle is an understanding of how juvenile salmon distribute among alternative migration routes once they enter the Delta. Even though survival may differ drastically among migration routes, the magnitude with which each route contributes to population survival will depend on the fraction of the population using each route. For example, although survival for fish entering the interior Delta is lower than for the Sacramento River, if 90% of fish remain in the Sacramento River then the interior Delta will have little influence on survival of the population. Current knowledge suggests survival is lower for fish migrating through the interior Delta, yet there is poor understanding of how such differences among migration routes affects population-level survival through the Delta.

Two recent studies examined important components of survival in the Delta, with the specific goal of placing findings in a population context. First, Kimmerer and Nobriga (2008) used particle tracking models to examine dispersal of juvenile salmon migrating through the Delta. Their findings provided insights into the distribution of possible fates of passively moving particles in response to tides, exports, and operation of the Delta Cross Channel. However, as recognized by Kimmerer and Nobriga (2008), a major assumption is that fish move as passive particles. Furthermore, their study did not incorporate differential "survival" of particles among different routes, which will substantially influence the distribution of possible fates of particles. Kimmerer (2008) also used existing coded-wire tag data to estimate a mean of 10% of the total number of fish surviving to Chipps Island, but such estimates are highly uncertain due to limitations of coded wire tags noted above. Such analyses begin to consider the population-level consequences of management actions, but still lack the ability to

draw direct inference on the simultaneous dispersal-survival process of juvenile salmon in the Delta.

Currently lacking is a population-level approach that is capable of 1) quantifying dispersal of the population among migration routes, 2) estimating survival within these routes, and 3) explicitly linking each of these components to survival of the population. Water management actions in the Delta act on individual components of the population in different places at different times: e.g., some fraction of the population passes the Delta Cross Channel, of which some fraction enters the interior Delta, of which some fraction arrives at the pumping stations. Thus, a framework to estimate route-specific dispersal and survival will help fisheries managers better understand the how water management actions act on these individual components. But more importantly, such a framework would provide a means for explicitly relating each route-specific component back to the population of interest.

1.2.3 Filling in the Gaps

Although the framework above is conceptually appealing, feasible approaches to estimating the route-specific components of population survival are few. For example, to accomplish such a task with coded wire tags would require 1) releasing tagged fish upstream of the Delta and allowing them to naturally distribute among routes as they migrate through the Delta, 2) recapturing fish within each major migration route as they pass channel junctions, 3) recapturing fish at the convergence of major river channels, 4) recapturing fish as they exit the Delta, and 5) recapturing fish after they exit the Delta. While theoretically feasible, logistics and labor associated with such an effort detract from this approach. Furthermore, batch marks such as coded-wire tags (as opposed to individually identifiable tags) limit the statistical models that can be applied, the parameters that can be estimated, and the assumptions that can be tested (Skalski et al., 2009a). However, low capture probability is the biggest limitation with coded wire tags and other tags that require physical recapture of tagged fish. The precision of survival estimates is positively related to capture probability: the lower the capture probability, the poorer the precision (Burnham et al., 1987). In coded wire tag studies in the Delta, Newman (2008) estimated that median capture probabilities of the Chipps Island trawl were ≤0.0008, or 0.08% of the tagged fish passing Chipps Island being captured by the trawl.

Such low capture probabilities introduce high uncertainty in estimates of survival. For example, Newman (2008) estimated that 100 paired releases each with 150,000 coded-wire tagged fish would be needed to obtain a coefficient of variation of 20. Given that only one or two paired releases have been conducted each year in past studies, many years of study would be required before even moderate levels of precision were obtained.

Biotelemetry techniques combined with mark-recapture models offer one possible approach to simultaneously quantify dispersal and survival of juvenile salmon migrating through the Delta. This approach entails deployment of telemetry monitoring stations at key locations throughout the Delta, implanting small transmitters into juvenile salmon, and then tracking their migration through the Delta. A major impediment to estimating dispersal and survival through the Delta is the extreme spatial complexity of the Delta's channel network. However, in complex settings such as the Delta, biotelemetry has a number of advantages over traditional mark-recapture techniques that rely on the physical recapture of fish. First, uniquely identifiable transmitters provide detailed information about the temporal and spatial movements of individuals migrating through the Delta. Second, the "capture" process is passive, so that an individual may be "captured" numerous times as it migrates unimpeded through the Delta. Third, uniquely identifiable tags allow development of statistical models capable of estimating both survival and dispersal through the Delta. Fourth, the spatial arrangement of telemetry stations in Delta can be tailored to the Delta's complex channel structure to quantify both movement among and survival within given migration routes. Fifth, because detection probabilities are typically high (>0.75), small sample sizes can yield high precision of parameter estimates.

Telemetry techniques have long been used to quantify the temporal and spatial extents of fish migrations (Winter, 1996), but only recently has telemetry data been cast in a mark-recapture framework to explicitly estimate demographic parameters. Pollock et al. (1995) used telemetry to estimate survival over time, but here I am interested in estimating survival through space. Skalski et al. (1998, 2001) used mark-recapture models to estimate in-river survival of migrating juvenile salmon implanted with passive integrated transponders (PIT tags) and with radio-tags. These models are based on the classic models of Cormack (1964), Jolly (1965), and Seber (1965). As such, these models estimate survival through discrete reaches of river, but

have limited application for the Delta where we must also estimate the proportion of fish using each migration route. Skalski et al. (2002) also developed a mark-recapture model to simultaneously estimate the probability of passing through a given route at a dam (e.g., turbines and spillway) and the probability of surviving each passage route. This model comes closer to that needed for the Delta because it estimates both movement among routes and survival within routes. However, the channel structure of the Delta is much more complex than that of fish passing through a single dam. The Delta has a hierarchical channel structure where a main channel splits in two or more channels, and nested within each of these channels may be additional junctions among which fish may disperse. Thus, although telemetry techniques offer promise, statistical models must be developed and tailored the Delta's complex channel network to estimate survival and dispersal of juvenile salmon in the Delta.

1.3 Goals of this Research

The overarching goal of my research is to use mark-recapture models to estimate 1) survival of juvenile salmon within specific migration routes of the Delta and 2) the proportion of fish using different migration routes through the Delta. Furthermore, as noted above, my goal is to link each of these components to population-level survival in the Delta to better understand how each migration route contributes to population survival. In 2006, a three-year research program was initiated to estimate watershed-scale survival of acoustically tagged juvenile salmon and steelhead in the Sacramento River (http://californiafishtracking.ucdavis.edu/; accessed December 2009). Although not specifically focused on the Delta, the infrastructure of acoustic telemetry stations from this research project afforded the opportunity for other studies to release acoustically tagged fish focused on their own research goals. As such, in 2006, I was funded through the CALFED Science Fellowship Program to assist the US Fish and Wildlife Service (USFWS) in developing the statistical models necessary to estimate dispersal and survival of juvenile salmon in the Delta.

The central interest of this work to fisheries managers is better understanding of the effect of water management actions on population-level survival of juvenile salmon migrating through the Delta. Thus, my goal is to provide a framework within which the effects of water

management actions on specific components of the populations can be measured and related to the population at large. Given relatively small sample sizes, low release replication, a limited range of environmental conditions, and the novelty of acoustic telemetry in the Delta, my research just begins to shed light on the effects of water management actions on survival through the Delta. Nonetheless, I begin to uncover the dynamics of movement and survival of juvenile salmon in the Delta and provide an analytical framework within which effects of water management actions can be quantified.

In this dissertation, each chapter builds on the previous, beginning with building the statistical foundation of the mark-recapture models and culminating with a multiyear analysis of survival and dispersal through the Delta. In Chapter 2, I develop the foundation of mark-recapture models for the Delta, describing general model structure, detailing and assessing model assumptions, and examining requirements for identifiability of model parameters. In Chapter 3, I developed and applied the basic mark-recapture model that estimates both dispersal and survival among migration routes in the Delta to a small data set of acoustically tagged late-fall Chinook salmon released during the 2007 migration year (December 2006 – February 2007). Since such a study had never been conducted and sample size was small, the findings from Chapter 3 provided many new insights but also highlighted ways to improve the study. Thus, Chapter 4 expands the initial mark-recapture model and applies it to data from the 2008 migration year with the goals of 1) improving precision of parameter estimates both within and among migration routes, 2) obtaining more detailed information within migration routes, and 3) examining patterns of variation in reach-specific survival. In Chapter 5, I incorporate covariates into the mark-recapture model to quantify factors affecting survival during the three-year study. In Chapter 6, I analyzed the three-year data set to uncover factors affecting entrainment probabilities at an important river junction in Delta. Here, I examine how river flow, tidal fluctuations, and operation of the Delta Cross channel affect the probability of fish entering a particular migration route. In Chapter 7, I conclude with a discussion of the ramifications of my findings for management of the Delta and recovery of salmon populations. I also identify directions for future research to further improve knowledge of the complex migration and survival dynamics of juvenile salmon in the Delta.

Chapter 2

QUANTIFYING SURVIVAL IN THE DELTA: MODELING FRAMEWORK, ESTIMATION, AND ASSUMPTIONS

2.1 Introduction

In this chapter, my goal is to develop the basic building blocks for constructing statistical models to estimate survival of juvenile salmon migrating through the Delta. To develop these building blocks requires an understanding of the underlying problem at hand, the statistical methods to tackle the problem, and the assumptions involved with application of the statistical methods. Therefore, first I examine the role of the Delta in the context of the Chinook salmon's life cycle, showing how the Delta can be cast in terms of the demographic parameters of a matrix population model. Having set up the problem, I then discuss the class of statistical models that can be used to estimate the demographic parameters and the assumptions entailed with application of these models. Next I describe how the spatial structure of the Delta necessitates adapting the statistical models and how such adaptation can influence estimability of model parameters. Last, I discuss assumptions of these models with particular focus on how they apply to use of acoustic telemetry in the Delta.

In describing the models and assumptions, I used simple conceptual models of a river delta to focus on model construction techniques and assessment of assumptions. Given the channel complexity of the Delta and ability of telemetry to monitor any river channel, the range and scope of possible models that could be constructed is nearly limitless. Therefore, my goal here is to focus on the general techniques needed to construct any model, with particular emphasis on ensuring assumptions are fulfilled and parameters estimable. Given this "toolbox", it is then straightforward to tailor any model to the specific questions of a particular study to tackle the full channel complexity of the Delta.

2.2 A Matrix Population Model Perspective

2.2.1 The Delta in the life cycle of Chinook salmon

Recovery of endangered salmon populations in the Central Valley requires an understanding of how each life stage of the salmon's life cycle contributes to population growth rates. In turn, population growth rates are determined by vital rates of stage-specific survival and reproduction. Although my research focuses on one small aspect of the salmon's life cycle – the period of migration through the Sacramento-San Joaquin River Delta – this critical period could substantially influence population growth rates. To fully understand the influence of the Delta on population growth rates, the Delta must first be placed in the context of the salmon's life cycle. Here, I describe a generic stage-structured life-cycle of Chinook salmon in the Sacramento River (Figure 2.1). Using a simple representation of the Delta, I then show how the period of migration through the Delta can be explicitly included in the matrix representation of a salmon's life cycle.

Matrix population models provide a convenient mathematical framework for structuring the life cycle of pacific salmon and for examining the contribution of specific life stages to population growth rates (Caswell, 2001). Matrix population models have been used to examine the effects of climate change on population viability of salmon populations (Crozier and Zabel, 2006; Zabel et al., 2006; Crozier et al., 2008), to examine effects on population growth from improving survival during the freshwater migration phase (Kareiva et al., 2000), and to identify demographic parameters that most influence population growth rates (Wilson et al., 2003). Recently, an independent review panel recommended just such an approach to understand the influence of the CVP and SWP on endangered salmon populations in the Central Valley (CALFED Science Review Panel, 2008). Thus, understanding how the Delta fits into the life-cycle demographics of salmon is important to fully gauge the influence of this life stage on population dynamics. From this perspective, my research can be viewed as a focused effort to quantify demographic rates during a poorly understood, but possibly critical period of a salmon's life cycle that may be influenced by water management actions.
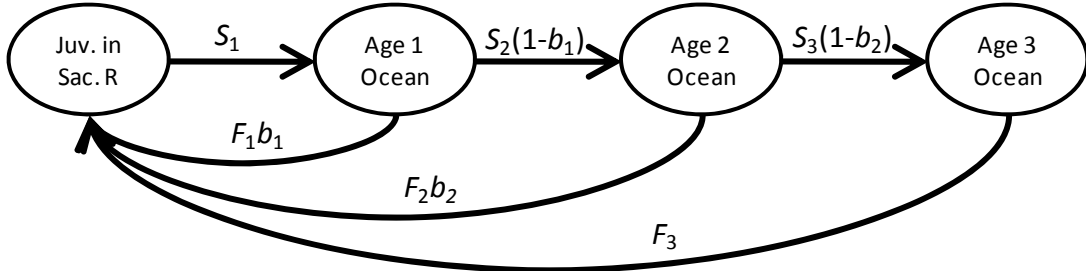
Figure 2.1. Stage-structured life cycle of salmon in the Sacramento River. Circles represent life stages, arrows represent transitions between time t and $t+1$, and demographic parameters of survival (S_i), breeding (b_j), and reproduction (F_j) govern the rate of transition between life stages.

I described a generic life cycle of Chinook salmon in the Central Valley using four life stages; the juvenile freshwater stage and three ocean age-classes (Figure 2.1). Transitions between life stages are governed by the probability of surviving, S_i, from life stage i to stage $i+1$ and the probability of returning to spawn after each year in the ocean, b_j. Each adult age class returning at time t contributes to the subsequent juvenile population at time $t+1$. I defined the juvenile life stage as ending when fish begin their downstream emigration from natal tributaries. Thus, F_j is the per-individual contribution of ocean age class j at time t to the population of emigrant juvenile salmon at time $t+1$. This life-cycle can be conveniently represented in matrix notation where the transition matrix $\mathbf{A}$ with entries a_{sr} represents the probability of transitioning from life stage r at time t (r indexes the columns) to life stage s at time $t+1$ (s indexes the rows):

$$\mathbf{A} = \begin{bmatrix} 0 & F_1 b_1 & F_2 b_2 & F_3 \\ S_1 & 0 & 0 & 0 \\ 0 & S_2(1-b_1) & 0 & 0 \\ 0 & 0 & S_3(1-b_3) & 0 \end{bmatrix}.$$

The demographic parameters forming the entries to the transition matrix are typically expressed as functions of more complex underlying processes. For example, each annual survival rate in the ocean may be expressed as a function of both fishing and natural mortality rates. Also, since F_j represents the contribution of spawning individuals to the juvenile emigrant population, F_j will be a function of 1) sex ratio, 2) survival of adults during the

upstream migration, 3) age-specific fecundity, 4) egg-to-fry survival, and 5) fry-to-emigrant survival. Since fish pass through the Delta during their transition from the juvenile freshwater stage to the ocean age 1 stage (Figure 2.1), my goal is to express S_1 as a function of the underlying demographic rates driving survival of the population during the transition between these life stages.

Fish move over large distances through diverse environments during their transition from the freshwater to ocean environment. Demographic rates during transition between these life stages are therefore best conceptualized as a spatially-structured population model with the population being censused at different points in space. As an example, I have shown the simplest representation of the Delta that captures the essence of three major migration routes that fish could use during transition between the freshwater and ocean life stages (Figure 2.2). At the first river junction, fish can take migration route B which bypasses the second river junction, and then all routes converge at the exit of the Delta. This network structure is important because fish that take migration route B are "immune" from entering route C. Such structure emulates the Delta where fish entering Sutter and Steamboat sloughs (route B) bypass the entrance to the Interior Delta (route C, See Figure 3.1). To incorporate this channel structure into a population model, the population is tallied just downstream of each river junction to measure within-route survival and the proportion of the population using each migration route at each river junction (Ψ).

2.2.2 The Delta as a stage-structured population model

The life-stage transitions between the freshwater and ocean can be structured as a series of spatially-dependent transition matrices, $\mathbf{A}_t$, where stages are represented by each of the possible migration routes (Figure 2.2). For example, for the first reach, two transitions are possible: fish may survive the first reach and move into route B or they may survive and remain in route A (see $\mathbf{A}_1$ in Figure 2.2). However, in the next reach, transition matrix $\mathbf{A}_2$ differs due to the spatial structure of that reach. The change in population size between freshwater and ocean life stages, S_1 in original matrix population model (Figure 2.1), is the 1,1 element of the pre-multiplied transition matrices:
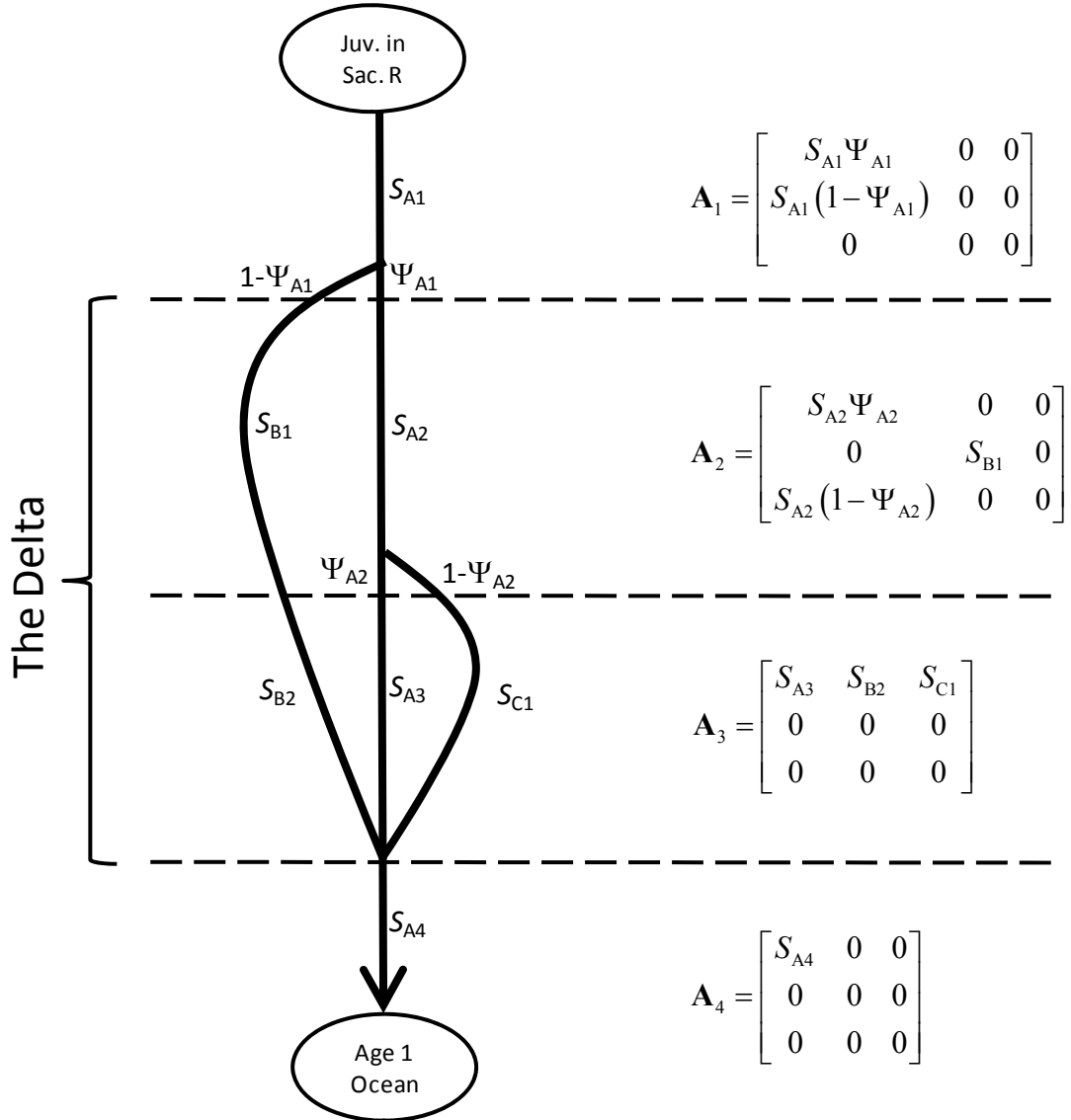
Figure 2.2. A simple representation of the Delta showing different migration routes that fish may take during their transition between freshwater and ocean life stages. Dashed lines mark the location of transitions among migration routes, with rates of transition governed by route-specific survival probabilities (S_{hi}) and probabilities of entering each migration route (Ψ_{hl}). Spatially dependent transition matrices ($\mathbf{A}_t$) show the probability of transitioning from route r (indexing the column) at location t to route s (indexing the row) at location $t+1$.

$$S_1 = \left(\mathbf{A}_1\mathbf{A}_2\mathbf{A}_3\mathbf{A}_4\right)_{1,1} = S_{A1}\left(\left(1-\Psi_{A1}\right)S_{B1}S_{B2} + S_{A2}\left(\Psi_{A2}S_{A3} + \left(1-\Psi_{A2}\right)S_{C1}\right)\right).$$

In essence, S_1 is the weighted average survival of fish that take different migration routes through the Delta where the weights are equal to the proportion of fish taking each unique migration route. Although the matrix notation used here may seem overly burdensome for describing the weighted average for such a simple example, it shows how this problem can be cast in terms of a matrix population model of a salmon's life cycle. Furthermore, as will be seen, this matrix representation will become very useful for constructing the likelihood of statistical models to estimate these parameters, especially when attempting to address the full spatial complexity of the Delta.

2.3 The Multistate Mark-Recapture Model

The central challenge of estimating parameters described in the population model above is sampling the population at different locations in the Delta. Acoustic telemetry provides a powerful technique for tracking the movements of individual fish. By placing autonomous telemetry stations at strategic locations in the Delta, detection data from the system of stations can be analyzed in mark-recapture statistical framework to estimate demographic parameters of interest (Skalski et al., 2001, 2002, 2009b). The Cormack-Jolly-Seber model has been used with telemetry data to estimate survival probabilities of juvenile salmon migrating to the ocean (LaCroix, 2008; Skalski et al., 2001). In our case, however, we are not only interested in estimating survival for each route, but also the proportion of fish using different migratory pathways. The multistate mark-recapture model provides just such a framework for estimating both survival and movement parameters.

Estimating movement rates among geographic areas from marked animals has received growing attention over the past 35 years. Arnason (1972) estimated movement rates and survival among two populations, and Arnason (1973) and Seber (1982) extended these models to three or more populations. Hilborn (1990) used a Poisson approximation to the multinomial distribution to estimate movement rates of skipjack tuna (*Katsuwonus pelamis*) from tag recovery data. Schwarz et al. (1993) fully generalized Arnason's models to allow for

any number of recapture occasions and geographic locations for application to band recovery data. Brownie et al. (1993) further generalized the model for application to multiple recaptures, and also constructed models that allow for non-Markovian transitions. Since these seminal papers, the multistate mark-recapture model has been used to model not only movement among geographic locations, but transition rates among any set of discrete states where transitions are stochastic (Lebreton et al., 2002; Nichols and Kendal, 1995). For example, this model has been used to estimate transitions among weight classes (Letcher and Horton, 2009) and between breeding and non-breeding states (Nichols et al., 1994). Thus, the multi-state mark-recapture model has become a very flexible estimation framework for answering diverse questions about important demographic parameters influencing population dynamics of animals.

2.3.1 The multistate model as an estimation framework

To describe the multistate model here, I use the notation of Brownie et al. (1993), and this notation is later used for the models I constructed for the Delta. The fundamental parameters estimated by the multistate model are:

ϕ_i^{rs} = joint probability of surviving from sampling occasion i to $i+1$ and moving from state r at occasion i to state s at occasion $i+1$.

p_i^s = probability of capture in state s at occasion i.

Given the multiple states, it is convenient to express these parameters in matrix form, here using three states for simplicity:

$$\phi_i = \begin{bmatrix} \phi_i^{11} & \phi_i^{12} & \phi_i^{13} \\ \phi_i^{21} & \phi_i^{22} & \phi_i^{23} \\ \phi_i^{31} & \phi_i^{32} & \phi_i^{33} \end{bmatrix},$$

$$p_i = \begin{bmatrix} p_i^1 & 0 & 0 \\ 0 & p_i^2 & 0 \\ 0 & 0 & p_i^3 \end{bmatrix}.$$

As opposed to the matrix population model, r indexes the rows and s indexes the columns. Under the most general model when all states are sampled at every occasion and animals move among all states, the multistate model is directly analogous to a Cormack-Jolly-Seber (CJS) model generalized to allow movement among multiple states (Cormack, 1964; Jolly, 1965; Seber, 1965). As with the CJS model, all parameters can be estimated for all sampling periods except for the final period, when joint movement-survival probabilities (ϕ_i^{rs}) are confounded with detection probability. Since the multistate model follows directly from the CJS model, assumptions of the multistate model, in large part, mirror those of the CJS model (see below).

Summary statistics and the associated likelihood can be formed from either the multistate extension of the m_{ij}-array or the complete capture histories of individuals (Burnham et al., 1987; Williams et al., 2002). Below, I present the m_{ij}-array approach for the standard multistate model, but for dealing with the particulars of the Delta, I use complete capture histories. Sufficient statistics reduce to the numbers of animals initially marked in each state and frequencies of marked animals subsequently recaptured in each state:

$$\underset{\sim}{R}_i = \begin{bmatrix} R_i^1 \\ R_i^2 \\ R_i^3 \end{bmatrix},$$

$$\mathbf{m}_{ij} = \begin{bmatrix} m_{ij}^{11} & m_{ij}^{12} & m_{ij}^{13} \\ m_{ij}^{21} & m_{ij}^{22} & m_{ij}^{23} \\ m_{ij}^{31} & m_{ij}^{32} & m_{ij}^{33} \end{bmatrix}.$$

Where R_i^r is the number of marked animals released at occasion i in state r, which includes both newly marked and recaptured/rereleased individuals; m_{ij}^{rs} is the number of individuals captured in state s during occasion j that were last captured and rereleased in state r at occasion i, and $i = 1, 2, \dots , k$ capture occasions. Following the notation of m_{ij}-array for CJS models, each row of $\mathbf{m}_{ij}$-array forms a multinomial distribution conditional on the number of animals released at occasion i (Table 2.1).

Table 2.1 The multistate extension of the m_{ij} array for a 4-occasion experiment showing release frequencies ($\underset{\sim}{R}_1$) and recapture counts ($\mathbf{m}_{ij}$). Also shown under each recapture count matrix is the associated matrix of multinomial cell probabilities, where $\mathbf{q}_i = \mathbf{I}\text{-}\mathbf{p}_i$ and $\mathbf{I}$ is the identity matrix of appropriate dimension.

Release occasion (i)	Number released	Recapture occasion (j)		
		2	3	4
1	$\underset{\sim}{R}_1$	$\mathbf{m}_{12}$ $\boldsymbol{\phi}_1\mathbf{p}_2$	$\mathbf{m}_{13}$ $\boldsymbol{\phi}_1\mathbf{q}_2\boldsymbol{\phi}_2\mathbf{p}_3$	$\mathbf{m}_{14}$ $\boldsymbol{\phi}_1\mathbf{q}_2\boldsymbol{\phi}_2\mathbf{q}_3\boldsymbol{\phi}_3\mathbf{p}_4$
2	$\underset{\sim}{R}_2$		$\mathbf{m}_{23}$ $\boldsymbol{\phi}_2\mathbf{p}_3$	$\mathbf{m}_{24}$ $\boldsymbol{\phi}_2\mathbf{q}_3\boldsymbol{\phi}_3\mathbf{p}_4$
3	$\underset{\sim}{R}_3$			$\mathbf{m}_{34}$ $\boldsymbol{\phi}_3\mathbf{p}_4$

In the parameterization above, ϕ_i^{rs} includes the underlying probabilities of both surviving and moving between states. Interest lies in estimating these underlying parameters, but they can only be estimated by imposing the assumption that all mortality occurs while in state r, and movement to state s occurs "instantaneously" just prior sampling. Under this assumption, the model can be reparameterized as a function of S_i^r, the probability of surviving from occasion i to $i+1$ conditional on being in state r at occasion i; and Ψ_i^{rs}, the probability of transitioning from state r at occasion i to state s at $i+1$, conditional on surviving to $i+1$. Using the three-state example, the reparameterization is

$$S_i^r = \phi_i^{r1} + \phi_i^{r2} + \phi_i^{r3} \tag{2.1}$$

$$\text{and} \qquad \Psi_i^{rs} = \frac{\phi_i^{rs}}{S_i^r}. \tag{2.2}$$

These parameters can be estimated as derived parameters with maximum likelihood estimates of ϕ_i^{rs}, or the likelihood can be reparameterized directly in terms of S_i^r and Ψ_i^{rs}. As will be seen, I mix both parameterizations within the same model, separating S_i^r and Ψ_i^{rs} when the assumption that survival occurs first and transition occurs last is met, but estimating the joint movement-survival parameters (ϕ_i^{rs}) when this assumption cannot be fulfilled (e.g., see Chapter 4).

2.3.2 Assumptions of the multistate model

Assumptions of the multistate model are analogous that of the CJS model, with a number of additional assumptions as alluded to above.

A1: Inferences drawn from the sampled population apply to the population of interest.

A2: Marked animals have the same survival and movement probabilities as the unmarked population.

A3: The sampling occasion is instantaneous relative to the sampling period.

A4: Marks are not lost or misread.

A5: The states occupied at each occasion are known without error.

A6: The fate of one individual has no influence on the fate of other individuals.

A7: All individuals alive in state *s* at occasion *i* have the same probability of capture.

A8: All individuals alive in state *r* at occasion *i* have the same probability of transitioning to state *s* at occasion *i*+1.

A9: Joint movement-survival probabilities arise through a first-order Markov process. In other words, the probability of transition from state *r* at occasion *i* to state *s* at *i*+1 depends only the on the state occupied at occasion *i*.

A10: For S_i^r and Ψ_i^{rs} to remain unbiased, all mortality must occur in state *r* and then movement to state *s* occurs just prior to sampling.

Assumptions A1-A3 involve the interpretation of the parameters with respect to their strict definition. Assumption A1 should be obvious, but is important to explicitly acknowledge since the marked population can often differ from the population upon which inference is desired. For example, in my study, inferences about endangered winter-run Chinook salmon are desired, but because of their endangered status, this population is unavailable for sampling. Instead, hatchery-origin late-fall Chinook salmon are used as a surrogate for winter-run Chinook salmon because hatchery fish are readily available and emigrate during the same time period as winter-run Chinook. Strict inferences apply only to the untagged population that mirrors the tagged population, although insights about other populations may also be inferred from findings on the marked population. I expand the discussion on assumption A1 in

Chapters 3 and 4. Assumption A2 requires that handling or marking of the animal does not influence its subsequent survival. For acoustic tags, a maximum tag-to-body mass ratio of 5% is often recommended to ensure that assumption A2 is fulfilled (Adams et al. 1998a, 1998b; Perry et al., 2001). However, if such a size limit restricts study of only the largest fish in a population, there will be less overlap between the sampled population and the population of interest. Assumption A3 is required for precise definition of survival between occasion i and i+1. If the sampling occasions take place over a long period of time (e.g., 5 days) relative to the time between mid-points of sampling occasions (e.g., 7 days), then the concept of a discrete interval over which survival takes place begins to lose meaning, and sampling occasions become blurred with the intervals between sampling. I expand discussion of this assumption below with respect to using telemetry techniques to sample across space in the Delta.

Assumptions A4 and A5 are particularly important when using telemetry, and these assumptions may be violated in a number of ways. First, mark loss may occur not only through physical loss of the tag, but may also occur if the tag's battery expires before the end of the study. Both processes negatively bias estimates of survival since tag loss cannot be distinguished from mortality. Physical loss of tags can be estimated using double tagging experiments (Seber, 1982), while battery failure rates can be estimated by conducting controlled tag "survival" experiments (Townsend et al., 2006; Cowen and Schwartz, 2005). Environmental acoustic noise may be interpreted by telemetry equipment as a valid transmission from a transmitter, and these false-positive detections can introduce positive bias into survival estimates. False-positive detections can be removed by judicious screening of telemetry data prior to mark-recapture analysis, which I discuss further in Chapter 3. Since telemetry equipment indicates the presence of a live tag and not necessarily a live fish, care must be taken to ensure that dead fish with live tags are not interpreted as live fish. Such a process would lead to positive bias in survival estimates and can be evaluated by releasing a known subsample of dead individuals with live tags. Assumption A5 can be caused by violation of assumption A4 through false-positive detections and will cause bias in movement probabilities. Assumption A5 may also be violated by certain combinations of the detection process and movement process among states, which I discuss below with respect to monitoring river junctions with telemetry equipment.

Assumptions A6 through A10 arise due to the underlying statistical distributions and structural form of the model used to estimate the parameters. The multinomial distribution assumes that observations on individuals are independent (A6) and identically distributed (A7 and A8). Violation of these assumptions will introduce heterogeneity into model parameters, which typically does not bias parameter estimates but can lead to bias in variance estimates. The Markov assumption (A9) may be violated if prior history influences future survival. For example, if migration through one route reduces survival in downstream reaches relative to fish that traveled through a different migration route, then the Markov assumption will be violated. As with A7 and A8, violation of this assumption will introduce heterogeneity and the variance will be underestimated, but the expectation of the average survival over all prior histories will remain unbiased.

Assumption A10 is often difficult to assess when sampling over time, but is easier to validate when estimating survival over space such as in my study. When estimating survival for time periods, assumption A10 requires all animals move from state r to state s "instantaneously" just prior sampling. However, the more likely scenario is that animals transition among states at various times throughout the interval, which results in the estimated survival between occasion i and $i+1$ being dependent on a unknown mixture of survival while in state r and state s. In contrast, when sampling periods are composed of survival of a population moving through space, the location of transition from one river channel (i.e., state) to another is know perfectly. Thus, to fulfill assumption A10, the population should be sampled such that telemetry stations are situated just downstream of a river junction. This ensures that the survival process takes places first, and then the transition from one route to another occurs at the very end of a river reach. This assumption is discussed in detail below.

2.4 Survival through the Delta as a Constrained Multistate Model

In my study, unique migration routes constitute the states of a multistate model, but as seen Figure 2.2, the transition matrix is constrained in each sampling period by the spatial structure of the channel network. Thus, this particular problem can be cast as a matrix population model formed by spatially dependent transition matrices $\mathbf{A}_t$ with a constrained version of a multistate mark-recapture model to estimate the parameters. To maintain the link

to matrix population models I retain the notation of section 2.2.1, but recognize that sampling occasions now refer to spatial locations indexed by t, and sampling periods represent river reaches between adjacent sampling occasions t and $t+1$.

As opposed to the fully generalized multistate model where all parameters are estimable in every occasion but the last, not all parameters in a constrained model may be estimable because transitions among each state do not occur during every sampling period. Furthermore, because the transition matrix varies across space, the structure of the multinomial likelihood must likewise accommodate the spatial structure of the Delta's channel network. Therefore, using the caricature of the Delta presented in Figure 2.2, I first develop an efficient method for constructing the likelihood of each capture history. Next, I discuss scenarios leading to inability to estimate parameters, minimal requirements to ensure parameter estimability, and approaches for determining whether all parameters are estimable in such models. Last, the spatial location of telemetry stations in the Delta directly affects the structure of the estimation model, the estimability of parameters, and validity of assumptions. Therefore, I explicitly show how a number of assumptions can be fulfilled or violated as a direct consequence of where telemetry stations are located relative to the parameters to be estimated.

2.4.1 Constructing the likelihood

Likelihoods for simple multinomial models with constrained state transitions can be constructed by specifying the probability function of each capture history "by hand" (e.g., see Chapter 3). However, given complex settings like the Delta, an efficient method of constructing the likelihood is needed to move beyond all but the simplest models of the Delta. For example, the model I present in Chapter 3 was comprised of nearly 1000 possible capture histories whereas the model in Chapter 4 had nearly 20,000 possible capture histories. Therefore, I adapted the methods of Fujiwara and Caswell (2002) to develop an efficient method of constructing the multinomial likelihood. Their approach proceeds by 1) defining transition matrices that include a "dead" state, 2) converting the state history vector defining the capture history into indicator matrices for each occasion, and 3) using matrix algebra to

construct the likelihood contribution of each individual from the transition, indicator, and detection matrices.

The example in Figure 2.2 has $S = 3$ states comprised of migration routes A, B, and C, to which I add state "0" representing death or non-detection. To estimate the parameters of the first three transition matrices, $k = 4$ sampling occasions are needed, which includes the initial capture, tagging, and release upstream of the Delta and the three occasions marked by dashed lines in Figure 2.2. At locations where dashed lines intersect river channels, tagged fish are monitored for presence-absence by telemetry stations. Associated with each transition matrix is a diagonal matrix of detection probabilities for each telemetry station. Thus, for the simple population model in Figure 2.2, the transition and detection matrices are:

$$\mathbf{A}_1 = \begin{bmatrix} S_{A1}\Psi_{A1} & 0 & 0 & 0 \\ S_{A1}(1-\Psi_{A1}) & 0 & 0 & 0 \\ 0 & 0 & 0 & 0 \\ 1-S_{A1} & 0 & 0 & 1 \end{bmatrix}, \qquad \mathbf{P}_2 = \begin{bmatrix} P_{A2} & 0 & 0 & 0 \\ 0 & P_{B1} & 0 & 0 \\ 0 & 0 & 0 & 0 \\ 0 & 0 & 0 & 0 \end{bmatrix},$$

$$\mathbf{A}_2 = \begin{bmatrix} S_{A2}\Psi_{A2} & 0 & 0 & 0 \\ 0 & S_{B1} & 0 & 0 \\ S_{A2}(1-\Psi_{A2}) & 0 & 0 & 0 \\ 1-S_{A2} & 1-S_{B1} & 0 & 1 \end{bmatrix}, \qquad \mathbf{P}_3 = \begin{bmatrix} P_{A3} & 0 & 0 & 0 \\ 0 & P_{B2} & 0 & 0 \\ 0 & 0 & P_{C1} & 0 \\ 0 & 0 & 0 & 0 \end{bmatrix}, \qquad (2.3)$$

$$\mathbf{A}_3 = \begin{bmatrix} S_{A3} & S_{B2} & S_{C1} & 0 \\ 0 & 0 & 0 & 0 \\ 0 & 0 & 0 & 0 \\ 1-S_{A3} & 1-S_{B1} & 1-S_{C1} & 1 \end{bmatrix}, \qquad \mathbf{P}_4 = \begin{bmatrix} P_{A4} & 0 & 0 & 0 \\ 0 & 0 & 0 & 0 \\ 0 & 0 & 0 & 0 \\ 0 & 0 & 0 & 0 \end{bmatrix}.$$

The $(S+1)\times(S+1)$ transition matrix $\mathbf{A}_t$ with entries a_{srt} defines the probability of transitioning from migration route r (indexing the columns, $r = 1, 2, \ldots, S+1$) at occasion t to migration route s (indexing the rows, $s = 1, 2, \ldots, S+1$) at occasion $t+1$. Note that I have separated the movement and survival process in this model; S_{hi} is the probability of survival from telemetry station i within route h ($h = \{A, B, C\}$) to the next downstream sampling location, Ψ_{hl} is the probability of entering route h at river junction l conditional on surviving to junction l ($l = \{1, 2\}$), and P_{hi} is the probability of detection at the ith telemetry station within

route h. The fourth row represents transitions to the death state, an absorbing state where $a_{SSt} =$ 1 and the probability of detection in this state is zero (i.e., $P_{0t} = 0$). Adding the death state makes these matrices column stochastic, and because of the assumption of a first-order Markov process, each column forms a conditionally independent multinomial distribution where the probability of transition from state r at occasion t to state s at $t+1$ depends only on state r at occasion t.

Next, define the detection history as the k-dimension vector indicating whether each fish was observed in route h at occasion t ($t = 1, 2, \dots , k$) or was not observed at occasion t. Likewise, let the state history represent the detection history in terms of the each route's index in the transition matrix. Thus, in the current example, route A = state 1, B = 2, C = 3, and 0 = 4. For example, the detection history AA0C can be represented as $\underset{\sim}{s} = \begin{bmatrix} 1 & 1 & 4 & 3 \end{bmatrix}^{\mathrm{T}}$. The next task is to translate the state history into indicator matrices for each occasion that will be used to select the appropriate entries in the transition and detection matrices. Let $\mathbf{E}_{mt}$ be the $(S+1) \times (S+1)$ matrix with a one in sth, sth position if the mth individual is detected in state s at occasion t:

$$\mathbf{E}_{mt} = \mathrm{D}\left(e_{\underset{\sim}{s}_t} \right).$$

Here, $\underset{\sim}{s}_t$ is the tth entry of the state history vector, $e_{\underset{\sim}{s}_t}$ is an $S+1$ length vector consisting of all zeros except for a one in the $\underset{\sim}{s}_t$ th position, and $\mathrm{D}\left(e_{\underset{\sim}{s}_t} \right)$ is the diagonal matrix formed from this vector. The probability of a given detection history can now be formed as a function of the transition ($\mathbf{A}_t$), detection ($\mathbf{P}_t$), and indicator ($\mathbf{E}_{mt}$) matrices:

$$\pi_m = \underset{\sim}{1}^{\mathrm{T}} \left(\prod_{t=1}^{k-1} \mathbf{U}_{t+1} \mathbf{E}_{m,t+1} \mathbf{A}_t \right) \underset{\sim}{1} \tag{2.4}$$

where π_m is the probability of observing the detection history of the mth individual, $\underset{\sim}{1}$ is an $S+1$ vector of ones, $\mathbf{U}_{t+1} = \mathbf{P}_{t+1}$ if the mth fish is detected (i.e., $\underset{\sim}{s}_{t+1} \neq S+1$) at occasion $t+1$, and $\mathbf{U}_{t+1} =$ $\mathbf{I}\text{-}\mathbf{P}_{t+1}$ if the mth fish is not detected (i.e., $\underset{\sim}{s}_{t+1} = S+1$) at occasion $t+1$. When a fish is detected in state s at $t+1$, $\mathbf{P}_{t+1}\mathbf{E}_{m,t+1}\mathbf{A}_t$ returns a matrix with a single entry representing the probability of surviving from t to $t+1$, of moving from state r to state s, and of being detected in state s. In contrast, when fish are not detected, $(\mathbf{I}\text{-}\mathbf{P}_{t+1})\mathbf{E}_{m,t+1}\mathbf{A}_t$ yields a matrix containing all possible

transitions from state *r* at time *t* to state *s* at time *t*+1. Thus, when fish are not detected at various locations in the Delta, Eqn. 2.4 yields the sum of the probability of each possible pathway that the fish could have taken through the Delta, in addition to the possibility that the fish could have died. The complete likelihood of the parameters (θ) given the data set is simply the product of π_m over all fish:

$$L\left(\underset{\sim}{\theta}\right) \propto \prod_{m=1}^{M} \pi_m$$

since π_m is the likelihood contribution of the *m*th fish and fish are assumed independent (assumption A6).

The example shown in Figure 2.2 is extremely simple for illustration purposes, but the strength of constructing the likelihood using the approach above is the ability to design models that can be tailored to the spatial complexity of the Delta's channel network. Structuring the likelihood in this fashion has two major advantages: 1) The complex channel network of the Delta can be broken down into a series of simple transition matrices that describe transitions from one occasion to the next in terms of survival and movement probabilities, and 2) The matrix algebra expressed in Eqn. 2.4 can be easily coded into computer programs to automatically build the likelihood from the detection histories and transition matrices.

2.4.2 Assumptions in the context of acoustic telemetry in the Delta

In this section, I evaluate a number of assumptions in terms of their relevance to monitoring migration of tagged fish in the Delta. Specifically I evaluate assumptions A3 (sampling is instantaneous), A5 (states are known without error), and A10 (movement from state *r* to *s* occurs just before sampling). I focus on these assumptions because they have arisen frequently when either assisting in the design of the telemetry system or when analyzing data where one of these assumptions may have been violated. Furthermore, except for A3, these assumptions apply almost exclusively to the monitoring of river junctions where the goal is to assign fish to migration routes and estimate the proportion of fish using each route. Most of these assumptions can be fulfilled if they are explicitly evaluated when designing and situating the telemetry stations within channels at a river junction. Therefore, I use simple examples to

show how these assumptions can be violated and how telemetry stations can be deployed such that assumptions are fulfilled.

Under assumption A5, the states occupied at each occasion are known without error. In terms of a river junction, this assumption means that there is no error in assigning fish to a migration route. This assumption may be violated in a number of ways. Consider the two examples in Figure 2.3 where the swimming path of a fish is shown relative to the detection zone of each telemetry station. In example A, the detection zone of the left channel extends into the right channel. Therefore, a fish taking the right channel could be detected by both telemetry stations, in which case no error would occur because the fish's migration route would be assigned based on the telemetry station where the fish was last detected. However, if the detection probability of the telemetry station in the right channel is imperfect and this fish were not detected (as indicated by the dashed line in Figure 2.3A), then this fish would be assigned to the left channel even though it had migrated through the right channel. This error could be identified if the fish were later detected at a downstream telemetry station within the right-hand migration route. However, if this fish had died before arriving at the next station then two types of bias will be introduced: 1) the probability of entering the left channel will be positively biased, and 2) the mortality that actually occurred in the right-hand channel will be assigned to the left hand channel, negatively biasing survival for the left hand channel.

This example shows that telemetry stations used to assign fish to a given migration route should have sufficient spatial specificity so as to detect only fish that have actually entered a given migration route. This can be accomplished by measuring the detection zone of each telemetry station and ensuring that only fish that have actually entered a specific migration route can be detected (Figure 2.3B). This approach will ensure that fish are not misassigned to a migration route regardless of whether they are detected at a given telemetry station. Even though the detection zones may be specific to a given channel, the swimming path of a fish may sometimes enter the mouth of one channel, but then swim out of that channel to enter the other channel. Again, the time series of detections would provide evidence of these events, in which case the telemetry stations should be situated some distance downstream of the river junction so as to detect only fish that are committed to a given route. Caution should be exercised; however, because moving the telemetry stations too far
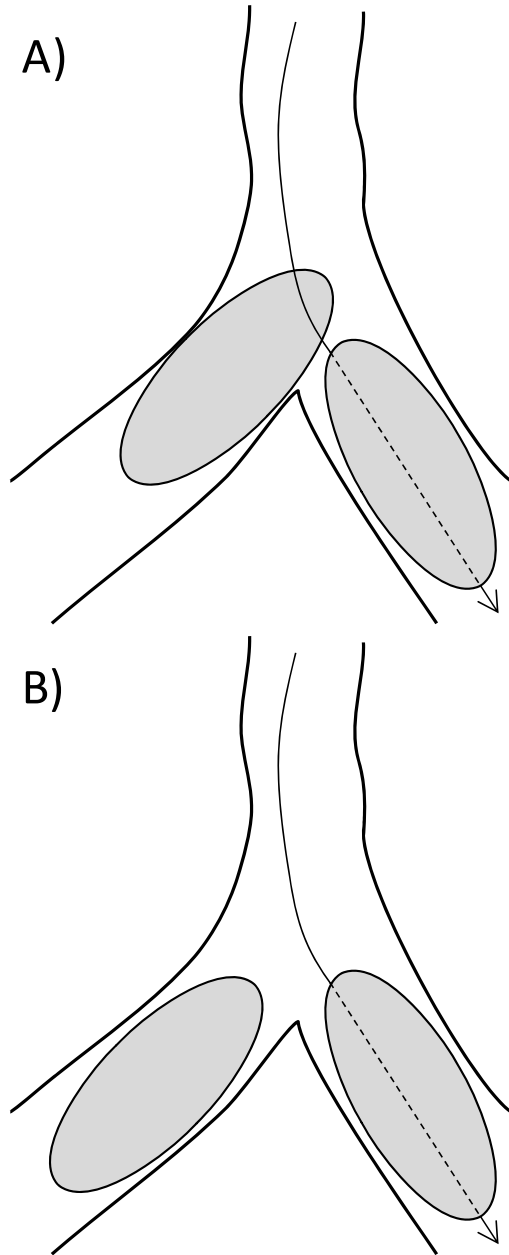
Figure 2.3. Schematic of a river junction under two scenarios with shaded ovals showing the detection zone of telemetry stations. The movement path of a fish is shown as a directed arrow. When the fish's path intersects the detection zone of each station, a solid line indicates the fish is detected and a dashed line indicates a fish is not detected. In scenario A, the fish would be wrongly assigned to the left-hand channel even though it remained in the right channel. In schematic B, no error would occur and mark-recapture models would account for the probability that the fish could have taken either route.

downstream of the river junction could violate assumption A10 (discussed next). Thus, design of the telemetry system involves a tradeoff between A5 and A10.

Although assumption A5 is important to facilitate system design, deployment, and testing of the telemetry system, perfect detection probabilities at a river junction will ensure that assumption A5 is fulfilled. That is, with perfect detection probabilities, the migration route of fish will be known without error regardless of complexity of movement paths through the telemetry stations at a river junction. Detection probabilities at river junctions were nearly perfect in all years at all river junctions in my study, implying that assumption A10 should take precedence over A5. However, planning of mark-recapture studies should occur with the expectation that detection probabilities will be imperfect, in which case consideration of assumption A5 is critical.

To separately estimate S_{hi} and Ψ_{hl} at a river junction, assumption A10 requires that all mortality occurs while in state r and then transition to state s occurs instantaneously just prior to sampling. In the spatial context of the Delta, this assumption means that all mortality should occur first within a reach, movement from one channel to another should occur last, and no mortality should occur between the point of entry to a channel and the location of the telemetry station within each channel. For example, consider a two-branch junction with the choice of placing hydrophones just downstream of a junction (points A_1 and B_1 in Figure 2.4) or some distance downstream of the river junction (points A_2 and B_2 in Figure 2.4). We might want to place the hydrophones at the downstream locations to ensure that fish were committed to a particular channel and not just temporarily "visiting" the entrance to that channel. This rationale is sound, but if mortality occurs downstream of the river junction, then the estimate of Ψ_h could be biased. Figure 2.4 shows the underlying survival probabilities upstream and downstream of the junction. The goal is to obtain unbiased estimates of survival and Ψ_h, the proportion of fish entering each channel.

First, consider the case when telemetry stations are placed at A_1 and B_1 (Figure 2.4). The mark-recapture model is capable of estimating two parameters between the upstream hydrophone (A_0) and the two downstream hydrophones (A_1 and B_1):

$$\hat{\phi}_{A0,B1} = S_{A0}\Psi_B$$

and $\quad \hat{\phi}_{A0,B1} = S_{A0}\left(1 - \Psi_B\right)$.

These estimable parameters follow directly from the definitions of ϕ_i^{rs}, S_i^r, Ψ_i^{rs} in the multistate model described in Section 2.2.1 and Eqns. 2.1 and 2.2. Our primary interest is in estimating the underlying survival and route entrainment probabilities. These underlying parameters can be estimated as:

$$\hat{S}_{total} = \hat{S}_{A0} = \hat{\phi}_{A0,B1} + \hat{\phi}_{A0,A1} \tag{2.5}$$

because $\mathrm{E}\left(S_{A0}\right) = \mathrm{E}\left(\phi_{A0,B1} + \phi_{A0,A1}\right) = S_{A0}\Psi_B + S_{A0}\left(1 - \Psi_B\right) = S_{A0}\left(\Psi_B + 1 - \Psi_B\right) = S_{A0}$

and

$$\hat{\Psi}_B = \frac{\hat{\phi}_{A0,B1}}{\hat{S}_{total}} \tag{2.6}$$

because $\quad \mathrm{E}\left(\hat{\Psi}_B\right) = \mathrm{E}\left(\dfrac{\phi_{A0,B1}}{S_{total}}\right) \doteq \dfrac{S_{A0}\Psi_B}{S_{A0}} = \Psi_B$.

Thus, when telemetry stations are located just downstream of a river junction, all mortality occurs first, movement into each channel occurs last, assumption A10 is fulfilled, and the underlying true parameters of interest can be estimated without bias.
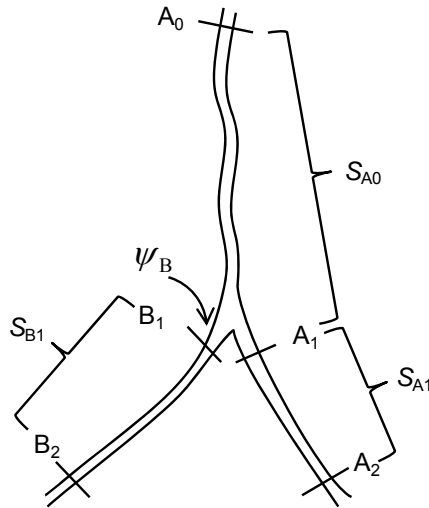
Figure 2.4. Schematic of a river junction showing potential locations of telemetry stations as hash marks across the river channel and brackets showing underlying survival probabilities between hash marks.

Now consider the case when telemetry stations are placed at the furthest downstream locations (A_2 and B_2) and *not* at A_1 and B_1 (Figure 2.4). In this case, the mark-recapture model is still capable of estimating only two parameters between the upstream hydrophone (A_0) and the two downstream hydrophones (A_2 and B_2), and these two parameters are functions of the underlying parameters:

$$E\left(\hat{\phi}_{A0,B2}\right) = S_{A0}\Psi_B S_{B1}$$

and $\quad E\left(\hat{\phi}_{A0,A2}\right) = S_{A0}\left(1-\Psi_B\right)S_{A1}.$

Using Eqns. 2.5 and 2.6, however, results in

$$E\left(\hat{S}_{total}\right) = E\left(\phi_{A0,B2} + \phi_{A0,A2}\right) = S_{A0}\left(\Psi_B S_{B1} + \left(1-\Psi_B\right)S_{A1}\right)$$

and $\quad E\left(\hat{\Psi}_B\right) = E\left(\dfrac{\phi_{A0,B2}}{S_{total}}\right) \doteq \dfrac{S_{A0}\Psi_B S_{B1}}{S_{A0}\left(\Psi_B S_{B1} + \left(1-\Psi_B\right)S_{A1}\right)} = \dfrac{\Psi_B S_{B1}}{\psi_B S_{B1} + (1-\Psi_B)S_{A1}}.$ $\quad$ (2.7)

In this case, $E(S_{total})$ is unbiased and estimates a function of the underlying parameters representing the product of survival through the upstream reach and the weighted average survival through the two downstream channels. In essence, S_{total} estimates the probability of surviving from the upstream telemetry station to either of the downstream stations. However, when mortality occurs between the river junction and the downstream telemetry stations, $E\left(\hat{\Psi}_B\right) \neq \Psi_B$, showing that $\hat{\Psi}_B$ will likely be biased. In fact, the only situation when $\hat{\Psi}_B$ will remain unbiased is when survival is equal in the two reaches downstream of the river junction. Setting $S_{A1} = S_{B1}$, we have

$$E\left(\hat{\Psi}_B\right) = \dfrac{\Psi_B S_{B1}}{\Psi_B S_{B1} + (1-\Psi_B)S_{A1}} = \dfrac{\Psi_B S_{B1}}{\Psi_B S_{B1} + (1-\Psi_B)S_{B1}} = \dfrac{\Psi_B S_{B1}}{S_{B1}(\Psi_B - 1 - \psi_B)} = \dfrac{\Psi_B S_{B1}}{S_{B1}} = \Psi_B.$$

Under any other circumstance, $\hat{\Psi}_B$ will be biased when mortality occurs between the river junction and the next downstream hydrophone. For a concrete example, assume the following true parameter values: $S_{A0} = 0.60$, $S_{A1} = 0.97$, $S_{B1} = 0.60$, and $\Psi_B = 0.50$. With these true values, $\hat{\Psi}_B = 0.382$ and Bias($\hat{\Psi}_B$) = -0.118. The magnitude of bias will depend on the true value of $\hat{\Psi}_B$ and the magnitude of the difference between S_{B1} and S_{A1}. When $S_{B1} < S_{A1}$, $\hat{\Psi}_B$ will be negatively biased; when $S_{B1} > S_{B2}$, $\hat{\Psi}_B$ will be positively biased; and as $S_{B1} - S_{A1}$

approaches zero, bias approaches zero. Bias with respect to $\hat{\Psi}_B$ follows a parabolic function

and approaches zero as $\hat{\Psi}_B$ approaches either zero or one. Thus, absolute bias with respect to

Ψ_B is at its maximum when

$$\frac{\partial}{\partial \Psi_B}\left(\hat{\Psi}_B - \Psi_B\right) = 0,$$

which has the solution

$$\Psi_B = \frac{S_{A2} - \sqrt{S_{B1}S_{A2}}}{S_{A2} - S_{B1}}.$$

With the survival probabilities in the example above, absolute bias in $\hat{\Psi}_B$ will be at its

maximum value when the true value of Ψ_B is 0.56.

These examples show that if the goal is to estimate the proportion of fish entering a

given river channel at a river junction, then telemetry stations must be positioned such that fish

are detected as soon as possible after they enter a given river channel. Situating telemetry

stations using these guidelines will ensure that little mortality occurs after fish enter a given

channel and ensure that estimates of route entrainment probabilities remain unbiased. In cases

when it is impossible to fulfill assumption A10, the best course of action is to estimate the ϕ

parameters and S_{total} (see Eqns. 2.1, 2.2, 2.5, and 2.6). Although the ϕ parameters are difficult

to interpret, being a combination of the underlying survival and movement probabilities, both ϕ

and S_{total} will remain unbiased. I used this approach at a number of locations in the Delta where

fish could take multiple pathways, but telemetry stations were located well downstream of the

channel junctions (see Chapter 4).

How far downstream of a junction is too far (possible violation of assumption A10)

and how close to a junction is too close (possible violation of assumption A5)? Spatial scale

comes into play, as the realized bias in Ψ_{hl} through violation of A10 will depend on the rate of

mortality with respect to distance. For example, if moving a telemetry station 500 m

downstream of a junction avoids errors in assigning fish to migration routes, but survival is

0.98 through that 500 m stretch, then the realized bias will be extremely small. Using my

earlier example from Figure 2.4 and setting $S_{B1} = 0.98$ and $S_{A1} = 1$ results in $E(\Psi_B) = 0.495$

when the true $\Psi_B = 0.5$ (using Eqn. 2.7). In this case, the tradeoff between fulfilling both assumptions A10 and A5 might warrant moving the telemetry station downstream by 500 m. Evaluating these assumptions will often require conceptual exercises such as the examples used here to first hypothesize the underlying parameter values and then calculate the bias. Empirically evaluating such questions by estimating survival over a 500 m reach could be difficult because the detection range of telemetry stations is often on the scale of hundreds of meters. In this case, the sampling occasion (i.e., detection range) cannot be considered instantaneous relative to the interval over which survival is estimated, which leads to violation of assumption A3.

Often researchers may be interested in estimating survival over small distances, or questions may arise about how best to monitor a complex channel junction. The appropriate spatial scale for monitoring can often be answered by considering assumption A3 and comparing the spatial scale of the detection zone to the spatial scale of the survival process. Such a situation occurs at the junction of Sutter Slough and Steamboat Slough with the Sacramento River (Figure 1.2). Sutter Slough branches off the Sacramento River and then 2 km downstream, Steamboat Slough splits off the Sacramento River (Figure 2.5). The question is whether this area should be modeled as 2 two-branch junctions or a single three-branch junction.

During the winter of 2007 (December 2006 – February 2007), telemetry stations were deployed just below each river junction, which allowed me to evaluate the best approach for modeling this junction. Assuming instantaneous sampling of fish passing detection stations (assumption A3), this reach could be modeled as two river junctions with survival to the first junction, entrainment probability for the first junction, survival from the first to the second junction, and then entrainment into the second junction (Figure 2.5). When analyzing the telemetry data, however, I found that detections of fish at the two telemetry stations in the mainstem river (just downstream of each junction) were often separated by only seconds. Since telemetry stations can detect tags for hundreds of meters, the short time difference between detections suggested that the detection range of these telemetry stations nearly overlapped (Figure 2.5). In this case, the spatial scale over which survival is to be estimated is on the same order of the survival process, making it impossible to accurately measure survival

over such a short distance. Therefore, the best course of action was to model this reach as a single three-branch river junction since it was impossible to accurately estimate survival between the first and second river junction due to violation of assumption A3. When the scale of detection is on the order of hundreds of meters, assumption A3 suggests that the minimum spatial scale for estimating survival should be on the order of kilometers.
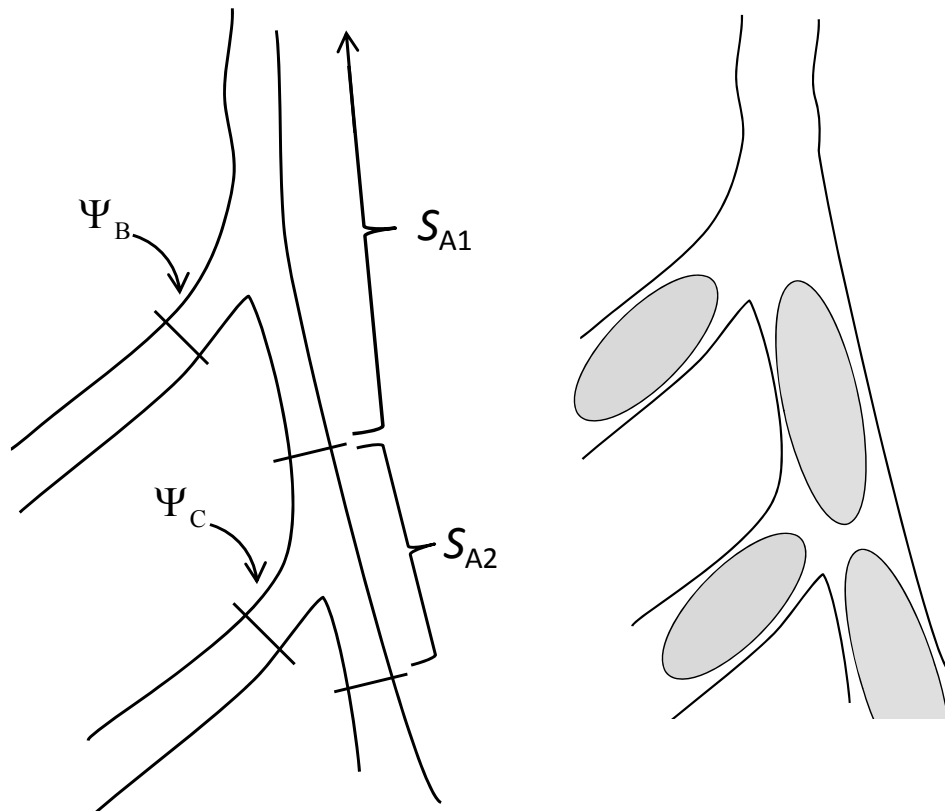
Figure 2.5. Schematic of the river junction at the Sacramento River with Sutter Slough and Steamboat Slough. Considering instantaneous sampling locations, this area could be modeled as 2 two-branch river junctions as shown at left. However, considering the detection zone of each telemetry station (shown as gray ovals on the right), indicates that the spatial scale of detection is on the same order of the survival process, suggesting this area should be modeled as a single three-branch river junction.

2.4.3 Parameter estimability under the constrained multistate model

Under the fully generalized multistate model described in Section 2.3, all parameters are estimable for all sampling periods but the last, but in a constrained model care is needed to ensure that all parameters are estimable. When the number of states sampled at each occasion varies, information contained in the recapture data may not be sufficient to separately estimate detection probabilities for each state and occasion. Inability to estimate detection probabilities typically leads to confounding between detection probabilities and survival and transition parameters, such as Ψ_{hl}. By contrast, ensuring detection probabilities are estimable at each telemetry station will also ensure that biological parameters can be estimated. Thus, understanding factors causing inability to estimate detection probabilities and features of system design that ensure identifiability of detection probabilities is crucial to designing a mark-recapture experiment that is capable of estimating the biological parameters of interest.

My goal in this section is to describe the techniques I used to evaluate identifiability of model parameters. Because the channel network of the Delta is hierarchical in nature, with secondary river junctions and migration routes nested within primary migration routes, ensuring estimability of parameters can be a difficult task. Therefore, I used both simulation and formal analytical techniques to evaluate parameter estimability of all models. Through this process, I identified a number of generalities for minimal requirements of system design that will ensure estimability of detection probabilities, and therefore, estimability of biological parameters. Such generalities will aid researchers during the initial design phase of a telemetry system, but only when a model is built, formally analyzed, and then fit to simulated data can we be absolutely certain that all parameters can be estimated from the mark-recapture data.

To simulate mark-recapture data, I built a mark-recapture model based on a given design of a telemetry system and then hypothesized a true set of parameter values for a given sample size of N fish. The probability of each detection history, π_i, was calculated from the hypothesized parameter values, and then the expected frequency of each capture history is calculated as $N\pi_i$. These expected frequencies were then used as the data set of detection history frequencies, the model was fit to the data to estimate the parameters, and the estimated parameters were compared to the true values. Substantial deviation between true and estimated

values or nonsensical variance estimates provides evidence that a given parameter may not be estimable.

A more formal approach involves the use of computer algebra packages to identify unestimable parameters (Catchpole et al., 2002; Gimenez et al., 2004). This approach can be used to test for both "intrinsic and extrinsic parameter redundancy" (*sensu* Catchpole et al., 2002). Intrinsic redundancy is defined as inability to estimate some parameters due to the fundamental structure of the model and occurs independently of any particular data set. A classic example is the inability to separately estimate survival and capture probability in the last reach (or time-period) of a CJS model (Seber 1982). Intrinsic redundancy is evaluated by forming the matrix of derivatives of $\ln(\pi_i)$ with respect to θ_j (i.e., a matrix of derivatives of the log of each multinomial cell probability with respect to each parameter). The rank of this matrix yields the number of (theoretically) estimable parameters. The model is considered full rank and all parameters estimable if the number of parameters equals the rank of the derivative matrix.

Extrinsic redundancy is defined as the inability to estimate some parameters due to the structure of a particular data set and can occur when data are sparse or when parameter estimates occur on the boundary of zero or one. Extrinsic redundancy is evaluated as described above, except only multinomial cell probabilities with non-zero counts are used in forming the derivative matrix. For example, perfect detection probabilities cause extrinsic redundancy. Consider the maximum likelihood estimator of P_t for the CJS model:

$$\hat{P}_t = \frac{r_t}{r_t + z_t}$$

where r_t is the number of fish detected downstream of occasion t of those detected at occasion t and z_t is the number of fish not detected at t but detected downstream of t (Seber, 1982; Burnham et al., 1987). When all fish detected downstream of a particular station were also detected at that station, $z_t = 0$ and $\hat{P}_t = 1$. However, under these circumstances, the likelihood function has no unique maximum in the neighborhood of $P_t = 1$, causing inability to estimate P_t through iterative maximization of the likelihood. Thus, it is important to identify parameters on a boundary, and then set them to appropriate constant values prior to estimating parameters via optimization routines.

In constrained multistate models for the Delta, the ability to estimate route-specific biological parameters rests on whether route-specific detection probabilities can be estimated at river junctions. When detection probabilities at a river junction cannot be estimated for a particular route, survival and route entrainment probabilities become confounded with detection probability. Understanding minimal requirements for estimating detection probabilities at river junctions is therefore critical to designing studies capable of estimating biological parameters of interest.

If there are H routes at a river junction, then downstream of the river junction, at least H-1 routes must contain a telemetry station specific only to that route. To better understand this requirement, consider the example shown in Figure 2.6 where detection probabilities at the first two river junctions are defined as in Eqn. 2.6. For the first river junction, detection probabilities at both telemetry stations (P_{B1} and P_{A2}) can be estimated because each channel has a telemetry station unique to that channel at the next downstream occasion (i.e., location B_2 for P_{B1} and A_3 or C_1 for P_{A2}). For example, fish not detected at B_1 will be detected at B_2 providing the information needed to estimate P_{B1}. Given that both detection probabilities at the first junction are estimable, the probability of entering each route (Ψ_{A1} and 1-Ψ_{A1}) is also estimable.

However, for the second river junction, detection probabilities for route A and C (P_{A3} and P_{C1}) are confounded because the next downstream telemetry station (A_4) is not unique to either route. Because the final telemetry station at A_4 can detect fish from any route, detection data from A_4 provides no information with which to distinguish whether undetected fish were missed at A_3 or C_1. As a consequence, it is impossible to estimate separate detection probabilities for these sites. To ameliorate this problem, imagine that another telemetry station is located downstream of the second junction within route C. With this design, P_{C1} can now be estimated from the downstream telemetry station unique to route C. Even though the final telemetry station can detect fish from any route, given within-route telemetry stations for routes A and C, information from the final station can be used to estimate detection probability for route A at the second junction (P_{A3}). Thus, only two of the three downstream telemetry stations need be specific to a given river channel.

Interestingly, given the minimal requirements in the example above, all detection probabilities in Figure 2.6 become estimable even though it appears that three detection

probabilities (P_{A3}, P_{B2}, and P_{C2}) must be estimated from a common telemetry station at the final occasion (A4). Given estimable route-specific detection and entrainment probabilities at each river junction, information at both t-1 (upstream) and t+1 (downstream) can be used to estimate detection probabilities at occasion t. For example, fish detected at B1 and then A4 must have passed B2 without being detected (Figure 2.3), allowing P_{B2} to be estimated. This example shows that ability to estimate detection probabilities at the river junctions ensures all subsequent parameters within a route become estimable.
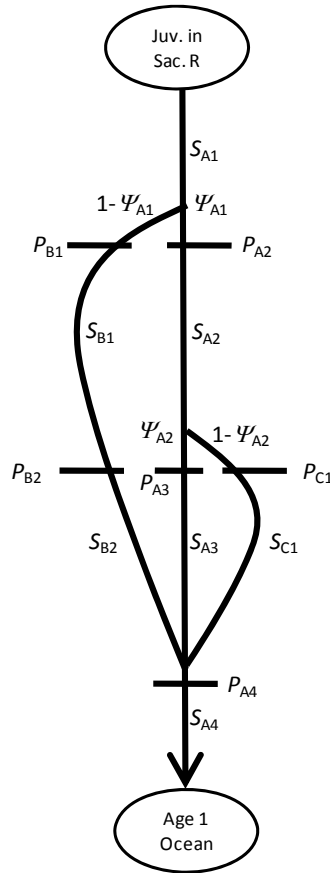
Figure 2.6. Schematic of the Delta with hash marks across the river channels showing locations where telemetry stations would be located according to Figure 2.2 to sample the population of tagged fish as it migrates through the Delta. Subscripts for detection probabilities identify each unique telemetry station within each route.

       In designing models for the Delta, H-1 within-route telemetry stations downstream of a junction for H routes at a junction arose time and again as the minimal requirements for ensuring estimability of all parameters. This generality was confirmed by using the techniques described above to evaluate parameter estimability. Thus, the "H-1" rule of thumb can be used to help design mark-recapture experiments for the Delta. However, because of the hierarchical nature of the Delta's channel network, initial design of the telemetry system must be followed by formal testing of the model to ensure that all parameters are estimable *before* the study is implemented.

Chapter 3

**ESTIMATING SURVIVAL AND MIGRATION ROUTE
PROBABILITIES OF JUVENILE CHINOOK SALMON MIGRATING
THROUGH THE SACRAMENTO-SAN JOAQUIN RIVER DELTA
DURING WINTER 2007**

3.1 Introduction

Many stocks of Chinook salmon (*Oncorhynchus tshawytscha*) in California,
Washington, and Oregon are listed as threatened or endangered under the Endangered Species
Act (Nehlsen et al., 1991; Myers et al., 1998). In the Central Valley of California, the winter,
spring, and fall/late fall runs of Chinook salmon are federally listed as endangered, threatened,
and a "species of concern," respectively (NMFS, 1997). Recently, due to below-target returns
of fall Chinook salmon to the Sacramento River, the National Marine Fisheries Service
declared a Federal Disaster and closed the 2008 salmon fishery along the West Coast (NOAA,
2008). Understanding factors affecting survival of salmon is therefore critical to devising
effective recovery strategies for these populations.

An important stage in the life history of Chinook salmon is the period of migration
from natal tributaries to the ocean, when juvenile salmon in the Sacramento River may suffer
mortality from a host of anthropogenic and natural factors (Brandes and McLain, 2001; Baker
and Morhardt, 2001; Williams, 2006). Juvenile Chinook salmon emigrating from the
Sacramento River must pass through the Sacramento-San Joaquin River Delta (hereafter, "the
Delta"), a complex network of natural and man-made river channels (Nichols et al., 1986).
Juvenile salmon may migrate through a number of routes on their journey to the ocean. For
example, they may migrate within the mainstem Sacramento River leading directly into San
Francisco Bay (see Route A in Figure 3.1). However, they may also migrate through longer
secondary routes such as the interior Delta, the network of channels to the south of the
mainstem Sacramento River (see Routes C and D in Figure 3.1).
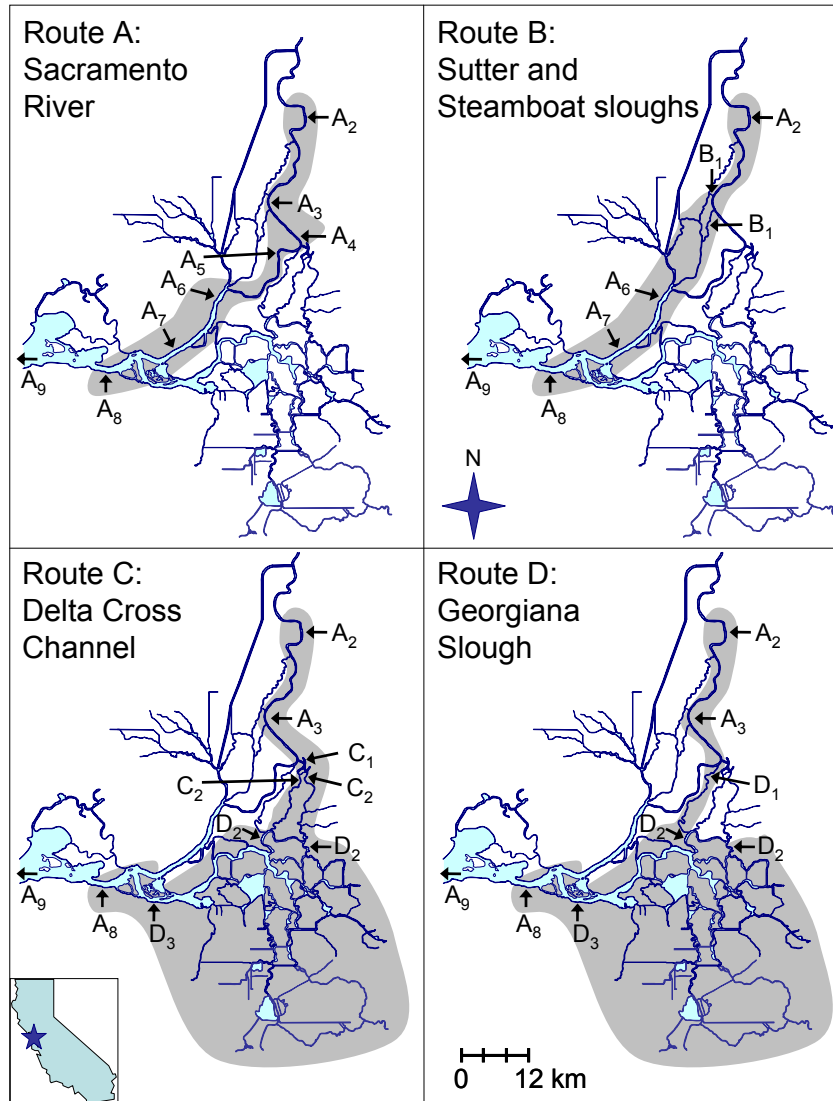
Figure 3.1. Maps of the Sacramento–San Joaquin River Delta with shaded regions showing river reaches that comprise survival through the Delta for four different migration routes. Arrows show the location of telemetry stations specific to each route. The Delta extends from station A_2 at Freeport to station A_8 at Chipps Island. The first river junction occurs where Sutter and Steamboat sloughs (B_1) diverge from the Sacramento River at station A_3. The second junction occurs where the Delta Cross Channel (C_1) and Georgiana Slough (D_1) diverge from the Sacramento River at station A_4. For routes C and D, the interior Delta is the large shaded region to the south of station D_2. Telemetry stations with the same label (B_1, C_2, and D_2) were pooled as one station in the mark-recapture model. Station A_3 was not operational during the first release in December, 2006. Station A_9 pools all telemetry stations in San Francisco Bay downstream of A_8. The release site (rkm 92) was 19 river kilometers upriver of station A_2 (rkm 73).

Both human actions and natural processes affect the magnitude and distribution of Sacramento River flow among the channel network of the Delta. Inflow into the Delta from the Sacramento River is largely controlled by upstream releases of water from storage reservoirs. Within the Delta, water distribution is affected by two water pumping projects in the southern Delta (the State Water Project and Central Valley Project). These projects pump water from the Delta for agricultural and municipal uses and can export up to 50% of the total inflow (Nichols et al., 1986). Associated with the water pumping projects is the Delta Cross Channel, a man-made channel that diverts river flow from the Sacramento River into the interior Delta (see C1 in Route C, Figure 3.1). In addition to these human influences on water flow through the Delta, natural processes include seasonal rainfall and snowmelt events in the winter and spring, respectively, and tidal cycles that vary on diel and bi-weekly time scales.

As juvenile salmon migrate among the complex channel network of the Delta, they are subject to channel-specific processes that affect their rate of migration, vulnerability to predation, feeding success, growth rates, and ultimately, survival. For example, growth of juvenile salmon in the Yolo Bypass, a seasonally inundated flood plain, was significantly greater than in the mainstem Sacramento River (Sommer et al., 2001). In contrast, juvenile salmon entering the interior Delta must traverse longer migration routes and are exposed to entrainment at the water pumping projects, both of which may decrease survival of fish using this migratory pathway (Brandes and McLain, 2001; Newman and Rice, 2002; Newman, 2003; Kimmerer, 2008; Newman and Brandes; 2010). These examples show that population-level survival rates of juvenile salmon migrating through the Delta will be driven by 1) the survival rates arising from the biotic and abiotic processes unique to each migration route, and 2) the proportion of the population using each migration route. In turn, natural and human-imposed variation in discharge and water distribution will affect population dispersal and survival rates within each channel, driving population-level survival through the Delta.

Currently, there is limited understanding of how water management actions in the Delta affect population distribution and route-specific survival of juvenile salmon. Evidence suggests that survival of fish migrating through the interior Delta decreases with increasing water exports (Brandes and McLain, 2001; Newman, 2003). Water exports could decrease survival by increasing migration times through the interior Delta, by increasing encounter rates

with predators, and by direct entrainment of fish at pumping facilities located in the interior Delta. Operation of the Delta Cross Channel likely affects the proportion of the population entering the interior Delta. To date, the proportion of fish migrating through the interior Delta has not been estimated, yet such estimates are critical to understand the relative effect of water management actions on the population as a whole (Newman and Brandes, 2010). Thus, currently lacking is a population-level approach that quantifies dispersal of the population among migration routes and measures survival within these routes to better understand the influence of management actions on population-level survival.

In this chapter, I develop a mark-recapture model for the Delta to explicitly estimate the probability of migrating through each of four migration routes and the probability of surviving through each route. Next, I quantify population-level survival through the Delta as a function of the route-specific migration and survival probabilities. I then apply this model to the first available acoustic telemetry data of juvenile late-fall run Chinook salmon collected during the winter of 2006/2007 (hereafter, "2007"). Acoustic telemetry is a passive "capture" technique enabling individual fish to be detected repeatedly by multiple telemetry stations as they migrate through the Delta. Given estimates of route-specific survival and movement through the Delta from the acoustic telemetry data, I then examine how each of these components interacted to affect survival of the population migrating through the Delta.

3.2 Methods

3.2.1 Telemetry system

Telemetry stations were deployed in the Delta to monitor movement of tagged fish among four major migration routes through the Delta (Figure 3.1): the mainstem Sacramento River (Route A); Sutter and Steamboat sloughs (Route B); the interior Delta via the Delta Cross Channel (Route C); and the interior Delta via Georgiana Slough (Route D). Although there are numerous possible migration pathways, I focused on these routes because management actions likely have the largest influence on movement and survival among these routes. For example, fish may enter the interior Delta from the Sacramento River through either the Delta Cross Channel or Georgiana Slough where they subsequently become

vulnerable to migration delays and entrainment at the water pumping projects. Steamboat and Sutter sloughs may be an important migration route because fish using this route bypass the Delta Cross Channel and Georgiana Slough (Figure 3.1). Thus, fish migrating through Steamboat and Sutter Slough are unable to enter the interior Delta through the Delta Cross Channel or Georgiana Slough.

Telemetry stations were labeled hierarchically to reflect the branching nature of channels at river junctions and their subsequent downstream convergence at the confluence of river channels (Figure 3.1). Each telemetry station consisted of single or multiple tag-detecting monitors (Vemco Ltd., Model VR2), depending on the number of monitors needed to maximize detection probabilities at each station. Since the Sacramento River is the primary migration route, the ith telemetry station within this route was denoted as A_i from the release site (A_1 located at river kilometer (rkm) 92) to the last telemetry station in the Delta at Chipps Island (A_8 at rkm -9; by convention, rkm 0 is defined at the southern tip of Sherman Island which is 9 river kilometers upstream of station A_8; see Figure 1.2). Migrating juvenile salmon first arrive at Sutter and Steamboat sloughs (B_1, rkm 43 and rkm 38), which diverge from the Sacramento River at the first river junction and converge again with the Sacramento River upstream of A_6 (rkm 19). Fish remaining in the Sacramento River then pass the Delta Cross Channel and Georgiana Slough at the second river junction. For the Delta Cross Channel, stations were labeled with C_i beginning where the Delta Cross Channel diverges from the Sacramento River at C_1 (rkm 60) and ending when these river channels converge with the interior Delta at D_2 (rkm 40 and rkm 47). Telemetry stations within Georgiana Slough and the interior Delta were labeled as D_i where Georgiana Slough branches off the mainstem Sacramento River (D_1, rkm 58) until convergence of the interior Delta with the Sacramento River at D_3 (rkm 5). Following this hierarchy, Routes A, B, C, and D contained 8, 1, 2, and 3 telemetry stations, respectively, for a total of 14 telemetry stations within the Delta. Parameter subscripting and coding of detection histories followed this hierarchical structure (see *Model Development* section below). With this configuration of telemetry stations, survival in the final reach is confounded with detection probability at the last telemetry station (Skalski et al., 2001). Therefore, to estimate survival to the terminus of the Delta and detection probability at the last station in the Delta (A_8), I formed one additional telemetry station by pooling

detections from numerous tag detecting monitors downstream of A_8 in San Francisco Bay. Most of these detections occurred at three primary stations that provided nearly complete cross-sectional coverage of San Francisco Bay at bridges located at rkm -37, rkm -64, and rkm -77, but single-monitor stations at other locations were also included.

3.2.2 Fish tagging and release

Juvenile late fall Chinook salmon were obtained from and surgically tagged at the Coleman National Fish Hatchery (rkm 431). For the first release in December, a 1.44-g tag (Vemco Ltd., Model V7-1L-R64K, 40-d expected battery life) was used and for the second release in January a 1.58-g tag was used (Vemco Ltd., Model V7-2L-R64K-2, 95-d expected battery life). Except for a minimum size criterion of 140 mm fork length, fish were randomly selected for tagging resulting in a mean fork length of 164.6 mm (SD = 10.9) and mean weight of 53.5 g (SD = 12.6). The tag weight represented 2.7% of the mean fish weight (range = 1.3%–3.8%) for the December release and 3.0% (range = 1.9%–4.9%) for the January release. Although recommendations for maximum tag-to-body weight ratios have varied (Jepsen et al., 2004), a 5% maximum tag-to-body weight ratio was followed based on the guidance of Adams et al. (1998a). Fish were fasted for 24 h prior to surgery to ensure they were in a post-absorptive state. To surgically implant transmitters, fish were anaesthetized in 90 mg/l tricaine methanesulfonate (MS-222) until they lost equilibrium. A fish was then placed in a light anesthetic bath (30 mg/l MS-222), ventral side up, and a small incision was made in the abdomen between the pectoral fins and the pelvic girdle. The transmitter was inserted into the peritoneal cavity, and the incision was closed with two interrupted sutures (4-0 nylon sutures with FS-2 cutting needle). Tagged fish were then returned to raceways and were allowed to recover for seven days prior to release.

Next, fish were transported to release sites in the Sacramento River near Sacramento, CA (rkm 92). Fish were then transferred to net pens (3-m square holding nets supported by pontoons) at the release site and held for 24 h in the Sacramento River prior to release to allow recovery from the transportation process. Fish were transported and held in four separate groups, and each group was released at roughly 6-h intervals over a 24-h period on 5 December 2006 (release 1) and again on 17 January 2007 (release 2). Each release was carried out over a

24-h period to distribute tagged fish over the tidal and diel cycle. The total sample size consisted of 64 acoustically tagged fish in December, 2006 and 80 acoustically tagged fish in January, 2007.

3.2.3 Model development

I developed a mark-recapture model that estimates three sets of parameters: detection (P_{hi}), survival (S_{hi}), and route entrainment probabilities (Ψ_{hl}). Detection probabilities (P_{hi}) estimate the probability of detecting a transmitter given a fish is alive and the transmitter operational at telemetry station i within route h (h = A, B, C, D; Figure 3.2). Survival probabilities (S_{hi}) estimate the probability of surviving from telemetry station i to i+1 within route h, conditional on surviving to station i (Figure 3.2). Route entrainment probabilities (Ψ_{hl}) estimate the probability of a fish entering route h at junction l (l = 1, 2), conditional on fish surviving to junction l (Figure 3.2). In addition, the parameter ω_{open} estimates the probability of fish passing junction 2 when the Delta Cross Channel was open. This model can be classified as a generalization of the standard Cormack-Jolly-Seber (CJS) mark-recapture model (Cormack, 1964; Jolly, 1965; Seber, 1965) and a special case of a multistate mark-recapture model where the route entrainment probabilities represent a constrained matrix of state transition probabilities (Lebreton and Pradel, 2002; Williams et al., 2002). Statistical assumptions associated with a model of this structure are detailed in Chapter 2.

The first river junction was modeled as a two-branch junction where detections at the entrance to either Sutter or Steamboat Slough (station B_1; Figure 3.1) were pooled to estimate a single route entrainment probability. Thus the parameter Ψ_{B1} estimates the probability of being entrained into either Sutter or Steamboat Slough at the first river junction (Figure 3.2). Conversely, $1 - \Psi_{B1} = \Psi_{A1}$ is the probability of remaining in the Sacramento River at the first junction (Figure 3.2). The second junction was modeled as a three-branch junction where $\Psi_{A2,}$ $\Psi_{C2,}$ and $1 - \Psi_{A2} - \Psi_{C2} = \Psi_{D2}$ estimate the probabilities of remaining in the Sacramento River (Route A), being entrained into the Delta Cross Channel (Route C), and entering Georgiana Slough (Route D) at junction 2 (Figure 3.2). Because $\Psi_{C2} = 0$ when the Delta Cross Channel is
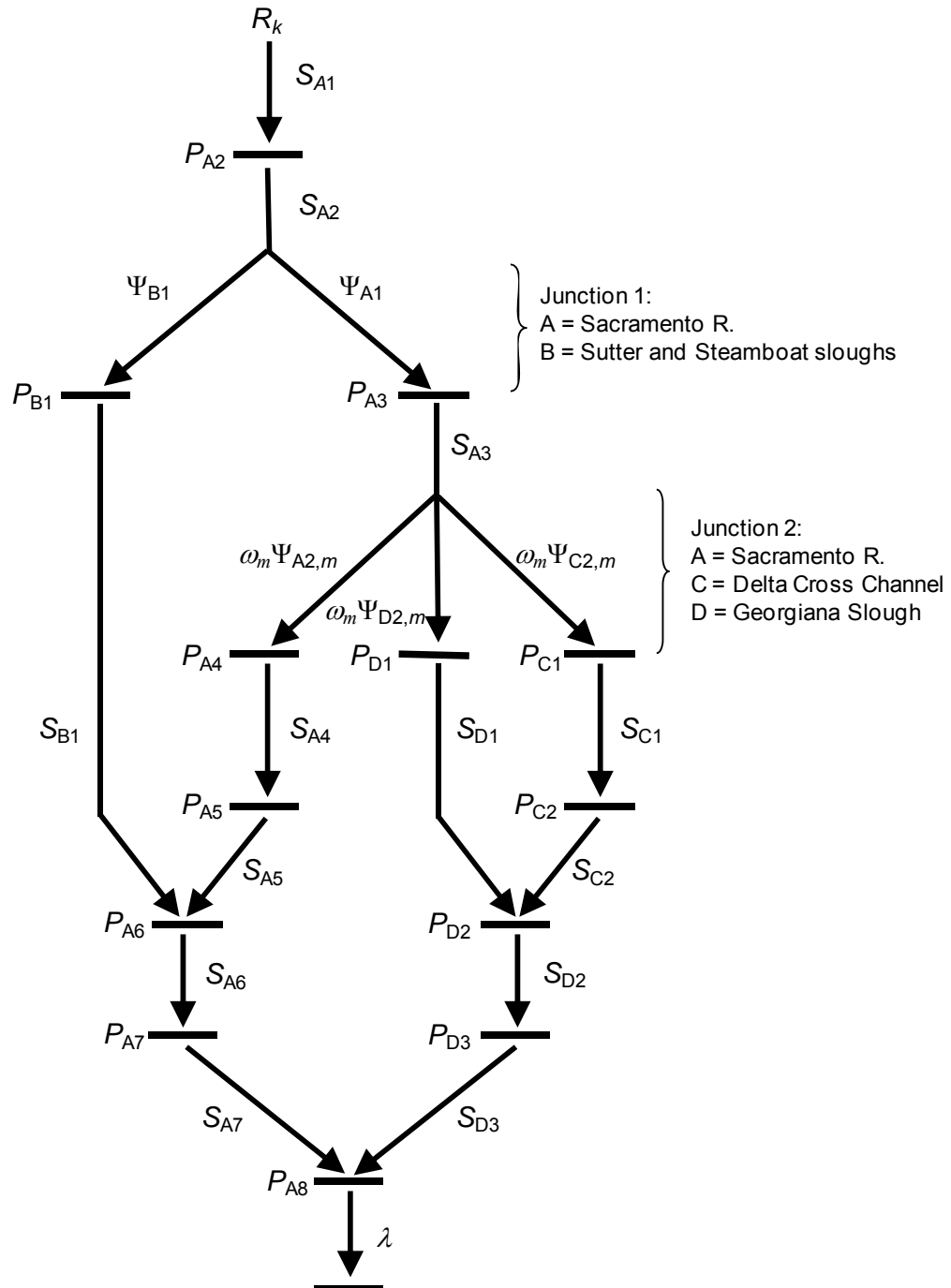
Figure 3.2. Schematic of the mark-recapture model used to estimate survival (S_{hi}), detection (P_{hi}), and route entrainment (Ψ_{hl}) probabilities of juvenile late-fall Chinook salmon migrating through the Sacramento–San Joaquin River Delta for releases made on 5 December 2006 and 17 January 2007.

closed, route entrainment probabilities at junction 2 depend on the position of the Delta Cross Channel gate when fish migrate past this location (Figure 3.2).

While some survival probabilities estimate survival within a given river channel from telemetry station i to $i+1$ (e.g., S_{A2}), others represent survival of fish migrating through a number of possible migration pathways. For example, fish entering Sutter or Steamboat Slough at B_1 may migrate through a northern or a southern channel (Figure 3.1). The parameter S_{B1}, estimating survival between sites B_1 and A_6, therefore represents an average of survival in each channel weighted by the proportion of fish using each channel. Note, however, that to separately estimate the underlying components of S_{B1}, additional telemetry stations would need to be placed at key channel junctions within this route. Similar survival probabilities include S_{C2} and S_{D2}, the latter of which encompasses much of the interior Delta (Figure 3.1).

With this model structure, the full model contains 33 parameters: 13 detection probabilities, 13 survival probabilities, 5 route entrainment probabilities, and ω_{open} (Figure 3.2). The final parameter, λ, estimates the joint probabilities of surviving downstream of A_8 and being detected at telemetry stations comprising A_9. Thus, λ has little biological meaning but must be included in the model in order to estimate survival to the terminus of the Delta at A_8.

3.2.4 Parameter estimation

Prior to parameter estimation, the records of tag-detections were processed to eliminate false positive detections using methods based on Skalski et al. (2002) and Pincock (2008). False positive detections of acoustic tags occur primarily when two or more tags are simultaneously present within the range of a given monitor, and simultaneous tag transmissions "collide" to produce a valid tag code that is not actually present at the monitor (Pincock 2008). My first criterion considered detections as valid if a minimum of two consecutive detections occurred within a 30-min period at a given telemetry station. Although this criterion minimizes the probability of accepting a false positive detection, Pincock (2008) showed that a pair of false positive detections with a time interval <30 min occurred on average once every 30 d when simulating ten tags simultaneously present at a monitor. Thus, my second criterion

considered records with two detections at a given location as valid only if these detections were consistent with the spatiotemporal history of a tagged fish moving through the system of telemetry stations (Skalski et al., 2002). The detection records of five tagged fish suggested they had been consumed by piscivorous predators as was evidenced by their directed upstream movement for long distance and against the flow. We truncated the detection record of these fish to the last known location of the live tagged fish. All other detections were considered to have been live juvenile salmon. In the lower Sacramento River (sites A_6–A_8), tag detection and discharge data showed that juvenile salmon were often advected upstream on the flood tides and downstream on the ebb tides. In these cases, we used the final downstream series of detections in forming the detection history.

I used maximum likelihood techniques to estimate parameters based on a multinomial probability model that categorized each fish into a mutually exclusive and exhaustive detection history. Detection histories compactly describe the migration and detection process of fish moving through the network of telemetry stations. For example, the history 1A0AAAAAA indicates a fish was released ("1"), detected in the Sacramento River at A_2 ("A"), not detected in the Sacramento River at A_3 ("0"), and then subsequently detected at every other telemetry station in the Sacramento River ("AAAAAA"). This model has 912 possible detection histories, but with release sample sizes of $R_1 = 64$ and $R_2 = 80$ tagged fish, not all histories are observed.

Each detection history represents one of the 912 cells of a multinomial distribution where the probability of each cell is defined as a function of the detection, survival, and route entrainment probabilities. For example, the probability of history 1A0AAAAAA can be expressed as:

$$S_{A1}P_{A2}S_{A2}\Psi_{A1} (1\text{-}P_{A3})S_{A3}\omega_{open}\Psi_{A2,open}P_{A4}S_{A4}P_{A5}S_{A5}P_{A6}S_{A6}P_{A7}S_{A7}P_{A8}\lambda$$

In words, the probability of this detection history is the joint probability of surviving the first reach (S_{A1}) and being detected at A_2 (P_{A2}); surviving the second reach (S_{A2}), remaining in the Sacramento River at junction 1 (Ψ_{A1}), and not being detected at A_3 ($1-P_{A3}$); and surviving the third reach (S_{A3}), remaining in the Sacramento River at junction 2 ($\Psi_{A2,open}$) when the Delta Cross Channel was open (ω_{open}), and surviving and being detected at all remaining stations in the Sacramento River (Figure 3.2).

Given the cell probabilities, the maximum likelihood estimates are found by maximizing the likelihood function of a multinomial distribution with respect to the parameters:

$$L\left(\underset{\sim}{\theta}\,|\,R_k,n_j\right) \propto \prod_{j=1}^{912} \pi_j^{n_j}$$

where R_k is the number of fish released in the kth release group ($k = 1, 2$), n_j is the number of fish with the jth detection history, and π_j is the probability of the jth detection history expressed as a function of the parameters ($\underset{\sim}{\theta}$). The likelihood was numerically maximized with respect to the parameters by using algorithms provided in the software programs R (R Development Core Team, 2008) and USER (Lady et al., 2008). The variance-covariance matrix was estimated as the inverse of the Hessian matrix. I used the delta method (Seber, 1982) to estimate the variance of parameters that are functions of the maximum likelihood estimates (e.g., $\Psi_{D2} = 1 - \Psi_{A2} - \Psi_{C2}$). Uncertainty in parameter estimates is presented both as standard errors and 95% profile likelihood confidence intervals.

Parameters were estimated separately for each release, but the model for each release was reduced from the full model because not all parameters could be estimated from the tag detection data. For the first release in December, $P_{A3} = 0$ because station A_3 was not operational, rendering limited ability to uniquely estimate the parameters S_{A2}, Ψ_{B1}, and S_{A3}. However, S_{A2} and Ψ_{B1} can be estimated under the assumption that $S_{A2} = S_{A3}$, which was supported by the similarity of S_{A2} and S_{A3} measured during the second release (for R_2: $\hat{S}_{A2} = 0.959$, $\widehat{SE} = 0.024$; $\hat{S}_{A3} = 0.976$, $\widehat{SE} = 0.025$). The Delta Cross Channel gate was closed for the second release, so ω_{open} and Ψ_{C2} were set to zero, which eliminated P_{C1}, S_{C1}, P_{C2}, and S_{C2} from the model. For both releases, a number of detection probabilities were set to 1 because of perfect detection data. Last, due to low detection frequencies in the interior Delta, the parameters S_{D1} and S_{D2} could not be estimated for the first release, but the product $S_{D1}S_{D2}$ was estimable as a single parameter. Likewise, for the second release only the product $S_{D1}S_{D2}S_{D3}$ was estimable as a single parameter.

3.2.5 Survival through the Delta

This mark-recapture model estimates the individual components that comprise survival of the population migrating through the Delta, defined as survival of tagged fish from the entrance to the Delta at station A_2 (Freeport, rkm 73) to the exit of the Delta at station A_8 (Chipps Island, rkm -9). Population-level survival through the Delta was estimated from the individual components as:

$$S_{\text{Delta}} = \sum_{h=A}^{D} \Psi_h S_h \qquad (3.1)$$

where S_h is the probability of surviving the Delta given the specific migration route taken through the Delta, and Ψ_h is the probability of migrating through the Delta via one of four migration routes (A = Sacramento River, B = Sutter and Steamboat sloughs, C = Delta Cross Channel, D = Georgiana Slough). Thus, population survival through the Delta is a weighted average of the route-specific survival probabilities with weights equal to the fraction of fish migrating through each route.

Migration route probabilities are a function of the route entrainment probabilities at each of the two river junctions:

$$\Psi_A = \Psi_{A1}\Psi_{A2} \qquad (3.2)$$

$$\Psi_B = \Psi_{B1} \qquad (3.3)$$

$$\Psi_C = \Psi_{A1}\Psi_{C2} \qquad (3.4)$$

$$\Psi_D = \Psi_{A1}\Psi_{D2} \qquad (3.5)$$

For instance, consider a fish that migrates through the Delta via the Delta Cross Channel (Route C). To enter the Delta Cross Channel, this fish first remains in the Sacramento River at junction 1 with probability Ψ_{A1}, after which it enters the Delta Cross Channel at the second river junction with probability Ψ_{C2}. Thus, the probability of a fish migrating through the Delta via the Delta Cross Channel (Ψ_C) is the product of these route entrainment probabilities, $\Psi_{A1}\Psi_{C2}$. However, for release 1, when the Delta Cross Channel was both open and closed, $\Psi_{h2} = \omega_{\text{open}}\Psi_{h2,\text{open}} + (1- \omega_{\text{open}}) \Psi_{h2,\text{closed}}$.

Survival through the Delta for a given migration route (S_h) is the product of the reach-specific survival probabilities that trace each migration path through the Delta between points A_2 and A_8 (Figure 3.1, Figure 3.2):

$$S_A = S_{A2}S_{A3}S_{A4}S_{A5}S_{A6}S_{A7} \tag{3.6}$$

$$S_B = S_{A2}S_{B1}S_{A6}S_{A7} \tag{3.7}$$

$$S_C = S_{A2}S_{A3}S_{C1}S_{C2}S_{D2}S_{D3} \tag{3.8}$$

$$S_D = S_{A2}S_{A3}S_{D1}S_{D2}S_{D3} \tag{3.9}$$

I also compared our estimates of S_{Delta} described above to estimates produced by a standard three-station CJS model. We included telemetry stations A_2, A_8, and A_9 in this model. Here, S_{Delta} is estimated directly from the model as the probability of surviving from station A_2 to A_8. I compared the two approaches to ensure they produced similar estimates and to examine the standard errors produced under each approach. Given that the CJS model contained many fewer parameters (4 for R_1 and 5 for R_2), I suspected that the CJS model might yield more precise estimates of S_{Delta}.

3.3 Results

3.3.1 River conditions and migration timing

For the first release in December, tagged fish passed the two river junctions when discharge of the Sacramento River at Freeport (US Geological Survey gauge 11447650 near station A_2; Figure 3.1) increased from 12,900 ft^3/s to 24,100 ft^3/s (Figure 3.3). The Delta Cross Channel was open when most of these fish passed the second river junction (Figure 3.3). However, the Delta Cross Channel closed at 1000 hours on 15 December 2006 and remained closed for the balance of the study (Figure 3.3). River discharge receded to about 12,000 ft^3/s when fish from the December release were migrating through the lower reaches of the Delta (Figure 3.3). In contrast to December, river discharge for the January release was low and stable during much of the migration period (Figure 3.3). Daily discharge of the Sacramento River remained near 12,000 ft^3/s until 9 February, after which discharge increased to 39,000

ft^3/s. However, this increase in flow occurred after most fish had passed through the lower reaches of the Delta (Figure 3.3). Water exports at the Delta pumping stations were stable within each migration period and averaged 10,789 ft^3/s for the December migration period and 6,823 ft^3/s for the January (Figure 3.3).
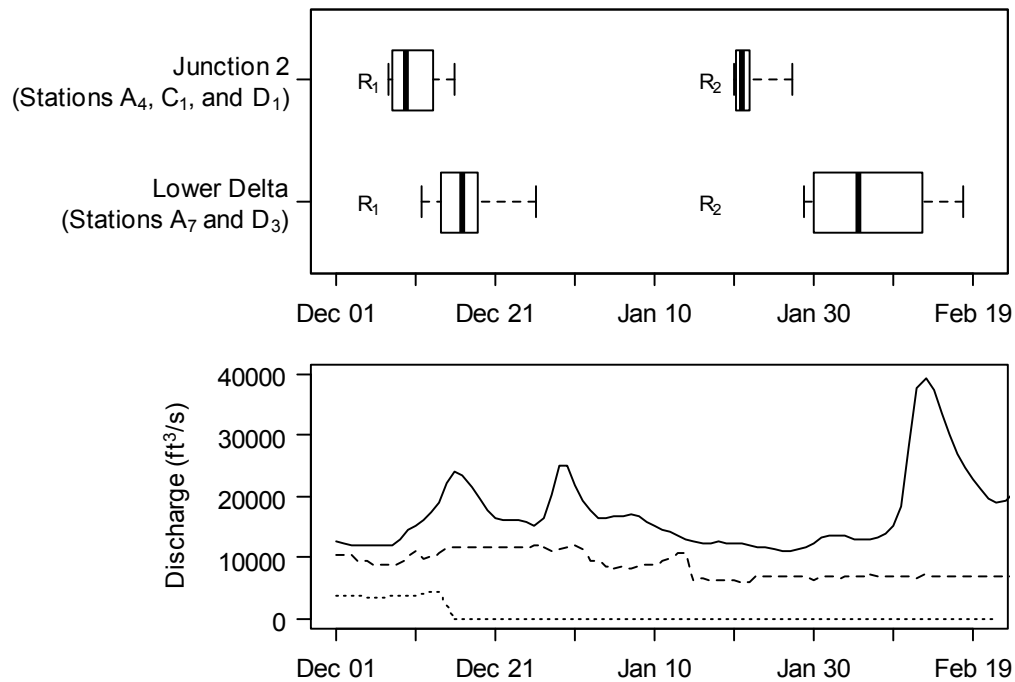
Figure 3.3. River discharge, water exports, and Delta Cross Channel discharge during the migration period of tagged juvenile Chinook salmon migrating through the Sacramento–San Joaquin River Delta during winter 2006/2007. Box plots show the distribution of arrival dates at Junction 2 on the Sacramento River and near the exit of the Delta. The two release dates are shown as R_1 = 5 December 2006 for a release size of 64 tagged fish and R_2 = 17 January 2007 for a release size of 80 fish. Whiskers represent the 10th and 90th percentiles, the box encompasses the 25th to 75th percentiles, and the line bisecting the box is the median arrival date. River discharge (solid line) is tidally filtered, daily discharge of the Sacramento River at Freeport (near telemetry station A_2), Delta Cross Channel discharge (dotted line) is the tidally filtered daily discharge, and water exports (dashed line) are the total daily discharge of water exported from the Delta at the pumping projects.

Coincident with lower river discharge, fish released in January took substantially longer to migrate through the Delta and exhibited higher variation in travel times relative to fish released in December (Figure 3.3). Among routes, travel times for the December release

from the release point to the lower Delta (stations A_7 and D_3) were quickest for fish migrating through Sutter and Steamboat sloughs (median = 7 d, interquartile range (25th – 75th percentile) = 6.1 – 11.7 d, n = 5) followed by the Sacramento River (median = 10.7 d, interquartile range = 9.3 – 12.5 d, n = 9) and the interior Delta via the Delta Cross Channel and Georgiana Slough (median = 13.8 d, interquartile range = 13.4 – 19.1 d, n = 5). For the January release, travel times were similar for fish migrating through the Sacramento River (median = 18.1 d, interquartile range = 13.2 – 23.9 d, n = 19) and Sutter and Steamboat Sloughs (median = 17.8 d, interquartile range = 12.7 – 27.3 d, n = 17). Travel times through the interior Delta were measured for only one fish in the January release, which took 33.9 d to travel from release to the lower Delta.

3.3.2 Migration routing

As juvenile salmon migrated past the first river junction, a large proportion of both release groups left the Sacramento River and migrated through Sutter and Steamboat sloughs (for R_1: $\hat{\Psi}_{B1}$ = 0.296; for R_2: $\hat{\Psi}_{B1}$ = 0.414). For the December release, most fish remaining in Sacramento River encountered the second river junction when the Delta Cross Channel was open ($\hat{\omega}_{open}$ = 0.861, $\widehat{SE}$ = 0.058), and 39% percent of these fish were entrained into the Delta Cross Channel ($\hat{\Psi}_{C2,open}$ = 0.387, $\widehat{SE}$ = 0.087). Regardless of release group or position of the Delta Cross Channel gate, similar fractions of fish passing junction 2 were entrained into Georgiana Slough (for R_1: $\hat{\Psi}_{D2,open}$ = 0.161, $\widehat{SE}$ = 0.066; $\hat{\Psi}_{D2,closed}$ = 0.200, $\widehat{SE}$ = 0.179; for R_2: $\hat{\Psi}_{D2,closed}$ = 0.150, $\widehat{SE}$ = 0.056). The remaining 45% of fish passing junction 2 when the Delta Cross Channel was open stayed in the Sacramento River ($\hat{\Psi}_{A2,open}$ = 0.452, $\widehat{SE}$ = 0.089), whereas nearly twice that fraction remained in Sacramento River when the Delta Cross Channel was closed (for R_1: $\hat{\Psi}_{A2,closed}$ = 0.800, $\widehat{SE}$ = 0.179; for R_2: $\hat{\Psi}_{A2,closed}$ = 0.850, $\widehat{SE}$ = 0.056).

A substantial proportion of fish migrating past junction 2 entered the interior Delta through the Delta Cross Channel and Georgiana Slough. However, a lower proportion of the

population entered the interior Delta because some fish bypassed the second river junction by migrating through Sutter and Steamboat sloughs (Figure 3.1). Accounting for population distribution among all routes, 23.5% were entrained into the Delta Cross Channel ($\hat{\Psi}_C$), 11.7% entered Georgiana Slough ($\hat{\Psi}_D$), and 35.2% migrated within the Sacramento River ($\hat{\Psi}_A$) for the December release when the Delta Cross Channel was open during much of the migration period (Table 3.1). In contrast, 8.8% migrated through Georgiana Slough and 49.8% remained in the Sacramento River in January when the Delta Cross Channel was closed (Table 3.1). Because Sutter and Steamboat sloughs rejoin the Sacramento River upstream of telemetry station A_6, much of this migration route through the Delta (Route B) consists of the mainstem Sacramento River (Figure 3.1). Thus for the December release, 64.8% of fish took migration routes largely consisting of the Sacramento River ($\hat{\Psi}_A + \hat{\Psi}_B$) and 35.2% were entrained into the interior Delta via the Delta Cross Channel and Georgiana Slough ($\hat{\Psi}_C + \hat{\Psi}_D$; Table 3.1). In contrast, only 8.8% percent of fish were entrained into the interior Delta through Georgiana Slough in January when the Delta Cross Channel was closed, with the remaining 91.2% migrating mostly within the Sacramento River ($\hat{\Psi}_A + \hat{\Psi}_B$; Table 3.1).

I found that migration route probabilities (Ψ_h) corresponded well with the fraction of total river discharge in each route (Figure 3.4). Distribution of river flow among the four migration routes was calculated as the fraction of mean discharge of each route relative to the mean discharge of the Sacramento River at Freeport (near station A_2), upstream of the two river junctions. Steamboat and Sutter Slough diverted 33.4% and 37.6% of the mean flow of the Sacramento River during the December and January migration period, accounting for the large proportion of fish using this migration route (Figure 3.4). At the second river junction, operation of the Delta Cross Channel influenced the relative discharge of the Sacramento River, with flow in the Sacramento River downstream of junction 2 representing 25.6% of its total discharge when the Delta Cross Channel was open (December release) compared to 40.0% when the Delta Cross Channel was closed (January release). The increase in relative flow of the Sacramento River due to closure of the Delta Cross Channel was accompanied by an increase in the fraction of fish migrating through this route (Figure 3.4). For both releases the proportion of fish migrating within the Sacramento River was about 10 percentage points

higher than the fraction of flow remaining in the Sacramento River, and for the January release the fraction migrating through Georgiana Slough was about 10% lower than the fraction of flow (Figure 3.4).

Table 3.1. Route-specific survival through the Sacramento–San Joaquin River Delta ($\hat{S}_h$) and the probability of migrating through each route ($\hat{\Psi}_h$) for acoustically tagged fall-run juvenile Chinook salmon released on 5 December 2006 (R_1) and 17 January 2007 (R_2). Also shown is population survival through the Delta (S_{Delta}), which is the average of route-specific survival weighted by the probability of migrating through each route.

Migration route	$\hat{S}_h$ ($\widehat{\text{SE}}$)	95% Profile Likelihood Interval	$\hat{\Psi}_h$ ($\widehat{\text{SE}}$)	95% Profile Likelihood Interval
R_1: December, 2006				
A) Sacramento R.	0.443 (0.146)	0.222, 0.910	0.352 (0.066)	0.231, 0.487
B) Steamboat & Sutter S.	0.263 (0.112)	0.102, 0.607	0.296 (0.062)	0.186, 0.426
C) Delta Cross Channel	0.332 (0.152)	0.116, 0.783	0.235 (0.059)	0.133, 0.361
D) Georgiana S.	0.332 (0.179)	0.087, 0.848	0.117 (0.045)	0.048, 0.223
S_{Delta} (All routes)	0.351 (0.101)	0.200, 0.692		
R_2: January, 2007				
A) Sacramento R.	0.564 (0.086)	0.403, 0.741	0.498 (0.060)	0.383, 0.614
B) Steamboat & Sutter S.	0.561 (0.092)	0.388, 0.747	0.414 (0.059)	0.303, 0.531
C) Delta Cross Channel	NA		0.000	NA
D) Georgiana S.	0.344 (0.200)	0.067, 0.753	0.088 (0.034)	0.036, 0.170
S_{Delta} (All routes)	0.543 (0.070)	0.416, 0.691		

3.3.3 Survival through the Delta

Overall, the estimate of survival through the Delta for the December release was lower than for January (for R_1: $\hat{S}_{\text{Delta}} = 0.351$, for R_2: $\hat{S}_{\text{Delta}} = 0.543$, Table 3.1) despite higher discharge and shorter travel times through the Delta for the December release (Figure 3.2). The CJS model produced nearly the same point estimates and standard errors (for R_1: $\hat{S}_{\text{Delta}} = 0.351$, $\widehat{\text{SE}} = 0.101$; for R_2: $\hat{S}_{\text{Delta}} = 0.536$, $\widehat{\text{SE}} = 0.070$). This finding supports the validity of our more complex model to reconstruct survival through the Delta from the individual components of reach-specific survival and route entrainment probabilities, while also

maintaining precision about $\hat{S}_{\text{Delta}}$. Relative to the small sample size of this study, precision was favorable due to high detection probabilities at most telemetry stations (Appendix Table 1.2).
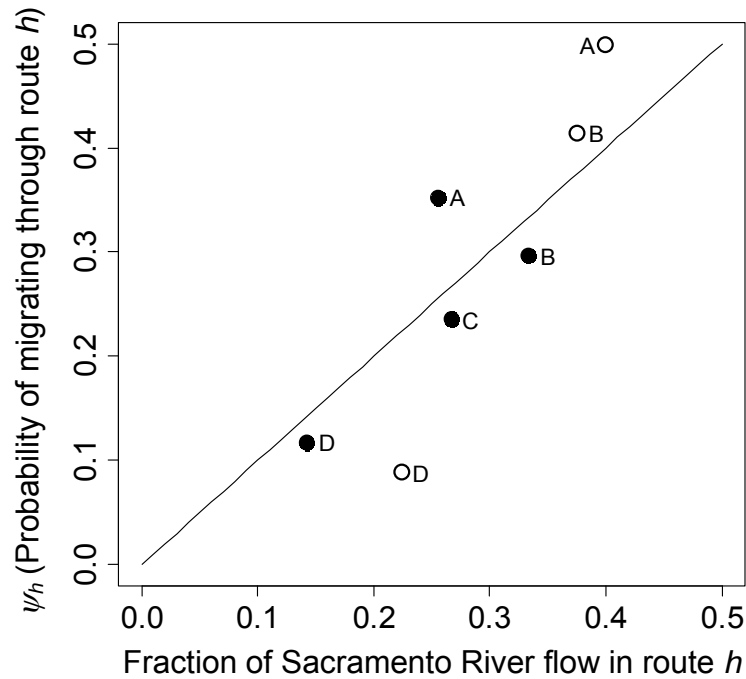
Figure 3.4. The probability of migrating through route h (Ψ_h) as a function of the proportion of total river flow in route h for tagged late-fall juvenile Chinook salmon released on 5 December 2006 (filled symbols) and 17 January 2007 (open symbols). Data labels A–D represent the Sacramento River, Steamboat and Sutter sloughs, the Delta Cross Channel, and Georgiana Slough, respectively. The reference line shows where the fraction migrating through each route is equal to the proportion of flow in each route (i.e., 1:1 ratio).

3.3.4 Relative contributions to S_{Delta}

Estimates of S_{Delta} were driven by 1) variation among routes in survival through the Delta (S_h) and 2) the relative contribution of each route-specific survival to S_{Delta} as measured by migration route probabilities (Ψ_h). For the December release, fish migrating within the Sacramento River exhibited the highest survival through the Delta ($\hat{S}_A$) relative to all other

routes, but only 35% of the population migrated through this route ($\hat{\Psi}_A$), representing a relatively small contribution to $\hat{S}_{\text{Delta}}$ (Figure 3.5, Table 3.1). In contrast, relative to survival in the Sacramento River, survival through all other routes reduced $\hat{S}_{\text{Delta}}$ and comprised 65% of the population ($\hat{\Psi}_B + \hat{\Psi}_C + \hat{\Psi}_D$), thereby contributing substantially to $\hat{S}_{\text{Delta}}$ for the December release (Figure 3.5, Table 3.1). For the January release, 91% of the population ($\hat{\Psi}_A + \hat{\Psi}_B$) migrated through routes with the highest survival, and thus survival through these routes comprised the bulk of $\hat{S}_{\text{Delta}}$ for the January release (Figure 3.5, Table 3.1). In comparison, survival for the interior Delta via Georgiana Slough ($\hat{S}_D$) was lower than the other routes, but this route accounted for only 9% of the population ($\hat{\Psi}_D$), having little influence on $\hat{S}_{\text{Delta}}$ (Figure 3.5, Table 3.1).
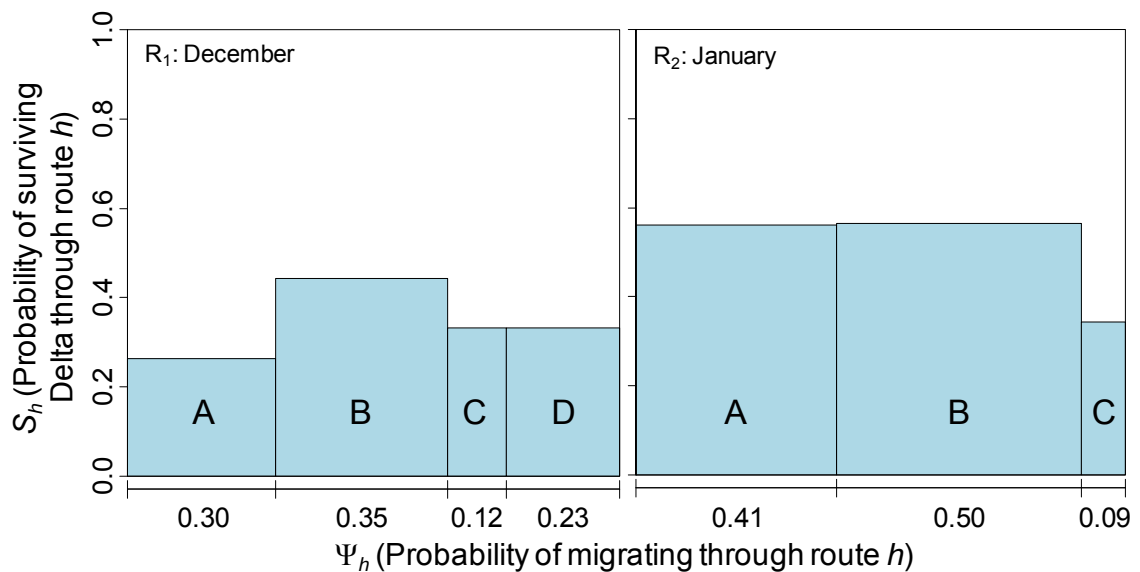
Figure 3.5. Probability of surviving migration through the Sacramento-San Joaquin River Delta (S_h) for each of four migration routes for tagged late-fall juvenile Chinook salmon released on 5 December 2006 (R_1) and 17 January 2007 (R_2). The width of each bar shows the fraction of fish migrating through each route (Ψ_h), and the total area of the bars yields S_{Delta}. Labels A–D represent Steamboat and Sutter sloughs, the Sacramento River, Georgiana Slough, and the Delta Cross Channel, respectively.

The observed difference in $\hat{S}_{\text{Delta}}$ between releases can be attributed to 1) a change in the relative contribution of each route-specific survival to $\hat{S}_{\text{Delta}}$, and 2) differences in survival for given migration routes. Survival estimates for interior Delta routes ($\hat{S}_{\text{C}}$ and $\hat{S}_{\text{D}}$) were lower than for the Sacramento River ($\hat{S}_{\text{A}}$) during both releases but contributed only 9% for the January release when the Delta Cross Channel was closed, compared to 35% ($\hat{\Psi}_{\text{C}} + \hat{\Psi}_{\text{D}}$) for the December release when the Delta Cross Channel was open (Figure 3.5, Table 3.1). Thus, lower contribution of interior Delta routes to $\hat{S}_{\text{Delta}}$ partly accounts for the higher $\hat{S}_{\text{Delta}}$ observed for the January release. However, higher $\hat{S}_{\text{Delta}}$ for January was also a consequence of changes in route-specific survival for the Sacramento River and Sutter and Steamboat sloughs, both of which were higher for the January release compared to December. These findings show how both survival through given routes and population distribution among routes interacted to affect $\hat{S}_{\text{Delta}}$ during the two releases.

3.4 Discussion

My study highlights the importance of quantifying both movement among migration routes and survival within routes to understand factors affecting population-level survival. Measuring survival through different migration routes (S_h) between the same beginning and end points (from telemetry station A_2 to A_8; Figure 3.1) provides direct insight into the effect of different migration routes on survival through the entire Delta. Furthermore, the migration route probabilities (Ψ_h) measure the contribution of each route-specific survival to the overall survival of the population migrating through the Delta. Thus, my modeling approach provides a natural framework for understanding how these route-specific components interact to affect population-level survival through the Delta. Operation of the Delta Cross Channel is an important water management action that may influence population-level survival by affecting the fraction of the population entering the interior Delta where survival is typically lower than alternative migration routes (this study, Newman and Brandes, 2010). Thus, without information about both population distribution among routes and survival within routes, it

would be difficult to quantify how management actions affect these underlying components that give rise to population-level survival.

I show that route-specific survival and movement among migration routes interact to influence population-level survival, but the next challenge is to quantify the mechanisms causing variation in route-specific survival. Within each release, travel times for fish migrating through the interior Delta were longer than alternative routes, possibly contributing to lower survival through the interior Delta. Relative to the December release, however, survival for the January release was higher for two migration routes (Sacramento River and Sutter and Steamboat sloughs) despite lower discharge and longer travel times through these routes during January (Figure 3.3). Thus, instantaneous mortality rates (i.e., per time) in these two routes were lower in January than in December suggesting that factors other than travel time also contribute to variation in survival within and among migration routes. Such factors may include variation in environmental conditions (e.g., water temperature, turbidity, tides) or temporal shifts in the spatial distribution of predators, both of which influence predator-prey interactions. This first year of study just begins to shed light on this variation, but with replication over a wide range of environmental conditions my analytical framework will allow researchers to explicitly quantify mechanisms influencing the route-specific components of population survival.

My findings are consistent with a series of studies that have estimated survival of juvenile salmon in the Delta with coded wire tags (Brandes and McLain, 2001; Newman and Rice, 2002; Newman, 2008; Newman and Brandes, 2010). In general, similar to my analysis, these studies found that survival of fish released into the interior Delta via Georgiana Slough was lower than survival of fish released into the Sacramento River downstream of Georgiana Slough (Newman, 2008; Newman and Brandes, 2010). Specifically, Newman and Brandes (2010) found that the ratio of survival for Georgiana Slough releases relative to Sacramento River releases was less than one for all release groups, indicating significantly lower survival for fish migrating through the interior Delta (see Table 2 in Newman and Brandes). In my analysis, an analogous estimate is $S_{D1}S_{D2}S_{D3}/S_{A5}S_{A6}S_{A7}$ (i.e., survival from D_1 to A_8 relative to A_5 to A_8; Figure 3.1). The estimate of this ratio was 0.625 ($\widehat{SE} = 0.352$) for the December release and 0.591 ($\widehat{SE} = 0.351$) for the January release. Although the standard errors indicate

that these estimates do not differ from one (i.e., equal survival), the point estimates parallel the previous studies and fall well within their observed release-to-release variation. This evidence continues to support the hypothesis that survival for fish migrating through the interior Delta is lower than for fish that remain in the Sacramento River. While past research has revealed differences in survival among migration routes, it was impossible to quantify how these survival differences influenced survival of the population. In contrast, my study builds on past research by explicitly estimating the relative contribution of route-specific survival to population-level survival, as quantified by migration route probabilities (Ψ_h).

Given that 30-40% of the population migrated through Sutter and Steamboat sloughs (Table 3.1), this migration route plays a key role in population-level survival by reducing the probability of fish entering the interior Delta. Fish migrating through Sutter and Steamboat sloughs do not encounter the Delta Cross Channel or Georgiana Slough, which directly reduces the fraction of fish entering the interior Delta via these routes. This relation is couched explicitly in my model: the probability of migrating through the interior Delta can be expressed as $\Psi_C + \Psi_D = (1 - \Psi_B)(\Psi_{C2} + \Psi_{D2})$. Note that the fraction entering the interior Delta ($\Psi_C + \Psi_D$) decreases as the fraction migrating through Sutter and Steamboat sloughs (Ψ_B) increases. This relationship highlights a critical linkage among migration routes that drives the dispersal process of juvenile salmon migrating through the Delta. Furthermore, closure of the Delta Cross Channel reduces channel capacity of the Sacramento River at the second river junction, which slightly increases the proportion of river flow diverted into Sutter and Steamboat sloughs at the first river junction (J.R. Burau, US Geological Survey, personal communication). Thus, in addition to eliminating a route through the interior Delta, closure of the Delta Cross Channel may decrease the proportion of fish entrained into the interior Delta by increasing the fraction of fish entering Sutter and Steamboat sloughs. However, whether population-level survival is increased by management actions that shift the population distribution among migration routes will depend on the relative difference in survival among alternative routes.

In general, migration route probabilities increased with the fraction of total river discharge in each migration route, but both the form of this relationship and the factors influencing migration route probabilities requires further study. Flow distribution among the

river channels at each junction varies with the tides on hourly time scales. Thus, migration route probabilities in my mark-recapture model represent an average of time-specific route entrainment probabilities that depend on the flow distribution when each fish passes a river junction. Furthermore, the spatial distribution of migrating salmon across a river channel may deviate from the spatial distribution of flow, which could cause a disproportionate number of salmon to be entrained into a given river channel relative to the proportion of flow in that channel. For example, in the Columbia River, juvenile salmon pass through shallow spillways at dams in higher proportions than the fraction of flow passing through spillways (Plumb et al., 2003; Zabel et al., 2008) because of the surface-biased distribution of salmon. Similar behavioral processes at river junctions in the Delta would manifest as consistently positive or negative deviations from the 1:1 line in Figure 3.4 (i.e., where the proportion of flow = proportion of fish in a given route). Given these processes and my initial findings, I hypothesize that 1) changes in the distribution of average river flow at river junctions will effect coincident changes in average migration route probabilities, 2) consistent deviations in migration route probabilities relative to flow distribution may arise from a mismatch in the spatial distribution of fish relative to flow, and 3) variability in release-specific migration route probabilities will be driven by the interaction between fish arrival timing at a river junction and hourly-scale changes in flow distribution at river junctions. In Chapter 6, I examine these hypotheses in detail by evaluating the effects of hydraulic variables on route entrainment probabilities of individuals when they migrated past the Delta Cross Channel and Georgiana Slough.

Strictly speaking, inferences from our study population apply directly to the population of hatchery-origin late fall Chinook salmon ≥140mm FL migrating through the Delta between December and mid-February under the environmental conditions observed during our study. However, four distinct populations of juvenile Chinook salmon (fall, late fall, winter, and spring) of both hatchery and wild origin use the Delta to varying degrees at different times of year during different life stages. Although our framework can be applied to any of these populations, inferences from our data should be considered in the context of the similarity of target populations to our study population. Between December and mid-February, most fish captured in midwater trawls in the lower Delta at Chipps Island (near station A_8) range in size

from about 110 mm to 200 mm (Brandes and McLain, 2001) and likely represent actively migrating smolts from the late fall and winter run of Chinook salmon (Hedgecock, 2001). Fall run fry (i.e., < 50 mm FL) begin appearing in the Delta in January and overlap with the arrival of spring run parr (>50 mm FL) in March, both of which rear and grow in the Delta to sizes <120 mm FL until complete emigration by late June (as presumed by absence in catch data; Williams, 2006 and references therein). Inferences from our data to fall run fry and spring run parr are not well supported due to differences in size, seasonal timing, and residence time in the Delta. In addition, survival of hatchery-origin fish may differ from wild fish (Reisenbichler and McIntyre, 1977; Kostow, 2004), but factors influencing relative differences in survival among migration routes (e.g., interior Delta relative to Sacramento River) are likely to act similarly on both wild and hatchery populations. Thus inferences about such relative differences may provide critical information for better understanding mechanisms influencing population-level survival of both hatchery and wild populations.

Estimating both movement and survival rates among different habitats is difficult yet critically important because these demographic parameters can have important consequences on population dynamics and viability (Beissinger and McCullough, 2002). In our study, strategically located telemetry stations yield information on the movement of individual fish, while the mark-recapture model allows unbiased estimation of demographic parameters by correcting for the imperfect detection probability of each telemetry station. Similar models have been applied extensively to estimate animal migration and survival rates among geographic areas over time (Hilborn et al., 1990; Hestbeck et al., 1991; Williams et al., 2002), but relatively few studies have focused on survival through space among alternative migration pathways (but see Skalski et al., 2002). Our framework could be applied to any migrating fish population that uses a number of alternative migration routes and is particularly well suited to dendritic networks such as river systems and their estuaries. For example, by situating telemetry stations at appropriate tributary confluences in a mainstem river, our modeling framework could be used to estimate both reach-specific survival and dispersal of adult salmonids among spawning tributaries. Here, movement rates (Ψ) estimate the proportion of the population using each tributary, providing important information about relative contribution of sub-populations in each tributary to the population as a whole. Our study

shows how combining telemetry with mark-recapture models provides a powerful approach to estimate demographic parameters in spatially complex settings.

This study has provided the first quantitative glimpse into the migration dynamics of juvenile salmon smolts in the Sacramento River. Route-specific survival through the Delta (S_h) measured the consequence of migrating through different routes on survival through the Delta, while migration route probabilities (Ψ_h) quantified the relative contribution of each route-specific survival to population-level survival. In years to come, increases in sample size and replication over variable environmental conditions will bolster inferences drawn from the acoustic-tag data and increase understanding of the mechanisms influencing survival. Cumulative knowledge gained from this population-level approach will identify the key management actions in the Delta that must be rectified if Sacramento River salmon populations are to recover.

Chapter 4

**IMPROVING THE PRECISION AND SPATIAL RESOLUTION OF
REACH SURVIVAL IN THE SACRAMENTO-SAN JOAQUIN RIVER
DELTA IN WINTER 2008**

4.1 Introduction

In the previous chapter, I developed a mark-recapture model to estimate the route-specific components of population-level survival for acoustically tagged late-fall Chinook salmon smolts migrating through the Sacramento–San Joaquin River Delta. The model was applied to data from tagged salmon that migrated through the Delta during the winter of 2006/2007 (hereafter "2007", Perry et al., 2008, 2010). This analysis provided the first quantitative estimates of route-specific survival through the Delta and the fraction of the population using each migration route. Furthermore, I explicitly quantified the relative contribution of each migration route to population-level survival. As with other authors (Newman and Brandes, 2010), I found that survival through the interior Delta was lower than survival of fish using the Sacramento River. I also found that the proportion of the population entering the interior Delta differed between releases, which influenced population-level survival by shifting a fraction of the population from a low-survival migration route (the interior Delta) to a high-survival route (the Sacramento River). However, I also found that differences between releases in population-level survival were caused by changes in survival for given migration routes. Thus, variation in population-level survival was driven both by variation in movement among routes as well as survival within routes.

In this chapter, I expand the model presented in Chapter 3 with the goal of increasing spatial resolution and improving precision of the subsequent study conducted during winter of 2007/2008 (hereafter "2008"). While many design aspects were maintained, I worked closely with the US Fish and Wildlife Service to incorporate a number of changes in study design based on insights from the first year of study. The most important limitation in 2007 was small

total sample size, as well as small sample size for specific migration routes. For example, because up to 40% of fish migrated through Sutter and Steamboat Slough at the first river junction (Route B in Figure 3.1), only 60% of fish remained in Sacramento River to pass the second river junction (Routes C and D leading to the interior Delta; Figure 3.1). This led to low sample size and poor precision of parameter estimates for routes through the interior Delta, which in turn led to low power to detect differences in survival among migration routes. Thus, I recommended two approaches to improve precision. First, the total sample size was tripled from 144 tagged fish in 2007 to 419 tagged fish in 2008. Second, because the interior Delta is an important migration route with many management concerns, we also released a subsample of fish directly into the interior Delta via Georgiana Slough (Route D in Figure 3.1).

To improve spatial resolution, many new telemetry stations were added, allowing survival to be better partitioned among specific reaches and to better quantify movement among channels within major migration routes. For example, in 2007, I observed a substantial difference between releases in survival for Sutter and Steamboat sloughs. However, because this migration route encompassed numerous unmonitored river channels it was impossible to determine whether changes in route-specific survival were due to shifts in mortality within a particular reach, or occurred due to changes in survival over all reaches with this route. Therefore, additional telemetry stations within this migration route allowed me to quantify the contribution of within-route reaches to overall route survival.

I first report results for population-level survival through the Delta, route-specific survival through the Delta, and dispersal among migration routes, contrasting estimates from this study to those from 2007. Given more detailed information within migration routes, I then examined patterns in reach-specific survival to understand whether variation in route-specific survival through the Delta was driven by particular reaches within a route. Last, in addition to dispersal among the major migration routes shown in Figure 3.1, I explicitly accounted for movement among other channels within routes, and discuss the influence of these movements on population-level migration and survival dynamics.

4.2 Methods

4.2.1 Telemetry system and fish tagging

The telemetry system, fish tagging, and fish releases followed the methods described in Chapter 3; therefore, only major departures from Chapter 3 are noted here. Telemetry stations were deployed to monitor movement of tagged fish among four major migration routes through the Delta (Figure 3.1): the mainstem Sacramento River (Route A), Steamboat and Sutter Slough (Route B), the interior Delta via the Delta Cross Channel (Route C), and the interior Delta via Georgiana Slough (Route D). Numerous telemetry stations were deployed within Sutter and Steamboat sloughs to better quantify survival and movement within this region, relative to the study in 2007 (see Chapter 3). Sutter Slough is labeled as B_1, the first sub-route within route B, and Steamboat Slough as B_2, the second sub-route. Specifically, Sutter Slough and Miner Slough form a northern route and stations along this route are labeled B_{11} (entrance to Sutter Slough), B_{12}, and B_{13} (Miner Slough; Figure 1.2 and 4.1). Steamboat Slough forms the southern route and these stations are labeled as B_{21}, B_{22}, and B_{23}. Relative to 2007, additional telemetry stations were also installed within the interior Delta (D_i). Routes A, B, C, and D contained 8, 6, 1, and 7 telemetry stations, whereas in 2007, the same routes contained 7, 1, 2, and 3 telemetry stations. In addition, to quantify movement between the lower Sacramento River and the lower San Joaquin River, we included a telemetry station within Three Mile Slough (E_1) for a total of 23 telemetry stations within the Delta.

In 2008, a 1.6-g tag with a 70-d expected battery life was used (Vemco Ltd., Model V7-2L-R64K), and fish had a mean fork length of 155.0 mm (SD = 10.2) and mean weight of 42.0 g (SD = 9.6). The tag weight represented 3.8% of the mean fish weight (range = 1.9%–5.4%). To release fish, they were first transported to release sites at either the Sacramento River near Sacramento, CA (20 km upstream of A_2) or Georgiana slough (about 5 km downstream from D_1; Figure 4.1). Fish were then transferred to perforated 19-L buckets (2 fish per bucket), held for 24 h in the Sacramento River prior to release to allow recovery from the transportation process, and then released at roughly hourly intervals over a 24-h period. The total sample size for the study was 419 acoustically tagged fish, with 208 fish released in
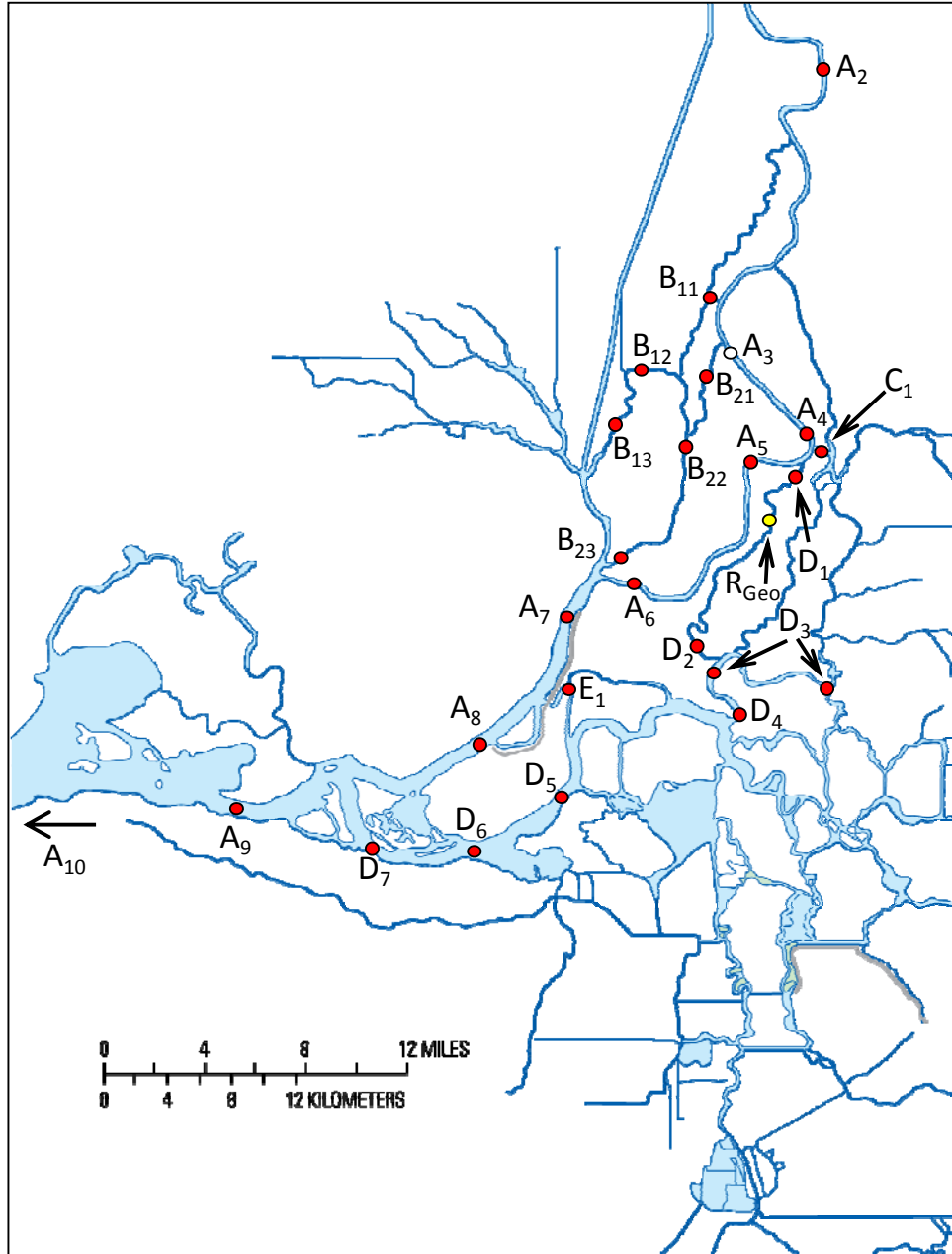
Figure 4.1. Location of telemetry stations used to estimate survival and migration route probabilities within four major migration routes of the Sacramento–San Joaquin River Delta during the winter of 2007/2008. Red-filled circles labeled as h_i show the location of telemetry station i with route h. Location A_3 is denoted by an unfilled circle to indicate that a telemetry station was not implemented at this location during the winter of 2007/2008. Station A_{10} pools all telemetry stations in San Francisco Bay downstream of A_9. The Sacramento release site was 19 river kilometers upriver of station A_2, and the Georgiana release site is noted as the yellow-filled circle labeled as R_{Geo}.

December when the Delta Cross Channel was open and 211 fish released in January when the Delta Cross Channel was closed (Table 4.1). For the first release, 28% of the fish were released into Georgiana Slough, but this fraction was increased to 38% for the second release in anticipation that a lower proportion of the Sacramento release group would enter the interior Delta with the Delta Cross Channel closed (Table 4.1). Fish were released into Georgiana Slough two days later than the Sacramento release group to match release times in Georgiana Slough with the travel time of fish from Sacramento to Georgiana Slough (R. Perry, unpublished data).

Table 4.1. Summary of release dates, locations, and sample size of acoustically tagged late-fall Chinook salmon released into the Delta during the winter of 2007/2008.

Release date	Release number	Release location	Sample size
4 December 2007	1	Sacramento	149
6 December 2007	1	Georgiana Slough	59
15 January 2008	2	Sacramento	130
17 January 2008	2	Georgiana Slough	81

4.2.2 Model development

As in my previous model, I estimated detection (P_{hi}), survival (S_{hi}), and route entrainment probabilities (Ψ_{hl}). However, to capture complexity in movement of fish among different channels I also estimated joint survival-entrainment probabilities ($\phi_{hi,jk}$) as described in Chapter 2 (Figure 4.2). Joint survival-entrainment probabilities ($\phi_{hi,jk}$) estimate the joint probability of surviving from site h_i to j_k and moving into route j. The $\phi_{hi,jk}$ parameters are estimated in reaches with river junctions that split into two channels, but where telemetry stations within each river channel are located some distance downstream the river junction. For example, fish passing station A_7 in the Sacramento River may enter Three Mile Slough (E_1) or remain the Sacramento River for another 5.5 km below this junction to pass station A_8 (Figure 4.2). Thus $\phi_{A7,A8}$ is the joint probability of surviving from A_7 to its junction with Three Mile Slough, remaining in the Sacramento River at this junction, and then surviving from the junction to A_8.
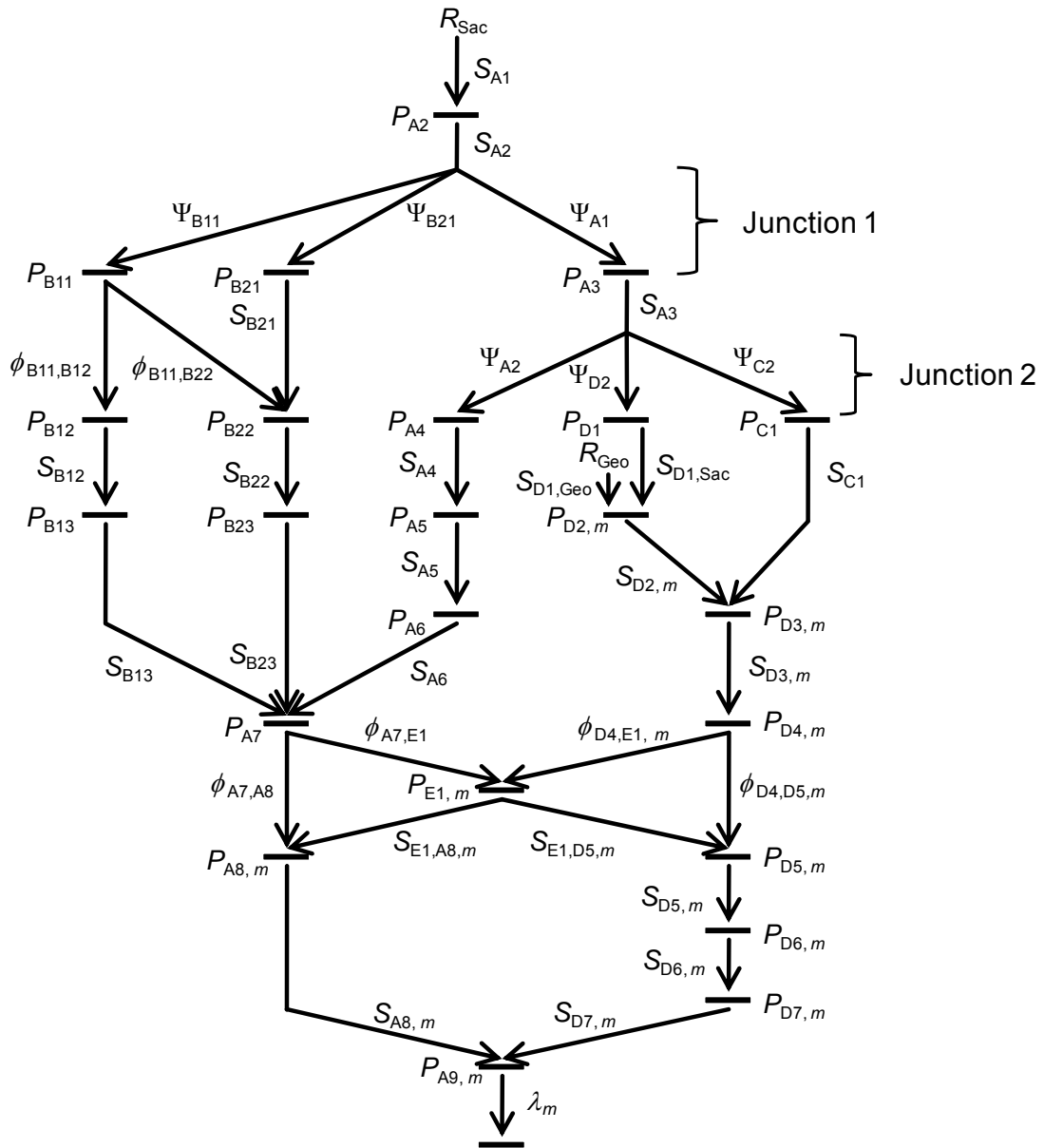
Figure 4.2. Schematic of the mark-recapture model used to estimate survival (S_{hi}), detection (P_{hi}), route entrainment (Ψ_{hl}), and joint survival-entrainment ($\phi_{hi,jk}$) probabilities of juvenile late-fall Chinook salmon migrating through the Sacramento–San Joaquin River Delta for releases made in December 2007 and January 2008. Release sites are denoted by R_m (m = Sac (Sacramento) and Geo (Georgiana Slough)), and parameters subscripted by m denote parameters which can be estimated separately for each release site.

In the 2007 study, telemetry arrays at the entrance to Sutter and Steamboat sloughs were pooled in the model to estimate a single route entrainment probability for both sloughs because within-route telemetry stations were not present. For this analysis, however, telemetry stations within Sutter and Steamboat slough downstream of each entrance allowed me to estimate route entrainment probabilities separately for each slough (Figures 4.1 and 4.2). Thus, the parameter Ψ_{B11} estimates the probability of being entrained into Sutter Slough at station B_{11} and Ψ_{B21} estimates the probability of being entrained into Steamboat Slough at station B_{21}. The probability of remaining in the Sacramento River at the first junction is $1 - \Psi_{B11} - \Psi_{B21} = \Psi_{A1}$ (Figures 4.1 and 4.2).

Joint survival-entrainment probabilities were estimated for three reaches where 1) fish entering Sutter Slough (B_{11}) may subsequently continue down either Miner Slough (B_{12}) or Steamboat Slough (B_{22}), 2) fish entering the San Joaquin River at D_4 may subsequently exit this reach through either Three Mile Slough at E_1 or the San Joaquin River at B_5, and 3) fish passing A_7 in the Sacramento River may exit this reach at either E_1 or A_8 (Figures 4.1 and 4.2). Each of these reaches consist a single river channel, a junction where the channel splits, and then two separate channels through which fish migrate before being detected at telemetry stations in each channel. In these locations, interest may lie in estimating the proportion of fish entering each channel, but as discussed in Chapter 2, Ψ_{hl} may be biased if survival probabilities downstream of the junction differ between the two channels. However, the joint probability of surviving and migrating through a given channel (i.e., $\phi_{hi,jk}$) will remain unbiased in these circumstances. Although the $\phi_{hi,jk}$ parameters are difficult to interpret biologically, being the joint probability of entrainment and survival, their sum yields the total reach survival. Thus, in the three reaches where $\phi_{hi,jk}$ parameters are estimated, $S_{B11} = \phi_{B11,B12} + \phi_{B11,B22}$, $S_{A7} = \phi_{A7,E1} + \phi_{A7,A8}$, and $S_{D4} = \phi_{D4,E1} + \phi_{D4,D5}$ are the probabilities of surviving from each upstream telemetry station to either of the next downstream stations.

Other than the differences noted above, the model structure for 2008 differed in two other aspects compared to 2007. First, in 2007, fish from a given release passed the Delta Cross Channel when it was both open and closed, requiring us to incorporate a parameter to

estimate the probability of fish passing the Delta Cross Channel under each condition (ω_{open}, see Chapter 3). However, for this study, only 3 fish released when the Delta Cross Channel was open passed the Delta Cross Channel after it had closed. Therefore, we did not include ω_{open} in the model because its effect on the route entrainment probabilities is minimal. Second, having two release sites leads to two estimates of the same parameter for reaches within the interior Delta (e.g., $S_{D3,m} = S_{D3,Sac}$ or $S_{D3,Geo}$; Figure 4.2). With this model structure, the full model contains 75 unique parameters; 55 parameters from the Sacramento release and 20 for the Georgiana Slough release (Figure 4.2).

4.2.3 Parameter estimation

Prior to parameter estimation, the records of tag-detections were processed to eliminate false positive detections as described in Chapter 3. The detection records of about 10% of tagged fish suggested they had been consumed by piscivorous predators as was evidenced by their directed upstream movement for long distance and against the flow. We truncated the detection record of these fish to the last known location of the live tagged fish. All other detections were considered to have been live juvenile salmon. In the lower Sacramento and San Joaquin rivers (sites A_7–A_8 and D_5–D_7), tag detection and discharge data showed that juvenile salmon were often advected upstream on the flood tides and downstream on the ebb tides. In these cases, we used the final downstream series of detections in forming the detection history.

Parameters were estimated using the maximum likelihood techniques described in Chapter 3, and the likelihood of each capture history was formed by adapting the methods of Fujiwara and Caswell (2002), as described in Chapter 2. Detection histories for 2008 were able to describe detailed movements of fish through the Delta. For example, a fish with the history AA0AAAAEDDDAA indicates it was released at Sacramento ("A"), detected in the Sacramento River at A_2 ("A"), and not detected in the Sacramento River at A_3 ("0"). This fish was subsequently detected at every other telemetry station as it emigrated from the Sacramento River ("AAAA") through Three Mile Slough ("E"), down the San Joaquin River ("DDD"), and finally past Chipps Island into San Francisco Bay ("AA"). Parameters were estimated separately for each release (k) but simultaneously for both release sites by expressing the joint

likelihood as the product of $L_{k,\text{Sac}}$ and $L_{k,\text{Geo}}$ (Sac = Sacramento release site, Geo = Georgiana Slough release site).

Although I suggested a telemetry station be deployed in the Sacramento River at junction 1 (station A_3), this station was not implemented in 2008, so I set P_{A3} to zero. Absence of this telemetry station makes it impossible to uniquely estimate the parameters S_{A2}, S_{A3}, Ψ_{B11}, and Ψ_{B11}. However, these parameters can be estimated by assuming that $S_{A2} = S_{A3}$. This assumption was supported by estimates of S_{A2} and S_{A3} in 2007 (See Chapter 3 and Appendix Table 1.2). Nonetheless, given that three of four releases thus far (in 2007 and 2008) occurred without a telemetry station at A_3, I undertook a sensitivity analysis to examine the magnitude of bias introduced into route entrainment probabilities due to deviation from the assumption that $S_{A2} = S_{A3}$ (see Appendix 2). Since it is impossible to apportion mortality between the reach above and below A_3, I examined bias under the extreme scenarios where all mortality occurs either upstream of the first river junction (i.e., $S_{A3} = 1$) or downstream of the first river junction (i.e., $S_{A2} = 1$).

For each release, the full model was considered as the model with the fewest parameter constraints which still allowed all parameters to be uniquely estimated. When parameter estimates occur at the boundaries of one (or zero) they cannot be estimated through iterative maximum likelihood techniques and must be set to one (or zero). In our study, many detection probabilities were set to one because all fish passing a given location were known to have been detected at that location. In some cases, survival probabilities were fixed to one because all fish detected at a given telemetry station were also detected at the next downstream location. In addition, parameters for Route C (the Delta Cross Channel) were set to zero for the second release when the Delta Cross Channel was closed. A full detailing of parameter constraints applied under the full model can be found in Appendix Table 3.2.

The purpose of including a separate release into Georgiana Slough was to improve precision within the interior Delta by boosting the sample size of fish migrating through this region. Pooling data across release sites can improve precision but assumes that the fish released into the Sacramento River and Georgiana Slough experience similar survival and detection probabilities in reaches through which both release groups migrate. Therefore, I used likelihood ratio tests (Casella and Berger, 2002) to evaluate hypotheses about equality in

detection and survival parameters between release sites. Lack of significance at $\alpha = 0.05$ indicated that the full model fit the data no better than the reduced model where parameters were set equal among releases, in which case the reduced model was selected over the full model. For each release, I first compared the full model to a reduced model where all parameters were set equal between releases. I then used parameter estimates from the selected model for estimating population-level and route-specific survival through the Delta.

4.2.4 Survival through the Delta

Population-level survival through the Delta was estimated using Eqn. 3.1, which is a weighted average of the route-specific survival probabilities (S_h) with weights proportional to the fraction of fish migrating through each route (Ψ_h).

Migration route probabilities Ψ_h are a function of the route entrainment probabilities (Ψ_{hl}) and estimate the probability of migrating through the Delta via particular migration route. I estimated the same migration route probabilities as described in Eqns. 3.1-3.4, except that $\Psi_B = \Psi_{B11} + \Psi_{B21}$. Since route entrainment probabilities can be estimated separately for Sutter Slough and Steamboat Slough, the probability of migrating through either Sutter or Steamboat Slough (Ψ_B) is the sum of the route-entrainment probabilities for each slough (Ψ_{B11} and Ψ_{B21})

When population level survival can be broken down into components of route-entrainment probabilities and reach specific survival, then survival through the Delta for a given migration route (S_h) is simply the product of the reach-specific survival probabilities that trace each migration path through the Delta between the points A_2 and A_9 (see Eqns 3.6-3.9). However, when joint survival-entrainment probabilities are included in the model, survival through a given route must take into account all possible within-route pathways that involve the $\phi_{hi,jk}$ parameters. For example, survival through the Delta for fish that remain in the Sacramento River through the first and second river junctions is expressed as:

$$S_A = S_{A2}S_{A3}S_{A4}S_{A5}S_{A6}\left(\phi_{A7,A8}S_{A8} + \phi_{A7,E1}S_{E1,D5}S_{D5}S_{D6}S_{D7}\right)$$

The bracketed term is the weighted average survival between A_7 (Rio Vista) and A_9 (Chipps Island) with the $\phi_{hi,jk}$ parameters weighting survival of fish that remain in the Sacramento River ($\phi_{A7,A8}S_{A8}$) and survival of fish that finish their migration in the lower San

Joaquin after passing through Three Mile Slough ($\phi_{A7,E1}S_{E1,D5}S_{D5}S_{D6}S_{D7}$). Thus, survival through the Delta for Route A (the Sacramento River) includes some mortality of fish that enter the interior Delta, and it is impossible to factor out this mortality without explicitly estimating route entrainment probabilities at the junction of the Sacramento River with Three Mile Slough. Nonetheless, the $\phi_{hi,jk}$ parameters provide information about the relative contribution of the interior Delta to survival through Route A. For example, $\phi_{A7,E1} \ll \phi_{A7,A8}$ would suggest that movement through Three Mile Slough is a small component of the total survival for fish that migrated in the Sacramento River up to that point. Survival through the Delta for fish taking the Delta Cross Channel (Route C) and Georgiana Slough (route D) is expressed similarly, and explicitly accounts for fish that pass through Three Mile Slough and finish their migration in the lower Sacramento River:

$$S_C = S_{A2}S_{A3}S_{C1}S_{D3}\left(\phi_{D4,D5}S_{D5}S_{D6}S_{D7} + \phi_{D4,E1}S_{E1,A8}S_{D8}\right),$$

and $\qquad S_D = S_{A2}S_{A3}S_{D1}S_{D2}S_{D3}\left(\phi_{D4,D5}S_{D5}S_{D6}S_{D7} + \phi_{D4,E1}S_{E1,A8}S_{D8}\right).$

To facilitate comparison with findings from our first year in 2007, we pooled Sutter and Steamboat Slough into a single migration route, but survival through the Delta can be estimated separately for fish that enter Sutter Slough and fish that enter Steamboat Slough:

$$S_B = \Psi_{B11}S_{B1} + \Psi_{B21}S_{B2}$$

where S_B is survival through the Delta for fish that enter either Sutter or Steamboat Slough, S_{B1} and S_{B2} are survival through the Delta for fish that enter Sutter Slough and Steamboat Slough, and where S_{B1} and S_{B2} are estimated as:

$$S_{B1} = S_{A2}\left(\phi_{B11,B12}S_{B12}S_{B13} + \phi_{B11,B22}S_{B22}S_{B23}\right)\left(\phi_{A7,A8}S_{A8} + \phi_{A7,E1}S_{E1,D5}S_{D5}S_{D6}S_{D7}\right),$$

and $\qquad S_{B2} = S_{A2}S_{B21}S_{B22}S_{B23}\left(\phi_{A7,A8}S_{A8} + \phi_{A7,E1}S_{E1,D5}S_{D5}S_{D6}S_{D7}\right).$

For fish entering Sutter Slough, note that the first bracketed term in S_{B1} accounts for survival of fish taking either Miner Slough ($S_{B12}S_{B13}$) or Steamboat Slough ($S_{B22}S_{B23}$) weighted by the joint probability of surviving and taking each of these routes ($\phi_{B11,B12}$ and $\phi_{B11,B22}$).

We used an approach similar to Newman and Brandes (2010) to quantify survival through each migration route relative to survival of fish that migrate within the Sacramento River:

$$\theta_h = \frac{S_h}{S_A} \qquad h \neq A$$

We measured survival through each route relative to route A because the Sacramento River is considered the primary migration route. For Georgiana Slough, θ_D is analogous to θ estimated by Newman and Brandes (2010), who estimated the ratio of recovery rates of coded wire tagged fish released into Georgiana Slough and the Sacramento River near A_4. Survival through the Delta for route h is equal to Route A when $\theta_h = 1$, and survival through route h is less (greater) than Route A when θ_h is less (greater) than one. I interpreted survival through route h as significantly different than Route A at $\alpha = 0.05$ when $\theta_h = 1$ fell outside the 95% profile likelihood confidence interval of $\hat{\theta}_h$.

To aid in interpreting differences in survival through the Delta among routes and between releases, I examined variation in reach-specific survival rates. Survival probabilities estimate the proportion of fish that survive through a given reach, but direct comparison of survival probabilities among reaches can be hampered by variation in the length of each reach. In our study, reach length varied from just a few kilometers to over 20 km. Therefore, we scaled survival probabilities relative to reach length by calculating survival per unit distance:

$$s_{hi} = \sqrt[x_{hi}]{S_{hi}} \tag{4.1}$$

where s_{hi} is the per-kilometer probability of surviving from telemetry station h_i to the next downstream station, x_{hi} is the distance (km) from telemetry station h_i to the next downstream telemetry station, and S_{hi} is the probability of surviving over x_{hi} kilometers. For reaches where more than one exit location is possible (reaches beginning at B_{11}, A_7, and D_4), I used the average distance to each of the exit points. The length of some reaches is ill-defined because fish may take multiple, unmonitored routes (e.g., the interior Delta between D_4 and D_5). For these reaches, reach length was calculated as the shortest distance between upstream and downstream telemetry stations (usually the main channel). If fish took longer routes which led to higher mortality, then survival probabilities (S_{hi}) scaled to the shortest possible migration route (s_{hi}) would appear low relative to other routes. Thus, this approach is of utility in identifying reaches of high mortality relative to the shortest possible pathway through a reach.

4.3 Results

4.3.1 River conditions and migration timing

River conditions differed for the two release groups and influenced their travel times through the Delta (Figure 4.3). For first release, tagged fish passed the two river junctions when discharge of the Sacramento River at Freeport was between 10,000 ft^3/s and 14,000 ft^3/s. The central 80% of this release group passed junction 2 (Stations A_4, C_1, and D_1; Figure 4.1) over a 5-day period between 7 December and 11 December. The Delta Cross Channel closed at 1138 hours on 14 December 2007 and remained closed for the balance of the study (Figure 4.3). In contrast, the second release group passed the two river junctions on the descending limb of a freshet, during which flows declined from about 19,000 ft^3/s to 14,000 ft^3/s. Under these flow conditions, the second release group passed junction 2 over a two-day period between 17 January and 19 January. Travel times from release to junction 2 were also shorter for the second release group, with a median travel time of 2.7 d for the first release compared to 1.5 d for the second release.

During their migration through the lower regions of the Delta, most of first release group experienced relatively low and stable discharge accompanied by declining water exports, whereas migration of the second release group coincided with a second freshet during which discharge increased to about 40,000 ft^3/s and exports remained stable (Figure 4.3). As a consequence, most of the first release group passed Chipps Island over a 29-d period (12 December to 10 January), but the second release group passed Chipps Island over only a 16-d period (24 January to 9 February). Although the median travel time from release to Chipps Island for the first release (9.7 d) was less than for the second release (12.9 d), the 90th percentile for the first release (35.9 d) was substantially longer than for the second release (23.9 d). These findings suggest that the main effect of the freshet during the second release was to compress the tail of the travel time distribution rather than shift its central tendency. For both releases, it was difficult to compare travel time among migration routes because ≤4 fish per route were detected at Chipps Island for all routes but the Sacramento River.
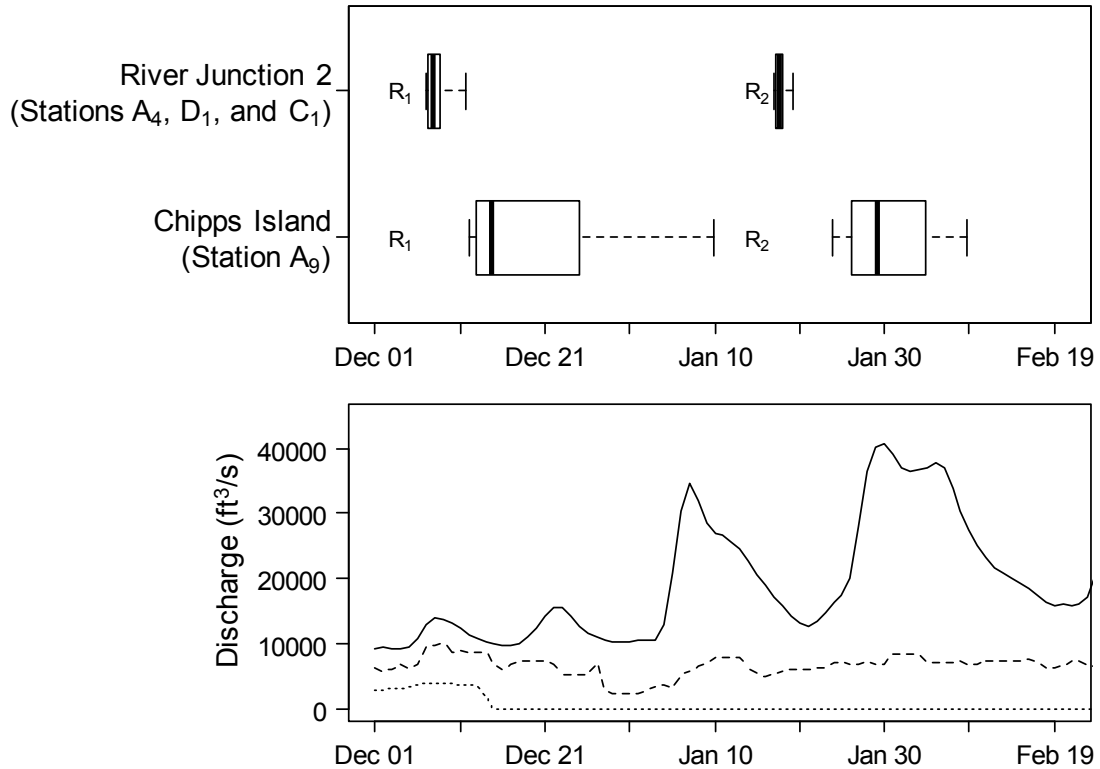
Figure 4.3. River discharge, water exports, and Delta Cross Channel discharge during the migration period of tagged juvenile Chinook salmon migrating through the Sacramento–San Joaquin River Delta during winter 2007/2008. Box plots show the distribution of arrival dates at Junction 2 on the Sacramento River (telemetry stations A4, C1, and D1) and at Chipps Island, the terminus of the Delta (telemetry station A9). The two release dates are shown as R_1 = 4 December 2006 for a release size of 149 tagged fish and R_2 = 15 January 2007 for a release size of 130 fish. Whiskers represent the 10th and 90th percentiles, the box encompasses the 25th to 75th percentiles, and the line bisecting the box is the median arrival date. River discharge (solid line) is tidally filtered, daily discharge of the Sacramento River at Freeport (near telemetry station A2), Delta Cross Channel discharge (dotted line) is the tidally filtered daily discharge, and water exports (dashed line) are the total daily discharge of water exported from the Delta at the pumping projects.

4.3.2 Route-specific survival through the Delta

Comparison of parameters between release sites (Sacramento and Georgiana Slough) suggested no difference in survival or detection probabilities, allowing me to set parameters equal between release sites to improve precision of survival estimates. For both releases, likelihood ratio tests were not significant (for December, χ_9^2=12.4, P = 0.192; for January, χ_9^2=14.8, P = 0.097), so the reduced model was used to estimate route-specific survival and S_{Delta}. I found little difference between releases in survival through the Delta. The probability of surviving through the Delta was 0.174 for the December release and 0.195 for the January release (Table 4.2). For the December release, fish remaining in the Sacramento River exhibited higher survival than all other routes ($\hat{S}_A$ = 0.283), whereas fish migrating through the interior Delta via the Delta Cross Channel and Georgiana Slough exhibited the lowest survival ($\hat{S}_C$ = 0.041, $\hat{S}_D$ = 0.087, Table 4.2 and Figure 4.4). In contrast, for the January release, fish migrating through Sutter and Steamboat sloughs exhibited similar survival ($\hat{S}_B$ = 0.245) as fish migrating within the Sacramento River ($\hat{S}_A$ = 0.244), whereas survival through the interior Delta via Georgiana Slough remained lower than the other migration routes ($\hat{S}_D$ = 0.086). For both releases, separate estimates of route-specific survival for Sutter Slough and Steamboat Slough revealed fish entering Steamboat Slough exhibited survival that was about 9 percentage points higher than for fish that entered Sutter Slough (Table 4.2).

I detected significant differences between survival for the Sacramento River and survival for other migration routes. For the December release, the ratio of survival for each major migration route relative to the Sacramento River (i.e., θ_h) ranged from 0.14 for the Delta Cross Channel to 0.48 for Sutter and Steamboat Slough, showing that survival through other routes was less than half that of the Sacramento River. Since θ_h = 1 fell outside the 95% confidence intervals of $\hat{\theta}_h$ for all major routes, these findings support the hypothesis that all routes had significantly lower survival than the Sacramento River (Table 4.3). Considering Sutter Slough and Steamboat Slough separately, only the estimate of θ_{B2} for Steamboat Slough

Table 4.2. Route-specific survival through the Sacramento–San Joaquin River Delta (S_h) and the probability of migrating through each route (Ψ_h) for acoustically tagged fall-run juvenile Chinook salmon released in December 2007 (R_1) and January 2008 (R_2). Also shown is population survival through the Delta (S_{Delta}), which is the average of route-specific survival weighted by the probability of migrating through each route.

Migration route	$\hat{S}_h$ ($\widehat{SE}$)	95% Profile likelihood interval	$\hat{\Psi}_h$ ($\widehat{SE}$)	95% Profile likelihood interval
R_1: December 2007				
A) Sacramento R.	0.283 (0.054)	0.187, 0.397	0.387 (0.044)	0.304, 0.475
B) Sutter & Steamboat S.	0.136 (0.039)	0.073, 0.225	0.345 (0.042)	0.267, 0.430
B_1) Sutter S.	0.107 (0.037)	0.050, 0.196	0.230 (0.037)	0.163, 0.308
B_2) Steamboat S.	0.193 (0.060)	0.095, 0.327	0.115 (0.028)	0.068, 0.178
C) Delta Cross Channel	0.041 (0.021)	0.013, 0.096	0.117 (0.029)	0.068, 0.182
D) Georgiana S.	0.087 (0.028)	0.043, 0.153	0.150 (0.033)	0.094, 0.221
S_{Delta} (All routes)	0.174 (0.031)	0.119, 0.242		
R_2: January 2008				
A) Sacramento R.	0.244 (0.048)	0.160, 0.346	0.490 (0.048)	0.397, 0.584
B) Sutter & Steamboat S.	0.245 (0.059)	0.143, 0.372	0.198 (0.037)	0.133, 0.278
B_1) Sutter S.	0.192 (0.070)	0.078, 0.343	0.086 (0.026)	0.044, 0.147
B_2) Steamboat S.	0.286 (0.070)	0.162, 0.430	0.112 (0.029)	0.033, 0.253
C) Delta Cross Channel	NA		0.000 (0.000)	
D) Georgiana S.	0.086 (0.023)	0.048, 0.140	0.311 (0.045)	0.229, 0.403
S_{Delta} (All routes)	0.195 (0.034)	0.135, 0.268		
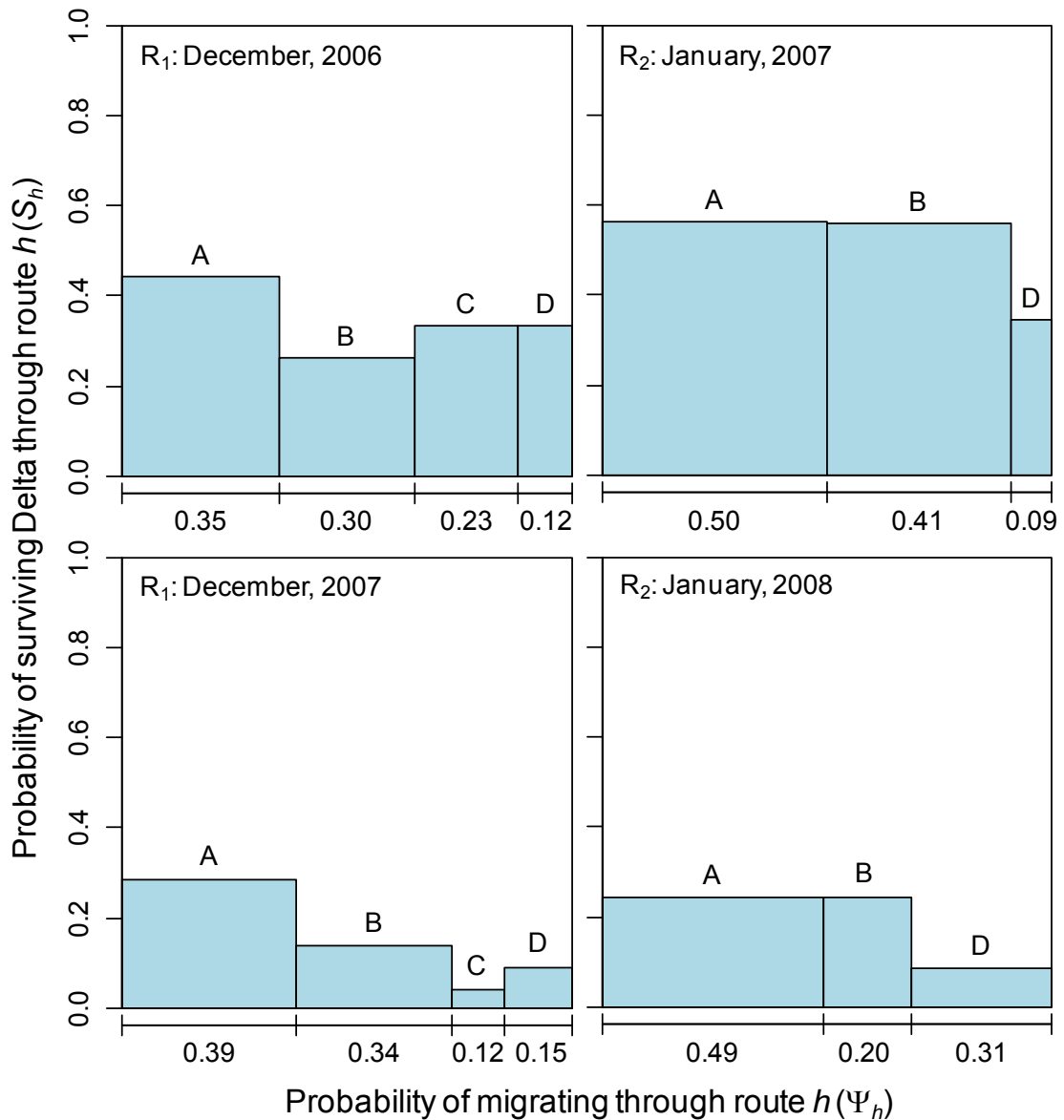
Figure 4.4. Probability of surviving migration through the Sacramento-San Joaquin River Delta (S_h) for each of four migration routes for tagged late-fall juvenile Chinook salmon emigrating from the Sacramento River. The width of each bar shows the fraction of fish migrating through each route (Ψ_h), and the total area under the bars yields S_{Delta}. The top panels show estimates from the winter of 2006/2007 (see Chapter 3), and the bottom panels show estimates from this study during the winter of 2007/2008. Labels A–D represent the Sacramento River, Steamboat and Sutter sloughs, the Delta Cross Channel, and Georgiana Slough, respectively.

was not significantly different from one, likely due to small sample size and low precision for this secondary route. In contrast, in January, $\hat{\theta}_B = 1.005$ whereas $\hat{\theta}_D = 0.352$, showing that survival through the interior Delta (Route D) was only about one third that of other available routes. Survival for the interior Delta was significantly lower than for the Sacramento River, but survival for Sutter and Steamboat Slough (and each slough separately) was not significantly different than the Sacramento River (Table 4.3).

Table 4.3. The ratio (θ_h) of survival through route h (S_h) to survival through the Sacramento River (S_A) for acoustically tagged late fall-run juvenile Chinook salmon released in December 2007 and January 2008.

Migration route	R_1: December 2007		R_2: January 2008	
	$\hat{\theta}_h$ ($\widehat{SE}$)	95% Profile likelihood interval	$\hat{\theta}_h$ ($\widehat{SE}$)	95% Profile likelihood interval
B) Sutter & Sutter S.	0.481 (0.132)	0.265, 0.794	1.005 (0.215)	0.621, 1.480
B$_1$) Sutter S.	0.380 (0.127)	0.182, 0.689	0.787 (0.273)	0.330, 1.365
B$_2$) Steamboat S.	0.683 (0.205)	0.346, 1.153	1.172 (0.255)	0.698, 1.714
C) Delta Cross Channel	0.146 (0.077)	0.044, 0.363	NA	
D) Georgiana S.	0.307 (0.109)	0.145, 0.596	0.352 (0.110)	0.186, 0.642

4.3.3 Migration routing

For some migration routes, I found that the proportion of the population migrating through a given route deviated from the fraction of mean discharge in a route. As juvenile salmon migrated passed the first river junction, 34.5% of fish left the Sacramento River to the migrate through Steamboat and Sutter Slough (Ψ_B, Figure 4.4 and Table 4.2), about 10 percentage points higher than the fraction of total discharge entering this route (Figure 4.5). In contrast, for the January release, only 19.8% of fish entered Sutter and Steamboat Slough (Figure 4.4 and Table 4.2) despite 37% of river discharge entering this route (Figure 4.5). Route entrainment probabilities for each slough showed that the difference in $\hat{\Psi}_B$ between releases occurred at the entrance to Sutter Slough (Table 4.2). In December, twice the fraction of fish entered Sutter Slough ($\hat{\Psi}_{B11} = 0.230$) as compared to Steamboat Slough ($\hat{\Psi}_{B21} = 0.115$), whereas in January, the proportion entering Sutter Slough declined to 0.086 while the

fraction entering Steamboat Slough remained unchanged at 0.112 (Table 4.2). As a consequence, 65% of fish remained in Sacramento River at the first river junction during the December release, whereas 80% remained in the Sacramento River for the January release (see Ψ_{A1} in Appendix Table 3.3). Thus, for the January release, a larger fraction of the population remained in the Sacramento River at the first junction, which increased exposure of the population to the second river junction where they could enter into the interior Delta.
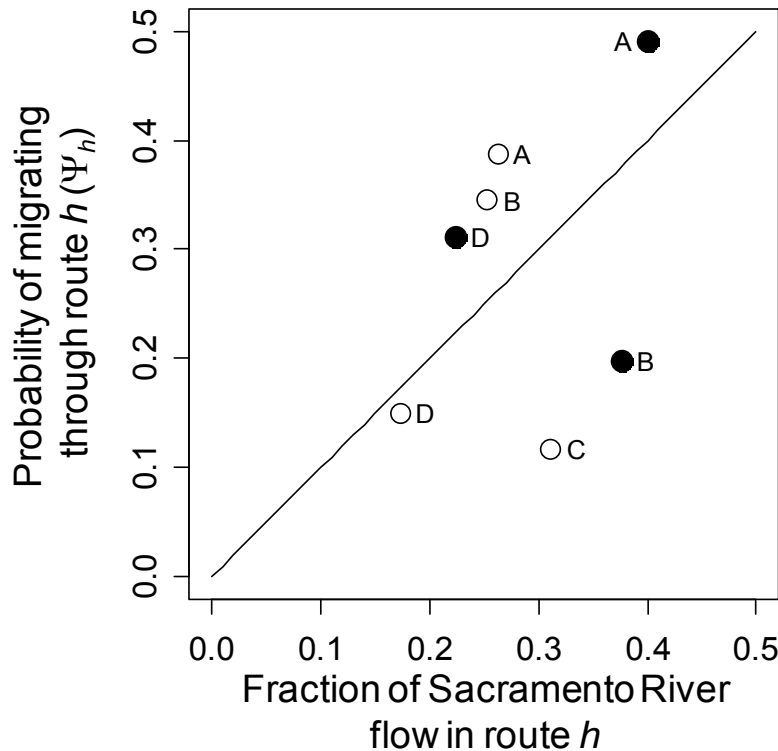
Figure 4.5. The probability of migrating through route h (Ψ_h) as a function of the proportion of total river flow in route h for tagged late-fall juvenile Chinook salmon released in December 2007 (open circles) and January 2008 (filled circles). Data labels A–D represent the Sacramento River, Steamboat and Sutter sloughs, the Delta Cross Channel, and Georgiana Slough, respectively. The fraction of river flow in each route was calculated as the proportion of tidally filtered daily discharge of each route relative to the total discharge of the Sacramento River at Freeport. The reference line shows where the fraction of fish migrating through each route is equal to the proportion of flow in each route (i.e., a 1:1 ratio).

For the December release, of fish that arrived at the second river junction where the Delta Cross Channel is located, 18% entered the Delta Cross Channel, 23% entered Georgiana Slough, and 59.2% remained in the Sacramento River (see Ψ_{C2}, Ψ_{D2}, and Ψ_{A2} in Appendix Table 3.3). In contrast, for the January release when the Delta Cross Channel was closed, 38.8% of fish arriving at the second river junction entered Georgiana Slough, with the remaining 61.2% migrating through the Sacramento River. Accounting for both river junctions, migration route probabilities for the December release indicated that 38.7% of the population migrated within the Sacramento River and 26.7% of the population entered the interior Delta. However, only 11.7% entered the interior Delta through the Delta Cross Channel even though 31% of the flow entered the Delta Cross Channel (Figures 4.4 and 4.5, Table 4.2). During January, nearly one third of the population was entrained into the interior Delta through Georgiana Slough (Figure 5, Table 2) despite the Delta Cross Channel being closed. Consequently, the fraction of the population entering the interior Delta was similar between release dates.

4.3.4 Relative contributions to S_{Delta}

Estimates of S_{Delta} were driven by 1) variation among routes in survival through the Delta ($\hat{S}_h$) and 2) the relative contribution of each route-specific survival to $\hat{S}_{Delta}$ as measured by migration route probabilities ($\hat{\Psi}_h$). For the December release, fish migrating within the Sacramento River exhibited the highest survival through the Delta ($\hat{S}_B$) relative to all other routes, but only 38.7% of the population migrated through this route ($\hat{\Psi}_B$), representing a relatively small contribution to $\hat{S}_{Delta}$ (Figure 4.4, Table 4.2). For the January release, 68.8% of the population ($\hat{\Psi}_A + \hat{\Psi}_B$) migrated through routes with the highest survival, since Sutter and Steamboat sloughs exhibited similar survival to the Sacramento River, but survival through the interior Delta was lower (Figure 4.4, Table 4.2). Because the fraction of the population entering the interior Delta was similar for both releases, lower survival through the interior Delta reduced population-level survival by a similar magnitude for both releases (Figure 4.4, Table 4.2).

4.3.5 Comparisons between 2007 and 2008

Some patterns in survival and migration route probabilities during 2008 differed considerably from 2007, whereas other patterns remained consistent. First, $\hat{S}_{\text{Delta}}$ for both releases in 2008 was lower than in 2007 (Table 3.1, Table 4.2, and Figure 4.4); $\hat{S}_{\text{Delta}}$ in 2007 was estimated at 0.351 and 0.543 for the December and January release groups compared to <0.20 for both releases in 2008. Although $\hat{S}_{\text{Delta}}$ was lower in 2008 relative to 2007, the pattern of survival probabilities among routes was similar between releases and years (Figure 4.4). In both years, all routes exhibited lower survival than the Sacramento River during the December release, but only fish entering the interior Delta exhibited lower survival than the Sacramento River for the January release (Figure 4.4). Larger sample size and the additional release site in Georgiana Slough during 2008 improved precision of route-specific survival compared to our 2007 study, allowing us to detect differences in survival among routes. We also found notable differences between years in route entrainment probabilities at the two primary river junctions. In 2007, migration route probabilities were similar to the fraction of flow in each route, but migration route probabilities deviated from this pattern in 2008. Consequently, in 2008 we found little difference between releases in the fraction of fish entering the interior Delta, whereas in 2007, the fraction of fish was lower during the January release when the Delta Cross Channel was closed (see Chapter 3).

4.3.6 Reach-specific patterns of survival and movement

I found high variation in per-km survival among reaches, ranging from as low as 0.867 km^{-1} to 1.0 km^{-1} for a few reaches where all fish survived. To put the magnitude of this survival in perspective, only 24% of fish will survive a 10-km reach at a rate of 0.867 km^{-1} (i.e., $= 0.867^{10} = 0.247$) and only 6% will remain after 20 km. In contrast, at a rate of 0.99 km^{-1}, 90% of fish will survive 10 km and 82% will still be alive after 20 km. Reaches with the lowest survival rates occurred downstream of telemetry stations B_{13}, B_{23}, and A_6 (i.e., the Cache Slough to Rio Vista region, Figure 4.6). Two out of three of these reaches were among

the four lowest survival probabilities observed in each release, highlighting a region of high local mortality relative to the length of these reaches. In contrast, other than survival probabilities that were fixed to one (Appendix Table 3.3), the highest per-km survival in both releases occurred in the first two reaches of the Sacramento River (downstream of A_2 and the Sacramento release site, A_1). These reaches were relatively long (~20 km each) and survival probabilities were >0.91 (see S_{A1} and S_{A2} in Appendix Table 3.3), leading to high survival relative to reach length.

Reach-specific survival was consistent with differences among routes in survival through the Delta. For the December release, 8 of the 11 reaches with the highest per-km survival were comprised of all 8 reaches in the Sacramento River (Route A, Figure 4.6). These reaches exhibited survival probabilities ≥ 0.96 km^{-1}. The remaining 11 reaches with the lowest per-km survival were comprised solely of the other three routes, with no particular route exhibiting consistently lower reach-specific survival rates. All of these reaches exhibited survival <0.96 km^{-1}. For the January release, the highest-ranking survival was still dominated by reaches within the Sacramento River (6 of the 11 highest per-km survival probabilities), but two reaches of the Sacramento River ranked in lowest 50 percent of survival rates (reaches beginning at A_6 and A_8).

Between releases, most reach-specific survival probabilities within the Sacramento River (Route A) and interior Delta (Route D) changed by less than 0.03 km^{-1} (Figure 4.7), and this finding agrees with the similarity in route-specific survival between releases for these routes (Figure 4.4). Furthermore, variation in survival between releases was low relative to the large variation in survival among reaches, especially for the Sacramento River (Figure 4.7). However, survival for all but one reach within Sutter and Steamboat sloughs increased substantially from December to January (Figure 4.7), which is consistent with the observed increase in survival through the Delta for this route. Thus, the observed difference in route-specific survival for Sutter and Steamboat sloughs was driven by coincident changes in survival rates for most reaches within this route and not by changes in survival within a specific reach.

One reach of particular management interest occurs downstream of D_4 in the interior Delta (see Figure 4.1). Although only about 17 km long by way of the San Joaquin River, this
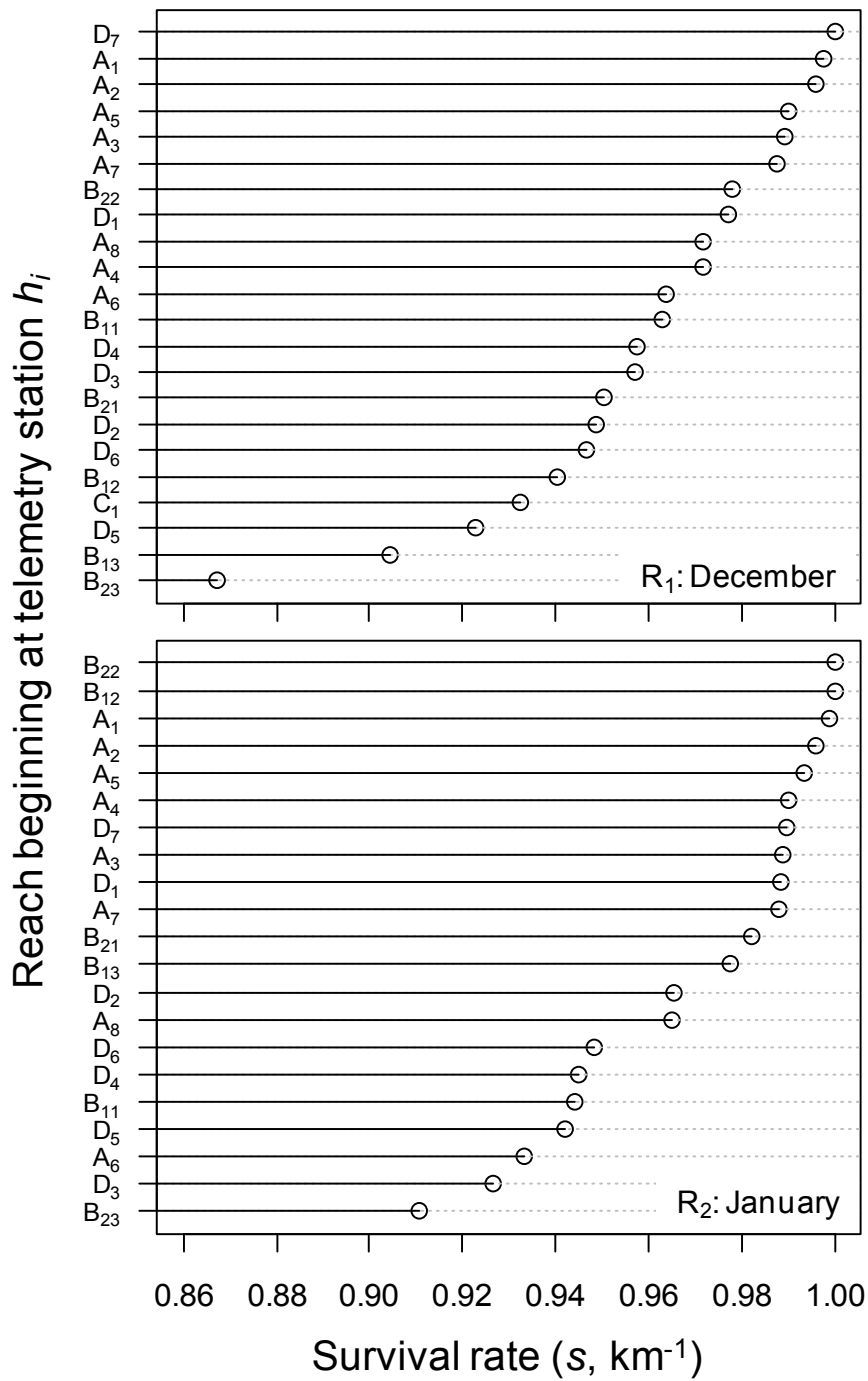
Figure 4.6. Reach-specific survival rates plotted in ascending order for tagged late fall Chinook salmon released in December 2007 (top) and January 2008 (bottom). Survival probabilities are scaled to the length of each reach from telemetry station h_i to the next downstream telemetry station (see Eqn. 4.1).
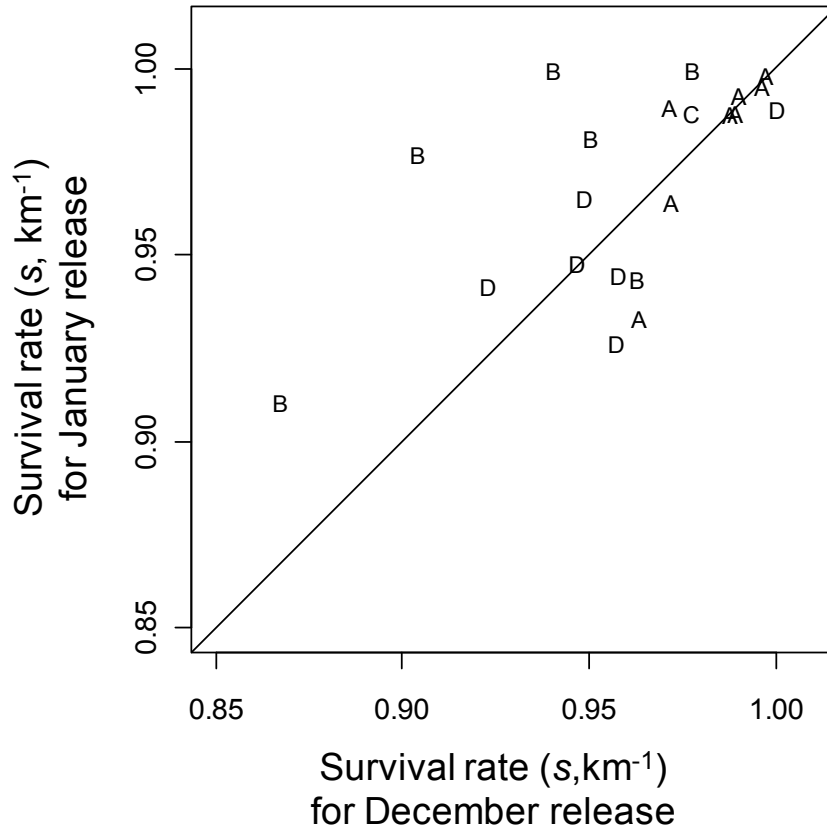
Figure 4.7. Reach-specific survival per km for the December 2007 release compared to the January 2008 release for acoustically tagged late fall Chinook salmon migrating through the Sacramento-San Joaquin River Delta. The reference line shows where survival rates are equal between releases. Letters correspond to reaches within A = Sacramento River, B = Sutter and Steamboat sloughs, and D = the interior Delta via Georgiana Slough.

reach encompasses a large network of channels and includes the pumping stations and fish salvage facilities in the southern Delta. This reach exhibited the lowest probability of survival of all reaches within the interior Delta, having observed survival probabilities of less than 50% (for R_1: $\hat{S}_{D4}$ = 0.484, $\widehat{SE}$ = 0.071; for R_2: $\hat{S}_{D4}$ = 0.395, $\widehat{SE}$ = 0.080; Appendix Table 3.3). However, when expressed as a function of reach length, other reaches within the interior Delta (Routes C and D) exhibited similar or lower survival rates than the reach downstream of D_4 (Figure 4.6). Direct mortality at the pumping stations appeared to contribute little to the estimate of S_{D4}. Both the State Water Project and Clifton Court Forebay were monitored by

telemetry stations, but these stations could not be incorporated into the survival model because too few fish were detected at these locations to warrant parameter estimation. However, of the 76 fish passing D_4 that were never detected at or downstream of D_5 or E_1 (indicating probable mortality in this reach), only one fish was detected at the pumping stations. Overall, six tagged fish were detected at the pumping stations, and five of these were later detected at or downstream of D_5 or E_1 suggesting they had been salvaged at the fish facilities and transported to the lower Delta. Thus, mortality rates appear high in many reaches of the interior Delta relative the Sacramento River, not just the reach that includes a primary point source of known mortality.

Although I could not estimate route entrainment probabilities at other junctions in the Delta, I explicitly accounted for observed movement among routes by estimating joint survival-entrainment probabilities. At the junction of Sutter Slough with Miner and Steamboat Slough (the reach downstream of B_{11}; Figure 2), $\hat{\phi}_{B11,B22}$ was about twice that of $\hat{\phi}_{B11,B12}$ during both releases (Appendix Table 3.3). If survival was similar for the two reaches downstream of the junction, then these findings suggest that about two-thirds of fish entering Sutter Slough migrated down Steamboat Slough and one-third traveled through Miner Slough.

For both releases I observed fish passing in both directions through Three Mile Slough (E_1 in Figure 4.1). However, Three Mile slough appears to play a relatively minor role in movement dynamics through the Delta relative to contribution of the major migration routes. In the Sacramento River, fish moving from A_7 to A_8 contributed a substantially larger fraction of the total survival through this reach (for R_1: $\hat{\phi}_{A7,A8} = 0.837$, $\widehat{SE} = 0.074$; for R_2: $\hat{\phi}_{A7,A8} = 0.781$, $\widehat{SE} = 0.070$) compared to fish moving from A_7 to E_1 (for R_1: $\hat{\phi}_{A7,E1} = 0.049$, $\widehat{SE} = 0.034$; for R_2: $\hat{\phi}_{A7,E1} = 0.109$, $\widehat{SE} = 0.046$). In the San Joaquin River, fish moving from D_4 to E_1 contributed more to the total reach survival for the first release compared to the second release. For the first release, $\hat{\phi}_{D4,E1} = 0.140$ ($\widehat{SE} = 0.049$) and $\hat{\phi}_{D4,D5} = 0.351$ ($\widehat{SE} = 0.070$), whereas for the second release $\hat{\phi}_{D4,E1} = 0.041$ ($\widehat{SE} = 0.023$) and $\hat{\phi}_{D4,D5} = 0.354$ ($\widehat{SE} = 0.079$). Whether a higher fraction of fish in the San Joaquin River passed through Three Mile Slough (E_1) during the first release is difficult to ascertain because lower survival in the San Joaquin River

downstream of its junction with Three-Mile Slough may also account for the observed difference.

4.4 Discussion

In 2007, $\hat{S}_{\text{Delta}}$ differed by nearly 20 percentage points between releases, and I attributed this observed difference to both a change in the proportion of fish entering the interior Delta and a change in survival within given migration routes (see Chapter 3). In contrast, for this study, I attribute lack of an observed difference in $\hat{S}_{\text{Delta}}$ between releases to 1) less variation between releases in survival for given migration routes, relative to 2007, 2) lower-than-expected entrainment into the Delta Cross Channel, 3) a decline in the proportion of fish entering Sutter and Steamboat sloughs in January, and 4) little difference in the proportion of fish entering the interior Delta between releases. In 2007, survival through the Delta for both the Sacramento River and Sutter and Steamboat slough increased substantially between December and January, partly driving the large observed difference in $\hat{S}_{\text{Delta}}$ between releases (Figure 4.4). However, during 2008 only Sutter and Steamboat sloughs exhibited a sizeable increase in survival from December to January. In 2008, although survival increased the proportion of fish entering Sutter and Steamboat sloughs declined from 0.34 to 0.20 from December to January. Had the proportion of fish entering Sutter and Steamboat sloughs remained unchanged, population-level survival would have received a larger boost from the increase in survival observed for this route. Given that survival for routes through the interior Delta were significantly lower than the Sacramento River during both releases, the fraction of fish entering the interior Delta dictated the magnitude of decrease in population-level survival due to fish using this migration route. Thus, the magnitude of decrease in population-level survival attributed to the interior Delta remained unchanged between releases because similar fractions of the population entered the interior Delta during both releases. However, because maximum survival for any given route during both releases was <0.30, population-level survival would remain low regardless of the fraction of fish entrained in the interior Delta.

That estimates of population-level survival were ≤0.20 for an 80-km section of river begs the question of whether the untagged population also experienced such low survival. To put the magnitude of these estimates in perspective, survival of hatchery-reared juvenile Chinook salmon over 600 km and through eight dams of the Snake and Columbia rivers ranged from 31%-59% (Williams et al. 2001). The absolute magnitude of survival relative to the distance traveled is clearly low compared to a similarly developed river system. However, factors such as source of the study fish and the effects of the transmitter could have reduced survival probabilities relative to untagged fish. Fish in this study were obtained directly from Coleman National Fish Hatchery, tagged, and then released about 40 km upstream of the first channel junction in the Delta. Initial "culling" of unfit hatchery fish obtained directly from a hatchery, a process suggested by Muir et al. (2001) and Newman (2003), could have lead to lower absolute survival compared to a population that had migrated in-river from natal tributaries or hatcheries to the Delta. If this process were pronounced in this study, I might have expected 1) low survival in the first reach following release, and 2) fish released at Sacramento to have higher survival probabilities through the interior Delta relative to fish that were released directly into the interior Delta at Georgiana Slough. In contrast, survival probabilities for the first reach of the Sacramento River were higher than all other reaches within this route (see S_{A1}, Appendix Table 3.3). Furthermore, the full model with different survival probabilities for each release site was not supported by the data. As for the effect of the transmitter, Hockersmith et al. (2003) found no difference in survival between radio tagged and PIT-tagged juvenile Chinook salmon over a similar distance as that studied here. Thus, I found little evidence to suggest that the low population-level survival through the Delta was a function of the source of fish or tagging methodology used for the study.

The strength of inferences from acoustic tag data to the untagged population depend on whether survival estimates are viewed from a relative or absolute point of view. Although I found no evidence that survival probabilities were lower than expected due to fish source or tagging method, I also have little basis with which to compare survival estimates from the study population to actively migrating populations of wild or hatchery origin in the Delta. However, regardless of the absolute magnitude of survival, differences among routes that influence survival should act similarly on all populations of salmon smolts migrating through

the Delta. For example, both tagged and untagged fish migrating through the interior Delta likely experienced lower survival through the Delta relative to fish migrating within the Sacramento River. Therefore, the relative difference in survival among routes from our data should provide stronger inference to untagged populations than will inferences about the absolute magnitude of survival probabilities. From this perspective, although survival was low for all migration routes during 2008, survival for routes through the interior Delta was at most 35% that of survival for fish remaining in the Sacramento River (Table 4.3). Future studies that include fish obtained from Coleman National Fish Hatchery paired with releases of in-river, actively migrating hatchery or wild fish would help to interpret the absolute magnitude of survival probabilities from this study in the context of other populations of interest.

The primary working hypothesis of management actions related to the operation of the Delta Cross Channel is that closing the Delta Cross Channel will increase population-level survival by reducing the fraction of the population entering the interior Delta where survival is lower than alternative migration routes. Implicit in this hypothesis is that the fraction of fish entering the interior Delta is proportional to the fraction of flow entering the interior Delta. In contrast to previous findings, I found that the proportion of fish entering each migration route did not necessarily agree with the proportion of mean discharge entering a route. Furthermore, deviations from this "expected" relationship acted to decrease the proportion of fish entering the interior Delta during the December release, but increase it during the January release. Based on distribution of mean discharge, closing the Delta Cross Channel reduced the total fraction of flow entering the interior Delta from 48.4% during the December release to 22.5% during the January release. However, for the December release, the proportion of fish entering the Delta Cross Channel was only about one-third the proportion of flow entering this route, whereas the proportion of fish entering Georgiana Slough was similar to the proportion of flow (Figure 4.5). Thus, the proportion of fish entering the interior Delta was less than might otherwise be expected based only on the distribution of river flow during the December release. During the January release, only about 20% of fish entered Sutter and Steamboat Slough even though 37% of Sacramento River flow entered this route (Figure 4.5). Therefore, a higher fraction of fish remained in the Sacramento River relative to that expected based on the proportion of flow in this route, which in turn exposed a higher fraction of the population to

entrainment into the interior Delta via Georgiana Slough. These findings show how variation in route entrainment probabilities at both major river junctions interacted to produce little observed difference between releases in the fraction of the population entering the Interior Delta, despite the Delta Cross Channel being open for the first release and closed for the second.

While dispersal of the population throughout the channel network of the Delta is likely driven in part by the distribution in mean river discharge among channels, my findings provide the first evidence that the distribution of fish entering each channel can deviate considerably from the distribution of flow entering each channel. Such deviation was expected by Burau et al. (2007), who identified a number of mechanisms likely to contribute to variation in route entrainment probabilities. First, flow distribution among the river channels at each junction varies with the tides on hourly time scales (Blake and Horn, 2003). Thus, diel patterns in migration behavior (Wilder and Ingram, 2006; Burau et al., 2007; Chapman et al., 2007) interacting with tidal fluctuations could produce route entrainment probabilities that deviate from that expected based on mean discharge. In addition, secondary circulation at river bends (Dinehart and Burau, 2005) combined with swimming behavior of juvenile salmon could concentrate the lateral distribution of migrating fish along the outside of river bends where they become more (or less) likely to be entrained into a given channel at a river junction (Burau et al., 2007). These fine-scale processes are an active area of research in the Delta (Burau et al., 2007) and should provide new insights into the mechanisms driving variability in route entrainment probabilities at river junctions.

While some aspects of migration and survival dynamics differed greatly between years, other patterns remained consistent. Although population-level survival in 2008 was lower than in 2007, the pattern of survival among routes was similar. During both releases, survival of fish migrating through the interior Delta was significantly less than for fish that remained in Sacramento River, which is consistent our findings in 2007 (Chapter 3) and with the findings of previous studies (Brandes and McLain, 2001; Newman and Rice, 2002; Newman, 2008; Brandes and Newman, 2010). This weight of evidence suggests that management actions that shift the distribution of the population from the interior Delta to the Sacramento River will improve population-level survival through the Delta. Similar to 2007, I

also found that survival through the Delta for fish migrating in Sutter and Steamboat Sloughs was significantly lower than the Sacramento River during the December release, but was comparable to the Sacramento River during the January release. Higher total river discharge (Figure 4.3) in January combined with a higher fraction of that discharge entering Sutter and Steamboat sloughs (Figure 4.5) could have improved migration conditions and reduced predation rates during the January release. Reach-specific survival rates increased for nearly all reaches of Sutter and Steamboat Slough (Figure 4.7), which is consistent with an increase in discharge through these reaches.

Quantifying survival rates per unit distance allowed me to identify patterns in reach-specific survival that generally followed the pattern of route-specific survival probabilities. Most reaches within the Sacramento River exhibited the highest survival rates during both releases, while most reaches within the interior Delta exhibited survival rates lower than the Sacramento River (Figure 4.6). These findings suggest that particular reaches within a route did not drive the observed differences in survival among migration routes. For instance, the lowest survival probabilities for the interior Delta were observed for the longest reach and included the most complex channel network with the pumping stations (see S_{D4} in Appendix Table 3.3). Yet survival rates for this reach were comparable to other reaches within this route when expressed as a function of reach length. In addition, I observed locally high mortality in the Cache Slough region downstream of station B_{13}, B_{23}, and A_6 for both releases. Last, survival rates in Sutter and Steamboat sloughs increased in January for nearly all reaches within this route. These patterns of variation among reaches suggest that factors influencing survival are operating at a spatial scale larger than an individual reach.

Reach-specific survival rates expressed with respect to distance traveled changed little between releases relative to the variability observed among reaches, especially for the Sacramento River (Figure 4.8). These findings suggest that factors other than migration distance (e.g., travel time) may also influence mortality rates. In contrast, in the Columbia River, survival rates of juvenile Chinook salmon have been significantly related to migration distance, but only weakly correlated to travel time (Muir et al., 2001; Anderson et al., 2005). Anderson et al. (2005) offered a hypothesis explaining this apparently contradictory finding. When prey migrate through a "gauntlet" of predators, predator-prey encounter rates will be

such that each prey encounters a predator at most once. Under these circumstances, predator-prey theory predicts that survival will be driven by distance traveled, but not by travel time. In contrast, when prey migration speeds are slow relative to predator swimming speeds such that multiple encounters are possible, then the situation reverses: the probability of survival becomes dependent on travel time. This hypothesis could partially explain the wide range in survival rates among reaches within the Sacramento River, but low variability between releases (Figure 4.7). Within our study area the Sacramento River transitions from river-driven discharge in the uppermost reaches to tidally driven discharge in the lower reaches. Coincident with this transition, fish movement patterns shift from downstream-only movements to both upstream and downstream movements in the lower reaches of the Delta. Thus, in lower reaches of the Delta fish may pass through a given reach more than once, which could increase predator encounter rates relative to the length of each reach.

This research continues to provide critical information to understand factors influencing migration and survival dynamics of juvenile Chinook salmon migration through the Delta. Improved precision of parameter estimates allowed me detect statistically significant differences in survival among migration routes. While some findings were similar to 2007, such as low survival through the Interior Delta relative to the Sacramento River, other findings deviated considerably between years. Survival through the Delta was less than 20% during 2008 (compared to 35%-54% in 2007), route-entrainment probabilities deviated from the fraction of mean river discharge entering each channel, and the proportion of the population entering the interior Delta was similar between releases despite closure of the Delta Cross Channel. Given the substantial variation in survival, route entrainment, and migration route probabilities observed among four releases and two years, I suspect that my analyses are just beginning to unmask the temporal and spatial variability in migration and survival dynamics in the Delta. Nonetheless, even with such variability, patterns in survival and movement dynamics are beginning to emerge. With the addition of migration data collected during the winter of 2008/2009, I plan to quantify factors that influence survival and migration route probabilities. Such information should provide insights into management actions that will improve survival of juvenile salmon populations migrating through the Sacramento-San Joaquin River Delta.

Chapter 5

**INDIVIDUAL-, RELEASE-, AND ROUTE-SPECIFIC VARIATION
IN SURVIVAL OF JUVENILE CHINOOK SALMON
MIGRATING THROUGH THE SACRAMENTO–SAN JOAQUIN
DELTA**

5.1 Introduction

In previous chapters, I developed an analytical framework for quantifying survival of
juvenile salmon migrating through the Sacramento-San Joaquin Delta. Key aspects of this
framework include estimating survival of fish migrating through different pathways in the
Delta and quantifying the fraction of the population using each migration route. Such an
approach allowed me to explicitly quantify how survival through each migration route
contributes to population-level survival. I applied this framework to acoustic tagging data from
two migration seasons and found that survival of fish migrating through the Interior Delta was
significantly lower than survival of fish remaining in the Sacramento River. While differences
among routes remained similar between years, survival through all routes in 2008 was
considerably lower than in 2007. In addition, I found that the distribution of fish among
migration routes generally followed the distribution of river flow, but sizeable deviations from
this relationship suggested that factors other than mean river flow also affect fish routing. The
final two chapters of my dissertation focus on quantifying the mechanisms responsible for
variability in survival and route entrainment probabilities. This chapter focuses on survival,
while questions related to route entrainment probabilities are reserved for the next chapter.

Past studies examining the relation between environmental variables and survival in
the Delta have identified Sacramento River flow, water temperature, tides, position of the Delta
Cross Channel gates, salinity, and to a lesser extent, water exports as important factors
affecting survival (Kjelson and Brandes, 1989; Newman and Rice, 2002; Newman, 2003, 2008,
Newman and Brandes, 2010). These experiments have provided critical information to
develop water management actions that aid in the recovery of endangered salmon. One

limitation, however, is that the response variable has often been the ratio of recapture rates of coded-wire-tagged fish (CWT) between different release locations, which reduces to the ratio of survival probabilities under the assumption of equal capture probabilities. Ratios of recapture rates have then been modeled as a function of covariates (e.g., exports). When modeling ratios, it is impossible to disentangle the relation of the covariate with each of the underlying survival rates, and therefore, inference about the effect of the covariate on survival is indirect. In contrast, acoustic telemetry data allow for direct modeling of the survival probabilities for each migration route as a function of the relevant environmental variables. Since population-level survival is driven by the relative differences in survival among routes, explicitly modeling survival rates within migration routes is critical to understand how differences among routes arise. In this chapter, I capitalize on these advantages of acoustic tags to understand differences in survival among migration routes and factors affecting survival within routes.

This chapter unfolds as follows: First I use the multistate mark-recapture model presented in earlier chapters to estimate survival and migration route probabilities from acoustic tagged fish migrating through the Delta during winter 2008/2009 (hereafter, "2009"). This analysis proceeds much as in Chapters 3 and 4, but excludes most of the methods already presented in earlier chapters. I then examine patterns of variation in route-specific survival over all years (2007–2009). Last, to explain variability in survival, I undertake an analysis of this three-year data set along with additional acoustic tag data from a study conducted by UC Davis and NOAA fisheries. Since this chapter focuses on survival, I simplified the mark-recapture framework by excluding route entrainment probabilities, and I used a Cormack-Jolly-Seber mark-recapture model to examine effects of covariates. I incorporate both group-level covariates (migration route, study, release group, year) and individual covariates (river flow, fish size), then select among a set of alternative models to identify factors responsible for variation in survival.

5.2 Methods

5.2.1 Survival and migration route probabilities in 2009

I used a modified version of the multistate mark-recapture model presented in previous chapters to estimate survival and migration route probabilities for the 2009 migration year. Since statistical methods were presented extensively in previous chapters and experimental design remained largely unchanged, here I present only details of the 2009 study that differed from previous years. Other details of the 2009 study, such as model schematic and reach-specific parameter estimates, can be found in Appendix 4.

Release timing, release locations, and telemetry system design closely followed the design used in 2008. A number of telemetry stations used in 2008 were not implemented in 2009 (Figure 5.1), but since these stations divided reaches within routes, the model structure remained essentially unchanged from that presented in Chapter 4 (compare Figure 4.2 to Appendix Figure 4.1). Release timing and release locations were similar to 2008, with fish released at Sacramento and also in Georgiana Slough to increase sample sizes of fish migrating through the Interior Delta (Table 5.1). All fish were surgically implanted with VEMCO acoustic tags at Coleman National Fish Hatchery and transported to release sites where they were held in-river for 24 h prior to release. At each location, fish were released in early December and again in mid-January.

The first release group was intended to pass the Delta Cross Channel when the cross channel gates were open, and the second release group when the gates were closed; but a substantial fraction of the first release group passed the Delta Cross Channel after the gates had closed. Therefore, as presented in Chapter 3, I incorporated a parameter to estimate the probability of fish passing this river junction when the gates were open (ω_{open}). I then estimated route entrainment probabilities conditional on gate position (i.e., $\Psi_{hl,open}$ and $\Psi_{hl,closed}$). Route-specific survival was estimated for each release as described in Chapter 4. Thus, for the first release group, route-specific survival represents the average survival over conditions experienced by this release-group; that is, with the Delta Cross Channel gates both open and closed.
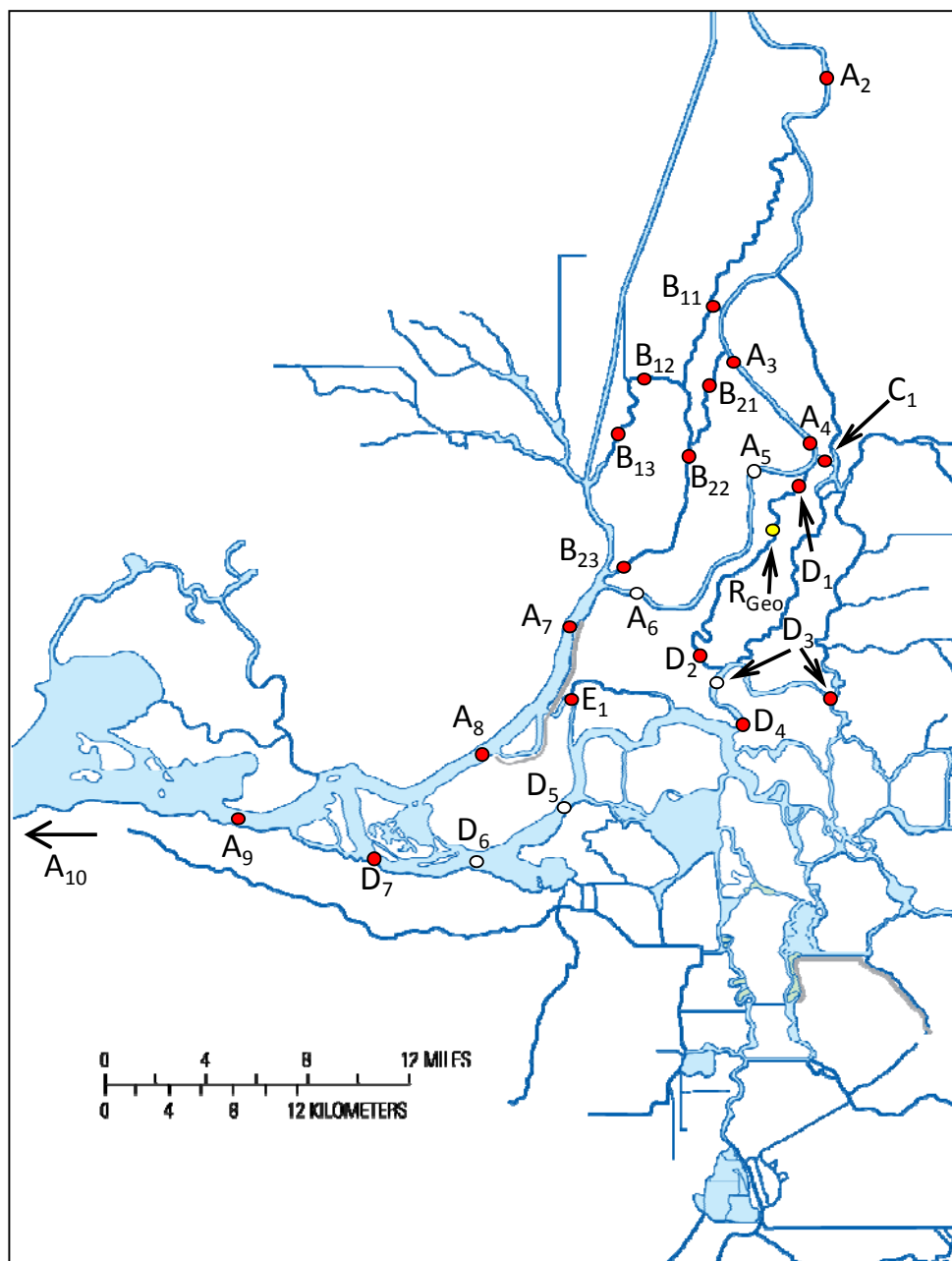
Figure 5.1. Location of telemetry stations used to estimate survival and migration route probabilities within four major migration routes of the Sacramento–San Joaquin River Delta during the winter of 2009. Red-filled circles labeled as h_i show the location of telemetry station i with route h. Locations denoted by unfilled circles show telemetry stations used in 2008 but not 2009. Station A_{10} pools all telemetry stations in San Francisco Bay downstream of A_9. The Sacramento release site was 19 river kilometers upriver of station A_2, and the Georgiana release site is noted as the yellow-filled circle labeled as R_{Geo}.

Table 5.1. Summary of release dates, release locations, and sample size of acoustically tagged late-fall Chinook salmon released into the Delta during the winter of 2009.

Release dates	Release number	Release location	Sample size
Nov 30 –Dec 4	1	Sacramento	192
Dec 2 –Dec 6	1	Georgiana Slough	100
Jan 13 – Jan 17	2	Sacramento	192
Jan 15 – Jan 19	2	Georgiana Slough	100

5.2.2 Multiyear analysis of route-specific survival

To quantify factors affecting survival over the three-year duration of this study, I incorporated covariates into a Cormack-Jolly-Seber (CJS) model that focused on a subset of the Delta (Cormack, 1964; Jolly, 1965; Seber, 1965). The CJS model was constructed to estimate survival to the exit of the Delta at Chipps Island from entry points into three major migration routes: 1) Sutter and Steamboat sloughs, 2) the Sacramento River, and 3) the interior Delta.

I examined a subset of the full multistate model for three reasons: First, the telemetry system differed in each year of study, resulting in year-specific multistate models that varied in their level of the spatial resolution. Second, my goal in this chapter was to examine factors affecting survival at the migration-route scale, rather than at the scale of reaches within routes. In Chapter 4, I found that changes in survival between releases occurred simultaneously for all reaches within a route (e.g., Sutter and Steamboat sloughs). This finding suggested that processes affecting survival acted at the migration-route scale rather than at the scale of reaches within routes. Last, I wanted to model survival as a function of individual covariates but imperfect detection probabilities for stations in the lower Delta made it impossible to use individual covariates due to missing covariate values for many fish. Rather, focusing the model on key entry points into migration routes where detection probabilities were nearly perfect allowed me to incorporate individual covariates without estimation and bias problems associated with missing covariate values (Catchpole et al., 2008).

Detections at key telemetry stations formed virtual "release" points where survival was modeled from the point of entry into each route. Virtual release points were formed from telemetry stations at the entry to Sutter and Steamboat sloughs (stations B_{11} and B_{21}), the

Sacramento River at its junction with the Delta Cross Channel and Georgiana Slough (station A_4), and the lower Mokulemne River where it enters the San Joaquin River (station D_4; Figure 5.1). Since detection probabilities at these locations were nearly perfect (See Appendix Tables 1.2, 3.3, and 4.3), conditioning the analysis on only detected fish resulted in little loss of information. Survival was then modeled for a single reach from each of these stations to Chipps Island. Reach length via the shortest possible pathway was 41.9 km for the interior Delta, 50.3 km for Sutter and Steamboat sloughs, and 51.9 km for the Sacramento River.

Reaches not included in this analysis are the Sacramento River from the release point at Sacramento to station A_4, the Delta Cross Channel from its junction with the Sacramento River to station D_4, and Georgiana Slough from the release location or from its junction with the Sacramento River to station D_4 (Figure 5.1). The upper reaches in the Sacramento River were excluded because telemetry stations were not implemented consistently in all years and survival in these reaches remained relatively high over all years of study (Appendix Tables 1.2, 3.3. and 4.3). The short reaches comprising Georgiana Slough, the Delta Cross Channel, and the North and South forks of the Mokelumne River were excluded so that survival of fish from both routes could be estimated simultaneously after they converge at the mouth of the Mokelumne River.

In addition to the USFWS study on which previous chapters are based, I also incorporated telemetry data from a CALFED-funded study (http://californiafishtracking. ucdavis.edu/, accessed December 2009). Telemetry data from both studies consisted of fish released during the winters of 2007, 2008, and 2009 from 11 release groups (Table 5.2). The CALFED and USFWS studies collaborated on tagging efforts, and the same personnel surgically implanted transmitters for both studies using methods described in Chapter 3. All juvenile salmon were monitored with same system of VEMCO telemetry stations. Although release sites varied among studies and years, all fish in the Sacramento River were released a minimum of 40 km upstream of entry points to migration routes used in the CJS model. By combining data from both studies, 932 fish were included in the analysis: 381 for the Sacramento River, 264 for Sutter and Steamboat sloughs, and 287 for the Interior Delta (Table 5.2).

Table 5.2. Route-specific sample sizes used in the CJS model for release groups of juvenile late-fall Chinook salmon implanted with acoustic tags during the winters of 2007 – 2009.

Study	Migration year	Release group	Release dates	Sacramento River	Steamboat and Sutter Slough	Interior Delta
USFWS	2007	1	Dec 5 – Dec 6	18	16	7
CALFED		2[*]	Jan 16–Feb 2	8	1	2
USFWS		3[*]	Jan 17 – Jan 18	33	29	2
USFWS	2008	4	Dec 4 – Dec 5	44	45	53
CALFED		5	Dec 7	22	12	8
USFWS		6	Jan 15 –Jan 16	52	23	73
CALFED		7	Jan 17	32	18	12
USFWS	2009	8	Nov 30 –Dec 4	56	48	48
CALFED		9	Dec 13	38	20	17
CALFED		10	Jan 11	19	15	6
USFWS		11	Jan 13 –Jan 17	59	37	59
All groups				381	264	287

[*]These release groups were pooled for analysis because sample sizes for release group 2 were inadequate for estimating route- and release-specific survival.

5.2.3 Incorporating covariates into the CJS model

The CJS model had two sampling occasions with four possible captures histories (111, 110, 101, and 100). The two occasions were formed from detections at station A_9 (Chipps Island) and station A_{10} (seaward of Chipps Island; Figure 5.1). I structured the negative log-likelihood of the CJS model following the approach of Skalski et al. (1993) where each individual's contribution to the likelihood is explicit:

$$\ln L\left(S_i, p_i, \lambda_i \mid \mathbf{Y}\right) = -\sum_{i=1}^{n} y_{i,111} \ln\left(S_i p_i \lambda_i\right) + y_{i,110} \ln\left(S_i p_i (1-\lambda_i)\right)$$
$$+ y_{i,101} \ln\left(S_i(1-p_i)\lambda_i\right) + y_{i,100} \ln\left(1 - S_i + S_i(1-p_i)(1-\lambda_i)\right). \tag{5.1}$$

Here, y_{ij} is an indicator variable resolving to 1 if the ith fish has the jth capture history, and zero otherwise, S_i is the probability of the ith fish surviving to Chipps Island from one of three starting points in the Delta, p_i is the detection probability of the ith fish at Chipps Island, and λ_i is the joint probability of the ith fish surviving and being detected at telemetry stations in San Francisco Bay. This model is overparameterized, and parameters for each individual are estimable only when constrained as a function of group-level or individual covariates.

I used the framework of generalized linear models (glm; McCullough and Nelder, 1989) to link a linear function of the CJS parameters, $g(\theta)$, to the covariates. I used a logit link function for all parameters:

$$g\left(\theta_i\right) = \ln\left(\frac{\theta_i}{1+\theta_i}\right) = \beta_0 + \beta_1 x_{i1} + ... + \beta_p x_{ip} = \boldsymbol{\beta}'\mathbf{x}_i \tag{5.2}$$

where $\theta_i = S_i, p_i,$ or λ_i; β_0 is the intercept; and β_j is the slope parameter for $j = 1, …, p$ covariates, x_{ij}. The covariates were introduced into the negative log-likelihood using the inverse logit function:

$$\theta_i = \frac{\exp\left(\boldsymbol{\beta}'\mathbf{x}_i\right)}{1+\exp\left(\boldsymbol{\beta}'\mathbf{x}_i\right)} \tag{5.3}$$

and the likelihood was iteratively minimized using optimization routines in the R statistical computing platform (R Development Core Team, 2008) to estimate the vector of β parameters. The variance-covariance matrix was estimated as the inverse of the observed Hessian matrix.

5.2.4 Defining group and individual covariates

I modeled survival through the Delta as function of both group-level and individual covariates. Individual covariates consisted of fork length and route-specific river discharge when individuals entered each route. Group-level covariates consisted of study (USFWS or CALFED), migration route, migration year, and mean river discharge for each release group and migration route.

I hypothesized that the 3-d period after fish entered a migration route was a critical period during which hydraulic conditions of the river could affect survival. Thus, individual covariates for river discharge were defined by mean discharge for the 3-d period after each fish entered the reach of interest. This time period was based on median travel times to the lower Sacramento River at Rio Vista (station A_7; Figure 5.1) from virtual release points in the Sacramento River (median = 2.4 d) and Sutter and Steamboat sloughs (median = 3.1 d). For the Interior Delta, I also focused on a 3-d period, hypothesizing that river conditions shortly after fish enter the San Joaquin River would influence their probability of moving towards the ocean or towards pumping stations in the southern Delta, which in turn, could affect survival.

For fish migrating through the Sacramento River, I modeled survival as a function of Sacramento River discharge just downstream of Georgiana Slough (Q_S, between stations A_4 and A_5 in Figure 5.1; also see Figure 6.1). Since the Delta Cross Channel diverts river flow upstream of this location, this gauging station measures flow remaining in the Sacramento River in response to operation of the cross channel gates. To capture the effect of tidal fluctuations on survival, I also considered the standard deviation of 15-min discharge over the 3-d period as a possible covariate. However, I found that the mean and standard deviation of discharge were highly correlated ($r = -0.864$, Figure 5.2). As inflow increases, tidal fluctuations are dampened; therefore, I used only mean discharge in the model because it quantifies both the effect of river inflow and the effect of inflow on tidal fluctuations.
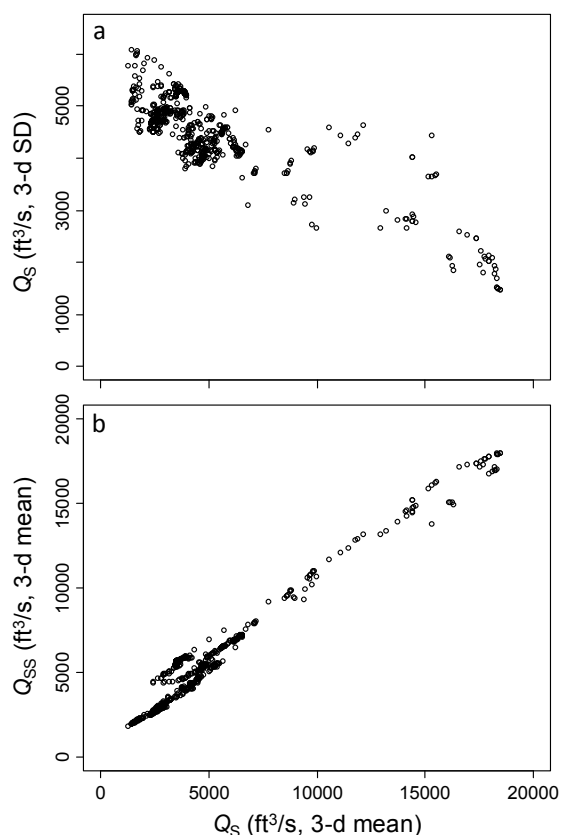
Figure 5.2. Relation between mean Sacramento River discharge measured downstream of Georgiana Slough (Q_S) with a) the standard deviation of Q_S, and b) the mean discharge entering Sutter and Steamboat sloughs (Q_{SS}). Means and standard deviations were calculated from 15-min flow data during the 3-d period following detection of tagged fish entering the Sacramento River and Sutter and Steamboat sloughs.

I also used Q_S for Sutter and Steamboat sloughs because 1) Q_S was highly correlated with discharge entering Sutter and Steamboat Slough ($r = 0.98$, Figure 5.2), 2) fish from both routes migrate through a common reach in the lower Sacramento River (Figure 5.1), and 3) using the same flow covariate allowed me to test whether the slope coefficients differed between migration routes. Specifically, the effect of Q_S on survival was modeled with the following structure (excluding the other covariates for clarity):

$$g(S) = \beta_1(I_{Sac} + I_{SS})Q_S + \beta_2 I_{SS}Q_S$$

where I_{Sac} and I_{SS} are dummy variables resolving to one when fish enter the Sacramento River (Sac) or Sutter and Steamboat sloughs (SS), and zero otherwise. With both terms in the model, the first estimates the slope for the Sacramento River and the second estimates the difference in slopes between the Sacramento River and Sutter and Steamboat sloughs. Thus, the null hypotheses $\beta_2 = 0$ explicitly tests whether the effect of Q_S on survival differs between migration routes.

River flow and migration routing in the interior Delta is more complex than the other migration routes. Once fish exit the Mokelumne River and enter the San Joaquin River, their probability of surviving may depend on whether they move seaward or inland towards the pumping stations. The probability of fish moving towards the pumps likely depends on the balance of flows exiting the Mokelumne River and the San Joaquin River relative to water exports at the pumping stations. Thus, individual covariates for the interior Delta were defined as mean 3-d discharge of water exports at the pumping stations (Q_E), of the Mokelumne River where fish enter the San Joaquin River (Q_M, near station D_4), and of the San Joaquin River at Jersey Point (Q_J, near station D_5, Figure 5.1).

I formed group-level covariates for river flow by averaging the individual covariates over each release group and migration route. This approach is equivalent to a weighted average with weights proportional to the distribution of entry times to each reach. All covariates were standardized by subtracting the mean from each observation and then dividing by the standard deviation.

5.2.5 Model selection

I used a three-phase approach to determine factors affecting route-specific survival: I first identified the best-fit model for p and λ and used this model as a basis fitting covariates to survival. Second, I modeled group-level covariates using analysis of deviance (ANODEV). Last, I selected among models with individual covariates using likelihood-ratio tests (LRT) and Akaike's Information Criterion (AIC; Burnham and Anderson, 2002).

I used ANODEV because it explicitly accounts for overdispersion and replication at the route- and release group-level. Since the analysis consisted of only 10 release groups and 3 reaches, ANODEV "penalizes" for this low level of replication through the effects of the "source" and "error" degrees of freedom on the F test. Furthermore, the error mean deviance quantifies overdispersion (release-to-release variability unexplained by covariates in the model), ensuring that test statistics for model selection remain unbiased. Because likelihood ratio tests (LRT) account for only multinomial sampling variability, they too often reject the null hypothesis of no covariate effect in the presence of variability that is unrelated to the group covariates (Skalski et al., 1993). In contrast, I used LRT for the individual covariates because LRT remains unbiased for individual covariates in the presence extra variability unrelated to the covariate (Skalski et al., 1993).

The fully saturated model estimated a unique p and λ for each release group and unique survival probabilities for each release group and migration route. Using the glm framework, this model was parameterized by including a main effect of release group for p and λ; and release group, route, and a release:route interaction for S (where ':' denotes interaction) . Given this saturated model, I evaluated reduced models for p and λ that consisted of year-specific parameters and constant p and λ over all years. I first selected the best model for λ and then fit models for p under the best λ model. The best-fit λ and p models were selected on the basis of LRT and AIC.

At the group level, I fit a model with all covariates which included route, year, study, Q_S for the Sacramento River and Sutter and Steamboat sloughs, and Q_M, Q_J, and Q_E for the Interior Delta. I then constructed an ANODEV table analogous to ANOVA tables that partition the variance among different sources of error (Skalski et al., 1993). To select

variables for inclusion in the model, I used stepwise selection, adding variables to the ANODEV table in order of the largest reduction in negative log-likelihood (NLL; Skalski et al., 1993). Interaction terms were always added to the model with their corresponding main effects. This approach results in a sequential ANODEV table where the *F* test for a given variable includes all other covariates previously added to the model.

For individual covariates, I added fork length (*L*) and flow variables to the saturated model for survival (i.e. to the model with route, release group, and route:release group). First, to test for differences in slopes among release groups, I considered interactions between release group and individual covariates. However, when simultaneously including all possible two-way interactions in the model, maximization of the likelihood became unstable and many parameters became inestimable, which was likely due to small sample size for some of the releases and routes (Table 5.2). Instead, prior to forming a full model, I added each covariate separately to the saturated model, crossed the covariate with release group, fixed inestimable slope parameters to zero, and then compared this model against the corresponding model lacking an interaction. None of the interactions were significant using LRT at $\alpha = 0.05$, so they were not included in the full model. Therefore, the full model with individual covariates estimated unique intercepts for each release group-route combination, but a common slope over all release groups.

Only the individual covariates were considered for model selection, keeping route, release, and route:release group in all models. The intent here was twofold: first, my goal was to explain within-release variation in survival over and above that accounted for by route and release group. Second, maintaining group-level structure ensured that group differences in survival were not wrongly attributed to the individual covariate. When covariate values do not overlap among groups, and group survival differs due to factors other than the covariate, LRT may falsely attribute a covariate effect to the group differences in survival (Hoffman and Skalski, 1995). However, Hoffman and Skalski (1995) showed that the LRT was unbiased when individual covariates were added to the fully saturated model. I used reverse elimination of covariates to identify the best-fit model, dropping terms one-at-a-time from the full model, eliminating the variable that least explained variation in survival (using LRT and AIC), re-fitting the reduced model, and then eliminating the next variable. Covariates were eliminated

until no variable could be dropped without resulting in a significantly poorer fit based on a substantial increase in AIC and evaluation of LRT at $\alpha = 0.05$.

5.3 Results

5.3.1 Migration routing and survival in 2009

Sacramento River discharge was less than 10,000 ft^3/s for much of the study period, and travel times of the first release group were substantially longer than observed in previous years (Figures 5.3 and 5.6). For the December release group, the median travel time to junction 2 (Stations A_4, C_1, and D_1; Figure 5.1) was 13 days, and the central 80% of this release group took 25 days to pass the second river junction. The January release group exhibited much shorter travel times to river junction 2 (median = 4.1 days) and a more compressed distribution, despite flows remaining low (Figure 5.3). These findings suggest that the first release group may not have been actively migrating smolts at the time of release. Travel times of the first release group to the outlet of the Delta were substantially longer than the second release group and their arrival distributions overlapped. For the first release group, the median travel time to Chipps Island was 25 days, but arrival at Chipps Island was distributed over nearly two months. For the second release group, the median travel time was 10.9 days and arrival times between the 10th and 90th percentile were distributed over 32 days. All fish exited the Delta with the onset of a freshet in late February.

Migration route probabilities varied according to the position of the Delta Cross Channel gate. The first release group was supposed to pass the Delta Cross Channel while its gates were open, but long travel times caused 45% of fish to pass the Cross Channel when the gates were closed (See ω_{open}, Appendix Table 4.3). For this release group, fish that passed when the Delta Cross was open distributed in thirds among the Sacramento River, Sutter and Steamboat Slough, and interior Delta (via the Delta Cross Channel or Georgiana Slough; Table 5.3). For routes leading to the interior Delta, 22.4% of the population entered through the Delta Cross Channel, whereas 12.4% entered through Georgiana Slough (Table 5.3). In contrast, of the fish from the first release group that passed the Delta Cross Channel when the gates were closed, 46.6% remained in the Sacramento River and 21.2% entered the Interior
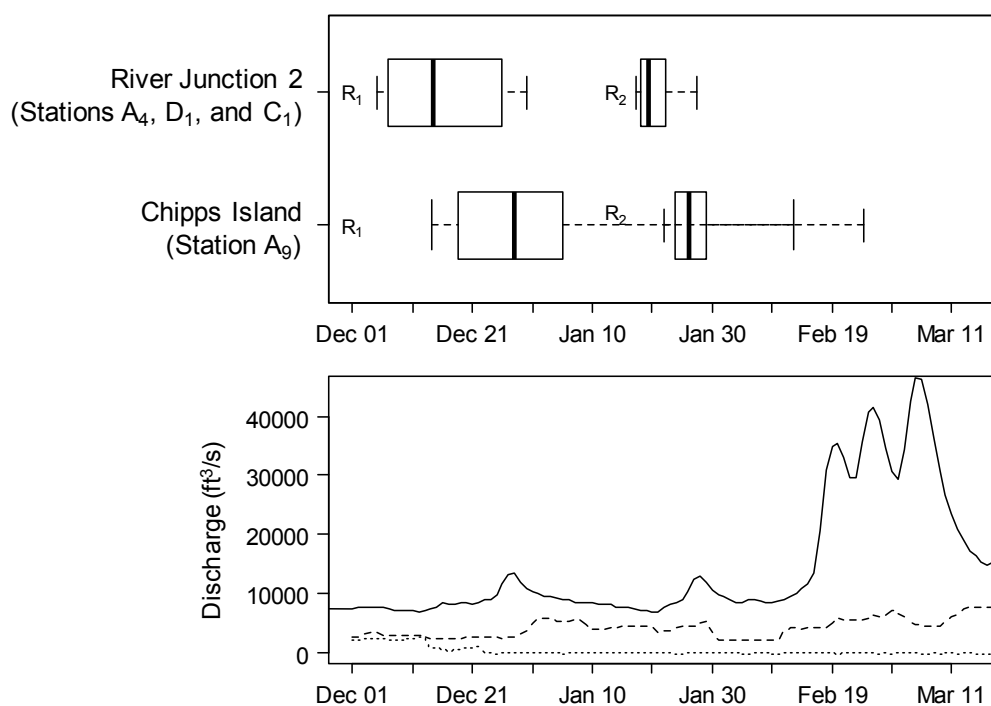
Figure 5.3. River discharge, water exports, and Delta Cross Channel discharge during the migration period of tagged juvenile Chinook salmon migrating through the Sacramento–San Joaquin River Delta during the winter of 2009. Box plots show the distribution of arrival dates at Junction 2 on the Sacramento River (telemetry stations A_4, C_1, and D_1) and at Chipps Island, the terminus of the Delta (telemetry station A_9). Release dates are shown as R_1 and R_2. Whiskers represent the 10th and 90th percentiles, the box encompasses the 25th to 75th percentiles, and the line bisecting the box is the median arrival date. For Chipps Island, whiskers have different widths to distinguish the overlap in arrival distributions. River discharge (solid line) is tidally filtered, daily discharge of the Sacramento River at Freeport (near telemetry station A2), Delta Cross Channel discharge (dotted line) is the tidally filtered daily discharge, and water exports (dashed line) are the total daily discharge of water exported from the Delta at the pumping projects.

Delta. Since the Delta Cross Channel was closed, migration route probabilities for the second release group were similar to those of the first release group that encountered a closed gate (Table 5.4). Closing the Delta Cross Channel increases discharge entering both the Sacramento River and Georgiana Slough. Coincident with this increase in flow, migration route probabilities for both releases indicate that the fraction of fish in both Georgiana Slough and the Sacramento River increased when the gate was closed. In Chapter 6, I expand on these findings to explicitly quantify entrainment probabilities as a function discharge entering each route.

Table 5.3. The probability of migrating through each route (Ψ_h) for acoustically tagged late fall-run juvenile Chinook salmon released in December 2008 as a function of gate position when fish passed the Delta Cross Channel.

Migration route	Cross Channel Open		Cross Channel Closed	
	$\hat{\Psi}_h$ ($\widehat{SE}$)	95% Profile likelihood interval	$\hat{\Psi}_h$ ($\widehat{SE}$)	95% Profile likelihood interval
A) Sacramento R.	0.331 (0.050)	0.238 , 0.431	0.466 (0.054)	0.360, 0.569
B) Sutter & Steamboat S.	0.321 (0.037)	0.251 , 0.397	0.321 (0.037)	0.251, 0.397
C) Delta Cross Channel	0.224 (0.045)	0.145 , 0.318	NA	
D) Georgiana S.	0.124 (0.036)	0.065 , 0.206	0.212 (0.049)	0.128, 0.315

Survival through the Delta was comparable between release groups even though the first release group had substantially longer travel times. Survival through the Delta was 0.386 for the first release group and 0.339 for the second release group (Table 5.4). Since half of the first release group encountered a closed Delta Cross Channel gate, migration route probabilities did not differ drastically between releases, resulting in similar contributions of route-specific survival to population-level survival. Among routes, fish migrating in the Sacramento River and Sutter and Steamboat sloughs exhibited the highest survival probabilities whereas fish migrating through the Delta Cross Channel and Georgiana Slough had lower survival (Table 5.4). For both releases, survival probabilities for the Sacramento River and Sutter and Steamboat sloughs ranged from 0.394 to 0.448. In contrast, survival probabilities ranged from 0.117 to 0.315 for fish migrating through the Interior Delta (Table 5.4).

The ratio of survival through each route relative to the Sacramento River (θ_h) indicated that fish entering the Interior Delta had significantly lower survival for two of the three survival probabilities. Fish entering the Delta Cross Channel exhibited significantly lower survival than the Sacramento River, as did fish entering Georgiana Slough from the second release group (Table 5.5). Although $\hat{\theta}_D = 0.70$ indicated lower survival of fish entering Georgiana Slough for the first release group, the 95% confidence interval encompassed one. For Sutter and Steamboat sloughs combined, θ_B was not different from one during either release. However, considering these routes separately, fish from the first release group entering Sutter Slough exhibited significantly lower survival but fish entering Steamboat

Slough had significantly higher survival than the Sacramento River. For the second release

group, fish within each of these routes experienced similar survival as fish remaining in the

Sacramento River (Table 5.5).

Table 5.4. Route-specific survival through the Sacramento–San Joaquin River Delta (S_h) and
the probability of migrating through each route (Ψ_h) for acoustically tagged late-fall juvenile
Chinook salmon released in December 2008 (R_1) and January 2009 (R_2). Also shown is
population survival through the Delta (S_{Delta}), which is the average of route-specific survival
weighted by the probability of migrating through each route.

Migration route	$\hat{S}_h\ (\widehat{SE})$	95% Profile likelihood interval	$\hat{\Psi}_h\ (\widehat{SE})$	95% Profile likelihood interval
R_1: December 2008				
A) Sacramento R.	0.448 (0.053)	0.348, 0.553	0.392 (0.040)	0.354, 0.458
B) Sutter & Steamboat S.	0.394 (0.056)	0.296, 0.507	0.321 (0.037)	0.251, 0.397
B$_1$) Sutter S.	0.281 (0.061)	0.172, 0.407	0.217 (0.033)	0.157, 0.288
B$_2$) Steamboat S.	0.632 (0.059)	0.509, 0.741	0.104 (0.025)	0.062, 0.158
C) Delta Cross Channel	0.117 (0.048)	0.044, 0.228	0.224 (0.045)	0.145, 0.318
D) Georgiana S.	0.315 (0.054)	0.216, 0.426	0.164 (0.164)	0.112, 0.226
S_{Delta} (All routes)	0.386 (0.038)	0.315, 0.463		
R_2: January 2009				
A) Sacramento R.	0.398 (0.051)	0.308, 0.484	0.459 (0.043)	0.404, 0.498
B) Sutter & Steamboat S.	0.432 (0.067)	0.394, 0.514	0.253 (0.036)	0.188, 0.328
B$_1$) Sutter S.	0.426 (0.086)	0.271, 0.468	0.096 (0.024)	0.055, 0.151
B$_2$) Steamboat S.	0.436 (0.075)	0.372, 0.518	0.158 (0.030)	0.105, 0.222
C) Delta Cross Channel	NA		0.000 (0.000)	
D) Georgiana S.	0.163 (0.033)	0.146, 0.204	0.288 (0.040)	0.219, 0.361
S_{Delta} (All routes)	0.339 (0.035)	0.310, 0.379		

Table 5.5. The ratio (θ_h) of survival through route h (S_h) to survival through the Sacramento River (S_A) for acoustically tagged late fall-run juvenile Chinook salmon released in December 2008 and January 2009.

| Migration route | R_1: December 2008 | | R_2: January 2009 | |
	$\hat{\theta}_h$ ($\widehat{SE}$)	95% Profile likelihood interval	$\hat{\theta}_h$ ($\widehat{SE}$)	95% Profile likelihood interval
B) Sutter & Sutter S.	0.879 (0.131)	0.644, 1.170	1.086 (0.199)	0.872, 1.251
B$_1$) Sutter S.	0.626 (0.139)	0.383, 0.925	1.070 (0.239)	0.832, 1.227
B$_2$) Steamboat S.	1.410 (0.144)	1.148, 1.728	1.096 (0.215)	0.977, 1.443
C) Delta Cross Channel	0.260 (0.109)	0.098, 0.527	NA	
D) Georgiana S.	0.703 (0.139)	0.466, 1.014	0.409 (0.094)	0.374, 0.449

5.3.2 Interannual patterns in route-specific survival

I observed substantial variation in the magnitude of within-route survival among years, yet stable patterns of survival across routes over all years. Among years, 2008 stands out as having the lowest survival at both the route scale and the Delta scale (Figure 5.4 and 5.5). Survival through the Delta was <0.20 for 2008, but > 0.33 for all other years and releases. In contrast, given that fish experienced the lowest flows in 2009 (Figure 5.6), estimates of S_{Delta} for 2009 were substantially higher than might be expected when compared relative to S_{Delta} for 2008 (Figure 5.4). Over all years, estimates of S_{Delta} exceeded 0.40 for only one release group (Dec. 2007), and only during 2007 did observed estimates of S_{Delta} differ between releases. Although rankings of route-specific survival vary somewhat across releases, one pattern remained constant: survival probabilities for the Sacramento River were always greater than survival for migration routes through the Interior Delta (via Georgiana Slough and the Delta Cross Channel; Figure 5.4). In addition, Sutter and Steamboat sloughs exhibited either similar survival to the Sacramento River (typically for January releases) or lower survival than the Sacramento River (typically for December releases). Except for the December release group in the 2007 migration year, observed survival estimates for Sutter and Steamboat Sloughs were greater than for routes leading to the Interior Delta. These findings clearly show that migration routes leading to the Interior Delta will reduce population survival proportional to the fraction of the population entering the interior Delta.
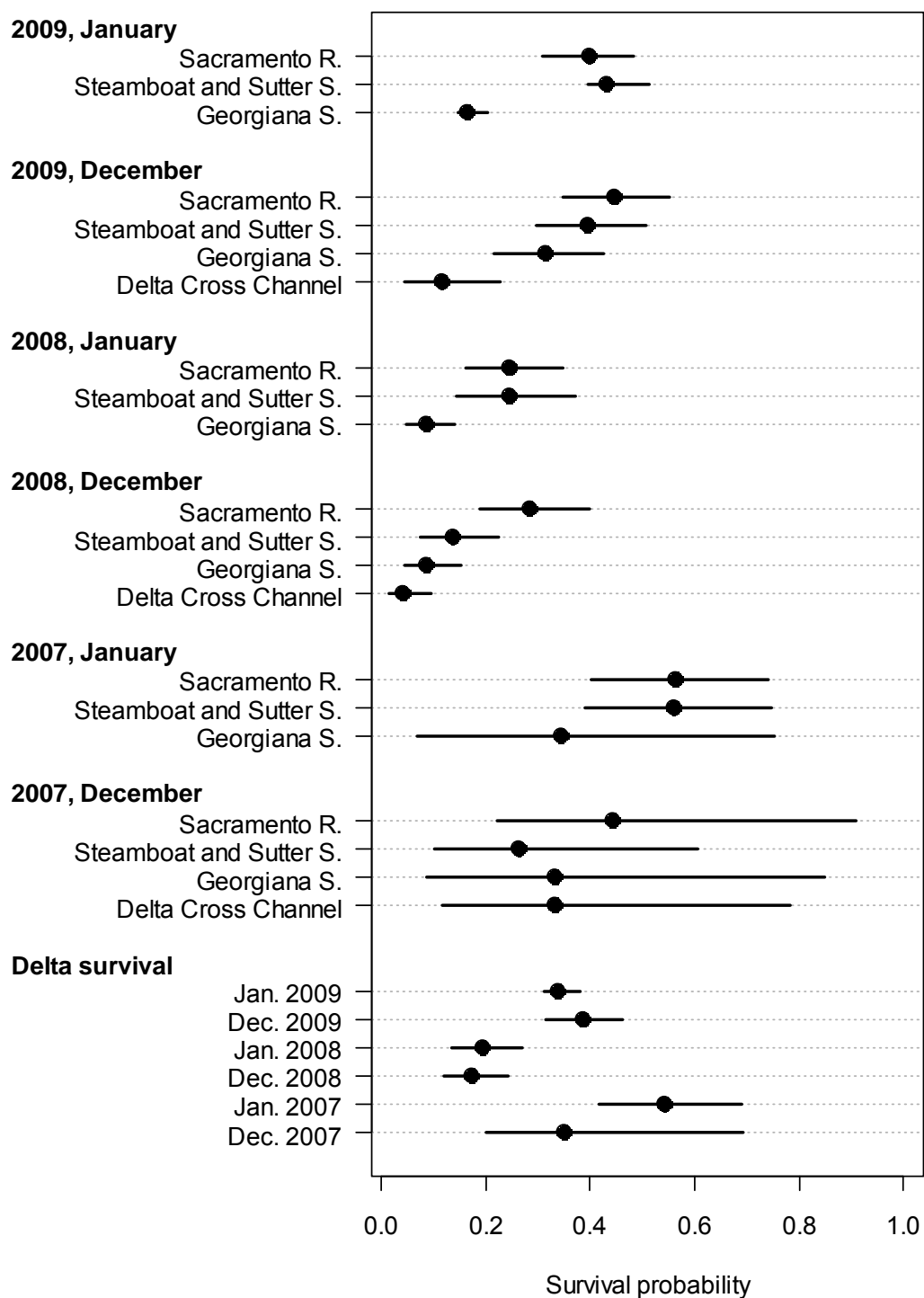
Figure 5.4. Summary of route-specific survival probabilities during migration years 2007–2009. Data points are organized by release group to facilitate comparison among routes within each release.
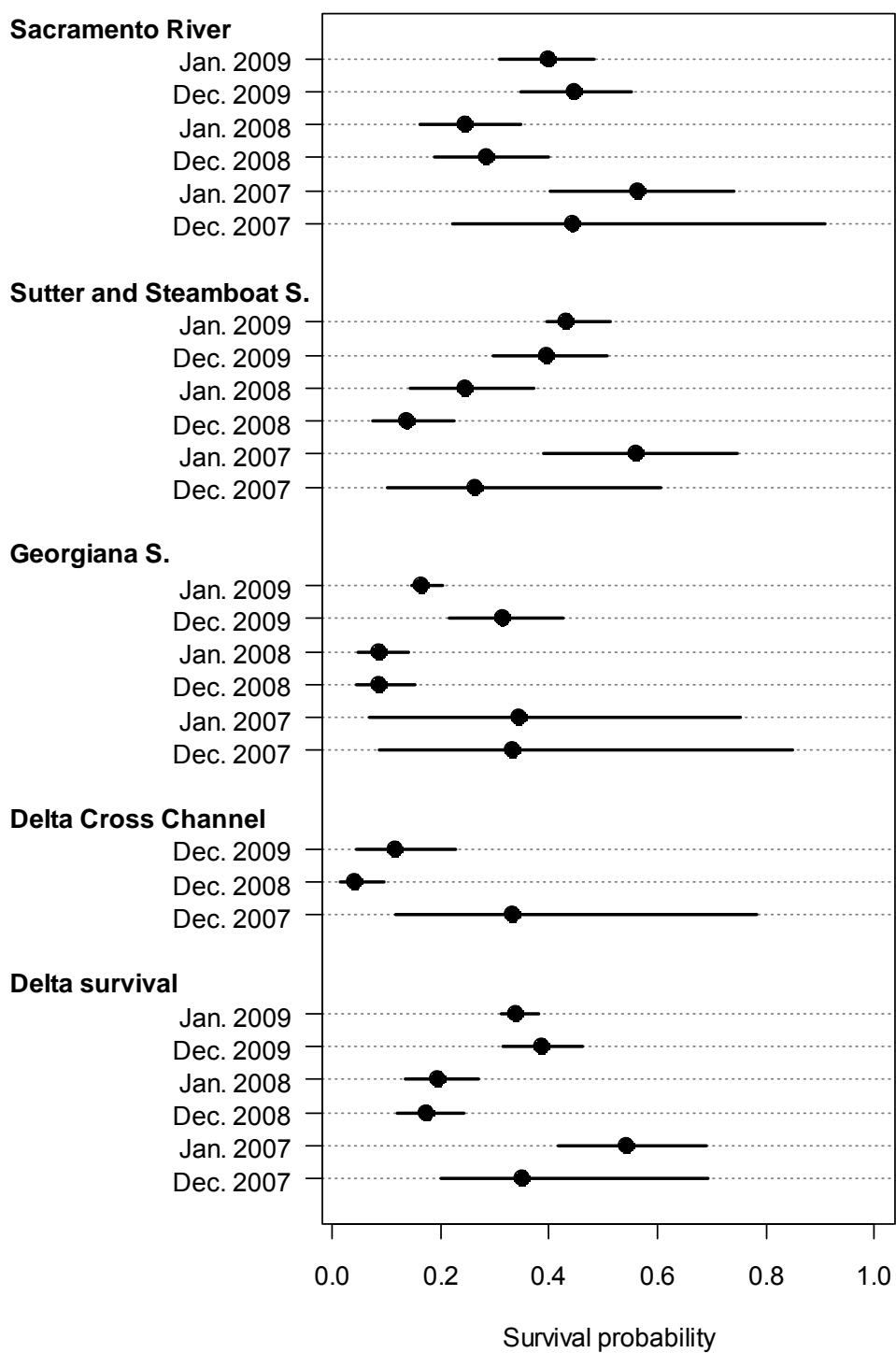
Figure 5.5. Summary of route-specific survival probabilities during migration years 2007–2009. Data points are organized by migration route to facilitate comparison among releases within each route.
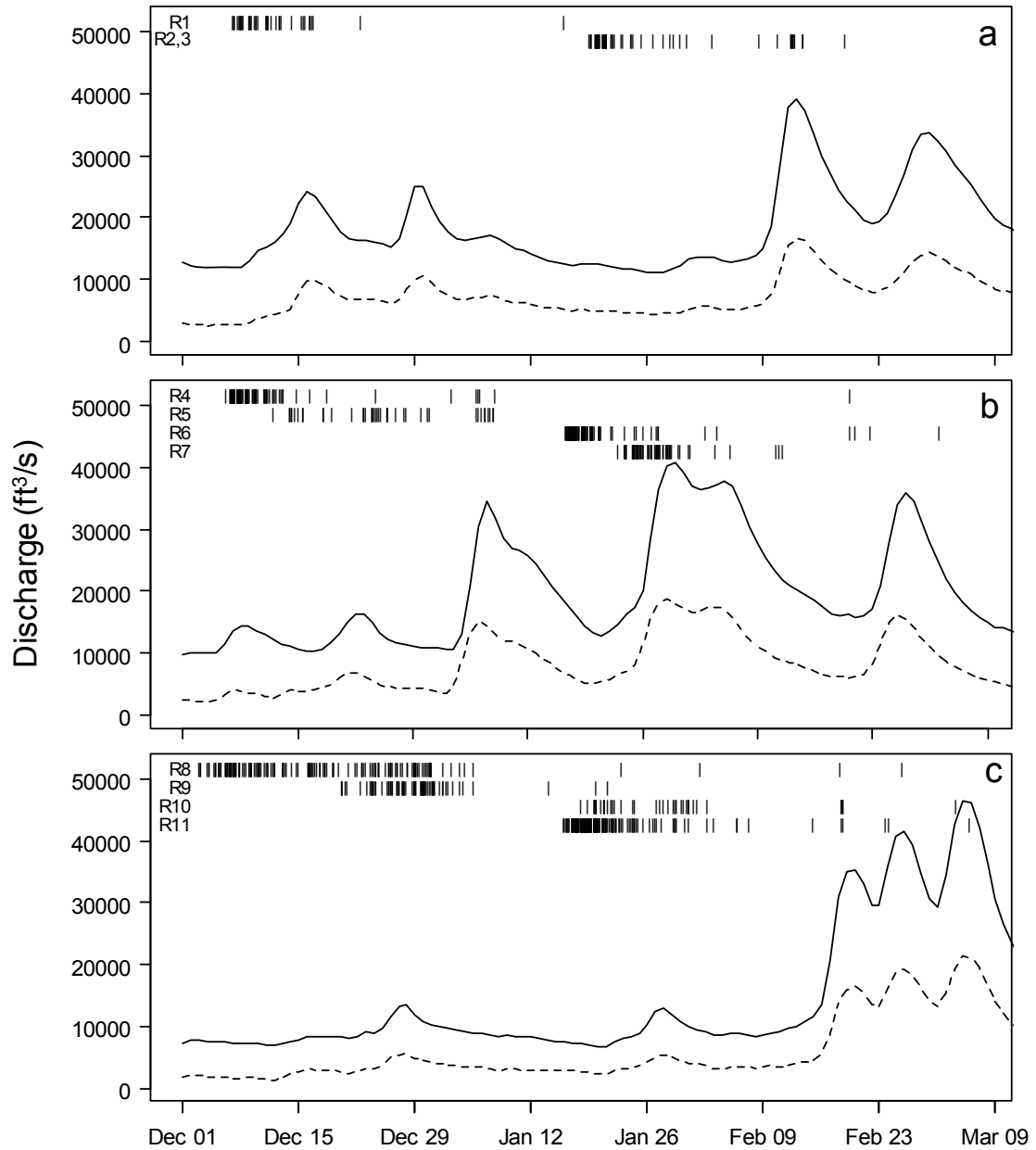
Figure 5.6. River conditions experienced by acoustic-tagged late-fall Chinook salmon smolts migrating through the Sacramento–San Joaquin River Delta during migration years a) 2007, b) 2008, and c) 2009. The solid line is mean daily discharge of the Sacramento River at Freeport and the dashed line is mean daily discharge of the Sacramento just downstream of Georgiana Slough. Tick marks show when tagged fish from each release group ($R_1 - R_{11}$) were detected at telemetry stations defining entry into migration routes used in the CJS survival model.

5.3.3 Factors affecting route-specific survival

For the CJS model, both λ and p varied among years, but not among releases within years. A model with a constant λ was not supported by AIC or LRT (Table 5.6). For constant p across years, the likelihood ratio test was significant at $\alpha = 0.05$, but not at $\alpha = 0.10$. However, since AIC increased with a 2-parameter decrease between models, I elected to use the year-specific p model for as the basis of model selection of group-level and individual-covariates (Table 5.6).

Table 5.6. Results of model selection to identify the best-fit CJS model for λ and p.

Parameter modeled	Model[*]	Number of parameters	AIC	NLL	LR	*P*
λ	$S(rt*rel)\,p(rel)\,\lambda(rel)$	49	1897.9	900.0		
	$S(rt*rel)\,p(rel)\,\lambda(yr)$	42	1889.2	902.6	5.3	0.63
	$S(rt*rel)\,p(rel)\,\lambda(.)$	40	1892.6	906.3	7.4	0.02
P	$S(rt*rel)\,p(yr)\,\lambda(yr)$	35	1879.1	904.6	5.8	0.57
	$S(rt*rel)\,p(.)\,\lambda(yr)$	33	1880.2	907.1	5.1	0.08

[*]Model notation is as follows: rel = release group, rt = route, and yr = migration year. An asterisk between variables indicates inclusion of both main effects and their interaction, and a period indicates an intercept-only model.

For group-level covariates, a nearly saturated model with route, year, study, and all possible interactions explained 85% of the discrepancy between the fully saturated and null models, whereas a model with only migration route and flow covariates explained 42%. These findings indicated that year and study shared common deviance with the flow covariates. The full covariate model explained 75.7% of the discrepancy in deviance between the saturated and null models, with year, study, and Q_S explaining most of this discrepancy (Table 5.7). I also found evidence of overdispersion as suggested by a mean error deviance of 1.5. Thus, even after accounting for the covariates, release-to-release variability was still greater than that expected by multinomial sampling variation. Year and study reduced the deviance more than any other variables and therefore appeared first in the ANODEV table (Table 5.7). Although route was not significant, it was entered next since the remaining flow variables were crossed with migration route indicator variables. Adding $(I_{Sac}+I_{SS}){:}Q_S$ to the model explained significant deviance over that explained by route, year, and study, but none of the other flow

variables were significant. Thus, the final model consisted of route, year, study, and $(I_{Sac}+I_{SS}):Q_S$. The inclusion of year and study in the final model shows that river flow could not fully account for differences in survival among years or between studies.

Table 5.7. Analysis of deviance table for group covariates in the CJS model. Survival was modeled with year-specific p and λ. Indicator variables are I_{ID}, I_{Sac}, and I_{SS} for fish entering the interior Delta, Sacramento River, and Sutter and Steamboat Sloughs, respectively.

Source	Degrees of freedom	Deviance	Mean deviance	F	P-value
Total (saturated model)	29[*]	904.6			
Intercept (null model)	1	960.8			
Corrected total	28	112.4			
Covariate total	10	85.0	8.5	5.59	<0.001
Study	1	21.9	21.9	14.43	0.001
Year	2	33.9	16.9	11.15	<0.001
Route	2	4.5	2.2	1.47	0.255
$(I_{Sac}+I_{SS}):Q_S$	1	18.1	18.1	11.94	0.003
$I_{ID}:Q_M$	1	4.8	4.8	3.15	0.092
$I_{ID}:Q_E$	1	1.1	1.1	0.70	0.414
$I_{SS}:Q_S$	1	0.7	0.7	0.45	0.512
$I_{ID}:Q_J$	1	0.1	0.1	0.07	0.800
Error	18	27.3	1.5		

[*]Release groups 2 and 3 were pooled as one group, and for this release group survival for the Interior Delta was fixed to 1 because all fish survived. For the saturated model, this led to 10 release groups, 3 routes, and 1 fixed parameter for a total of $10(3) - 1 = 29$ degrees of freedom.

Individual covariates added six parameters to the saturated model but decreased AIC by 11 units, indicating that individual covariates explained considerable within-release variation in survival (Table 5.8). Model selection for individual covariates paralleled that for group-level covariates: flow variables for the interior Delta survival were not significant, nor was there a difference in slopes for Q_S between the Sacramento River and Sutter and Steamboat Sloughs (Table 5.8). However, when either fork length or $(I_{Sac}+I_{SS}):Q_S$ were dropped from the model, model fit worsened considerably (Table 5.9). Thus, the best fit model with individual covariates consisted of release group, route, route:release group, $(I_{Sac}+I_{SS}):Q_S$, and fork length. Despite the individual covariate model having 24 more parameters than the best-fit group covariate model, AIC for the individual covariate model (AIC = 1862.8) was 6.3

units less than for the group covariate model (AIC = 1869.1), indicating that individual covariates explained more variation in survival than group covariates alone.

Table 5.8. Results of model selection for the effect of individual covariates on survival. Survival was modeled with year-specific p and λ. Indicator variables are I_{ID}, I_{Sac}, and I_{SS} for fish entering the interior Delta, Sacramento River, and Sutter and Steamboat Sloughs, respectively.

Model or covariate dropped	Number of parameters	AIC	NLL	LR	*P*-value
Route*Release + all covariates	41	1869.2	893.6		
Route*Release – all covariates	35	1879.1	904.6	21.9	0.001
$I_{ID}{:}Q_J$	40	1867.2	893.6	0.0	1.000
$I_{SS}{:}Q_S$	39	1865.2	893.6	<0.1	0.888
$I_{ID}{:}Q_E$	38	1863.4	893.7	0.22	0.639
$I_{ID}{:}Q_M$	37	1862.8	894.4	1.41	0.235

Table 5.9. Likelihood ratio tests and AIC when each variable is dropped from the best fit model with individual covariates. Indicator variables are I_{ID}, I_{Sac}, and I_{SS} for fish entering the interior Delta, Sacramento River, and Sutter and Steamboat Sloughs, respectively.

Variable dropped	Number of parameters	NLL	Likelihood Ratio	AIC	ΔAIC	*P*-value
None (best fit)	37	894.4		1862.8	0.0	
Fork length	36	898.8	8.8	1869.6	6.8	0.003
$(I_{Sac}{+}I_{SS}){:}Q_S$	36	899.9	11.0	1871.8	9.0	0.001

5.3.4 Parameter estimates and predicted survival probabilities

Significant effects of study and year indicated that differences in survival among release groups could not be fully accounted for by my migration route and river flow (Table 5.10). A negative coefficient of -0.37 suggests that on average, release groups for the USFWS study exhibited lower survival than for the CALFED study. For example, predicted survival of the reference group (Sacramento R., 2009, CALFED study) is logit^{-1}(0.71) = 0.67 at the mean flow of 5127 ft^3/s, whereas for the USFWS, predicted survival is logit^{-1}(0.71-0.37) = 0.58. Among years, 2008 had a large negative coefficient, suggesting lower survival than in 2009. For example, relative to the reference group at the mean flow, predicted survival for 2007 and

2008 is logit^{-1}(0.71-0.16) = 0.63 and logit^{-1}(0.71-1.19) = 0.38. Among routes, the interior Delta had the largest negative coefficient despite being the shortest direct route to Chipps Island. Relative to the reference group, predicted survival for the interior Delta is logit^{-1}(0.71-0.44) = 0.57. These patterns of variation are consistent with my observations from the multistate model (Figures 5.4 and 5.5).

Although flow variables could not account for all variation among release groups, Sacramento River flow still explained significant variability in survival for the Sacramento River and Sutter and Steamboat sloughs. Positive slope estimates under both the group- and individual-covariate models show that survival is positively associated with Q_S (Tables 5.10 and 5.11). Under the group covariate model, most of the release groups experienced average flows <8000 ft^3/s, and two data points at higher discharge appear to be driving the relationship (both from release group 7; Figure 5.7). The individual covariate model strengthens the findings of the group covariate model because individuals from multiple releases experienced river discharge >8000 ft^3/s (Figure 5.6 and 5.8). For example, when release group 7 is excluded, Q_S remains statistically significant in the individual covariate model, suggesting that this release group was not driving the relationship. Under both models, predicted survival increases by about 40 percentage points over the observed range of discharge, although the slope is less steep under the individual covariate model (Figures 5.7 and 5.8).

The individual covariate model also revealed effects of fork length on survival and substantial among-release variation in survival. The slope estimate for fork length was positive, indicating that larger size was associated with higher survival (Table 5.11). The estimated slope for fork length was about half that of Q_S, and thus, a 1-SD change in fork length, when holding Q_S constant, results in a smaller change in survival than a 1-SD change in flow (when holding length constant; Table 5.8, Figure 5.8). For example, at the mean observed discharge, predicted survival increases by about 25 percentage points over the range in fork length, compared to a 40 percentage point change over the range in flow. Despite the relation of survival with fork length and Q_S, considerable release-to-release variation in survival remains. Mechanisms driving this variation remain unknown.

Table 5.10. Parameter estimates on the logit scale for group-level covariates best explaining survival and detection probabilities of the CJS model. Parameter estimates for categorical variables (Route, Year, and Study) are estimated as differences from a reference category set as the intercept.

Parameter modeled	Variable	Group description	$\hat{\beta}$ (SE)	95% Confidence interval (± 1.96 SE)
S		Intercept (Sacramento R., CALFED, 2009)	0.71 (0.18)	0.35, 1.06
	Route	Sutter and Steamboat S.	-0.15 (0.18)	-0.49, 0.20
		Interior Delta	-0.44 (0.18)	-0.79, -0.09
	Year	2007	-0.16 (0.28)	-0.70, 0.39
		2008	-1.19 (0.19)	-1.56, -0.82
	Study	USFWS	-0.37 (0.20)	-0.77, 0.03
	$(I_{\text{Sac}}+I_{\text{SS}})Q_S$		0.74 (0.18)	0.38, 1.09
p	Year	Intercept (2009)	1.58 (0.20)	1.19, 1.96
		2007	-0.85 (0.38)	-1.60, -0.10
		2008	0.09 (0.34)	-0.58, 0.77
λ	Year	Intercept (2009)	1.75 (0.21)	1.34, 2.17
		2007	-0.95 (0.40)	-1.73, -0.18
		2008	-0.78 (0.30)	-1.37, -0.19

Table 5.11. Parameter estimates on the logit scale for individual-level covariates best explaining survival probabilities of the CJS model. Parameter estimates for categorical variables (Route and Release Group) are estimated as differences from a reference category set as the intercept. Parameter estimates for Release Group and Route:Release Group interaction terms can be found in Appendix Table 4.4.

Parameter modeled	Variable	Group description	$\hat{\beta}$ (SE)	95% Confidence interval (± 1.96 SE)
S		Intercept (Sacramento R., Release group 5)	0.13 (0.50)	-0.84, 1.10
	Route	Sutter and Steamboat S.	-0.01 (0.81)	-1.60, 1.58
		Interior Delta	-0.58 (0.91)	-2.36, 1.20
	Fork length		0.26 (0.09)	0.09, 0.43
	$(I_{\text{Sac}}+I_{\text{SS}})Q_S$		0.52 (0.18)	0.17, 0.87
p	Year	Intercept (2009)	1.59 (0.20)	1.20, 1.98
		2007	-0.80 (0.37)	-1.53, -0.06
		2008	0.02 (0.35)	-0.67, 0.70
λ	Year	Intercept (2009)	1.77 (0.21)	1.35, 2.18
		2007	-0.90 (0.39)	-1.66, -0.13
		2008	-0.83 (0.30)	-1.43, -0.24
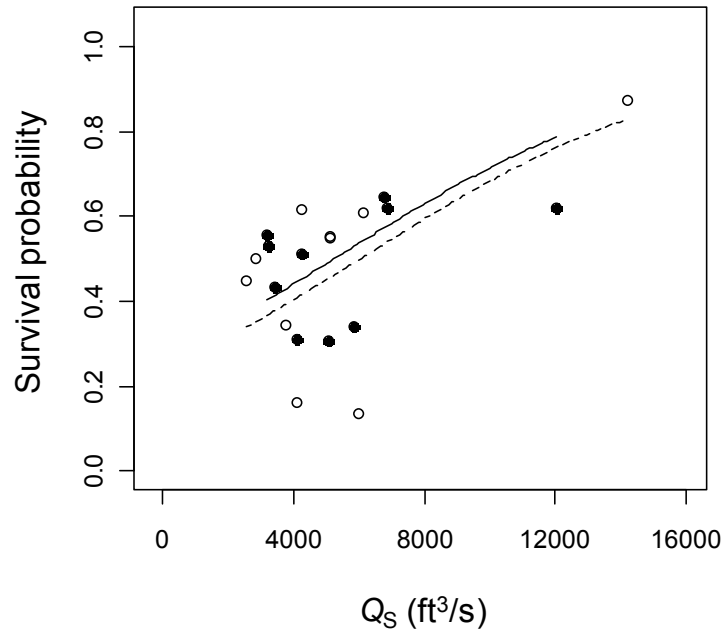
Figure 5.7. Predicted survival as a function of Q_S for the Sacramento River (solid line) and Sutter and Steamboat sloughs (dotted line) plotted against survival probabilities for the Sacramento River (filled circles) and Sutter and Steamboat sloughs (open circles). The fully saturated model was used to estimate route- and release group-specific survival probabilities. Predicted survival is plotted at the mean of group-specific intercepts estimated under the best-fit group covariate model.
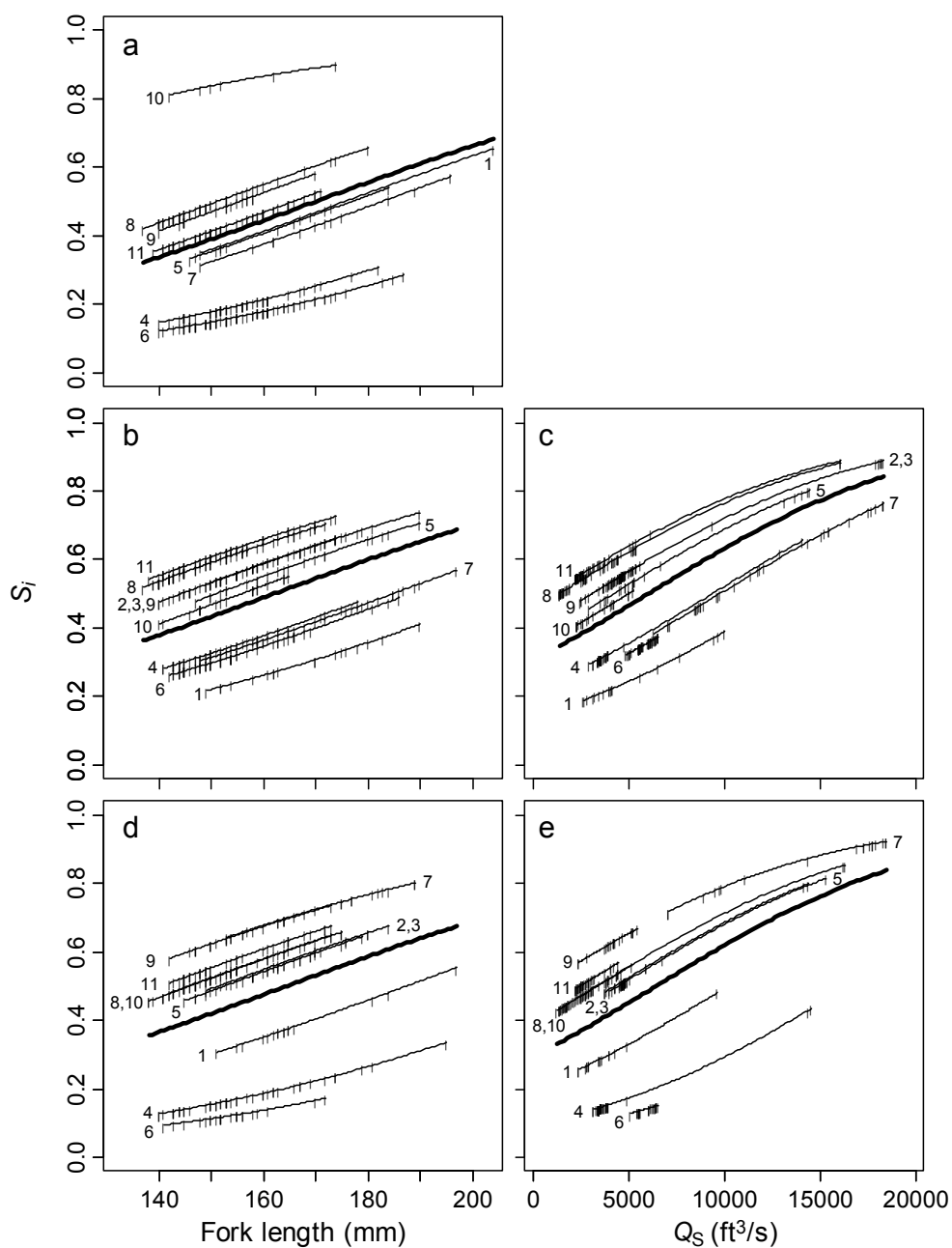
Figure 5.8. Predicted individual survival probabilities as a function of fork length (a, b, and d) and Q_S (c and e) for the interior Delta (a), the Sacramento River (b and c), and Sutter and Steamboat sloughs (d and e). Survival probabilities with respect to Q_S are calculated at the mean fork length (156.5 mm) and with respect to fork length are calculated at the mean discharge (5127 ft³/s). Symbols show either observed fork lengths (a, b, and d) or observed flows when each fish entered a migration route (c and e). Each line is labeled by release group as defined in Table 5.2. The heavy line shows predicted survival plotted at the mean of release group-specific intercepts.

5.4 Discussion

Over the three-year duration of this study, I identified substantial variability in survival related to migration route, river flow, and fish size. Although considerable variability in survival remains unexplained, quantifying effects of river flow and migration route on survival helps to understand how water management actions might influence population-level survival. I observed stable patterns of variability in survival across migration routes, with migration routes leading to the interior Delta having lower survival than the Sacramento River or Sutter and Steamboat sloughs. Thus, water management actions affecting routing of fish through the Delta will influence population-level survival. My findings also suggest that decreases in discharge of the Sacramento River could reduce survival of fish migrating in the Sacramento River and Sutter and Steamboat sloughs. By combining both migration routing and survival in common framework, these relationships form the basis of dynamic models to simulate the effect of water management actions on population-level of survival.

The relation between Sacramento River flow and survival in Sacramento River and Sutter and Steamboat sloughs has important implications for management of water resources in the Delta. Climate change, upstream water withdrawals, and operation of the Delta Cross Channel alter river flow, and in turn, may affect survival of juvenile salmon. For example, at mean total inflows during this study (13642 ft^3/s at Freeport), flow of the Sacramento River downstream of the Delta Cross Channel increases from 2952 ft^3/s to 4791 ft^3/s upon closing the cross-channel gates (flows estimated from a regression model in Burau et al., 2007). My analysis suggests that survival would increase by about six percentage points due to this increase in discharge. Although relatively small, this change in survival must be considered simultaneously relative to survival in other routes and the fraction of fish using each migration. Closing the Delta Cross Channel reduces the fraction of fish entering the interior Delta where survival is low, and increases the fraction remaining in the Sacramento River where survival increases due to the increase in flow. Thus, water management actions that influence routing of fish as well as survival within routes can have a compounding effect on population survival.

Although smolt survival in two routes was positively associated with river flow, it is important to recognize that other variables correlated to river flow likely also affect survival. For example, tidal fluctuations may affect survival of juvenile salmon by influencing predator

encounter rates. As river inflow increases, tidal fluctuations is discharge are dampened (Figure 5.2; also see Figure 6.8). In turn, the point at which the Sacramento River reverses direction on flood tides moves further downstream. These hydrodynamics govern the movements of juvenile salmon by advecting fish upstream on flood tides. Tidal excursions are large when river inflow is low, which increases the distance that fish are advected upstream. Fish pass stationary predators at most once when river discharge is unidirectional, but fish may experience multiple encounters with predators when they are advected upstream with the tides. Thus, although survival decreased with discharge, survival was also inversely related to tidal fluctuations. I suspect that the steepness of flow-survival relation is driven by both river inflow and by tidal fluctuations that affect predator encounter rates. Due to the correlation of river flow with other variables that might affect survival, caution should be exercised when using the flow-survival relation to predict survival in response to water management actions. For example, structural changes to the Delta that alter the relation between river flow and tidal dynamics (e.g., levee breaches) could change the relation between river discharge and survival.

Inability to identify a relation between flow and survival for the interior Delta is not unexpected given the small sample size relative to the spatial and hydrodynamic complexity of the interior Delta. Only 287 fish entered the interior Delta whereas 645 fish from both the Sacramento River and Sutter and Steamboat sloughs were used to estimate the relation between survival and Q_S. To detect a significant covariate effect, Hoffman and Skalski (1995) showed that 300 fish were needed to achieve 70% power ($\alpha = 0.05$) when the individual covariate caused survival to range between 0.5 and 1.0. Baseline survival and capture probabilities in their simulation was on the same order of magnitude observed here, but their study was comprised of three intervals (i.e., reaches), all of which informed the estimate of the slope. In our case, we modeled a single reach and had smaller sample size. Thus, even if an underlying relation existed, power to detect such a relation was likely low.

The interior Delta is a complex environment with multiple alternative migration routes, which also makes it difficult to link mean river flows to survival. Each migration pathway through the interior Delta differs in biotic and abiotic processes that could influence survival. Furthermore, hydrodynamics in the interior Delta are affected not only by river inflow and water exports, but also by tidal dynamics. The particular migration route used by fish

migrating through the interior Delta is probably determined more by hourly-scale flow patterns when fish enter this region, rather than by daily scale mean flows as used in my analysis. In turn, the particular pathway used to migrate through the interior Delta could ultimately determine an individual's probability of surviving. Although the interplay between mean river inputs and exports may influence migration routing and survival, given the complexity of the interior Delta, substantially larger sample sizes over a wide range of conditions will likely be needed to detect such an effect. Newman and Brandes (2010) came to the same conclusion in an analysis of the export effects of survival of coded-wire-tagged juvenile salmon. Similar to my findings, they found that survival of fish through the Interior Delta was substantially lower than fish migrating through the Sacramento River. However, unexplained environmental variability was so large that an effect of exports on survival could not be detected.

Although a positive relation between survival and fish size in unsurprising, mechanisms driving this relation are less clear. Large juvenile salmon are better able to evade predators and preclude consumption by smaller predators (Sogard, 1997). However, a tag effect could also partially explain size-dependent survival. In this study, fish size was restricted above 140 mm to maintain tag-to-body mass ratios below 5%, a threshold beyond which growth and swimming performance of tagged juvenile salmon declines (Adams et al., 1998a, 1998b). Nonetheless, negative effects of the transmitter may persist: larger fish are better able to carry a tag of a given size. Thus, the magnitude with which size affects survival may be influenced by both predation and the effect of the tag. That is, smaller tagged fish may be less capable of evading predators than similarly sized untagged fish, whereas differences in survival between tagged and untagged fish may disappear as fish size increases. Such an interaction would increase the slope of the relation between fish size and survival relative to that expected for untagged fish. This potential interaction should be kept in mind when interpreting size-dependent survival observed in this study.

Among release groups, I identified systematic differences in survival among years and between studies. Mechanisms driving release-, year- and study-specific differences in survival remain unknown, but I present three potential hypotheses: 1) episodic events related to handling and release of tagged fish, 2) differences in expression of post-release mortality experienced by fish released at different locations, and 3) environmental factors that may have

influenced survival but were not included in the model. First, the nature of mark-recapture studies requires that animals be handled, tagged, transported, and released; therefore, such studies are subject to unforeseen events that may subsequently compromise the survival of tagged animals. For example, release group 1 may have experienced handling mortality due to buckling of the net pen in which fish were held (P. Brandes, USFWS, personal communication), but the extent of this mortality is unknown.

A second possible mechanism explaining study-specific differences in survival is initial culling of unfit hatchery fish that occurs shortly after release. On average, fish released for the USFWS study exhibited lower survival, but were also released into the Sacramento River >176 km downstream of fish from the CALFED study. Since late-fall Chinook used in this study were obtained directly from a hatchery, all fish were naïve to the natural river environment and likely underwent some period of acclimation during which they could have been subject to higher mortality. If fish released further upriver experienced such mortality prior to arrival in Delta whereas fish released downriver had not yet fully expressed this mortality upon entering the Delta, then differences in route-specific survival might be expected. Such differential mortality among groups of fish released in different locations has been suspected in the both the Columbia River (Muir et al., 2001; Skalski et al., 2009b) and the Sacramento River (Newman, 2003). Although a plausible explanation, this hypothesis is not supported by observed survival estimates for 2009. Release locations in 2009 were the same as in 2008 yet survival estimates for between studies were similar (Figure 5.8).

A third explanation is that I failed to include critical variables that would explain the remaining variability among release groups not accounted for by migration route, river flow, or fish size. Since predation is a major source of juvenile salmon mortality in the Delta (Lindley and Mohr, 2003), mechanisms influencing predation rates could account for unexplained variability in survival. For example, turbidity can affect predation rates by affecting the reaction distance at which predators can detect prey (Gregory and Levings, 1998), and recapture ratios of juvenile salmon in the Delta have been positively associated with turbidity (Newman, 2003). In addition, since arrival timing at entry points to migration routes did not completely overlap among release groups, shifts in the spatial distribution of predators could cause differential mortality among release groups over and above that expected from river

flow. High temperature has also been shown to negatively affect survival of juvenile salmon in the Delta (Baker, 1995; Newman and Rice, 2002; Newman, 2003), but fish migrating between December and February experience a much narrower range of temperatures (about $6 – 12$ °C) than observed in these studies (e.g., mean temperature was 18.7°C in Newman's 2003 analysis). These hypotheses remain fruitful avenues of exploration to explain release-to-release variation in survival not explained by migration route, river flow, and fish size.

In a system complex as the Delta, management models are needed to understand how human- and natural-caused changes to the Delta influence dynamics of endangered fish populations. However, parameterizing such models with empirical data is difficult precisely due to the Delta's complexity. My analysis has taken an important step by providing a modeling framework and quantifying important mechanisms affecting survival. In this chapter, I found that survival differed among migration routes and was influenced by fish size and route-specific river flow. These relationships can be incorporated into the multistate framework to quantify population-level survival in response to survival in different migration routes. Although route-specific survival is clearly an important component of population survival, understanding the dynamics of migration routing is also critical. Therefore, in the next chapter, I focus on modeling entrainment probabilities as a function of tides, river flow, and gate operations. Given dynamic relationships for both migration routing and survival, managers can begin to understand how both components change simultaneously to drive survival of juvenile salmon emigrating through the Delta.

Chapter 6

**EFFECT OF TIDES, RIVER FLOW, AND GATE OPERATIONS ON
ENTRAINMENT OF JUVENILE SALMON INTO
THE INTERIOR DELTA**

6.1 Introduction

Understanding how juvenile salmon distribute among migration routes in the
Sacramento-San Joaquin River Delta is critical to devise management strategies that improve
survival through the Delta. Juvenile salmon that enter the interior Delta via the Delta Cross
Channel and Georgiana Slough survive at a lower rate than fish migrating within the
Sacramento River (Chapter 4; Perry et al. 2010; Newman and Brandes, 2010). Consequently,
the Delta Cross Channel is prescriptively closed in mid-December each year under the
rationale that fish distribute among migration routes in proportion to the discharge entering
each route (Low et al., 2006). Closing the Delta Cross Channel reduces the fraction of mean
Sacramento River inflow entering the interior Delta by about 30 percentage points. A
coincident reduction in entrainment into the Interior Delta would increase population survival
by shifting fish from low- to high-survival migration routes. However, the nature of the
relationship between flow distribution and fish distribution is poorly quantified. The mean
proportion of flow entering the interior Delta has been positively related to counts of juvenile
Chinook salmon at pumping facilities, but these relations are driven by two influential
observations (Low et al., 2006). Furthermore, recent analyses of acoustic telemetry data have
shown that the proportion of fish entering each migration route can deviate considerably from
the proportion of flow (Chapter 4). Identifying mechanisms that affect entrainment into the
interior Delta will therefore provide a basis for quantifying how management actions affect
survival of juvenile salmon.

At a given river junction, a number of factors influence whether a fish enters a
particular river channel. Both the relative distribution of flow among river channels and the

spatial distribution of fish migrating through a river junction will influence the probability of entering a given river channel. Intuitively, fish migrating through a river junction close to one shore will likely remain in the channel along that shore, whereas fish along the opposite shore will tend to enter the opposite channel. How fish are distributed in the channel cross-section relative to longitudinal division of flow vectors entering each channel will dictate the proportion of fish entering each channel relative to the proportion of flow. This conceptual model suggests that fish distribution relative to flow distribution will remain constant at a given set of river conditions for a given population of juvenile salmon. However, it is unclear whether the ratio of fish to flow, here defined as the entrainment efficiency of a given channel, will remain constant as total discharge varies.

Interactions between behavioral and physical processes affect the spatial distribution of fish, and in turn, the relationship between river discharge and entrainment efficiency. Secondary circulation at river bends is a phenomenon where surface velocity vectors are directed towards the outside of a river bend, dive toward the bottom, and then return toward the inside of the bend along the river bottom (Dinehart and Burau, 2005a). Surface-oriented behavior of juvenile salmon could interact with secondary circulation to concentrate juvenile salmon on the outside of river bends. Since the strength of secondary circulation increases with total discharge, entrainment efficiencies for channels on the outside of a river bend could increase with discharge, implying a relationship between fish and flow that is not strictly proportional. The vertical distribution of juvenile salmon may also vary on a diel basis (Beeman and Maule, 2006). At the junction of the Delta Cross Channel and Sacramento River, juvenile salmon are typically shallower at night than during the day (Blake and Horn, 2003, 2006). The consequence of these behavioral responses in terms of probability of entrainment into a given channel will depend on river conditions when fish arrive at a river junction.

River discharge at many junctions in the Delta varies not only on daily and seasonal time scales, but also on hourly time scales due to tidal forcing. At the junction of the Sacramento River, Delta Cross Channel, and Georgiana Slough, the Sacramento River often reverses direction and flows upstream on flood tides, with water entering Georgiana Slough and the Delta Cross Channel from both the upstream and downstream directions (Dinehart and Burau, 2005b; Blake and Horn, 2003, 2006). Clearly, if juvenile salmon arrive at the river

junction when all water is flowing into the interior Delta, they will have a high probability of entering the interior Delta. Only a few hours later on the peak ebb tide, very little water flows into the Delta Cross Channel even though the gates are open. Fish arriving during this tidal stage will have a low probability of entering the Delta Cross Channel. Between these extremes, transition between tidal stages affect the cross-sectional distribution of fish in river junction (Blake and Horn, 2003, 2006), which in turn will influence entrainment probabilities. Hourly variation in entrainment probabilities integrate over each day of the juvenile salmon migration season, ultimately determining the fraction of the population entrained into the interior Delta. Linking the influence of hourly variation in entrainment probabilities on population-level entrainment into the interior Delta remains a formidable challenge in understanding the effects of management actions on juvenile salmon distribution.

The objective of this chapter is to understand how entrainment probabilities vary with hourly, diel, daily, and seasonal variation in river discharge at the junction of the Sacramento River with the Delta Cross Channel and Georgiana Slough. Ultimately, managers need models informed by reliable data to understand biological consequences of water management actions such as operation of the Delta Cross Channel. With this end in mind, I first develop a multinomial regression model to quantify entrainment probabilities of individual fish in response in flow variables. I then use this model to 1) examine variation in predicted entrainment probabilities at a range of temporal scales and 2) determine whether fish are likely to distribute in direct proportionality to the fraction of mean flow entering the interior Delta. Last, I illustrate how my model can be used to understand the effect of alternative management actions on entrainment of fish into the interior Delta by simulating entrainment probabilities under two scenarios of Delta Cross Channel gate operations.

6.2 Methods

I used a multinomial regression model to quantify the effect of hydraulic conditions of the river junction on the migration routes used by acoustically tagged fish. I used all acoustic telemetry data to date (winters of 2007-2009) where the migration of tagged fish was monitored at the junction of the Sacramento River with the Delta Cross Channel and Georgiana Slough. Gauging stations at this junction provide a nearly continuous record of river discharge

entering each of these channels, providing the covariates for analysis. A multinomial model with individual covariates is an attractive framework for this problem: For each fish, the model estimates the probability that it will enter one of three river channels given the river conditions when it entered the junction.

6.2.1 Telemetry data

I used telemetry data on Late-fall Chinook salmon from three studies: 1) the U.S. Fish and Wildlife Service (referred to as "USFWS"; Perry et al., 2010), 2) NOAA Fisheries and University of California at Davis (referred to as "CALFED"; http://californiafishtracking. ucdavis.edu/, accessed December 2009), and 3) and the U. S. Geological Survey (referred to as "USGS"; Vogel, 2008; Table 6.1). For the first two studies, all fish were monitored by the same set of VEMCO telemetry equipment, as described in Chapters 3 and 4. The USGS study used telemetry equipment from HTI (Hydroacoustic Technologies Inc., Seattle, WA). For all studies, telemetry stations were situated just downstream of the entrance to the Delta Cross Channel and Georgiana Slough to detect fish as they left the Sacramento River and entered these routes (Figure 6.1). In the Sacramento River, telemetry stations were located from just upstream of the Delta Cross Channel to just downstream of Georgiana Slough (Figure 6.1). The location of telemetry stations varied among studies and years but all stations were ≤1 km from the entrance of the Delta Cross Channel or Georgiana Slough. Each telemetry station recorded the date and time when tagged fish passed by each telemetry station.

Telemetry data consisted of fish released during the winters of 2007, 2008, and 2009 in 13 different release groups (Table 6.1). All studies used late-fall Chinook salmon from Coleman National Fish Hatchery. All transmitters were surgically implanted and fish were released using methods similar to those described in Chapter 3. Although release sites varied among studies and years, all fish were released a minimum of 40 km upstream of the river junction (Figure 6.1). The fraction of each release group arriving at the river junction depended on upstream mortality rates and the proportion of fish entering Sutter and Steamboat sloughs, which diverges from the Sacramento River upstream of the Delta Cross Channel and Georgiana Slough. Overall, 714 fish were detected at the river junction, representing 38% of all fish released. About 29% of fish detected at the junction passed the Delta Cross Channel

when its gates were open with the remainder passing the junction with the gates closed (Table 6.1).

Table 6.1 Sample sizes for release groups of juvenile late-fall Chinook salmon implanted with acoustic tags during the winters of 2007 – 2009. DCC = Delta Cross Channel.

Release group	Study	Year	Release dates	Number released	Number detected at junction	Number with DCC open	Fraction detected at night
1	USFWS	2006	Dec 5 – Dec 6	64	36	32	0.86
2	USGS		Dec 11– Dec 12	96	57	49	0.70
3	USFWS	2007	Jan 17 – Jan 18	80	39	0	0.85
4	USGS		Jan 12 –Jan 23	166	55	0	0.85
5	CALFED		Jan 16–Feb 2	200	11	0	0.55
6	USFWS		Dec 4 – Dec 5	149	76	73	0.79
7	CALFED		Dec 7	150	36	3	0.72
8	USFWS	2008	Jan 15 –Jan 16	130	85	0	0.72
9	CALFED		Jan 17	154	49	0	0.63
10	USFWS		Nov 30 –Dec 4	192	91	47	0.81
11	CALFED		Dec 13	149	57	1	0.82
12	CALFED	2009	Jan 11	151	30	0	0.70
13	USFWS		Jan 13 –Jan 17	192	92	0	0.64
All groups				1873	714	205	0.75

Telemetry data were organized into discrete detection events, and the fate of each fish was assigned to one of the three river channels based on the time series of detection events. The minimum criterion for a detection event consisted of two consecutive detections within 30-min period at a given telemetry station (Skalski et al., 2001; Pincock, 2008; Perry et al., 2010). Detections failing this criterion were considered inadequate for route assignment and excluded from analysis. A detection event ended with a time lapse of >1 h between detections at a given station, or when fish were detected at a different location. A migration route (S = Sacramento River, G = Georgiana Slough, and D = Delta Cross Channel) was assigned to each fish based on its final detection location in the time series of detection events at the river junction (Figure 6.1). The time of entrance to each channel was defined by the first detection of the final detection event upon entering a given river channel.
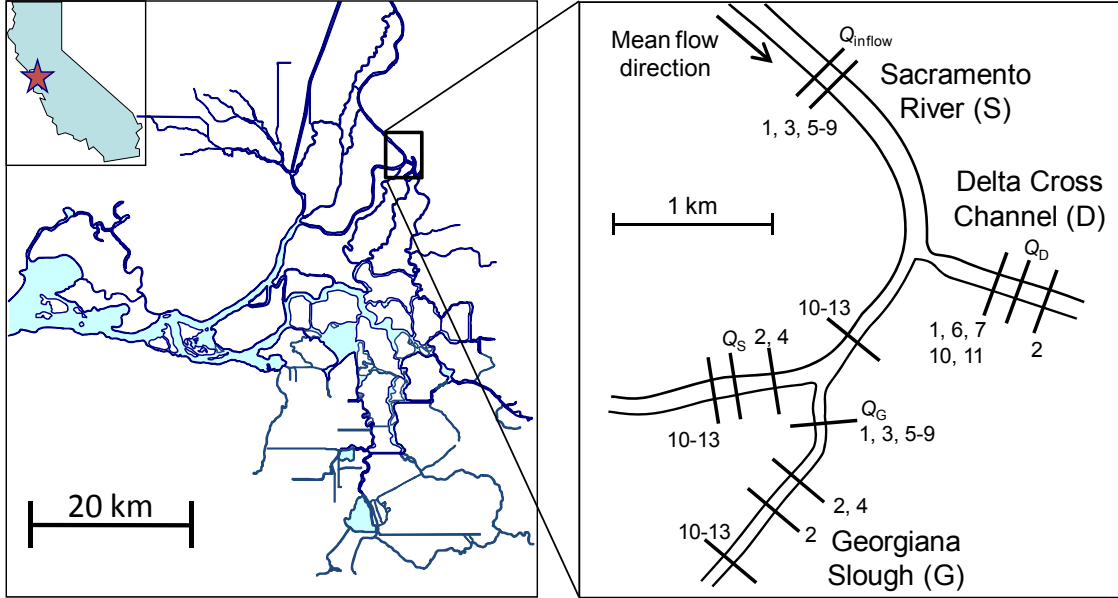
Figure 6.1. Map of the Sacramento–San Joaquin River Delta and the junction of the Sacramento River with the Delta Cross Channel and Georgiana Slough showing the location of telemetry stations and discharge gauging stations. Discharge gauging stations in each channel a labeled as Q. Telemetry stations are labeled by the particular release groups monitored at that location (see Table 6.1 for detail on release groups).

6.2.2 Model development

The three migration routes (S, G, D) used by each fish form a categorical response variable that is distributed as trinomial when the Delta Cross Channel gate is open and binomial when the gate is closed. The probability distribution for each individual can be expressed as

$$P\left(Y_{ij} = y_{ij}\right) = \pi_{i,\mathrm{D}}^{y_{i,\mathrm{D}}} \pi_{i,\mathrm{G}}^{y_{i,\mathrm{G}}} \pi_{i,\mathrm{S}}^{y_{i,\mathrm{S}}} \qquad \text{when the Delta Cross Channel is open}$$

and $\quad P\left(Y_{ij} = y_{ij}\right) = \pi_{i,\mathrm{G}}^{y_{i,\mathrm{G}}} \pi_{i,\mathrm{S}}^{y_{i,\mathrm{S}}} \qquad$ when the Delta Cross Channel is closed,

where $y_{ij} = 1$ when the ith fish enters the jth river channel and zero otherwise, and π_{ij} is the probability of the ith individual entering the jth river channel. The probability of entering the interior Delta, π_{ID}, is $\pi_{\mathrm{D}} + \pi_{\mathrm{G}} = 1 - \pi_{\mathrm{S}}$. More generally, the distribution for each individual can be represented as

$$P\left(Y_{ij} = y_{ij}\right) = \pi_{i,\mathrm{D}}^{y_{i,\mathrm{D}} I_{i,\mathrm{D}}} \pi_{i,\mathrm{G}}^{y_{i,\mathrm{G}}} \pi_{i,\mathrm{S}}^{y_{i,\mathrm{S}}} \tag{6.1}$$

where $I_{i,\mathrm{D}}$ is an indicator variable resolving to one if the ith fish passes the river junction when the Delta Cross Channel gate is open and zero if it passes the junction when the gate is closed.

I also explored an alternative formulation of the distribution using conditional branching probabilities. With only downstream river flow, fish first past by the Delta Cross Channel but can enter Georgiana Slough only if they fail to enter the Delta Cross Channel. Under this rationale, the probability distribution when the Delta Cross Channel is open can be constructed as

$$P\left(Y_{ij} = y_{ij}\right) = \pi_{i,\mathrm{D}}^{y_{i,\mathrm{D}}} \left(\left(1 - \pi_{i,\mathrm{D}}\right)\pi_{i,\mathrm{G|S}}\right)^{y_{i,\mathrm{G}}} \left(\left(1 - \pi_{i,\mathrm{D}}\right)\left(1 - \pi_{i,\mathrm{G|S}}\right)\right)^{1 - y_{i,\mathrm{D}} - y_{i,\mathrm{G}}} \tag{6.2}$$

where $\pi_{i,\mathrm{G|S}}$ is the probability of an individual entering Georgiana Slough conditional on remaining in the Sacramento River at the Delta Cross Channel (Figure 6.1). I found that likelihood functions formed from either Eqns. 6.1 or 6.2 were maximized at the same value. Therefore, use of either parameterization is a matter of interpretation rather than goodness-of-fit. Since the river flows in both directions at this junction, fish can pass by both routes D and G, only to be advected upstream with the tides to ultimately enter either route. Therefore, I chose to use unconditional probabilities represented in Eqn. 6.1 because fish movement through this junction does not strictly adhere to a conditional branching process. Multi-route river junctions with unidirectional river flow may be better modeled with the conditional branching structure of Eqn. 6.2. Such a junction occurs where Sutter Slough and Steamboat Slough branch off the Sacramento River (see Figures 1.2 and 2.7).

My goal was to model entrainment probabilities (π_{ij}) as a function the hydraulic conditions of the river junction at the time the ith fish entered the jth migration route. I used a generalized linear model framework with a baseline-category logit function to link $g(\pi_{ij})$ to a linear combination of the explanatory variables

$$g\left(\pi_{ij}\right) = \ln\left(\frac{\pi_{ij}}{\pi_{iJ}}\right) = \beta_{j0} + \beta_{j1}x_{ij1} + \dots + \beta_{jp}x_{ijp} = \boldsymbol{\beta}_j' \mathbf{x}_{ij} \tag{6.3}$$

where π_{ij} is measured relative to the baseline category π_{iJ}, β_{j0} is the intercept for the jth migration route, and β_{jk} are slope parameters for $k = 1, \dots, p$ explanatory variables (x_{ijk}) for the ith individual and jth route. I used the Sacramento River route ($J = \mathrm{S}$) as the baseline category against which to measure the probabilities of entering the Delta Cross Channel and Georgiana

Slough. I modeled each baseline logit function with its own set of explanatory variables, allowing a different set of variables to affect the probability of entrainment into each river channel. Entrainment probabilities are expressed directly as a function of the explanatory variables by taking the inverse of the baseline-category logits:

$$\pi_{ij} = \frac{\exp\left(\boldsymbol{\beta}'_j \mathbf{x}_{ij}\right)}{\displaystyle\sum_{h=1}^{J} \exp\left(\boldsymbol{\beta}'_h \mathbf{x}_{ih}\right)} \tag{6.4}$$

where $\boldsymbol{\beta}_J$ for the baseline category ($J = $ S) is set to zero.

I estimated the regression parameters by maximizing the log likelihood function of the joint probability distribution over all individuals. The log-likelihood function for the data set of n fish is

$$\ln L\left(\boldsymbol{\pi} \mid \mathbf{Y}\right) = \ln\left(\prod_{i=1}^{n} \pi_{i,\mathrm{D}}^{y_{i,\mathrm{D}} I_{i,\mathrm{D}}} \pi_{i,\mathrm{G}}^{y_{i,\mathrm{G}}} \left(1 - I_{i,\mathrm{D}} \pi_{i,\mathrm{D}} - \pi_{i,\mathrm{G}}\right)^{1 - y_{i,\mathrm{D}} I_{i,\mathrm{D}} - y_{i,\mathrm{G}}}\right)$$

$$= \sum_{i=1}^{n} y_{i,\mathrm{D}} I_{i,\mathrm{D}} \ln \pi_{i,\mathrm{D}} + y_{i,\mathrm{G}} \ln \pi_{i,\mathrm{G}} + \left(1 - y_{i,\mathrm{D}} I_{i,\mathrm{D}} - y_{i,\mathrm{G}}\right) \ln\left(1 - I_{i,\mathrm{D}} \pi_{i,\mathrm{D}} - \pi_{i,\mathrm{G}}\right)$$

$$= \sum_{i=1}^{n} y_{i,\mathrm{D}} I_{i,\mathrm{D}} \ln \pi_{i,\mathrm{D}} + y_{i,\mathrm{G}} \ln \pi_{i,\mathrm{G}} + \ln\left(1 - I_{i,\mathrm{D}} \pi_{i,\mathrm{D}} - \pi_{i,\mathrm{G}}\right) - y_{i,\mathrm{D}} I_{i,\mathrm{D}} \ln\left(1 - I_{i,\mathrm{D}} \pi_{i,\mathrm{D}} - \pi_{i,\mathrm{G}}\right)$$

$$- y_{i,\mathrm{G}} \ln\left(1 - I_{i,\mathrm{D}} \pi_{i,\mathrm{D}} - \pi_{i,\mathrm{G}}\right)$$

$$= \sum_{i=1}^{n} y_{i,\mathrm{D}} I_{i,\mathrm{D}} \ln\left(\frac{\pi_{i,\mathrm{D}}}{1 - I_{i,\mathrm{D}} \pi_{i,\mathrm{D}} - \pi_{i,\mathrm{G}}}\right) + y_{i,\mathrm{G}} \ln\left(\frac{\pi_{i,\mathrm{G}}}{1 - I_{i,\mathrm{D}} \pi_{i,\mathrm{D}} - \pi_{i,\mathrm{G}}}\right) + \ln\left(1 - I_{i,\mathrm{D}} \pi_{i,\mathrm{D}} - \pi_{i,\mathrm{G}}\right) \tag{6.5}$$

Since the probabilities must sum to one, $\pi_{i,\mathrm{S}} = 1 - \pi_{i,\mathrm{D}} - \pi_{i,\mathrm{G}}$ for the baseline category. Eqn. 6.5 shows explicitly how the baseline category logits given in Eqn. 6.3 arise as the natural parameters of the multinomial distribution (Agresti, 2002).

To express the likelihood function in terms of the explanatory variables (x_{ijk}) and regression parameters (β), the baseline-category logits in the first two terms of Eqn. 6.5 are replaced with Eqn. 6.4, and π_{ij} in the last term is substituted with Eqn. 6.4, which reduces to:

$$\ln L\left(\boldsymbol{\pi} \mid \mathbf{Y}\right) = \sum_{i=1}^{n} \left[y_{i,\mathrm{D}} I_{i,\mathrm{D}} \left(\boldsymbol{\beta}'_\mathrm{D} \mathbf{x}_{i,\mathrm{D}}\right) + y_{i,\mathrm{G}} \left(\boldsymbol{\beta}'_\mathrm{G} \mathbf{x}_{i,\mathrm{G}}\right) + \ln\left(1 + I_{i,\mathrm{D}} \exp\left(\boldsymbol{\beta}'_\mathrm{D} \mathbf{x}_{i,\mathrm{D}}\right) + \exp\left(\boldsymbol{\beta}'_\mathrm{G} \mathbf{x}_{i,\mathrm{G}}\right)\right) \right].$$

The parameters were estimated using optimization routines in the R statistical computing platform (R Development Core Team, 2008) to minimize the negative log-likelihood function with respect to the parameters. The variance of the parameter estimates were estimated using the diagonal elements of the inverse of the Hessian matrix.

6.2.3 Explanatory variables

River discharge (Q_j), water velocity (V_j), and the proportion of total outflow (p_{Q_j}) entering each river channel were the primary variables used to explain variation in entrainment probabilities. USGS gauging stations are located just downstream of the entrance to these channels (Q_S, Q_D, and Q_G) and total discharge entering the junction is measured by a gauging station just upstream of the river junction (Q_{inflow}, Figure 6.1). These gauging stations record discharge and water velocity every 15 min, providing detailed information about the hydraulic conditions that tagged fish experienced when they migrated through the river junction.

Hydraulic conditions of the river junction were assigned to each fish based on the time of detection in each river channel. However, inconsistency in the location of telemetry stations among release groups (Figure 6.1, Table 6.1) introduced variability when basing covariate values on detection times at a given station. For example, because flow changes quickly with the tides, discharge of Georgiana Slough when a fish passes the telemetry station located near this flow gauge (Q_G in Figure 6.1) could differ substantially from the discharge when the same fish passes the telemetry station 1 km downstream of the flow gauge (Figure 6.1). To account for this variability, I referenced all detection times to a common spatial location in each channel by estimating the transit time of each fish from telemetry station to gauging station. Transit times were estimated from cross-sectional water velocities and distances between each telemetry station and gauging station. Thus, let Q_{ij} represent the discharge entering channel *j* when the *i*th fish is estimated to have passed a gauging station. The full model based on covariates from spatially-referenced detection times fit the data much better than did the same model with unreferenced times: Akaike's Information Criterion (AIC) = 800.8 and the minimum negative log-likelihood (NLL) = 384.4 for spatially referenced covariates compared

to AIC = 876.8 and NLL = 422.4 for unreferenced covariates (lower values indicate better fit for both measures; Burnham and Anderson, 2002).

The effect of tidal fluctuations on hydraulic conditions of the river junction was captured by two variables. First, I calculated the rate of change in discharge of the Sacramento River as $\Delta Q_S(t) = Q_S(t+1) - Q_S(t)$ where t is measured in units of 15 minutes. This variable accounts for hydraulic conditions that may be quite different on a flood-to-ebb transition compared to an ebb-to-flood transition, even though total discharge may be similar during each transition. When ΔQ_S is negative, discharge is decreasing, which typically occurs during the transition from an ebb tide to a flood tide. In contrast, when ΔQ_S is positive, discharge is increasing, as typified by the transition from a flood to an ebb tide. Second, U is a dummy variable set to one when water is flowing upstream in the Sacramento River (i.e., $U = 1$ when $Q_S < 0$), and zero otherwise. Statistical significance of this variable indicates that water flowing upstream into the junction affects entrainment probabilities over and above the influence of Q_{ij}.

I included a number of other variables in the analysis unrelated to hydraulic conditions but that may also affect the probability of fish entering a given migration route. These variables included fork length (L, mean = 155.9 mm, range = 118 – 204 mm), time of day (a dummy variable where $D = 1$ for fish detected during day and $D = 0$ for night), and daily water temperature (T, mean = 9.4, range = 6.6 – 12.4 degrees) when fish passed through the river junction.

6.2.4 Model selection

To identify variables that affect entrainment probabilities, I formed an initial full model that included all possible explanatory variables and then eliminated variables that failed to improve model fit to the data. Each variable in $g(\pi_D)$ or $g(\pi_G)$ was dropped one-at-a-time from the full model, fit to the data, and a likelihood ratio test used to determine whether dropping the variable resulted in a significantly poorer fit of the model to the data. The variable with the largest *P*-value was eliminated from the model, a new "full" model was formed, and variables were again dropped one-at-a-time and fit to the data. This process was repeated until no

further variables could be dropped from the model at $\alpha = 0.05$. Given a fully reduced model of main effects, I then formed all possible two-way interactions (i.e., products of variables) and used reverse elimination of interaction terms to arrive at a final model.

Due to the high correlation among Q_j, V_j, and p_{Q_j} variables, I formed three full models, one for each type of predictor variable. In addition, I excluded flow variables from the Delta Cross Channel (Q_D) and the upstream gauging station (Q_{inflow}) because they were highly correlated with those from downstream gauge on the Sacramento River (e.g., $r = -0.84$ between Q_D and Q_S) and caused variance inflation factors > 20. Variance inflation factors (VIFs) provide an index of multicollinearity by measuring the magnitude with which the variances of parameter estimates are inflated compared to when the explanatory variables are uncorrelated (Kutner et al., 2005). With these flow stations excluded, all variance inflation factors were < 5 (Kutner et al., 2005 recommend VIFs < 10). Using Q_j as an example, each full model had the following structure:

$$\ln\left(\frac{\pi_j}{\pi_S}\right) = \beta_{j0} + \beta_{j1}Q_S + \beta_{j2}Q_G + \beta_{j3}\Delta Q_S + \beta_{j4}U + \beta_{j5}T + \beta_{j6}D + \beta_{j7}L . \qquad (6.6)$$

Because final models based on Q_j, V_j, and p_{Q_j} were not nested, I used Akaike's Information Criterion to compare these models (Burnham and Anderson, 2002).

All continuous explanatory variables were standardized by subtracting each observation from the mean and dividing by the standard deviation. Standardizing puts all variables on the same quantitative scale, facilitating comparison of parameters on different absolute scales. Parameter estimates based on standardized variables are interpreted as the magnitude of effect of each variable on entrainment probabilities for a one standard deviation change when holding the remaining variables constant.

6.2.5 Goodness of fit

I assessed model fit to the data using both quantitative and descriptive techniques. To check for systematic deviations of predicted from observed values, I grouped data into discrete classes, plotted mean observed versus predicted values, and performed approximate Pearson χ^2 tests. I also used the Hosmer-Lemeshow test, formed by 1) grouping the data set into 10

classes of equal sample size based on the ordered predicted probabilities, $\hat{\pi}_{ij}$; 2) calculating the

$\hat{C}$ test statistic based on squared differences between observed and expected frequencies in

each class; and 3) comparing $\hat{C}$ to a χ^2 distribution with 8 df (Hosmer and Lemeshow, 2000).

Since the multinomial model produces two predicted probabilities ($\hat{\pi}_{iD}$ and $\hat{\pi}_{iG}$), I conducted

the Hosmer-Lemeshow test for each. I used two grouping methods to visually inspect model

fit to the data. First, data were discretized into 14 groups based on fixed cutpoints of the

predicted probabilities. This approach leads to unequal sample size among groups but spans

the range of predicted probabilities. I also compared mean predicted probabilities of each

release group to the observed proportions in each group that entered each channel. This

grouping approach tends to average over hydraulic conditions that might lead to very different

predicted probabilities among individuals, but provides a natural classification for a group of

fish that experienced the same set of average environmental conditions.

I calculated the area under the receiver operating curve (AUC) to quantify how well

the model predicts the fates of fish (Hosmer and Lemeshow, 2000). The AUC is calculated as

follows: if estimated probabilities of π_{ij} are greater than an arbitrary cutoff value of π_j, then the

ith fish is assigned to route j. For a particular cutoff value, the actual route used by each fish is

compared to the predicted route, and the false-positive and true-positive rate calculated. The

receiver operating curve (ROC) plots the true-positive rate versus the false-positive rate for all

possible cutoff values, and AUC is the area under this curve. An AUC of 0.5 indicates the

model has no ability to predict the fish's migration route, whereas AUC = 1 indicates perfect

classification ability. In practice, AUC between 0.7 and 0.8 is considered "acceptable" and

between 0.8 and 0.9 is considered "excellent" (Hosmer and Lemeshow, 2000).

6.2.6 Variation in predicted entrainment probabilities

I used the best-fit model 1) to understand how entrainment probabilities vary over a

range of time scales, 2) to evaluate the assumption that the daily fraction of fish is proportional

to the mean daily fraction of flow entering the interior Delta, and 3) to examine the effect of

river inputs and tides on the daily fraction of fish entering the interior Delta. Time-specific

entrainment probabilities reveal the individual consequences of arriving at the junction at a

particular time of day and tidal cycle. At the population level, however, the fraction of fish entering each route depends on 1) fluctuation in time-specific entrainment probabilities over each day and 2) the distribution of fish arrival times at the junction over the diel cycle.

For time-specific entrainment probabilities that vary among individuals, the expected number of fish entering migration route j on day d, n_{jd}, is

$$E\left(n_{jd}\right)=\sum_{i=1}^{N_d} \pi_{ijd}$$

where N_d is the total number of fish migrating past the junction on day d. The expected fraction of fish entering route j is then

$$\frac{E\left(n_{jd}\right)}{N_d}=\frac{1}{N_d}\sum_{i=1}^{N_d} \pi_{ijd} = \bar{\pi}_{jd}, \tag{6.7}$$

showing that the expected fraction is equivalent the mean entrainment probability on a given day. I used Eqn. 6.7 as the basis for extending individual probabilities to population-level entrainment.

First, I predicted entrainment probabilities using Eqn. 6.4 for the three-year time series of 15-min flow data at the river junction for the period December 1 to February 28. At the finest temporal scale I examined how π_{ij} varied over the tidal cycle under average conditions during the study. Next, I used the three-year time series to calculate $\bar{\pi}_{ID,d}$, the daily fraction of fish entering the interior Delta. Here, entrainment probabilities at the 15-min scale were averaged over each day, and also over day and night periods within each day. This approach assumes that fish arrive at the river junction uniformly over the diel cycle, and $\bar{\pi}_{ID,d}$ for day and night periods help understand how non-uniform arrival distributions affect population-level entrainment. Each day was defined to begin at sunrise (for sunrise, range = 0657-0728 hours; for sunset, range = 1640-1743 hours).

Entrainment efficiency on day d, $E_{ID,d}$, was calculated as

$$E_{ID,d} = \frac{\bar{\pi}_{ID,d}}{p_{\bar{Q}_{ID},d}}$$

where $p_{\bar{Q}_{ID},d}$ is the proportion of mean discharge on day d entering the interior Delta. Entrainment efficiencies <1 indicate lower mean probabilities of entering the interior Delta

relative to the fraction of flow entering the interior Delta, whereas $E_{ID,d} > 1$ suggest more fish than the fraction of flow enter the interior Delta. Entrainment efficiencies remaining constant with respect to $p_{\bar{Q}_{ID},d}$ indicate that the probability of entrainment into the interior Delta is directly proportional to the fraction of flow entering the interior Delta, with $E_{ID,d}$ measuring the constant of proportionality.

Last, I examined the contribution of river inputs and tides to variation in daily entrainment and water distribution. I compared $p_{\bar{Q}_{ID},d}$ and $\bar{\pi}_{ID,d}$ to mean daily discharge entering the river junction ($\bar{Q}_{inflow,d}$). I calculated two measures to quantify the effect of tides on a given day, 1) the fraction of each day with upstream river flow into the junction (i.e., $Q_S <$ 0), and 2) the coefficient of variation in Q_S. The CV is the standard deviation of 15-min flows on each day divided by the daily mean flow of the Sacramento River downstream of the river junction. Since tidal fluctuations decrease as total river discharge increases, the CV measures the relative strength of tides at the river junction on a given day.

6.2.7 Simulating alternative gate operations

To illustrate the utility of an entrainment probability model for informing management decisions, I simulated entrainment probabilities under a management scenario where the Delta Cross Channel was open during the day but closed at night. The premise of this management action is that most of the water entering the interior Delta occurs during large daytime flood tides, whereas most of the tagged fish passed the river junction at night (see Table 6.1). Thus, the rationale is that closing the gates at night minimizes the risk of entrainment for most of the fish population, while opening the gates during the day still allows substantial water to be diverted to the interior Delta. Closed-at-night gate operations were implemented experimentally in 2009 and results are pending. However, given a model for predicting time-specific entrainment probabilities, an alternative approach is to simulate the effect closed-at-night gate operations.

I simulated closed-at-night gate operations for the period Nov 1 to Jan 31 based on current regulations for gate operations. Delta Cross Channel gates are mandated to be closed from Feb 1 to May 20 for fisheries protection (SWRCB, 1995). However, 45 days of

discretionary gate closures for fishery protection are allowed between Nov 1 and Jan 31 (SWRCB, 1995). I focused simulations on this period when managers have considerable flexibility in operating the Delta Cross Channel.

I used the Delta Simulation Model II (DSM2) to simulate 15-min river flows at the river junction under a closed-at-night gate operation (CADWR, 2010). DSM2 is a model for simulating one-dimensional, unsteady, open-channel flow in the Delta in response to river inflows, tidal forcing, and water management actions. I used the most recent calibration of the model and the latest historical simulation. DSM2 was recently recalibrated for use in the Bay Delta Conservation Plan, and historical simulations of Delta hydrodynamics under this recalibration extend through the winter of 2007 (CH2MHILL, 2009). Since the historical simulation did not extend beyond 2007, I used simulated data for the period November 1, 2006 through January 31, 2007, which overlapped the first year that telemetry data were available.

I predicted entrainment probabilities under two scenarios: 1) the historical simulation, which matched inflows, tides, and gate operations during the period of interest, and 2) a closed-at-night simulation, which differed from the historical simulation only in the position of the Delta Cross Channel gates. Recall that under the historical conditions, the Delta Cross Channel gate was open prior to December 15 and closed thereafter (see Figure 3.3). In contrast, for the closed-at-night simulation, I opened the Delta Cross Channel gates at sunrise and closed the gates at sunset for the entire simulation period. Given flow data simulated under these scenarios, I then predicted entrainment probabilities for each 15-min observation using Eqn. 6.4.

I evaluated the two scenarios by 1) examining entrainment probabilities at a range of temporal scales, 2) comparing the distribution of daily entrainment probabilities, and 3) assessing the effect of diel activity patterns on daily entrainment probabilities. To evaluate the consequence of different diel activity patterns of fish, I assumed either a uniform arrival distribution, 85% of fish arriving at the junction during night, or 85% of fish arriving during the day. For predominant diurnal or nocturnal migration, the daily mean probability of entering the interior Delta was calculated as:

$$\bar{\pi}_{\mathrm{ID},d} = A_{\mathrm{Day}}\bar{\pi}_{\mathrm{ID},d,\mathrm{Day}} + \left(1 - A_{\mathrm{Day}}\right)\bar{\pi}_{\mathrm{ID},d,\mathrm{Night}}$$

where A_{Day} is the probability of arriving at the junction during daylight hours, $\bar{\pi}_{\text{ID},d,\text{Day}}$ is the mean probability of entering the interior Delta during daylight hours on day d, and $\bar{\pi}_{\text{ID},d,\text{Night}}$ is the mean probability of entering the interior Delta during night.

6.3 Results

6.3.1 Model selection

Although the full model with discharge variables consisted of 16 parameters, many of these variables failed to improve model fit (Table 6.2), yielding a final model comprised of 7 parameters and 4 explanatory variables (Table 6.3). Water temperature, fork length, and time of day were eliminated entirely from the model because likelihood ratio tests showed that these factors did not significantly improve model fit. Upstream flow in the Sacramento River (U) and Q_{G} did not affect entrainment probabilities for the Delta Cross Channel, whereas ΔQ_{S} did not influence π_{G} (Table 6.1). None of the remaining variables could be eliminated without significantly increasing the negative log-likelihood (Table 6.3), and none of the two-way interactions among the remaining variables were significant (Table 6.2). Including water velocity instead of discharge did not change the structure of the final model (Appendix Table 5.1 and 5.2), and only marginally improved the fit of the model to the data (AIC = 786.8 for the best-fit V_j model; AIC = 787.6 for the best-fit Q_j model). Using the proportion of total outflow did not lead to a more parsimonious model (Appendix Table 5.3 and 5.4); ΔAIC = 9.5 when comparing the best-fit p_{Q_j} model (AIC = 797.1) with the best-fit Q_j model (Table 6.3). Therefore, I used the best fit model with discharge variables for subsequent analyses.

6.3.2 Goodness of fit

I found little evidence of systematic departures of predicted from observed values. The goodness-of-fit tests were not significant (for $g(\pi_{\text{D}})$: $\hat{C}$ = 4.84, P = 0.775; for $g(\pi_{\text{G}})$: $\hat{C}$ = 5.19, P = 0.737). Plots of mean observed versus predicted probabilities supported the statistical tests, showing no evidence of systematic deviations (Figure 6.2). These plots also revealed

Table 6.2. Results of reverse model selection for discharge variables (Q_j) showing the likelihood ratio test and associated statistics for the model with the given variable dropped relative to the preceding model with one additional variable.

Variable dropped	Linear predictor	Number of parameters	AIC	–Log-likelihood	Likelihood Ratio	*P*-value
None (full model)		16	800.8	384.4		
D (time of day)	$g(\pi_G)$	15	798.8	384.4	0.01	0.920
T (temperature)	$g(\pi_D)$	14	796.9	384.4	0.02	0.888
L (fork length)	$g(\pi_G)$	13	794.9	384.5	0.05	0.823
U (upstream flow)	$g(\pi_D)$	12	793.1	384.5	0.15	0.699
D (time of day)	$g(\pi_D)$	11	791.4	384.7	0.30	0.584
Q_G	$g(\pi_D)$	10	789.7	384.9	0.35	0.554
L (fork length)	$g(\pi_D)$	9	788.6	385.3	0.35	0.354
T (temperature)	$g(\pi_G)$	8	787.6	385.8	1.06	0.303
ΔQ_S	$g(\pi_G)$	7	787.6	386.8	1.98	0.159
None (all interactions)		11	790.3	384.2		
$Q_S \times U$	$g(\pi_G)$	10	788.3	384.4	0.03	0.863
$Q_S \times Q_G$	$g(\pi_G)$	9	786.9	384.5	0.57	0.450
$Q_G \times U$	$g(\pi_G)$	8	786.5	385.3	1.63	0.202
$Q_S \times \Delta Q_S$	$g(\pi_D)$	7	787.6	386.8	3.08	0.079

Table 6.3. Likelihood ratio tests when each variable is dropped from the best fit Q_j model.

Variable dropped	Number of parameters	Linear predictor	–Log-likelihood	Likelihood Ratio	AIC	P-value
None (best fit)	7		386.8		787.6	
Q_S	6	$g(\pi_G)$	417.6	61.5	847.1	<0.001
Q_G	6	$g(\pi_G)$	420.0	66.5	852.1	<0.001
U	6	$g(\pi_G)$	392.3	11.0	796.6	<0.001
Q_S	6	$g(\pi_D)$	449.0	124.5	910.1	<0.001
ΔQ_S	6	$g(\pi_D)$	391.8	10.0	795.6	0.002
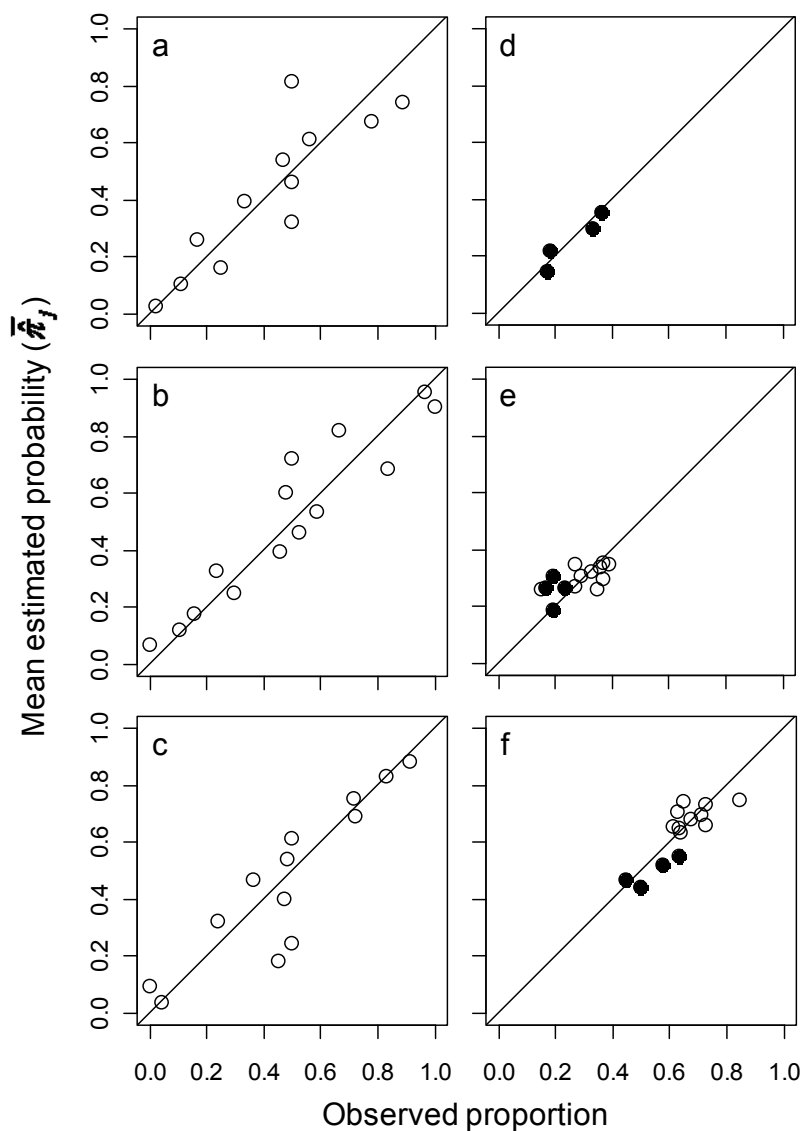
Figure 6.2. Observed proportions of fish entering the Delta Cross Channel (a and d), Georgiana Slough (b and e), and the Sacramento River (c and f) compared to the mean predicted probabilities entering each channel. For the left column (a-c), groups were formed by discretizing predicted probabilities into 14 intervals of equal-probability width. For the right column (d-f), means are calculated for each release group and Delta Cross Channel gate position (unfilled symbols = closed gate, filled symbols = open gate). For d-f, groups with ≤10 fish are not shown.

good agreement between predicted and observed values, regardless of how the data were grouped, with no large deviations between expected and observed values. I found that AUC = 0.785 for $\hat{\pi}_{i,G}$, 0.873 for $\hat{\pi}_{i,D}$, 0.841 for $\hat{\pi}_{i,S}$, indicating that the model has excellent ability to predict the ultimate fates of fish. For example, $\hat{\pi}_S > 0.7$ correctly predicts 80% of fish that actually remained in the Sacramento River, while 75% of fish that entered the interior Delta are also correctly classified (Appendix Figure 5.1). Taken together, the goodness-of-fit measures suggest little evidence of lack-of-fit, close agreement between predicted and observed values, and good ability to predict the likelihood of entering migration routes in response hydraulic dynamics.

6.3.3 Estimated parameters and entrainment probabilities

Under the best-fit model, Q_S, Q_G, and U significantly affected the probability of entering Georgiana Slough (π_G), whereas Q_S and ΔQ_S affected the probability of entering the Delta Cross Channel (π_D; Table 6.3). Parameter estimates indicate both the direction and magnitude of the effect of these variables on entrainment probabilities when holding the remaining variables constant (Table 6.4). For π_G, the slope parameter for Q_S is negative, indicating that increases in Q_S decreased the probability of entering Georgiana Slough (Figure 6.3b). In contrast, the positive slope estimate for Q_G indicates that π_G increased with Q_G (Figure 6.3f). Slope estimates for Q_G and Q_S are of similar magnitude, showing that a 1 SD change in either variable affected π_G by a similar magnitude, but in opposite directions. The positive parameter estimate for U indicates that water flowing upstream from the Sacramento River into the river junction increased the probability of entering Georgiana Slough (Figure 6.3n). For the Delta Cross Channel, decreases in both Q_S and ΔQ_S increased the probability of fish entering the Delta Cross Channel, but the slope estimate for Q_S is five times that for ΔQ_S, indicating that Q_S was the dominant factor driving entrainment probabilities into the Delta Cross Channel (Table 6.4, Figure 6.3c and 6.3k).
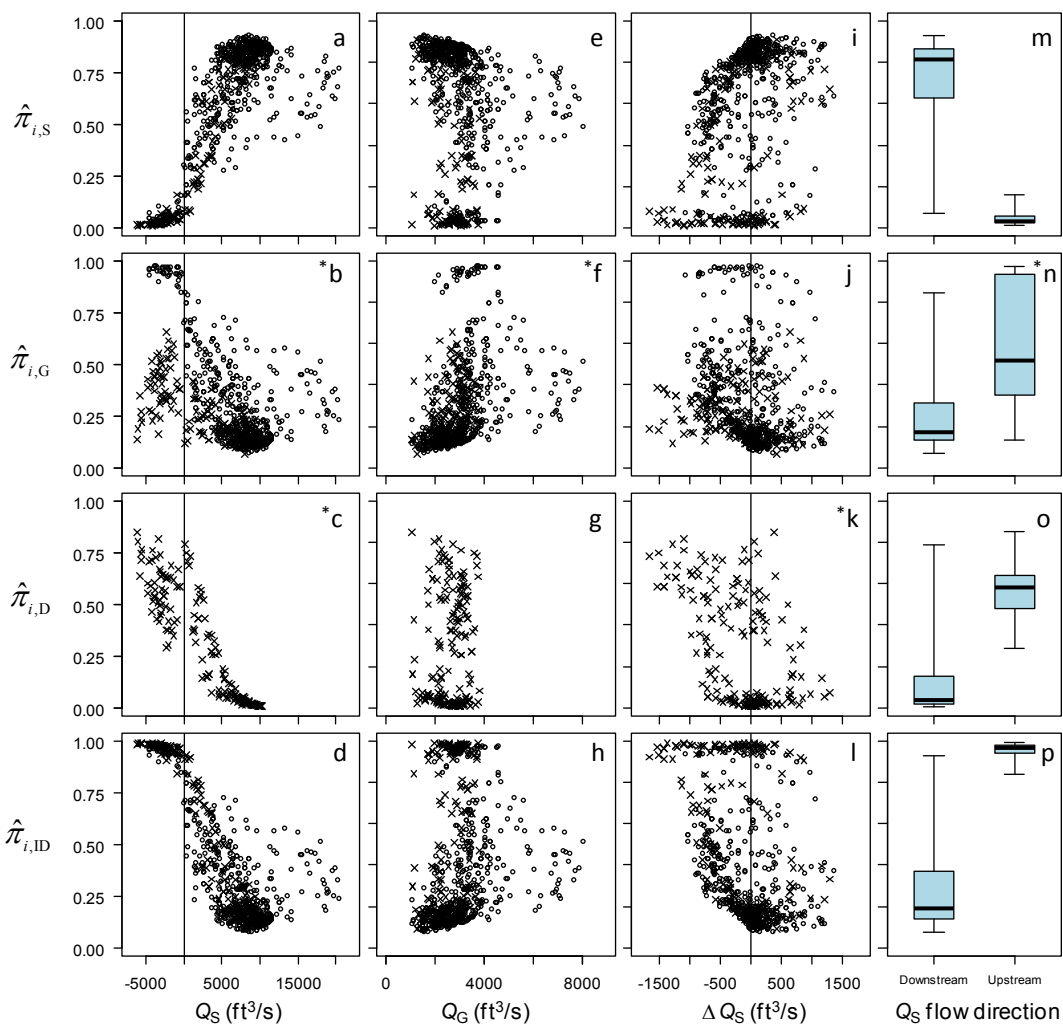
Figure 6.3. Plots of estimated entrainment probabilities ($\hat{\pi}_{ij}$) for route j and individual (i) as a function of flow variables in the best fit model. Panels with an asterisk indicate the driving relationships in the best fit model (see Tables 6.3 and 6.4). Box plots show the range, median, 25th, and 75th percentiles. Circles indicate fish that arrived at the river junction when the Delta Cross Channel was closed, and Xs indicate fish arriving when the Delta Cross Channel was open. Subscripts are as follows: S = Sacramento River, G = Georgiana Slough, D = Delta Cross Channel, and ID = Interior Delta.

Table 6.4 Maximum likelihood parameter estimates for the best fit model relating entrainment probability into Georgiana Slough (G) and the Delta Cross Channel (D) to hydraulic variables of the river junction.

Variable	Parameter	Estimate	Standard error
Intercept	β_{G0}	-0.900	0.106
Q_S	β_{G1}	-1.163	0.154
Q_G	β_{G2}	0.852	0.107
U	β_{G4}	1.595	0.512
Intercept	β_{D0}	-2.337	0.391
Q_S	β_{D1}	-2.694	0.337
ΔQ_S	β_{D3}	-0.474	0.158

6.3.4 Hourly variation in predicted entrainment probabilities

At mean river flows observed during our study (Table 6.5), flood tides caused the Sacramento River to reverse direction twice daily (Figure 6.4a and 6.5a). Under these conditions, discharge of the Sacramento River downstream of the junction (Q_S) varied substantially from -5,000 ft^3/s during the full flood tide to 10,000 ft^3/s during the full ebb tide only a few hours later (Figure 6.4a and 6.5a). Flow into the Delta Cross Channel was inversely related to the Sacramento River, increasing rapidly during the transition from ebb tide to flood tide as Q_S decreased (i.e., when $\Delta Q_S < 0$). Relative to Q_S and Q_D, discharge of Georgiana Slough exhibited much less variability regardless of whether the Delta Cross Channel gates were open or closed (Figure 6.4a and 6.5a).

Table 6.5. Summary of flow conditions experienced by juvenile salmon detected at the junction of the Sacramento River (Q_S, ΔQ_S) with the Delta Cross Channel (DCC, Q_D) and Georgiana Slough (Q_G). Discharge at Freeport is the mean daily discharge of the Sacramento River upstream of the Delta on dates fish were detected at the river junction.

Flow variable (ft^3/s)	Overall Mean (SD)	Range	DCC open Mean (SD)	DCC closed Mean (SD)
Q at Freeport	13,800 (6,483)	6,800 – 40,700	13,350 (3,999)	13,990 (7,243)
Q_{inflow}	10,350 (4,483)	-2,170 – 28,200	10,100 (3,219)	10,450 (4,900)
Q_S	6,254 (4,918)	-6,120 – 20,400	3,770 (5,112)	7,255 (4,468)
Q_G	3,044 (1,143)	1,070 – 8,073	2,663 (599)	3,198 (1,268)
Q_D	1,102 (2,246)	-1,370 – 9,140	3,838 (2,662)	0
ΔQ_S	-74 (476)	-1,659 – 1,360	-173 (556)	-33 (434)
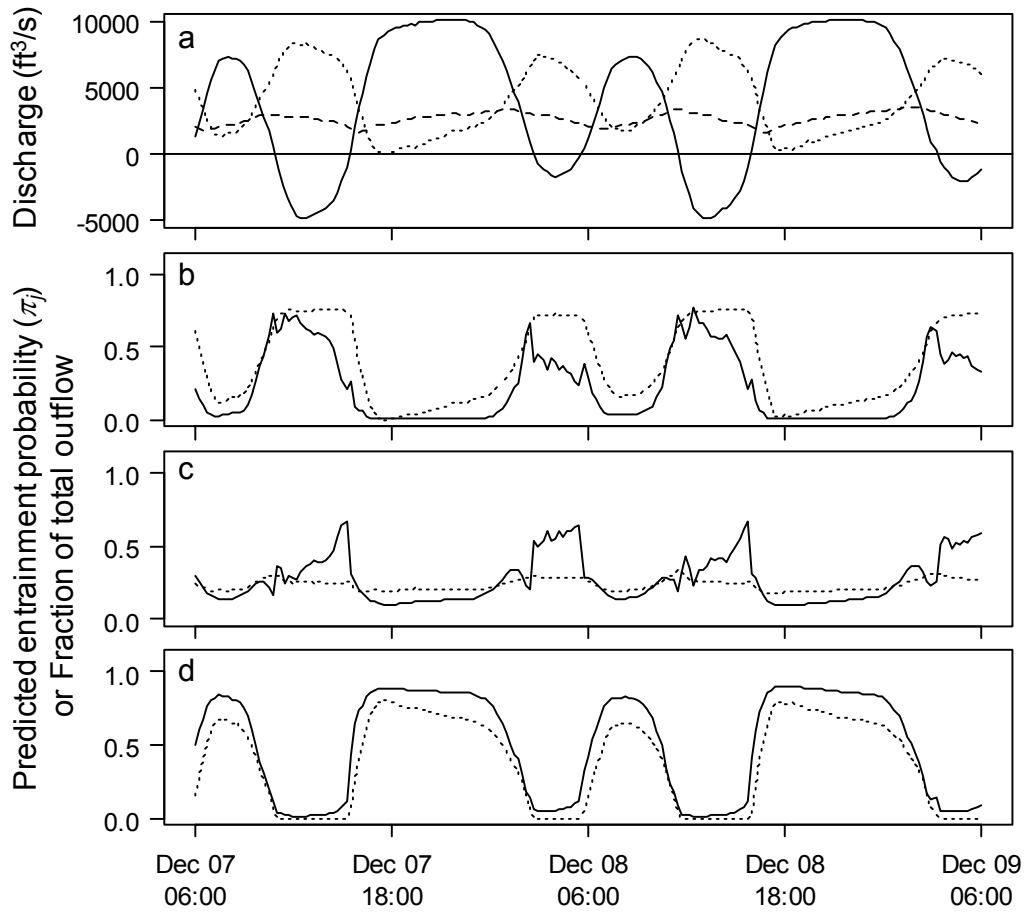
Figure 6.4. Predicted entrainment probability into route *j* as a function of river flow entering each channel for two days in December 2007 under average flow conditions with the Delta Cross Channel open. The top panel (a) shows river discharge just downstream of the river junction in the Sacramento River (Q_S, solid line), the Delta Cross Channel (Q_D, dotted line), and Georgiana Slough (Q_G, dashed line). Panels b-d show the predicted probability of entering each channel (π_j, solid line) and the fraction of total outflow entering each channel (p_{Q_j}, dotted line). Panel b = Delta Cross Channel, c = Georgiana Slough, and d = Sacramento River.
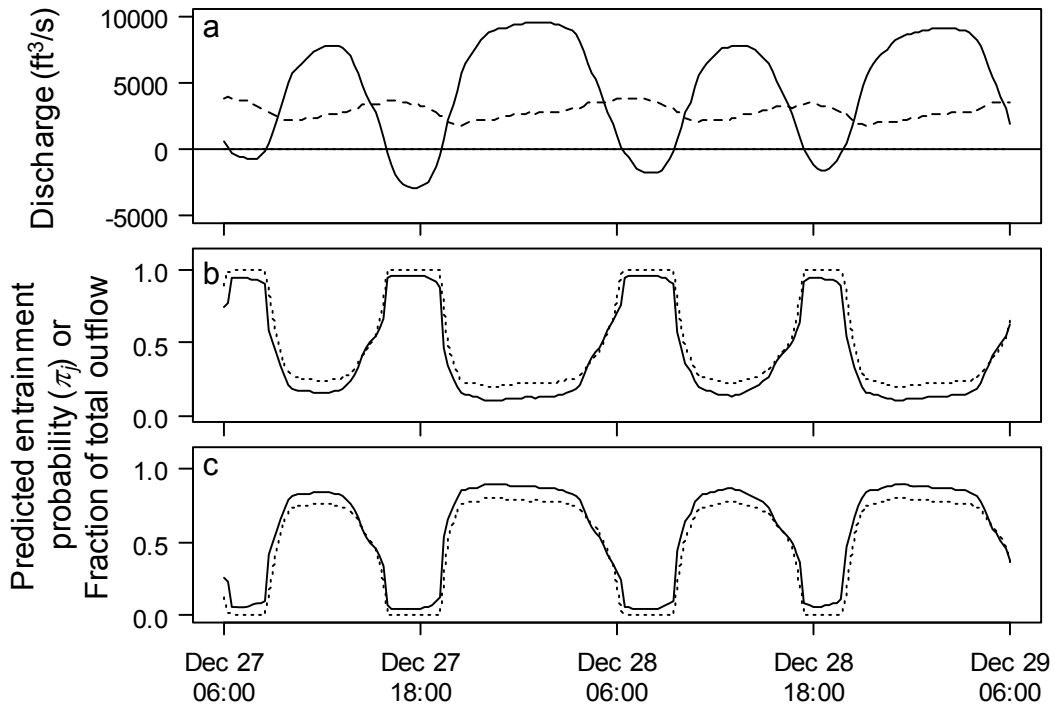
Figure 6.5. Predicted entrainment probability into route *j* as a function of river flow entering each channel for two days in December 2007 under average flow conditions with the Delta Cross Channel gate closed. The top panel (a) shows river discharge just downstream of the river junction in the Sacramento River (Q_S, solid line) and Georgiana Slough (Q_G, dashed line). Panels b-c show the predicted probability of entering each channel (π_j, solid line) and the fraction of total outflow entering each channel (p_{Q_j}, dotted line). Panel b = Georgiana Slough, and c = Sacramento River.

In response to fluctuating river flows driven by the tides, entrainment probabilities vary substantially throughout the day. For the Delta Cross Channel, π_D closely tracks Q_D and is inversely related to Q_S (Figure 6.4b). Thus, π_D is close to zero during the full ebb tide when flow of the Sacramento River is at its maximum and cross channel flow is minimal. As the tide transitions from ebb to flood, flow decreases in the Sacramento River and π_D increases to a maximum of about 75% just as Sacramento River reaches the full flood tide. The probability of entering the Delta Cross Channel is nearly always less than the fraction of total discharge entering the cross channel, except when Q_S declines from ebb to flood tide. During this tidal stage, π_D is similar to the fraction of Q_D. Following the peak of the flood tide, however, π_D begins to decline despite the proportion of flow entering the cross channel remaining relatively constant through the flood tide. This pattern is driven by the relative contributions of Q_S and ΔQ_S in the equation for π_D (Table 6.4). The negative slope for ΔQ_S increases π_D when Q_S declines during ebb-to-flood transitions, but decreases π_D when Q_S increases during flood-to-ebb transitions (Figure 6.4b).

Discharge of Georgiana Slough varies much less than Q_D or Q_S, yet the probability of entering Georgiana Slough varies substantially throughout the day (Figure 6.4c and 6.5b). When the Delta Cross Channel gate is open and Q_S is positive, π_G tends to track the fraction of discharge entering Georgiana Slough (Figure 6.4c). However, during flood tides that cause upstream flow in the Sacramento River, π_G increases substantially despite a constant fraction of discharge entering Georgiana Slough. In contrast, with the Delta Cross Channel closed, the fraction of discharge entering Georgiana Slough varies between 20% and 100% as Q_S cycles between negative and positive flow about a relatively constant Q_G (Figure 6.5b). Consequently, π_G closely tracks the fraction of flow entering Georgiana Slough, and ranges from approximately 0.10 during the full ebb tide to 0.95 during the flood tide. During flood tides with the Delta Cross Channel gates closed, the probability of entering Georgiana Slough is higher than when the gates are open (Figure 6.4c and 6.5b). This pattern also arises in the estimated entrainment probabilities where $\hat{\pi}_{i,G}$ tends to be higher with the gates closed compared to open for a given Q_S less than 5,000 ft^3/s (Figure 6.2b).

Since π_G increases when the Delta Cross Channel is closed, π_S follows as similar pattern regardless of the whether the cross channel gates are open or closed (Figure 6.4d and 6.5c). In general, π_S follows a step function, switching quickly from a high probability of remaining in the Sacramento River during an ebb tide to a very low probability during the flood tide (Figure 6.4d and 6.5c). During the full ebb tide, π_S remains at about 0.90 regardless of gate position. However, with the cross channel gate open during a flood tide, π_S is near zero, indicating that fish migrating through the river junction during this tidal stage will almost certainly enter either the Delta Cross Channel or Georgiana Slough (Figure 6.4d, also see Figure 6.2a and 6.2d). Although π_S remains low during flood tides when the gate is closed, fish still have 5-10% chance of remaining in the Sacramento River (Figure 6.4d).

6.3.5 Daily and diel variation in mean entrainment probabilities

At the daily scale, the mean probability of entering the interior Delta ($\bar{\pi}_{ID,d}$) tends to follow the seasonal trend in the fraction of discharge entering the interior Delta, but the difference between fish entrainment and water distribution varies over time (Figure 6.5b and Appendix Figures 5.2 and 5.3). For example, in December 2006 when the Delta Cross Channel was open, the fraction of mean flow entering the interior Delta is higher than $\bar{\pi}_{ID,d}$ (Figure 6.6b). However, when the Delta Cross Channel was closed, the fraction of flow entering the interior Delta declines much more than $\bar{\pi}_{ID,d}$ and remains less than $\bar{\pi}_{ID,d}$ for the remainder of the winter. The difference between total discharge entering the junction and the interior Delta increases as total discharge increases, which decreases the fraction of discharge, and in turn, the mean probability of entering the interior Delta (Figure 6.6a and 6.6b). Although $\bar{\pi}_{ID,d}$ generally tracks the fraction of flow entering the interior Delta, these findings suggest their relationship is not directly proportional.

I also found substantial differences between mean entrainment probabilities for day and night, with daytime entrainment probabilities cycling over a two-week period according to the spring-neap tidal cycle (Figure 6.6c and Appendix Figures 5.2 and 5.3). Semidiurnal tides
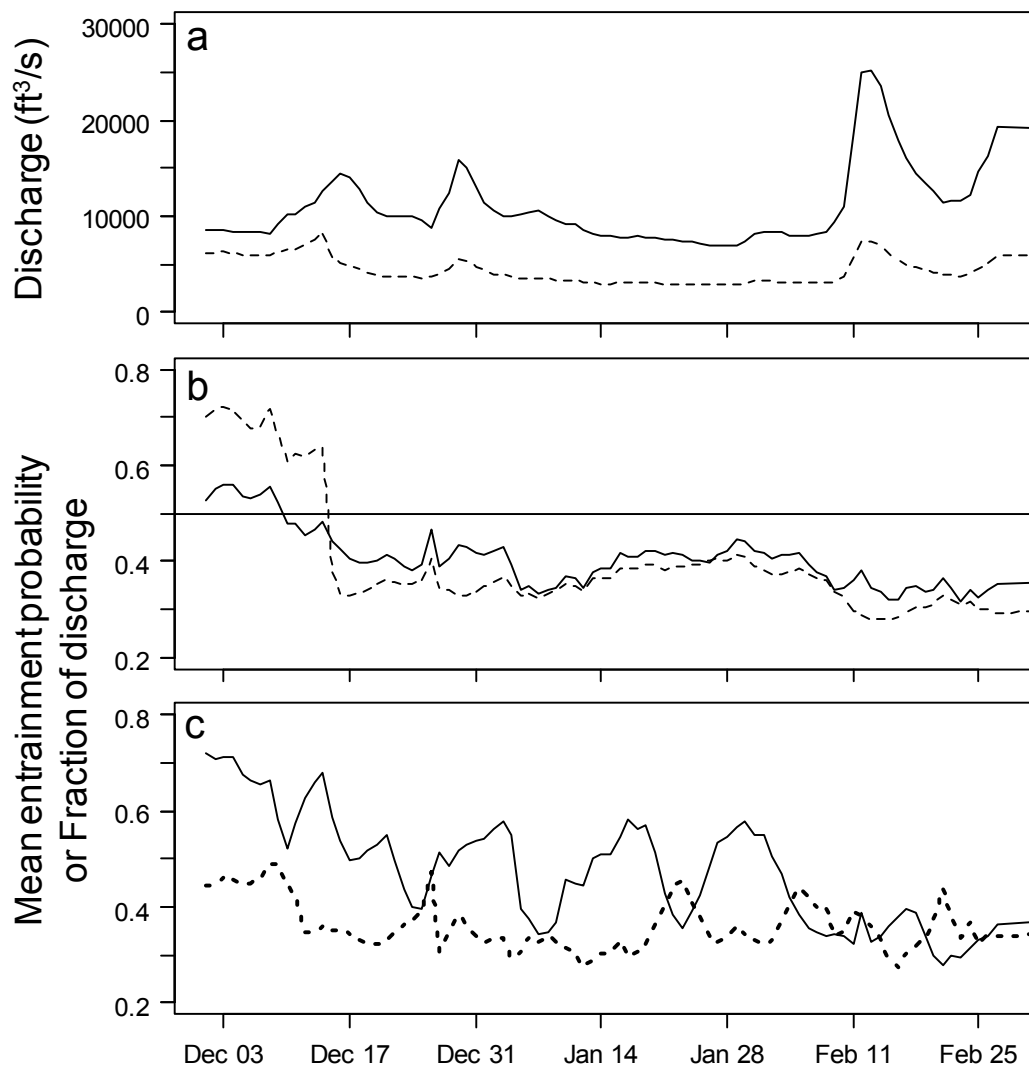
Figure 6.6. Mean daily river flow (a) and mean predicted probability of entrainment into the interior Delta (b and c) during winter 2006/2007. The top panel (a) shows mean daily discharge entering the river junction (Q_{inflow}, solid line) and mean daily discharge entering the interior Delta through both the Delta Cross Channel and Georgiana Slough (dotted line). Panel b shows the mean daily probability of entering the interior Delta ($\bar{\pi}_{\text{ID},d}$, solid line) and the fraction of mean daily discharge entering the interior Delta ($p_{\bar{Q}_{\text{ID},d}}$, dashed line). Panel c shows the mean entrainment probability for day (solid line) and night (heavy dotted line) diel periods. The Delta Cross Channel was open prior to December 15, 2006 and closed thereafter.

at this river junction are characterized by two tidal cycles each day, one with a large tidal range and one with a smaller tidal range (tidal range is the difference in water elevation between peak flood tide and the next ebb tide). On large ebb tides, the probability of remaining in the Sacramento River remains high for a long period of time (e.g., 7 h for the nighttime floods in Figure 6.4d) relative to the following ebb tide when π_S is high for only brief periods (e.g., about 2 h for the daytime floods in Figure 6.4d). When the large ebb tide followed by the small flood tide occurs mostly at night, fish arriving at night, on average, have a high probability of remaining in the Sacramento River (conversely, a low probability of entering the interior Delta). However, the very next tide during the day is typically comprised of a small ebb tide and a large flood tide. Thus, when integrated over the daytime period, the average probability of entering the interior Delta is much higher for a fish that arrives at the river junction during the day (Figure 6.6). As tides shift by about an hour each day, the alternating high-low floods and ebbs switch between day and night, inducing cycles in the mean probability of entering the interior Delta during day and night. These findings indicate that seasonal migration timing combined with diel activity patterns of fish could substantially influence the fraction of the population entrained into the interior Delta. However, at higher total discharge, tidal cycles have less influence on hourly discharge and entrainment probabilities, and thus mean day and night entrainment probabilities are similar (e.g., late February in Figure 6.6c).

6.3.6 Expected relation between entrainment probability and flow distribution

Mean daily entrainment probabilities are positively related to the fraction of flow entering the interior Delta (Figure 6.7b). However, entrainment probabilities are not directly proportional to the fraction of river flow entering the interior Delta, nor is there a 1:1 relation between the entrainment probability and the fraction of flow. First, a slope of 0.47 indicates that, on average, a unit decrease in the fraction of discharge entering the interior Delta reduces the mean daily entrainment probability by only 0.47 units (Figure 6.7b). For instance, reducing the proportion of flow into the interior Delta by 30 percentage points (e.g., from 65% to 35%) is expected to reduce the mean entrainment probability by only about 15 percentage points. Second, mean entrainment probabilities are not directly proportional to the fraction of flow
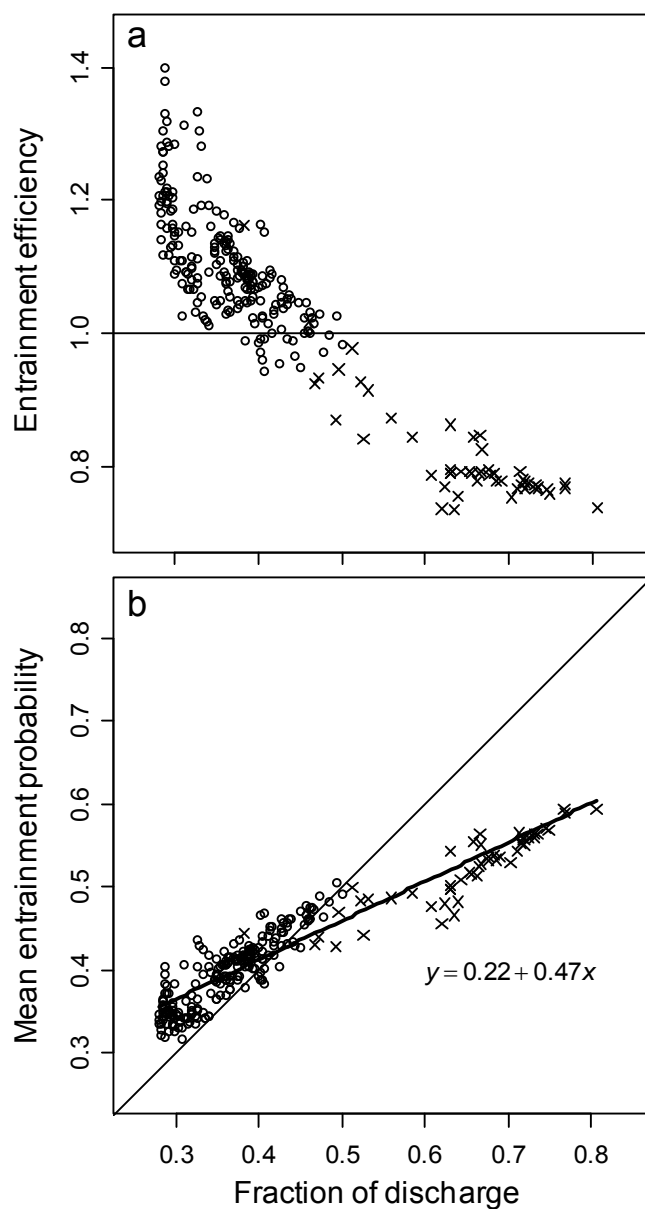
Figure 6.7. Entrainment efficiency (a; $E_{ID} = \bar{\pi}_{ID} / p_{\bar{Q}_{ID}}$) and mean daily probability of entering the interior Delta (b; $\bar{\pi}_{ID}$) as a function the proportion of mean inflow entering the interior Delta ($p_{\bar{Q}_{ID}}$) for the period Dec 1 – Feb 28 during the winters of 2007 to 2009. Circles are days when the Delta Cross Channel was closed, and Xs are days when the Delta Cross Channel was open during some part of that day. The horizontal line at $E_{ID} = 1$ in the top panel and the 45° line in the bottom panel show where the mean entrainment probability is equal to the fraction of flow entering the interior Delta.

since entrainment efficiency is not constant with respect to the fraction of flow (Figure 6.6a).
Entrainment efficiency is greater than one when the fraction of flow entering the interior Delta
is low, but decreases below one as the fraction of discharge entering the interior Delta
increases. Thus, opening the Delta Cross Channel will increase the fraction of fish entering the
interior Delta, but by considerably less than the increase in the fraction of flow.

6.3.7 Contribution of river inputs and tides

Both river flows and gate position affect the strength of the tides at the river junction
(Figure 6.8), and in turn, the fraction of river flow entering the interior Delta. With increasing
inflow to the junction, tidal forces are dampened (Figure 6.8b) and the fraction of each day
with upstream flow declines (Figure 6.8a). For example, with the gates closed, reverse flows
comprise 40% of the day at the lowest observed inflows, but the Sacramento River ceases to
reverse direction at inflows exceeding about 12,000 ft^3/s (Figure 6.8a). At given inflows
<15,000 ft^3/s, an open cross channel gate increases both CV(Q_S) and the fraction of time with
upstream river flow at Q_S (Figure 6.8). The fraction of mean daily discharge entering the
interior Delta increases with the strength of the tides (Figure 6.9d) because much of the water
entering the interior Delta occurs during flood tides (Figure 6.4 and 6.5). However, as river
inflows increase, the fraction of discharge entering the interior Delta approaches an asymptote
at just less than 30% (Figure 6.9b), the point at which tidal strength approaches zero (Figure
6.8b and 6.9d). With the gates open, the fraction of flow entering the interior Delta remains
about 30 percentage points higher than with the gates closed (Figure 6.9c). These hydraulic
relationships play a critical role in the likelihood that fish will be entrained into the interior
Delta.

River inputs, tidal forces, and the position of the Delta Cross Channel gate influence
the entrainment probability into the interior Delta. Mean daily entrainment probabilities follow
the same pattern as the fraction of flow, initially decreasing as total discharge increases (Figure
6.9a). This pattern arises due to the effect of tides: Entrainment probabilities are highest when
tides are strong (Figure 6.9c), which occurs at low inflows (Figure 6.8). Daily entrainment
probabilities are highest at low inflow because the Sacramento River reverses direction for a
substantial fraction of the day (Figure 6.8a), and under these conditions $\pi_{i,\mathrm{ID}}$ is at its maximum
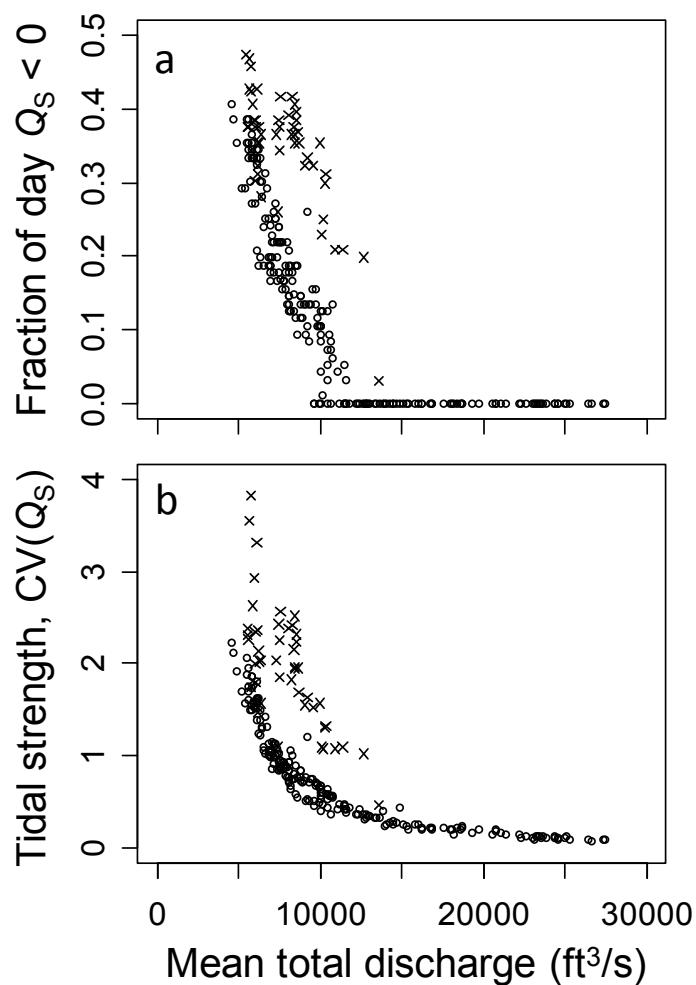
Figure 6.8. The proportion of each day with upstream flow into the junction (a) and tidal strength (b; coefficient of variation in Q_S) as a function of mean daily river discharge entering the junction ($\bar{Q}_{\text{inflow},d}$). Circles are days when the Delta Cross Channel was closed, and Xs are days when the Delta Cross Channel was open during some part of that day. Three data points with $4 > CV(Q_S) < 6$ are not shown.
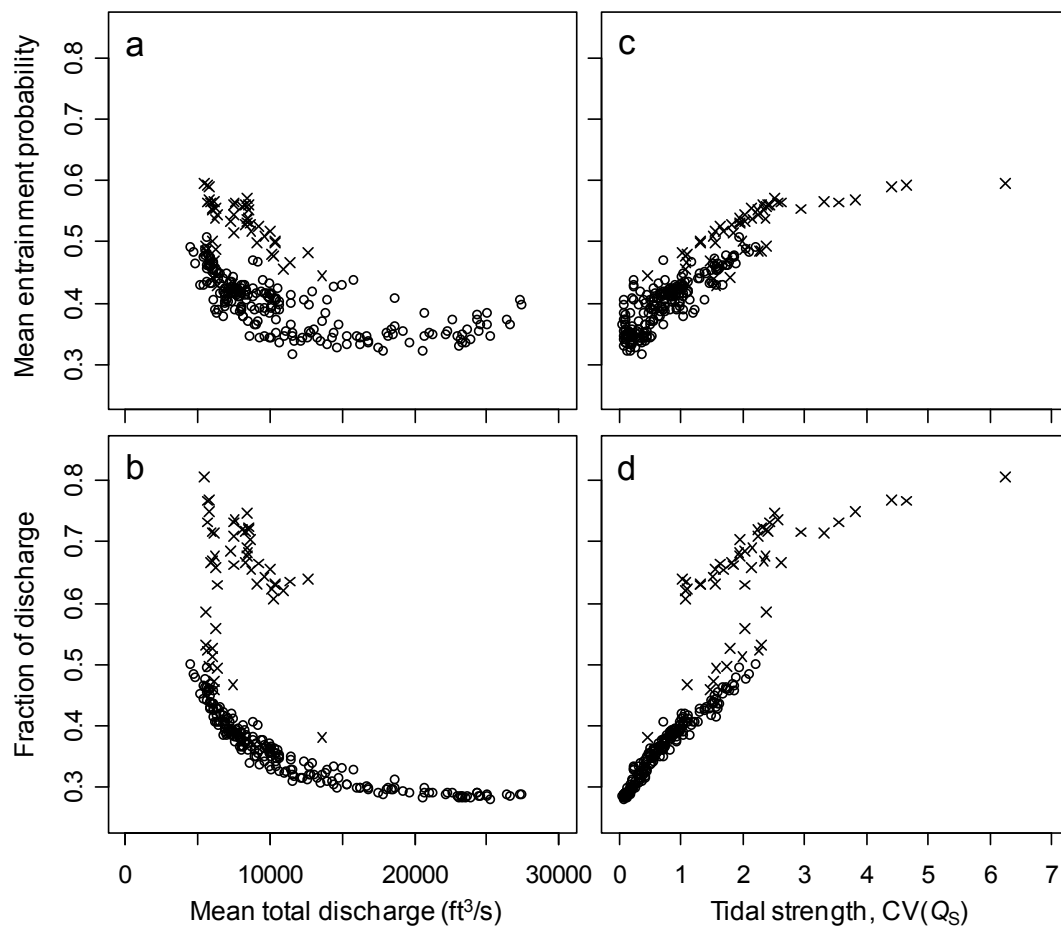
Figure 6.9. Mean daily probability of entering the interior Delta (a and c; $\bar{\pi}_{\mathrm{ID}}$) and the proportion of mean inflow entering the interior Delta (b and d; $p_{\bar{Q}_{\mathrm{ID}}}$) as a function of mean daily discharge entering the river junction (a and b; $\bar{Q}_{\mathrm{inflow},d}$) and tidal strength (c and d; coefficient of variation in Q_{S}) for the period Dec 1 – Feb 28 during the winters of 2007–2009. Circles are days when the Delta Cross Channel was closed, and Xs are days when the Delta Cross Channel was open during some part of that day. In the bottom panels (b and d), variability in $p_{\bar{Q}_{\mathrm{ID}}}$ with the Delta Cross Channel open at low discharge is due to experimental gate operations in 2009 when the cross channel was open during the day but closed at night.

 (Figure 6.3d). Mean daily entrainment probabilities approach a minimum at inflows of about 12,000 ft^3/s (Figure 6.9a), the point at which the Sacramento River ceases to reverse direction (Figure 6.8a).

The difference in entrainment probability between cross channel gates open and closed (at a given total discharge) is only about 15 percentage points, half the difference in the fraction of flow between gates open and closed (Figure 6.9a and 6.9b). This finding illustrates the effect of the slope (0.47) in the relation between entrainment probability and fraction of discharge shown in Figure 6.6.

6.3.8 Simulating alternative gate operations

Closing the Delta Cross Channel at night had a large influence on the fraction of discharge entering the interior Delta, but much less effect on daily entrainment probabilities for the interior Delta (Figure 6.10 and 6.11). Prior to December 15, the period when the Delta Cross Channel is historically open, the closed-at-night operation reduces the interior Delta flow proportion by 15 percentage points (Figure 6.10a and 6.11a). In contrast, daily entrainment probabilities decrease on average by 5, 7, and 1.5 percentage points for uniform, 85% night, and 85% day arrival distributions at the junction (Figure 6.10b-6.10d). After December 15 when the gate is historically closed, switching to the closed-at-night operation increases the interior Delta flow proportion by 11 percentage points (Figure 6.10a and 6.11b). In this case, daily entrainment probabilities increase, on average, by 3, 1.3, and 6 percentage points for the uniform, 85% night, and 85% day arrival distributions at the junction (Figure 6.10b-6.10d). Thus, when switching from a fully closed gate position, opening the gates during the day has little effect on entrainment if most migration occurs at night, but a larger increase when migration occurs mostly during the day. Regardless of diel activity pattern, however, the change in daily entrainment probabilities is considerably less than the change in the fraction of discharge.

Hourly time series of route-specific entrainment probabilities reveal why gate operations affect flow proportions more than population-level entrainment. The probability of remaining in the Sacramento River (π_S) changes little in response to changes in gate position (Figure 6.12 and 6.13). For example, when the Delta Cross Channel is open, switching to
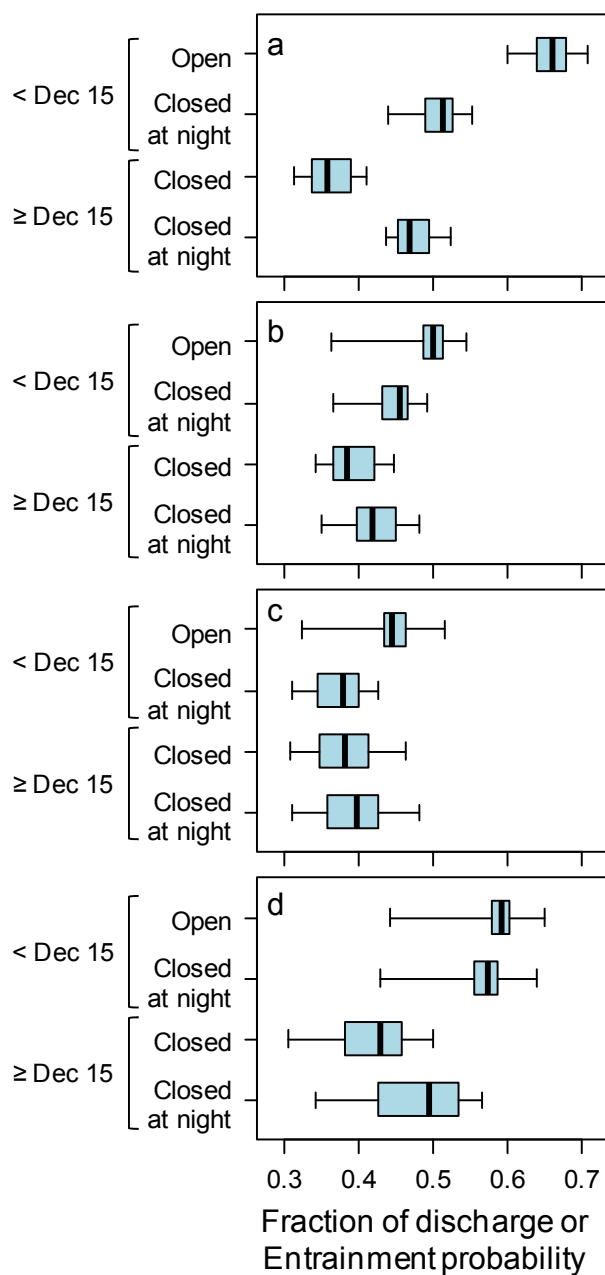
Figure 6.10. Distribution of the daily proportion of discharge entering the interior Delta (a) and predicted daily entrainment probabilities for the interior Delta (b-d) assuming b) a uniform diel arrival distribution at the junction, c) 85% of fish arriving at night, and d) 85% of fish arriving during the day. Entrainment probabilities were predicted from simulating flow data for the period November 1, 2006 – January 31, 2007 under two scenarios: 1) the historical gate operations where the Delta Cross Channel was open until December 15 and closed thereafter, and 2) operations where the gate was closed at night but open during the day for the entire simulation period.
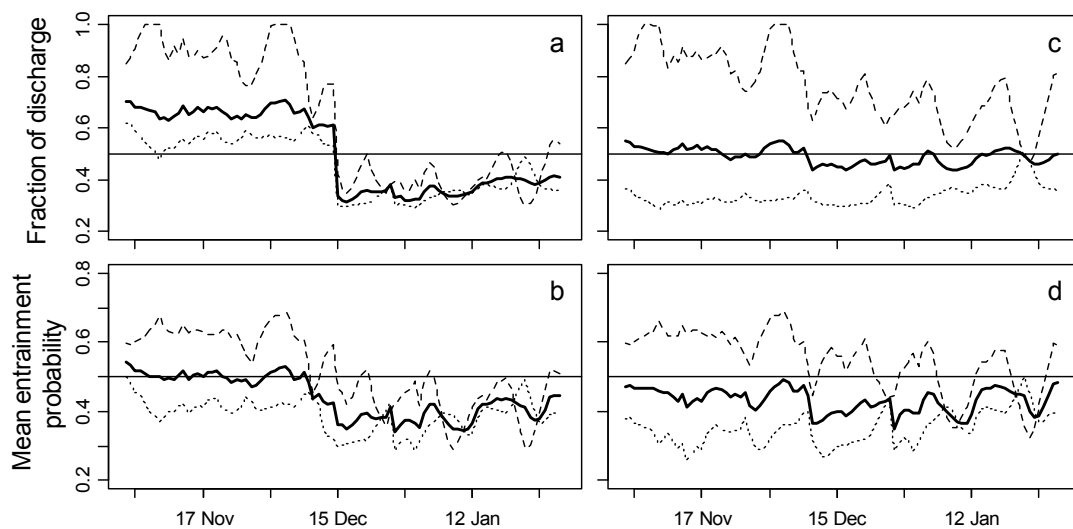
Figure 6.11. Daily fraction of discharge (a and c) and mean probability of entrainment (b and d) into the interior Delta under two simulated flow scenarios. Simulations were conducted for the period November 1, 2006 – January 31, 2007 under the historical gate operations where the Delta Cross Channel was open until December 15 and closed thereafter (a and b), and closed-at-night operations where the gate was closed at night but open during the day for the entire simulation period (c and d). The top panels (a and c) show the fraction of junction inflow entering the interior Delta for each day (solid line) and for day and night periods within each day (dashed and dotted lines). The bottom panels (b and d) show mean daily entrainment probabilities assuming uniform diel arrival at the junction (solid line), 85% of fish arriving during day (dotted line), and 85% of fish arriving at night (dashed line).
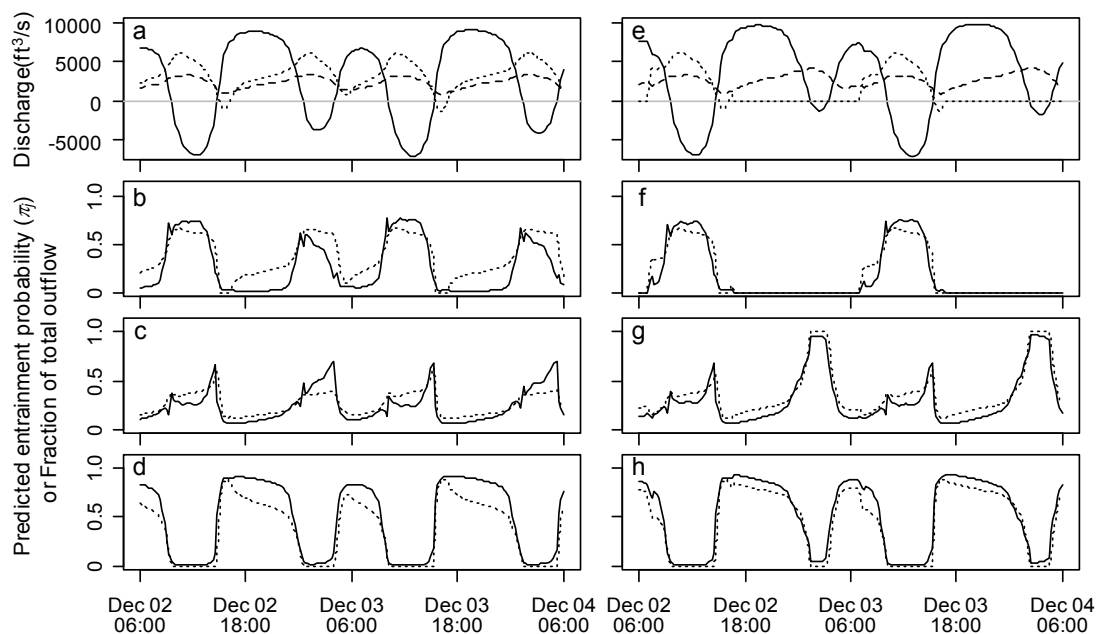
Figure 6.12. Predicted entrainment probability into route *j* as a function of simulated river flows entering each channel for two days in December 2006. Panels a-d = historical gate operations where the Delta Cross Channel was open until December 15, and e-h = closed-at-night operations where the gate was closed at night but open during the day for the entire simulation period. The top panels (a and e) show river discharge just downstream of the river junction in the Sacramento River (Q_S, solid line), Georgiana Slough (Q_G, dashed line), and the Delta Cross Channel (Q_D, dotted line). Lower panels (b-d and f-h) show the predicted probability of entering each route (π_j, solid line) and the fraction of total outflow entering each route (p_{Q_j} , dotted line). Panels b and f = the Delta Cross Channel, c and g = Georgiana Slough, and d and h = Sacramento River.

Figure 6.13. Predicted entrainment probability into route *j* as a function of simulated river flows entering each channel for two days in January 2007. Panels a-d = the historical gate operations where the Delta Cross Channel was closed after December 15, and e-h = closed-at-night operations where the gate was closed at night but open during the day for the entire simulation period. The top panels (a and e) show river discharge just downstream of the river junction in the Sacramento River (Q_S, solid line), Georgiana Slough (Q_G, dashed line), and the Delta Cross Channel (Q_D, dotted line). Lower panels (b-d and f-h) show the predicted probability of entering each route (π_j, solid line) and the fraction of total outflow entering each route (p_{Q_j}, dotted line). Panels b and f = the Delta Cross Channel, c and g = Georgiana Slough, and d and h = Sacramento River.

closed-at-night operations prevents fish from entering the cross channel but substantially increases their chances of entering Georgiana Slough during the flood tide (Figure 6.12). Thus, the only noticeable change in π_S is that it remains high for slightly longer during each ebb tide. When integrated over the 24-h period, daily entrainment into the interior delta decreases, but less than is expected based solely on changes in flow distribution. These findings illustrate how my model can be used to understand the effect of management actions on routing of fish in the Delta.

6.4 Discussion

Recovering endangered salmon populations in the Sacramento River requires a detailed understanding of how water management actions affect life history events that determine population dynamics. For a juvenile salmon migrating through the Delta, entering one of many migration routes is an important event that may determine its eventual fate. Entrainment events occur at small spatial and temporal scales at numerous river junctions, but how these events unfold over time determine population-level distribution among migration routes. At the individual level, I found that the probability of entering a given route varies on hourly timescales with the tides. At the population level, the fraction of fish entering a route varies on diel and fortnightly scales due to the spring-neap cycle, and on daily and seasonal scales due to river inflows and gate operations. These findings form the basis for understanding how water management actions affect entrainment into the interior Delta. As shown by simulating closed-at-night gate operations, my model can be used for predicting how fish distribute among routes in response to water management actions. Such management tools are critical for understanding the response of endangered salmon populations to water management actions in the Delta.

My findings show that flood tides causing the Sacramento River to reverse direction substantially increase the probability of entering both Georgiana Slough and the Delta Cross Channel. Parameter estimates indicate that entrainment probabilities into both the Delta Cross Channel and Georgiana Slough are at a maximum when 1) Q_S is at a minimum (increases both π_G and π_D), 2) the ebb tide transitions to a flood tide (increases π_D), 3) Q_G is at a maximum

(increases π_G), and 4) discharge at Q_S is negative (increases π_G; Figure 6.4 and 6.5, Table 6.3). These conditions coincide and persist for the longest period of time during flood tides when mean river discharge entering the junction is low (Figure 6.8). As a consequence, daily entrainment into the interior Delta is highest at the lowest mean daily river discharge (Figure 6.9). As mean river discharge increases, tidal fluctuations are dampened and the river ceases to reverse direction on flood tides, causing daily entrainment probabilities to decrease as total inflow to the junction increases. These processes suggest that reduced inflows to the Delta will increase the frequency and duration of negative-flow flood tides at this river junction, increasing the fraction of juvenile salmon populations entrained into the interior Delta. In the future, inflows to the Delta may decrease through climate change or through water management actions that reduce discharge of the Sacramento River.

Overall, predicted daily entrainment into the interior Delta varied from about 30% to 60%. This range is driven by operation of the Delta Cross Channel and the interaction between river inflows and tides (Figure 6.9). Given the current physical setting of the Delta, reducing entrainment from the highest to lowest levels requires 1) closing the Delta Cross Channel gate and 2) maintaining mean daily inflows to the junction above 12,000 ft^3/s. Closing the gate is expected to reduce entrainment into the interior Delta by 10-15 percentage points. With the gates closed, entrainment probabilities decline an additional 15-20 percentage points from about 0.5 at the lowest inflow to 0.3 at about 12,000 ft^3/s. Increasing river inflow reduces tidal forces until about 12,000 ft^3/s, in turn reducing mean daily entrainment probabilities. At higher inflows, entrainment probabilities remain relatively constant, suggesting a shift from tidally dominated dynamics at hourly scales to inflow-dominated dynamics at daily scales. A third approach to reduce entrainment probabilities involves structural changes to the Delta that alter the relation between inflows and tides at this river junction. For example, wetland restoration at key locations in the Delta could absorb tidal forces, reducing upstream propagation of tides in the Sacramento River. Such actions would lower the inflow threshold at which tides begin to increase entrainment into the interior Delta by shifting the curves in Figure 6.8 to the left.

My analysis shows that low river inflows affect entrainment probabilities as much as operation of the Delta Cross Channel. This is an important finding because low inflows may have a compounding effect on population-level survival if survival through the interior Delta is

negatively related to inflow. Under constant survival within routes, population-level survival (i.e., S_{Delta}) decreases with increasing entrainment into the interior Delta because survival in the interior Delta is lower than survival in the Sacramento River (Perry et al., 2010; Newman and Brandes, 2010; Chapter 4). However, if survival through the interior Delta decreases with inflow, then population-level survival may decline quickly because entrainment into the interior Delta increases while survival in the interior Delta is declining. Although the relation between inflow and survival through the interior Delta has yet to be firmly established (Newman and Brandes, 2010), my study highlights how river flow, route-specific survival, and entrainment into the interior Delta can act synergistically to affect population-level survival.

Understanding the relation between fish and flow distribution is important for quantifying both the economic and biological costs of water management actions. I found that predicted entrainment into the interior Delta was positively related but disproportional to discharge entering the interior Delta. Furthermore, entrainment efficiency was inversely related to the fraction of discharge entering the interior Delta, declining from 1.4 at low flow proportions when the Delta Cross Channel was closed, to 0.7 at high flow proportions with the Delta Cross Channel open (Figure 6.7). Thus, assuming a 1:1 relation between fish and flow considerably overestimates the fraction of fish entrained when the Delta Cross Channel is open. Nonetheless, reducing the interior Delta flow proportion reduces fish entrainment, but at a rate less than the change in flow. Specifically, the fraction of fish changes by only about half the change in the fraction of flow entering the interior Delta. Thus, each unit change in the fraction of fish entrained "costs" two units of fractional discharge. Understanding this relationship will allow managers to better quantify tradeoffs between the benefits of reducing fish entrainment relative to the costs of reduced water pumping associated with closure of the Delta Cross Channel.

Interaction between tides and diel migration behavior substantially affects the fraction of fish entrained into the interior Delta, especially during low inflows to the junction. During the winter migration period, flood tides during the day tend to be larger than at night, causing higher mean entrainment probabilities during the day. Consequently, relative to uniform diel migration, preferential diurnal migration will increase the fraction of fish entrained into the interior Delta, whereas nocturnal migration reduces entrainment. This finding was illustrated

in my simulations of alternative gate operations: regardless of gate operations, mean entrainment probabilities were highest when 85% of fish migrated during the day, lowest when 85% of fish migrated at night, and intermediate when fish migrated uniformly over the diel cycle (Figure 6.10 and 6.11).

Increasing river inflow reduces tidal fluctuations at the river junction and in turn, reduces differences between day and night entrainment probabilities. Thus, day and night entrainment probabilities are similar when river flow exceeds the threshold at which at tidal strength approaches zero (about 12,000 ft^3/s). This pattern is illustrated in Figure 6.6 where day and night entrainment probabilities differed considerably during low flow in January, but were similar during February when inflow increased. Diel activity patterns affect population-level entrainment when river flow is low and tidal strength high, but will have little influence on entrainment at higher inflows when tidal strength is low. Given the relatively low flows observed during this three-year study, understanding diel activity patterns of migrating juvenile salmon is critical for quantifying entrainment into the interior Delta and identifying management actions that minimize entrainment.

In general, factors driving diel movement patterns in the Delta are poorly understood but will probably vary with season, environment, life stage, and life history strategy of juvenile salmon. In my study, the proportion of fish detected at night averaged 75% even though night comprised about 60% of the 24-h period. More importantly, nighttime arrival varied from 55% to 86% among release groups, ranging from diel arrival proportional to the availability of daylight hours to substantial nocturnal migration (Table 6.1). Such variation is not surprising given that diel activity patterns can switch from day to night in response to interactions between predation risk, physiological state, and environmental cues (Metcalfe et al. 1998, 1999). For example, an increase in nighttime activity with decreasing temperature is hypothesized as a behavioral response to lower metabolic requirements, reducing the need for juvenile salmon to feed during the day when predation risk is high. In my study, some preference for nocturnal migration is expected given that the study occurred during winter at water temperatures ranging from 6-12 °C. At higher temperatures, evidence suggests that juvenile salmon in the Delta may migrate preferentially during the day (Wilder and Ingram, 2006).

The primary strength of my model is its ability to estimate time-specific probabilities of entering each migration route in response to tidally varying flows. This property allows management actions to be simulated at hourly scales, but also permits assessment of different diel activity patterns. Diel activity of a given population can vary considerably, such as observed in this study. Furthermore, species, life stages, and rearing types (e.g., hatchery versus wild) that migrate simultaneously may exhibit different diel activity patterns. By simulating a range of diel activity patterns, management actions robust to uncertainty in diel activity can be identified. Simulations of closed-at-night gate operations provided one example of how my model could be used to optimize water management actions by maximizing water diversion and minimizing fish entrainment. Additional applications include simulating the effect of changes in mean river inputs and changes in tidal dynamics (e.g., through wetland restoration or levee breaches); both of which are critical factors affecting entrainment into the interior Delta.

It is important to recognize that population distribution among migration routes will depend on entrainment probabilities at a number of critical river junctions. First, many juvenile salmon never encounter the Delta Cross Channel or Georgiana Slough because 20-40% of the population enters Sutter and Steamboat Slough, the first major river junction in the Delta that juvenile salmon must negotiate (Perry et al., 2010; Chapter 4). Second, downstream of both river junctions, juvenile salmon may also enter the interior Delta through Three Mile Slough or at the confluence of the Sacramento and San Joaquin rivers near the terminus of the Delta. Future efforts to quantify channel-specific entrainment probabilities as a function of flow at other river junctions will help to predict Delta-wide movement of the population in response water management actions.

Prior to this study, fisheries managers had little mechanistic information to guide water management actions intent on minimizing entrainment into the interior Delta. Uncertainty about driving mechanisms forces fisheries managers to act in a precautionary manner, implementing actions least likely to harm endangered populations at the expense of consumptive water use. Furthermore, lack of understanding key mechanisms limits development of solutions that both minimize biological consequences, but also minimize costs to water users. Operation of the Delta Cross Channel is an obvious action that managers can

control. Less obvious but equally important is the effect of river inflow on entrainment into the interior Delta. I quantified how these mechanisms affect route entrainment probabilities and developed a model that managers can use to assess the effect of a wide range of water management actions. This study takes an important step towards providing tools to understand how future water management in the Delta might influence migration and survival dynamics of juvenile salmon.

Chapter 7

SUMMARY AND CONCLUSIONS

Historically, California's Central Valley was among the most productive salmon-bearing watersheds in the continental United States. Today, the Sacramento-San Joaquin River Delta has the distinction as one of the most human-altered estuaries in the world. Yet such alteration has allowed water from the Delta to support 20 million Californians and the country's largest agricultural industry. Salmon and other endemic fish populations have suffered the consequence of this economic prosperity and are now but a wisp of their former magnitude. State and federal governments are wrestling with recovering endangered fishes while maintaining ecosystem services in the face of climate change and human population growth. My dissertation research takes place against this backdrop, but this general storyline has played out in many large rivers and estuaries across the nation.

Managers require detailed information about the response of endangered fish populations to alternative water management actions. Given the extreme spatial and hydrodynamic complexity of the Delta, unraveling migration and survival dynamics of juvenile salmon is a formidable challenge. Traditional capture-recapture techniques have limited utility in this setting, but acoustic telemetry allows the migration of individuals to be tracked at fine temporal and spatial scales to match the complexity of the Delta's channel network. Although acoustic telemetry provides a means for collecting reams of detailed data, lacking are statistical models to translate this data from mere descriptive assessments to population-level inferences. My dissertation takes a significant step towards coupling modern capture-recapture models with detailed information afforded by telemetry. The models presented in this dissertation illustrate the inferential power obtained when combining telemetry with statistical models to tackle complex problems in fisheries science.

At the outset of this research project, significant questions loomed not only about survival of juvenile salmon, but also about their movement patterns through the Delta. For the past 30 years, survival studies using coded wire tags provided an incomplete picture of

population status. Annual survival indices indicated that mortality in some migration routes was lower than others. Without information about movement among routes, however, it was impossible to quantify the contribution of a particular migration route to survival of the population. This gap made it impossible to explicitly quantify the effects of management actions at the population level. My first goal, therefore, was to link survival in each migration route to population-level survival. In Chapter 2, I cast this problem as a spatially structured population model comprised of two sets of vital rates: 1) route-specific survival probabilities and 2) transition probabilities that governed movement among routes.

To estimate parameters of this spatially stratified model, I adapted the general class of models known as multistate mark-recapture models (Brownie et al., 1993; Lebreton and Pradel, 2002). I explicitly evaluated critical assumptions of the model in the context of using telemetry to sample individuals moving through space. I showed how the spatial location of telemetry stations could violate model assumptions, leading to biased estimates of transition probabilities. In addition, the dendritic, hierarchical structure of the Delta's channel network results in a constrained version of the general multistate model, which can cause confounding among parameters. I used formal statistical techniques and simulation to arrive at general principles for telemetry system design that both fulfills model assumptions and ensures estimability of parameters. My findings illustrate the direct link between developing a model containing parameters of interest, designing the telemetry system to estimate these parameters, and then testing the model to be sure parameters can be estimated from the data. Given the explosion in the use of remote detection systems for monitoring fish populations (Hewitt et al., 2010, McMichael et al., 2010), this work contributes directly towards understanding how to design both detection systems and statistical models capable of estimating parameters of interest.

In Chapters 3 and 4, I applied the multistate models to the first available telemetry data on Delta-scale movements of juvenile Chinook salmon. New insights were immediate. For the first time, managers could begin to understand how movement and survival at multiple spatial scales interact to affect population survival. At the finest spatial scale, transition probabilities quantified the chances of a fish being entrained into a particular channel at a given river junction. At the next scale, joint entrainment probabilities across multiple river junctions

yielded the fraction of the population migrating through a particular pathway in the Delta. Understanding movement at both scales is critical to water management in the Delta. At the scale of a single junction, consequences of water management actions on fish entrainment can be directly quantified (e.g., operation of the Delta Cross Channel). At the scale of multiple junctions, the probability of migrating through a unique pathway quantifies the contribution of route-specific survival to population-level survival. For example, I showed that the survival in the Sacramento River was consistently higher than other migration routes, yet for some releases, less than half of the population migrated through the Delta via the Sacramento River. Without a spatially-structured model coupled with telemetry data to estimate the parameters, such insights would be impossible.

Matrix population models cast in the framework of a population viability analysis are a powerful approach to assess recovery of endangered species in response to alternative scenarios (Caswell, 2001; Morris and Doak, 2002). However, to understand how population growth rates are affected by a given management action on a particular life stage at a specific location, sufficient detail must be built into the model. Such detail often translates into numerous parameters for which few empirical estimates exist. By structuring the Delta as a series of spatially stratified transition matrices, I showed how the Delta can be fit neatly into the larger framework of a matrix population model for the complete salmon life cycle. Furthermore, the multistate mark-recapture model provides a natural framework for estimating the parameters of a matrix population model (Caswell and Fujiwara, 2004). Thus, my research has provided both the framework and the parameter estimates with which to quantify how management actions in the Delta affect not only juvenile survival, but population growth rates (e.g., see CALFED Science Review Panel, 2008). Linking spatial dynamics to a population model *and* estimating the parameters of such a model is a major strength of my work that has broad applicability to other systems.

My modeling approach stresses estimation of individual components of the population that can be reconstructed at different levels of organization to gain insights into population dynamics. Reach-specific survival probabilities and entrainment probabilities at a river junction form the basic building blocks of population-level survival. In and of themselves, these fundamental parameters yield insights into movement and survival dynamics at a local

scale. In Chapter 4, for example, I found that reach-specific survival shifted simultaneously for all reaches within a route, shedding light on the spatial scale of variability in survival processes. More important, however, functions of the fundamental parameters provide insights at larger scales of organization. A key example is route-specific survival, the product of reach-specific survival probabilities tracing a particular migration pathway through the Delta. Ability to quantify survival between the same beginning and end points for fish traversing different pathways allows migration routes to be directly compared on the same spatial scale. Furthermore, with a unifying estimation framework, measures of uncertainty for both fundamental parameters and their functions can be readily obtained. Similar approaches are starting to be implemented and models being developed to deconstruct population survival into its component parts (Skalski et al., 2002; Buchanan, 2005). All rely on remote detection of tagged individuals, development of novel estimation models, and reconstruction of fundamental parameters into population-level parameters.

Given a three-year set of telemetry data, in Chapters 5 and 6 I began to tackle the dynamics of movement and survival in response to environmental factors. These analyses focused on individuals because the environment varied at temporal scales likely to impose substantial variation in the fates of individuals. Survival of individuals in two migration routes depended on hydraulic conditions (river flow and tidal strength) during the three days after fish entered a migration route. This finding is of direct use to managers that must quantify the effects of upstream water withdrawals on salmon populations. The Delta Cross Channel has long been the focus of intense scrutiny for both its importance to water users and its effect on juvenile salmon survival. Until my research, entrainment into the Delta Cross Channel was never quantified except for indirect measurements at the pumping facilities. I not only obtained release-specific point estimates of both junction- and population-level entrainment probabilities into the Delta Cross Channel, but I quantified how river flow, tides, and gate operations influenced daily entrainment probabilities into the interior Delta. I then showed how a dynamic model for entrainment probabilities could be used to understand the effect of water management actions on fish routing. This model can be applied immediately in Delta planning processes such as the Delta Bay Conservation Plan to understand how different water management actions affect migration routing in the Delta.

Although the dynamics of the Delta are complex, my findings are intuitive. Most fish are entrained into the interior Delta when all water flows into the interior Delta. Survival is low when fish migrate via a route in which more water can flow inland than towards the ocean. Survival increases when river flow speeds fish past hungry predators. Survival of big fish is greater than that of small fish. To some extent, each of these statements can be supported without data, based on common sense and first principles. Yet in the absence of data these statements stand as mere hypotheses to be challenged. The beauty of science lies in uncovering what should make sense; the central challenge, figuring out how to uncover it; the reward, finding out that indeed, the intuitive hypothesis is supported by the data. But collecting data is not enough. Telemetry techniques allow us to collect millions of detailed observations on individuals, but scientific insights remain hidden without mathematical models to extend individual observations to population-level inferences. My contribution to science is not my findings per se, but developing the mathematical frameworks that allow us to distill apparent complexity into a series of seemingly simple relationships. After all, it is the interaction of myriad simple relationships from which complexity arises. By breaking down systems into their component parts, developing models to relate the pieces to the whole, and applying modern technology to inform models with data, I have taken an important step towards unraveling the complexity of human and natural factors affecting survival of juvenile salmon in the Delta.

BIBLIOGRAPHY

Adams, N. S., D. W. Rondorf, S. D. Evans, J. E. Kelly, and R. W. Perry. 1998a. Effects of surgically and gastrically implanted radio transmitters on swimming performance and predator avoidance of juvenile Chinook salmon (*Oncorhynchus tshawytscha*). Canadian Journal of Fisheries and Aquatic Sciences. 55:781–787.

Adams, N. S., D. W. Rondorf, S. D. Evans, and J. E. Kelly. 1998b. Effects of surgically and gastrically implanted radio transmitters on growth and feeding behavior of juvenile Chinook salmon. Transactions of the American Fisheries Society. 127: 128–136.

Anderson, J. J., E. Gurarie, R. W. Zabel. 2005. Mean free-path length theory of predator-prey interactions: application to juvenile salmon migration. Ecological modeling. 186: 196–211.

Agresti, A. 2002. Categorical data analysis. John Wiley and Sons, Inc., Hoboken, New Jersey.

Arnason, A. N. 1972. Parameter estimation for mark-recapture experiments on two population subject to migration and death. Researches in Population Ecology. 13: 97–13.

Arnason, A. N. 1973. The estimation of population size, migration rates, and survival in a stratified population. Researches in Population Ecology. 15: 1–8.

Baker, P. F., T. P. Speed, and F. K. Lignon. 1995. Estimating the influence of temperature on the survival of Chinook salmon smolts (*Oncorhynchus tshawytscha*) migrating through the Sacramento-San Joaquin River Delta of California. Canadian Journal of Fisheries and Aquatic Sciences. 52:855–863.

Baker, P. F. and J. E. Morhardt. 2001. Survival of Chinook salmon smolts in the Sacramento-San Joaquin Delta and Pacific Ocean. Pages 163 – 182 in R.L. Brown, Editor. Contributions to the Biology of Central Valley Salmonids, Volume 2, Fish Bulletin 179. California Department of Fish and Game, Sacramento, California.

Beissinger, S. R. and D. R. McCullough. 2002. Population Viability Analysis. The University of Chicago Press, Chicago, Illinois.

Beeman, J.W., and J.G. Maule. 2006. Migration depths of juvenile Chinook salmon and steelhead relative to total dissolved gas supersaturation in a Columbia River reservoir. Transactions of the American Fisheries Society. 135: 584–594.

Black, M. 1995. Tragic Remedies: A century of failed fishery policy on California's Sacramento River. The Pacific Historical Review. 64:37–70.

Blake, A. and M. J. Horn. 2003. Acoustic tracking of juvenile Chinook salmon movement in the vicinity of the Delta Cross Channel, Sacramento River, California – 2001 study results. US Bureau of Reclamation Technical Memorandum No. 8220-04-04.

Blake, A. and M. J. Horn. 2006. Acoustic tracking of juvenile Chinook salmon movement in the vicinity of the Delta Cross Channel, Sacramento River, California – 2003 study results. Report by the US Geological Survey, California Water Science Center, Sacramento, California.

Brandes, P.L. and J.S. McLain. 2001. Juvenile Chinook salmon abundance, distribution, and survival in the Sacramento-San Joaquin Estuary. Pages 39 – 138 *in* R.L. Brown, editor. Contributions to the Biology of Central Valley Salmonids, Volume 2, Fish Bulletin 179. California Department of Fish and Game, Sacramento, California.

Brown, L.R. and D. Michniuk. 2007. Littoral fish assemblages of the Alien-dominated Sacramento-San Joaquin Delta, California, 1980–1983 and 2001–2003. Estuaries and Coasts. 30:186–200.

Brown, R. and W. Kimmerer. 2006. An Interpretive Summary of the May 27, 2005 Delta Action 8 Workshop. Report to California Bay-Delta authority. (available: http://www.deltacouncil.ca.gov/delta_science_program/pdf/review_vamp_support_EWA_workshop_DeltaAction8_summary_040606.pdf, accessed May 2010)

Brownie, C., J.E. Hines, J.D. Nichols, K.H. Pollock, and J.B. Hestbeck. 1993. Capture–recapture studies for multiple strata including non-markovian transitions. Biometrics. 49:1173–1187.

Buchanan, R. A. 2005. Release-recapture models for migrating juvenile and adult salmon in the Columbia and Snake Rivers using PIT-Tag and radiotelemetry data. Ph.D. Dissertation, University of Washington, Seattle, Washington.

Burau, J., A. Blake, and R. Perry. 2007. Sacramento/San Joaquin River Delta regional salmon outmigration study plan: Developing understanding for management and restoration. Available: http://baydeltaoffice.water.ca.gov/ndelta/salmon/documents /RegionalSalmonStudyPlan_2008.01.07.pdf. (May 2009).

Burnham, K. P., D. R. Anderson, G. C. White, C. Brownie, and K. H. Pollock. 1987. Design and Analysis Methods for Fish Survival Experiments Based on Release-Recapture, American Fisheries Society, Monograph 5, Bethesda, Maryland.

Burnham, K. P. and D. R. Anderson. 2002. Model selection and multimodel inference: a practical information-theoretic approach. Springer, New York, New York.

CALFED Science Review Panel. 2008. Independent Review of the 2008 NMFS analytical framework for its OCAP biological opinion. Available: http://www.science.calwater. ca.gov/pdf/reviews/OCAP_NMFS_AF_review_final.pdf. (May 2010).

CADWR (California Department of Water Resources). 2010. Delta Simulation Model II – DSM2. Available: http://baydeltaoffice.water.ca.gov/modeling/deltamodeling/ models/dsm2/dsm2.cfm (January 2010).

CH2MHILL. 2009. DSM2 Recalibration.Report to California Department of Water Resources, Sacramento, CA. Available: ftp://ftpmodeling.water.ca.gov/pub/delta/ DSM2_Users_Group/BDCP/DSM2_Recalibration_102709_doc.pdf. (May 2010).

Casella, G. and R.L. Berger. 2002. Statistical inference. Duxbury/Thompson Learning Inc., Pacific Grove, California.

Caswell, H. 2001. Matrix Population Models: Construction, Analysis, and Interpretation. Sinauer Associates, Inc., Sunderland, Massachusetts.

Caswell, H. and M. Fujiwara. 2004. Beyond survival estimation: mark-recatpure, matrix population models, and population dynamics. Animal Biodiversity and Conservation. 27:471–488.

Catchpole, E.A., B.J.T. Morgan, and A. Viallefont. 2002. Solving problems in parameter redundancy using computer algebra. Journal of Applied Statistics. 29:625–636.

Catchpole, E. A., B. J. T. Morgan, and G. Tavecchia. 2008. A new method for analysing discrete life history data with missing covariate values. Journal of the Royal Statistical Society B. 70: 445–460.

Chapman, E. D., P. T. Sandstrom, A. J. Ammann, C. Michel, A. P. Klimley, R. B. MacFarlane, and S. L. Lindley. 2007. Diel Migrations of Salmon Smolts in the Sacramento River, Delta, and San Francisco Bay Estuary. Poster presented at the State of the Estuary Conference, 2007. Available: http://californiafishtracking.ucdavis.edu/ publication.html (accessed May 2009).

Clark, K. W., M. D. Bowen, R. B. Mayfield, K. P. Zehfuss, J. D. Taplin, and C. H. Hanson. 2009. Quantification of pre-screen loss of juvenile steelhead in Clifton Court Forebay. California Department of Water Resources, Sacramento, CA. Available: http://baydeltaoffice.water.ca.gov/ndelta/fishery/documents/2009_clark_et_al_quantifi cation_of_steelhead_pre-screen_loss.pdf (accessed January 2009).

Cormack, R. M. 1964. Estimates of survival from the sighting of marked animals. Biometrika 51:429–438.

Cowan, L.L. and C.J. Schwartz. 2005. Capture–reapture studies using radio telemetry with premature radio-tag failure. Biometrics. 61:657–664.

Crozier, L. and R.W. Zabel. 2006. Climate impacts at multiple scales: evidence for differential population responses in juvenile Chinook salmon. Journal of Animal Ecology. 75:100–1109.

Crozier, L.G., R.W. Zabel, and A.F. Hamlet. 2008. Predicting differential effects of climate change at the population level with life-cycle models of spring Chinook salmon. Global Change Biology. 14:236–249.

Culberson, C., L. Bottorf, M. Roberson, and E. Soderstrom. 2008. Geophysical setting and consequences of management in the Bay-Delta. Pages 37–55 in M. Healy, M. Dettinger, and R. Norgaard, editors. The State of Bay-Delta Science, 2008. The CALFED Science Program, Sacramento, California. Available: http://www.science.calwater.ca. gov/publications/sbds.hml (August 2009)

CVPIA. 1992. The Central Valley Project Improvement Act. Available: http://www.fws.gov/ sacramento/CAMP/CAMP_documents/Central_Valley_Project_Improvement_Act.pdf. (May 2010).

Dinehart R.L. and J.R. Burau. 2005a. Averaged indicators of secondary flow in repeated acoustic Doppler current profiler crossing of bends. Water Resources Research, VOL. 41, W09405, doi:10.1029/2005WR004050.

Dinehart R.L. and J.R. Burau. 2005b. Repeated surveys by acoustic Doppler current profiler for flow and sedimante dynamics in a tidal river. Journal of Hydrology. 314:1–21.

Feyrer, F. and M.P. Healy. 2003. Fish community structure and environmental correlates in the highly altered southern Sacramento–San Joaquin Delta. Environmental Biology of Fishes. 66:123–132.

Fisher, F. W. 1994. Past and present status of Central Valley Chinook salmon. Conservation Biology. 3:870:873.

Fujiwara, M and H. Caswell. 2002. Estimating population projection matrices from multi-stage mark-recapture data. Ecology. 83:3257–3265.

Gimenez, O., A. Viallefont, E.A. Catchpole, R. Choquet, and B.J.T. Morgan. 2004. Methods for investigating parameter redundancy. Animal Biodiversity and Conservation. 27:561–572.

Gregory, R. S. and C. D. Levings. 1998. Turbidity reduces predation on migrating juvenile Pacific salmon. Transactions of the American Fisheries Society. 127:275–285.

Gringas, M. 1997. Mark/recapture experiments at Clifton Court Forebay to estimate pre-screening loss to entrained juvenile fishes: 1976-1993. IEP Technical Report No. 55. Available: http://iep.water.ca.gov/report/reports.html (May 2010).

Healey, M. C., M. D. Dettinger, and R. B. Norgaard. 2008. The State of Bay-Delta Science, 2008. Sacramento, California.

Healy, M. 2008. Science and the Bay-Delta. Pages 19–36 in M. Healy, M. Dettinger, and R. Norgaard, editors. The State of Bay-Delta Science, 2008. The CALFED Science Program, Sacramento, California. Available: http://www.science.calwater.ca. gov/publications/sbds.hml (August 2009)

Hedgecock, D., M. A. Banks, V. K. Rashbrook, C. A. Dean, and S. M. Blankenship. 2001. Applications of population genetics to conservation of Chinook salmon diversity in the Central Valley. Pages 45–70 *in* R.L. Brown, editor. Contributions to the Biology of Central Valley Salmonids, Volume 1, Fish Bulletin 179. California Department of Fish and Game, Sacramento, California.

Hestbeck, J. B., J. D. Nichols, and R. A. Malecki. 1991. Estimates of movement and site fidelity using mark-resight data of wintering Canada geese. Ecology. 72:523–533.

Hewitt, D. A., E. C. Janney, B. S. Hayes, and R. S. Shively. 2010. Improving inferences from fisheries capture-recapture studies through remote detection of PIT Tags. Fisheries. 35: 217–231.

Hilborn, R. 1990. Determination of fish movement patterns from tag recoveries using maximum likelihood estimators. Canadian Journal of Fisheries and Aquatic Sciences. 47:635–643.

Hockersmith, E. E., W. D. Muir, S. G. Smith, B. P. Sandford, R. W. Perry, N. S. Adams, and D. W. Rondorf. 2003. Comparison of migration rate and survival between radio-tagged and PIT-tagged migrant yearling chinook salmon in the Snake and Columbia rivers. North American Journal of Fisheries Management 23:404–413.

Hosmer, D.W. and S. Lemeshow. 2000. Applied logistic regression. John Wiley and Sons, New York, New York.

Jepsen, N., Schreck, C., Clement, S. & Thorstad, E. 2004. A brief discussion of the 2% tag/bodymass rule. Pages 255–259 in M. T. Spedicato, B. Marmulla, and G. Lembo, editors. Aquatic Telemetry: Advances and Applications. Food and Agriculture Organization of the United Nations, Rome, Italy.

Jolly, G. M. 1965. Explicit estimates from capture-recapture data with both death and immigration-stochastic model. Biometrika 52:225–247.

Kimmerer, W. J. 2008. Losses of Sacramento River Chinook salmon and delta smelt to entrainment in Water Diversions in the Sacramento–San Joaquin Delta. San Francisco Estuary and Watershed Science 6:2(Article 2):1–27.

Kimmerer, W. J. and Nobriga, M. L. 2008. Investigating particle transport and fate in the Sacramento-San Joaquin Delta using a particle tracking model. San Francisco Estuary and Watershed Science. 6:1(Article 4):1–26.

Kimmerer, W. J., L. Brown, S. Culberson, P. Moyle, and M. Nobriga. 2008. Aquatic ecosystems. Pages 73–102 in M. Healy, M. Dettinger, and R. Norgaard, editors. The State of Bay-Delta Science, 2008. The CALFED Science Program, Sacramento, CA. Available: http://www.science.calwater.ca. gov/publications/sbds.hml (August 2009)

Kjelson, M.A., P.F Raquel, and F.W Fisher. 1981. Influences of freshwater inflow on chinook salmon (Oncorhynchus tshawytscha) in the Sacramento-San Joaquin Estuary, pp. 88-108. In: R.D Cross and D.L. Williams (eds.), Proceedings of the National Symposium Freshwater inflow to Estuaries. U.S. Dept. of Interior, Fish and wildlife Service. FWS/OBS-81/04 Vol. 2.

Kjelson, M.A. and Brandes, P. B. 1989 . The use of smolt survival estimates to quantify the effects of habitat changes on salmonid stocks in the Sacramento-San Joaquin Rivers, California. In: Levings, C.D., Holtby L. B., and Henderson, M. A., editors. Proceedings of the National Workshop on the Effects of Habitat Alteration on Salmonid Stocks. Canadian Special Publications in Fisheries and Aquatic Sciences. 105:100–115.

Kostow, K. E. 2004. Differences in juvenile phenotypes and survival between hatchery stocks and a natural population provide evidence for modified selection due to captive breeding. Canadian Journal of Fisheries and Aquatic Sciences. 61:577–589.

Kutner, M. H., C. J. Nachtsheim, J. Neter, and W. Li. 2005. Applied linear statistical models. McGraw Hill, Boston.

LaCroix, G.L. 2008. Influence of origin on migration and survival of Atlantic salmon (*Salmo salar*) in the Bay of Fundy, Canada. Canadian Journal of Fisheries and Aquatic Sciences. 65:2063–2079.

Lady, J. M., P. Westhagen, and J. R. Skalski. 2008. USER 4: User specified estimation routine. School of Aquatic and Fishery Sciences, University of Washington, Seattle, Washington. Available: http://www.cbr.washington.edu/paramest/user/. (May 2009).

Lebreton, J. D., and R. Pradel. 2002. Multistate recapture models: modeling incomplete individual histories. Journal of Applied Statistics 29: 353–369.

Letcher, B.H. and G.E. Horton. 2009. Seasonal variation in size-dependent survival of juvenile Atlantic salmon (*Salmo salar*): performance of multistate capture-mark-recapture models. Canadian Journal of Fisheries and Aquatic Sciences. 65:1649–1666.

Lindley and Mohr, 2003. Modeling the effect of striped bass (*Morone saxatilis*) on the population viability of Sacramento River winter-run Chinook salmon (*Oncorhynchus tshawytscha*). Fishery Bulletin. 101: 321–331.

Lindley, S. T., M. S. Mohr, R. B. Schick, P. May, J. J. Anderson, S. Greene, C. Hanson, A. Low, D. McEwan, R. B. MacFarlane, C. Swanson, J. G. Williams. 2004. Population structure of threatened and endangered Chinook salmon ESUs in California's Central Valley Basin. NOAA-TN-NMFS-SWFSC-370.

Lindley, S.T., C.B. Grimes, M.S. Mohr, W. Peterson, J. Stein, J.T. Anderson, L.W. Botsford, D.L. Bottom, C.A. Busack, T.K. Collier, J. Ferguson. J.C. Garza, A.M. Grover, D.G. Hankin, R.G. Kope, P.W. Lawson, A. Low, R.B MacFarlane, K. Moore, M. Palmer-Zwahlen, F.B. Schwing, J. Smith, C. Tracy, R. Webb, B.K. Wells, and T.H. Williams. 2009. What caused the Sacramento River fall Chinook stock collapse? Pre-publication report to the Pacific Fishery Management Council. Available: http://swr.nmfs.noaa.gov/media/SalmonDeclineReport.pdf. (May 2010).

Low, A.F., J. White, and E. Chappel. 2006. Relationship of Delta Cross Cahnnel gate operations to loss of juvenile winter-run Chinook salmon at the CVP?SWP Delta Facilities. California Department of Fish and Game. Available: http://science.calwater.ca.gov/pdf/ewa/EWA_delta_cross_channel_closures_06_111406.pdf (accessed February 2010).

McCullough, P. and Nelder, J. A. 1989. Generalized Linear Models. Chapman and Hall, New York.

McMichael, G. A., M. B. Eppard, T. J. Carlson, J. A. Carter, B. D. Ebberts, R. S. Brown, M. Weiland, G. R. Ploskey, R. A. Harnish, and D. Deng. 2010. The juvenile salmon acoustic telemetry system: a new tool. Fisheries. 35:9–22.

Metcalfe, N. B., N. H. C. Fraser, and M. D. Burns. 1998. State-dependent shifts between nocturnal and diurnal activity in salmon. Proceedings of the Royal Society of London B. 265: 1503–1507.

Metcalfe, N. B., N. H. C. Fraser, and M. D. Burns 1999. Food availability and the nocturnal vs[diurnal foraging trade-off in juvenile salmon. Journal of Animal Ecology. 68: 371–381.

Morris, W. F. and D. F. Doak. 2002. Quantitative Conservation Biology: Theory and Practice of Population Viability Analysis. Sinauer Associates, Inc., Sunderland, Massachusetts.

Moyle, P. B. 2002. Inland Fishes of California. University of California Press, Berkely, California.

Muir, W. D., S. G. Smith, J. G. Williams, E. E. Hockersmith, and J. R. Skalsi. 2001. Survival estimates for migrant yearling Chinook salmon and steelhead tagged with passive integrated transponders in the lower Snake and lower Columbia rivers, 1993–1998. 21: 269–282.

Myers, J. M., R. G. Kope, G. J. Bryant, D. Teel, L. J. Lierheimer, T. C. Wainwright, W. S. Grant, F. W. Waknitz, K. Neely, S. T. Lindley, and R. S. Waples. 1998. Status review of Chinook salmon from Washington, Idaho, Oregon, and California. NOAA Technical Memorandum. NFMS-NWFSC-35. U.S. Department of Commerce, National Oceanic and Atmospheric Administration.

Myrick, C. A., and J. J. Cech, Jr. 2004. Temperature effects on juvenile anadromous salmonids in California's Central Valley: what don't we know? Reviews in Fish Biology and Fisheries. 14:113-123.

Nehlsen, W., J. E. Williams, and J. A. Lichatowich. 1991. Pacific salmon at the crossroads: stocks at risk from California, Oregon, Idaho, and Washington. Fisheries 16: 4 – 21.

Newman, K. B., and J. Rice. 2002. Modeling the survival of Chinook salmon smolts outmigrating through the lower Sacramento River system. Journal of the American Statistical Association. 97: 983–993.

Newman, K. B. 2003. Modelling paired release–recovery data in the presence of survival and capture heterogeneity with application to marked juvenile salmon. Statistical Modelling 3:157–177.

Newman, K. B. 2008. An evaluation of four Sacramento–San Joaquin River Delta juvenile salmon survival studies. Project number SCI-06-G06-299. U.S. Fish and Wildlife Service, Stockton, California. Available: http://www.science.calwater.ca.gov/pdf/ psp/PSP_2004_final/PSP_CalFed_FWS_salmon_studies_final_033108.pdf (August 2008).

Newman, K. B. and P. L. Brandes. 2010. Hierarchical modeling of juvenile Chinook salmon survival as a function of Sacramento–San Joaquin Delta water exports. North American Journal of Fisheries Management. 30:157-169.

Nichols, F. H., J. E. Cloern, S. N. Luoma, and D. H. Peterson. 1986. The modification of an estuary. Science 4738:567-573.

Nichols, J.D., J.E. Hines, K.H. Pollock, R.L. Hinz, and W.A. Link. 1994. Estimating breeding proportions and testing hypotheses about costs of reproduction with capture-recapture data. Ecology. 75:2052–2065.

Nichols, J.D, and W.L. Kendal. 1995. The use of multi-state capture–recapture models to address questions in evolutionary ecology. Journal of Applied Statistics. 22:835–846.

NMFS (National Marine Fisheries Service). 1997. NMFS proposed recovery plan for the
Sacramento River winter-run Chinook. National Marine Fisheries Service, Southwest
Regional Office, Long Beach, CA.

NOAA (National Oceanic and Atmospheric Administration). 2008. Fisheries off West Coast
States and in the Western Pacific; West Coast salmon fisheries; 2008 management
measures and a temporary rule. Federal Register 73:23971–23981.

Perry, R. W., N. S. Adams, and D. W. Rondorf. 2001. Buoyancy compensation of juvenile
Chinook salmon implanted with two different size dummy transmitters. Transactions
of the American Fisheries Society. 130:46–52.

Perry R. W. and J. R. Skalski. 2008. Migration and survival of juvenile Chinook salmon
through the Sacramento–San Joaquin River Delta during the winter of 2006-2007.
Report to U.S. Fish and Wildlife Services, Stockton, California.

Perry, R. W., P. L. Brandes, P. T. Sandstrom, A. Ammann, B. MacFarlane, A. P. Klimley, and
J. R. Skalski. 2010. Estimating survival and migration route probabilities of juvenile
Chinook salmon in the Sacramento–San Joaquin River Delta. North American Journal
of Fisheries Management. 30:142–156.

Pincock, D. G. 2008. False detections: what they are and how to remove them from detection
data. VEMCO division of AMIRIX Systems Inc. Available: http://www.vemco.com/
pdf/false_detections.pdf. (May 2009).

Plumb, J.M., A.C. Braatz, J.N. Lucchesi, S.D. Fielding, J.M. Sprando, G.T. George, N.S.
Adams, and D.W. Rondorf. 2003. Behavior of radio-tagged juvenile Chinook salmon
and steelhead and performance of a removable spillway weir at Lower Granite Dam,
Washington, 2002. Report of the U.S. Geological Survey to the U.S. Army Corps of
Engineers, Walla Walla, Washington.

Pollock, K. H., C. M. Bunck, S. R. Winterstein, and C.-L. Chen. 1995. A capture-recapture survival analysis model for radio-tagged animals. Journal of Applied Statistics. 22:661–672.

R Development Core Team. 2008. R: A language and environment for statistical computing. R Foundation for Statistical Computing, Vienna, Austria. Available: http://www.R-project.org. (May 2009).

Reisenbichler, R. R. and J. D. McIntyre. 1977. Genetic differences in growth and survival of juvenile hatchery and wild steelhead trout, *Salmo gairdneri*. Journal of the Fisheries Research Board of Canada. 34:123–128.

Schwarz, C. J., J. F. Schweigert, and A. N. Arnason. 1993. Post-release stratification in band-recovery models. Biometrics. 44:765–785.

Seber, G. A. F. 1965. A note on the multiple recapture census. Biometrika 52:249–259.

Seber, G. A. F. 1982. The estimation of animal abundance and related parameters. Macmillan, New York.

Skalski, J. R., A. Hoffman, and S. G. Smith. 1993. Testing the significance of individual- and cohort-level covariates in animal survival studies. Pages 9–28 in J.-D. Lebreton and P. M. North, editors. Marked Individuals in the Study of Bird Populations. Birkhauser-Verlag-Basel, Switzerland.

Skalski, J. R., S. G. Smith, R. N. Iwamoto, J. G. Williams, and A. Hoffmann. 1998. Use of passive integrated transponder tags to estimate survival of migrant juvenile salmonids in the Snake and Columbia rivers. Canadian Journal of Fisheries and Aquatic Sciences. 55:1484–1493.

Skalski, J. R., J. Lady, R. Townsend, A. E. Giorgi, J. R. Stevenson, C. M. Peven, and R. D. McDonald. 2001. Estimating in-river survival of migrating salmonid smolts using radiotelemetry. Canadian Journal of Fisheries and Aquatic Sciences. 58:1987–1997.

Skalski, J. R., R. Townsend, J. Lady, A. E. Giorgi, J. R. Stevenson, and R. D. McDonald. 2002. Estimating route-specific passage and survival probabilities at a hydroelectric project from smolt radiotelemetry studies. Canadian Journal of Fisheries and Aquatic Sciences 59:1385–1393.

Skalski, J. R., R. A. Buchanan, and J. Griswold. 2009a. Review of marking methods and release-recapture designs for estimating the survival of very small fish: Examples from the assessment of salmonid fry survival. Reviews in Fisheries Science. 17:391–401.

Skalski, J. R., R. A. Buchanan, R. L. Townsend, T. W. Steig, and S. Hemstrom. 2009b. A multiple-release model to estimate route-specific and dam passage survival at a hydroelectric project. North American Journal of Fisheries Management. 29:670–679.

SWRCB (State Water Resources Control Board). 1995. Water quality control plan for the San Francisco Bay/Sacramento-San Juoaquin Delta Estuary. Available: http://www.swrcb.ca.gov/. (May 2010).

Sogard, S. M. 1997. Size-selective mortality in the juvenile stage of teleost fishes: A review. Bulletin of Marine Science. 60:1129–1157.

Sommer, T. R., M. L. Nobriga, W. C. Harrell, W. Batham, and W. J. Kimmerer. 2001. Floodplain rearing of juvenile Chinook salmon: evidence of enhanced growth and survival. Canadian Journal of Fisheries and Aquatic Sciences 58: 325–333.

Stone, L. 1897. The artificial propagation of salmon on the Pacific Coast of the United States, with Notes on the natural history of the quinnat salmon. Bulletin of the U.S. Fisheries Commission. 16:203–235.

Townsend, R.L., J.R. Skalski, P. Dillingham, and T.W. Steig. 2006. Correcting bias in survival estimation resulting from tag failure in acoustic and radiotelemetry studies. Journalof Agricultural, Biological, and Environmental Statistics. 11:183–196.

Vogel, D. A. 2008. Pilot study to evaluate acoustic-tagged juvenile Chinook salmon smolt migration in the northern Sacramento – San Joaquin Delta 2006-2007. Available: http://baydeltaoffice.water.ca.gov/ndelta/TDF/documents/NorthDeltaSalmonMigration%20PilotStudy%20Report.pdf (accessed Dec. 2010).

Wilder, R. M. and J. F. Ingram. 2006. Temporal patterns in catch rates of juvenile Chinook salmon and trawl net efficiencies in the Lower Sacramento River. IEP Newsletter 19: 18–28.

Williams, B. K., J. D. Nichols, and M. J. Conroy. 2002. Analysis and management of animal populations. Academic Press, San Diego.

Williams, J. G., S. G. Smith, and W. D. Muir. 2001. Survival estimates for downstream migrant yearling juvenile salmonids through the Snake and Columbia rivers hydropower system, 1966–1980 and 1993–1999. North American Journal of Fisheries Management. 21: 310-317.

Williams, J. G. 2006. Central Valley salmon: a perspective on Chinook and steelhead in the Central Valley of California. San Francisco Estuary and Watershed Science 4(3, Article 2):1–398.

Wilson, P. H. 2003. Using population projection matrices to evaluate recovery strategies for Snake River Spring Chinook Salmon. Conservation Biology. 17:782–794.

Winter, J.D. 1996. Advances in underwater biotelemetry. Pages 555–590 in B.R. Murphy and D.W. Willis, Editors. Fisheries Techniques, 2nd Edition. American Fisheries Society, Bethesda, Maryland.

Yoshiyama, R. M., E. R. Gerstung, F. W. Fisher, and P. B. Moyle. 2001. Historical and present distribution of Chinook salmon in the Central Valley drainage of California. Pages 71 – 176 in R. L. Brown, editor. Contributions to the Biology of Central Valley Salmonids, Volume 1, Fish Bulletin 179. California Department of Fish and Game, Sacramento, California.

Zabel, R.W., and Anderson, J.J. 1997. A model of the travel time of migrating juvenile salmon, with an application to Snake River spring chinook. North American Journal of Fisheries Management. 17: 93–100.

Zabel, R. W., J. Faulkner, S. G. Smith, J. J. Anderson, C. Van Holmes, N. Beer, S. Iltis, J. Krinke, G. Fredericks, B. Bellerud, J. Sweet, A. Giorgi. 2008. Comprehensive passage (COMPASS) model: a model of downstream migration and survival of juvenile salmonids through a hydropower system. Hydrobiologia. 609:289–300.

Zabel, R. W., M. D. Scheuerell, M. M. McClure, and J. G. Williams. 2006. The interplay between climate variability and density dependence in the population viability of Chinook salmon. Conservation Biology. 20:190–200.

Appendix 1

ADDITIONAL FIGURES AND TABLES FOR CHAPTER 3

Appendix Table 1.1. Counts of detection histories for the full model shown in Figure 3.2 for a release of $R_1 = 64$ fish on 5 December 2006 and $R_2 = 80$ fish on 17 January 2007. Counts for all other detection histories were zero and are not shown here. Each digit of the detection history indicates detection at telemetry stations within each of four migration routes (labeled A–D), with a "0" indicating a fish was not detected. Since some routes contained fewer telemetry stations than others, the "*" notation acts as a place holder to maintain information about the jth telemetry station in the jth position of the detection history. In the fourth position of the detection history, the history for junction 2, a capital letter indicates a fish passed junction 2 when the Delta Cross Channel was open, and a lower-case letter indicates the Delta Cross Channel was closed when a fish passed junction 2.

R_1: December 2006		R_2: January 2007	
Detection history	Frequency	Detection history	Frequency
1BA**BBBB	1	1BA**BBBB	4
1BA**BB0B	2	1BA**0BBB	2
1BA**BBB0	2	1BA**00BB	1
1BA**B000	1	1BA**BB0B	4
1BA**0000	10	1BA**0B0B	1
1B0BB0BBB	1	1BA**BBB0	1
1B0BB0B0B	1	1BA**0BB0	2
1B0BBBBB0	1	1BA**BB00	3
1B0BBBB00	4	1BA**B000	1
1B0BBB000	3	1BA**0000	10
1B0BB0000	3	1BBbBBBBB	5
1B0B00000	1	1B0bBBBBB	1
1B0000000	5	1BBbB0BBB	3
100000000	7	10BbB0BBB	1
1B0bBBBBB	2	1BBbB00BB	1
1B0b00000	2	1BBbBBB0B	4
1B0C*C0BB	1	1BB0BBB0B	1
1B0C*C000	2	1BBbBBBB0	1
1B0C*0000	2	1BBbB0BB0	2
1B0c*0000	1	1BBbBBB00	1
1B0DDC00B	1	1BBbB0B00	1
1B0DD000B	1	1BBbBB000	2
1B0DDC0B0	1	1BBbB0000	10
1B0DD00B0	1	1BBb00000	1
1B0DDC000	2	1BB000000	1

Appendix Table 1.1 Continued.

1B0DD0000	5	1B0000000	3
1B0D00000	1	100000000	7
		1BBc***BB	1
		1BBc***B0	1
		1BBc***00	4
Total released (R_k)	64		80

Appendix Table 1.2. Parameter estimates for the mark-recapture shown in Figure 3.2 for releases of acoustically tagged late-fall juvenile Chinook salmon made in December, 2006 (R_1) and January, 2007 (R_2). Parameters not estimated are indicated by an "NA" in the estimate column, and parameters fixed at a constant value are noted by an "NA" in the profile likelihood column.

Parameter	R_1: December 2006 Estimate ($\widehat{SE}$)	95% Profile likelihood interval	R_2: January, 2007 Estimate ($\widehat{SE}$)	95% Profile likelihood interval
S_{B1}	0.389 (0.126)	0.176, 0.645	0.681 (0.093)	0.492, 0.850
S_{A1}	0.891 (0.039)	0.799, 0.951	0.913 (0.032)	0.838, 0.962
S_{A2}	0.947 (0.023)	0.890, 0.981	0.959 (0.024)	0.896, 0.990
S_{A3}	0.947 (0.023)	0.890, 0.981	0.976 (0.025)	0.895, 1.000
S_{A4}	0.833 (0.088)	0.623, 0.956	0.970 (0.030)	0.873, 0.998
S_{A5}	0.830 (0.110)	0.578, 1.000	0.725 (0.085)	0.549, 0.879
S_{A6}	0.750 (0.108)	0.511, 0.915	0.900 (0.059)	0.751, 0.983
S_{A7}	0.952 (0.237)	0.566, 1.000	0.953 (0.077)	0.794, 1.000
S_{D1}	0.648 (0.302)	0.193, 1.000	NA	
$S_{D2}S_{D3}$	0.571 (0.270)	0.166, 1.000	NA	
$S_{D1}S_{D2}S_{D3}$	NA		0.368 (0.213)	0.071, 0.802
S_{C1}	0.917 (0.080)	0.681, 0.995	NA	
S_{C2}	0.707 (0.252)	0.322, 1.000	NA	
Ψ_{B1}	0.296 (0.062)	0.186, 0.426	0.414 (0.059)	0.303, 0.531
Ψ_{A1}	0.704 (0.062)	0.574, 0.814	0.586 (0.059)	0.469, 0.697
ω_{open}	0.861 (0.058)	0.725 , 0.948	0.000	NA
ω_{closed}	0.139 (0.058)	0.052 , 0.275	1.000	NA
$\Psi_{A2,open}$	0.452 (0.089)	0.286 , 0.625	0.000	NA
$\Psi_{D2,open}$	0.161 (0.066)	0.061 , 0.315	0.000	NA
$\Psi_{C2,open}$	0.387 (0.087)	0.230 , 0.562	0.000	NA
$\Psi_{A2,closed}$	0.800 (0.179)	0.372 , 0.987	0.850 (0.056)	0.719, 0.938
$\Psi_{D2,closed}$	0.200 (0.179)	0.013 , 0.628	0.150 (0.056)	0.062, 0.281
P_{B1}	1.000	NA	1.000	NA
P_{A2}	1.000	NA	0.986 (0.014)	0.939, 0.999
P_{A3}	1.000	NA	0.975 (0.025)	0.895, 0.999
P_{A4}	1.000	NA	0.970 (0.030)	0.873, 0.998
P_{A5}	1.000	NA	1.000	NA
P_{A6}	0.857 (0.094)	0.621, 0.975	0.641 (0.077)	0.485, 0.779
P_{A7}	1.000	NA	0.941 (0.040)	0.829, 0.990
P_{A8}	0.500 (0.158)	0.218, 0.782	0.655 (0.088)	0.474, 0.810
P_{D1}	1.000	NA	1.000	NA
P_{D2}	0.600 (0.219)	0.199, 0.919	NA	
P_{D3}	1.000	NA	NA	
P_{C1}	1.000	NA	NA	
P_{C2}	1.000	NA	NA	
λ	0.500 (0.158)	0.218, 0.782	0.731 (0.087)	0.544, 0.874

Appendix 2

ASSESSING THE CONSEQUENCE OF ASSUMING $S_{A2} = S_{A3}$

Since a telemetry station at location A_3 was not implemented during 2008 nor for the December release in 2007, the parameters S_{A2}, S_{A3}, Ψ_{B11}, and Ψ_{B21} could not be uniquely estimated without imposing constraints on the parameters. Therefore, I estimated these parameters under the constraint that $S_{A2} = S_{A3}$. Although estimates from the January release in 2007 showed little difference between S_{A2} and S_{A3} (Appendix Table 1.2), station A_3 has not been monitored for three of the four releases thus far. If S_{A2} is not equal to S_{A3}, then associated estimates of route entrainment and survival probabilities will be biased. Here I evaluate the magnitude of bias introduced by assuming $S_{A2} = S_{A3}$, when in fact S_{A2} differs from S_{A3}.

To illustrate the potential bias that might be incurred, I first simplified the problem by assuming a two-branch junction (Appendix Figure 2.1). I was interested not only in bias in Ψ_B, but also in bias that might occur in the product $S_{A2}S_{A3}$. This product appears in equations for route specific survival through the Delta for Routes A, C, and D (i.e., S_h). Thus, bias in this product is more relevant than bias in each of the reach-specific survival probabilities. Appendix Figure 2.1 shows a schematic of the problem with the underlying survival and route entrainment parameters. Without a telemetry station at location A_3, only two parameters can be estimated from information provided by telemetry stations at B_1 and A_4. The two estimable parameters are the joint probabilities of the underlying parameters between stations A_2 and B_1, and between A_2 and A_4:

$$\phi_{A2,\,B1} = S_{A2}\Psi_B \tag{A2.1}$$

$$\phi_{A2,\,A4} = S_{A2}S_{A3}\left(1 - \Psi_B\right) \tag{A2.2}$$

Where $\phi_{A2,B1}$ is the joint probability of surviving the first reach and entering channel B, and $\phi_{A2,A4}$ is the joint probability of surviving the first reach, remaining in channel A, and surviving the second reach. As discussed in Chapter 2, these two parameters can always be

estimated without bias from the data, as can the total survival from A_2 to either of the downstream exit points:

$$S_{total} = \phi_{A2,\,B1} + \phi_{A2,\,A4} \qquad\qquad (A2.3)$$
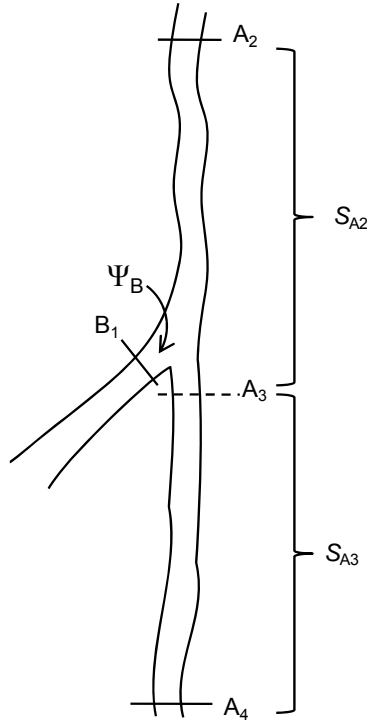
Appendix Figure 2.1. Schematic of a two-branch river junction showing location of telemetry stations at A_2, B_2, and A_4. The dashed line notes lack of a telemetry station at A_3. Brackets show the probability of surviving between A_2 and A_3 and between A_3 and A_4. The probability of entering Channel B is Ψ_B, and the probability of remaining in Channel A is 1-Ψ_B.

To quantify bias, I substituted Eqns. A2.1 and A2.2 into Eqn. A2.3, set $S_{A3} = S_{A2}$, and then solved Eqn. A2.3 for S_{A2} and Eqn. A2.1 for Ψ_B:

$$\tilde{S}_{A2} = \frac{\Psi_B - \sqrt{\Psi_B{}^2 - 4S_{total}\left(\Psi_B - 1\right)}}{2\left(\Psi_B - 1\right)} \qquad\qquad (A2.4)$$

$$\tilde{\Psi}_B = \frac{\phi_{A2,\,B1}}{\tilde{S}_{A2}} \qquad\qquad (A2.5)$$

Here, $\tilde{S}_{A2}$ and $\tilde{\Psi}_B$ will be the biased estimates that result when assuming $S_{A2} = S_{A3}$ when in fact $S_{A2} \neq S_{A3}$; and S_{total} and $\phi_{A2,B1}$ are calculated using hypothesized true values of S_{A2}, S_{A3}, and Ψ_B.

Estimates of S_{total} from my data will be unbiased regardless of bias that might be present in estimates of S_{A2}, S_{A3}, or Ψ_B, and we used this fact to establish the maximum possible bias that could arise by assuming $S_{A2} = S_{A3}$. For example, for the first release in 2008, I estimated $\hat{\Psi}_B = 0.345$ and $\hat{S}_{A2} = \hat{S}_{A3} = 0.919$ (Appendix Table 3.3), resulting in $\hat{S}_{total} = 0.87$. Now suppose $\hat{\Psi}_B = \tilde{\Psi}_B = 0.345$ is the biased estimate of Ψ_B: What true values of Ψ_B, S_{A2}, and S_{A3} could have produced the observed estimate, $\tilde{\Psi}_B$? First, the true parameter values Ψ_B, S_{A2}, and S_{A3} are constrained such that $\hat{S}_{total} = 0.87$ (according to Eqn. A2.3) and $\tilde{\Psi}_B = 0.345$ (according to Eqn. A2.5). Also, given that $\hat{S}_{total} = 0.87$, S_{A2} and S_{A3} are further constrained such that all of the observed mortality could have occurred in either the first reach (i.e., $S_{A3} = 1$) or the second reach (i.e., $S_{A2} = 1$). Clearly, mortality will occur in both reaches, but I used these two scenarios to bound the extremes of bias that could possibly occur given that $\hat{S}_{total} = 0.87$ and $\tilde{\Psi}_B = 0.345$. Thus, maximum bias is calculated by setting $S_{A2} = 1$ (or $S_{A3} = 1$), and then finding the true values of S_{A3} (or S_{A2}) and Ψ_B that satisfy $S_{total} = 0.87$ and $\tilde{\Psi}_B = 0.345$. Should the maximum possible bias be low under these extreme scenarios, then I can infer that the realized bias would be even less.

Under these extreme scenarios, I found that maximum possible bias was quite low. For the December release, maximum absolute bias in Ψ_B was less than 0.028, and bias in $S_{A2}S_{A3}$ was less than 0.035 (Appendix Table 2.1). Maximum possible bias for the January release was even less (Appendix Table 2.1). These findings suggest that the realized bias in these parameters will be much less than the maximum possible bias, given that we know mortality occurs in both reaches, and that past evidence suggests little difference between S_{A2} and S_{A3} (see Appendix Table 3.3). Parameter stimates are robust to deviations from $S_{A2} = S_{A3}$ partly due to the relatively high total survival (S_{total}) observed in this reach. Since S_{total} constrains the range of possible true values of S_{A2} and S_{A3}, as S_{total} decreases S_{A2} and S_{A3} may

take on a wider range of values between 0 and 1. Thus, as S_{total} decreases, the possible maximum bias will increase under the extreme scenarios of all mortality occurring in either one reach or another.

Although this sensitivity analysis shows that bias was likely minimal, the appropriate course of action is to ensure a telemetry station is implemented at A_3 in future years. Given the influence of Sutter and Steamboat sloughs on migration dynamics through the entire Delta, this river junction is too important to rest future research on such assumptions.

Appendix Table 2.1. Maximum possible bias induced by assuming $S_{A2} = S_{A3}$, when in fact, all mortality occurs in either the upstream reach or the downstream reach.

Release	True values				Estimates when assuming $S_{A2} = S_{A3}$		Bias	
	S_{A2}	S_{A3}	Ψ_B	S_{total}	$\tilde{S}_{A2}$	$\tilde{\Psi}_B$	$\Psi_B - \tilde{\Psi}_B$	$S_{A2}S_{A3} - \tilde{S}_{A2}^2$
R_1: December	0.870	1.000	0.364	0.870	0.918	0.345	-0.019	-0.025
	1.000	0.810	0.318	0.870	0.920	0.345	0.028	0.035
R_2: January	0.852	1.000	0.213	0.852	0.914	0.198	-0.014	-0.016
	1.000	0.819	0.182	0.852	0.915	0.198	0.017	0.017

Appendix 3

ADDITIONAL FIGURES AND TABLES FOR CHAPTER 4

Appendix Table 3.1. Counts of detection histories for the model shown in Figure 4.2 for a release of $R_1 = 208$ fish on 4 December 2007 and $R_2 = 211$ fish on 16 January 2008. Counts for all other detection histories were zero and are not shown here. Each digit of the detection history indicates detection at telemetry stations within each of four migration routes (labeled A–D) and Three Mile Slough (E). A "0" indicating either a fish was not detected or a telemetry station within that route was not implemented at that position in the capture history (since some routes had more telemetry stations than others). Detection histories beginning with "0 0 0 D" indicate fish released in Georgiana Slough whereas those beginning with "A" are fish released into the Sacramento River.

R_1: December 2006		R_2: January 2007	
Detection history	Frequency	Detection history	Frequency
0 0 0 D 0 0 0 0 0 0 0 0	11	0 0 0 D 0 0 0 0 0 0 0 0	5
0 0 0 D D 0 0 0 0 0 0 0	5	0 0 0 D D 0 0 0 0 0 0 0	4
0 0 0 D D D 0 0 0 0 0 0	7	0 0 0 D D D 0 0 0 0 0 0	21
0 0 0 D D D D 0 0 0 0 0	20	0 0 0 D D D D 0 0 0 0 0	32
0 0 0 D D D D D 0 0 0 0	6	0 0 0 D D D D D 0 0 0 0	4
0 0 0 D D D D E 0 0 0 0	3	0 0 0 D D D D E 0 0 0 0	1
0 0 0 D D D D D 0 D 0 0 0	2	0 0 0 D D D D 0 0 D 0 0 0	1
0 0 0 D D D D D 0 D D A 0	1	0 0 0 D D D D D 0 D 0 0 0	2
0 0 0 D D D D E A 0 0 A A	2	0 0 0 D D D D 0 0 D D 0 0	1
0 0 0 D D D D D 0 0 D A A	1	0 0 0 D D D D 0 0 0 0 A 0	1
0 0 0 D D D D D 0 D D A A	1	0 0 0 D D D D E A 0 0 0 A	1
A 0 0 0 0 0 0 0 0 0 0 0	8	0 0 0 D D D D D 0 D D 0 A	1
A A 0 0 0 0 0 0 0 0 0 0	18	0 0 0 D D D D 0 0 0 0 A A	1
A 0 B1 0 0 0 0 0 0 0 0 0	1	0 0 0 D D D D D 0 0 0 A A	1
A A B1 0 0 0 0 0 0 0 0 0	8	0 0 0 D D D D E A 0 0 A A	1
A A B2 0 0 0 0 0 0 0 0 0	3	0 0 0 D D D D D 0 D 0 A A	2
A A 0 A 0 0 0 0 0 0 0 0	7	0 0 0 D D D 0 D 0 0 D A A	1
A A B1 B1 0 0 0 0 0 0 0 0	4	0 0 0 D D D D D 0 0 D A A	1
A A B1 B2 0 0 0 0 0 0 0 0	1	A 0 0 0 0 0 0 0 0 0 0 0	6
A 0 B2 B2 0 0 0 0 0 0 0 0	1	A A 0 0 0 0 0 0 0 0 0 0	16
A A B2 B2 0 0 0 0 0 0 0 0	2	A A B1 0 0 0 0 0 0 0 0 0	4
A 0 0 C 0 0 0 0 0 0 0 0	1	A A B2 0 0 0 0 0 0 0 0 0	1
A A 0 C 0 0 0 0 0 0 0 0	9	A A 0 A 0 0 0 0 0 0 0 0	3
A A 0 D 0 0 0 0 0 0 0 0	6	A 0 0 D 0 0 0 0 0 0 0 0	2

Appendix Table 3.1. Continued.

Genotype	R_k	Genotype	R_k
A 0 0 A A 0 0 0 0 0 0 0	1	A A 0 D 0 0 0 0 0 0 0 0 0	4
A A 0 A A 0 0 0 0 0 0 0	5	A 0 0 A A 0 0 0 0 0 0 0	1
A A B1 B1 B1 0 0 0 0 0 0 0	7	A A 0 A A 0 0 0 0 0 0 0	6
A A B1 B2 B2 0 0 0 0 0 0 0	4	A 0 B1 B1 B1 0 0 0 0 0 0 0	1
A A B2 B2 B2 0 0 0 0 0 0 0	2	A 0 B2 B2 B2 0 0 0 0 0 0 0	1
A A 0 D D 0 0 0 0 0 0 0	1	A A B2 B2 B2 0 0 0 0 0 0 0	3
A A 0 0 A A 0 0 0 0 0 0	1	A A 0 D D 0 0 0 0 0 0 0	3
A A 0 A A A 0 0 0 0 0 0	4	A A 0 A A A 0 0 0 0 0 0	10
A A 0 D D D 0 0 0 0 0 0	1	A 0 0 D D D 0 0 0 0 0 0	1
A A 0 A A 0 A 0 0 0 0 0	1	A A 0 D D D 0 0 0 0 0 0	2
A A B1 B2 B2 0 A 0 0 0 0 0	1	A A B1 B2 B2 0 A 0 0 0 0 0	1
A A B2 B2 B2 0 A 0 0 0 0 0	1	A A B2 B2 B2 0 A 0 0 0 0 0	1
A A 0 A A A A 0 0 0 0 0	2	A 0 0 A A A A 0 0 0 0 0	1
A A 0 C 0 D D 0 0 0 0 0	3	A A 0 A A A A 0 0 0 0 0	2
A A 0 D D D D 0 0 0 0 0	3	A 0 0 D D D D 0 0 0 0 0	4
A A B2 B2 B2 0 0 A 0 0 0 0	1	A A 0 D D D D 0 0 0 0 0	12
A A 0 A A 0 A A 0 0 0 0	1	A A B1 B1 B1 0 0 A 0 0 0 0	1
A A B1 B1 B1 0 A A 0 0 0 0	1	A 0 B1 B2 B2 0 0 A 0 0 0 0	1
A A B2 B2 B2 0 A A 0 0 0 0	1	A A B2 B2 B2 0 0 A 0 0 0 0	1
A 0 0 A A A A 0 0 0 0 0	1	A A 0 A A A 0 A 0 0 0 0	2
A A 0 A A A A A 0 0 0 0	9	A A 0 A A 0 A A 0 0 0 0	1
A A 0 D D D D D 0 0 0 0	1	A A B1 B1 B1 0 A A 0 0 0 0	2
A A 0 D D D D E 0 0 0 0	1	A A B2 B2 B2 0 A A 0 0 0 0	3
A A 0 D D D D 0 0 D 0 0 0	1	A 0 0 A A A A 0 0 0 0 0	1
A A 0 A A 0 0 A 0 0 0 A 0	1	A A 0 A A A A 0 0 0 0 0	5
A A B1 B2 B2 0 A A 0 0 0 A 0	1	A A 0 D D D D 0 0 0 0 0	2
A A B2 B2 B2 0 A A 0 0 0 A 0	1	A A 0 A A A A E 0 0 0 0	2
A A 0 A A A A A 0 0 0 A 0	2	A A 0 A A 0 A E 0 D 0 0 0	1
A A B1 0 B1 0 0 E D D D A 0	1	A A 0 A A A A 0 0 0 0 A 0	1
A A 0 0 A 0 A 0 0 0 0 0 A	1	A A 0 A A A A A 0 0 0 A 0	3
A A 0 D D D D D 0 D D 0 A	2	A A 0 A A A A E 0 D 0 A 0	1
A A 0 A A A A E D D D 0 A	1	A A 0 D D D D D 0 D D A 0	1
A A 0 A A A A 0 0 0 0 A A	1	A A 0 A A 0 A A 0 0 0 0 A	1
A A B2 B2 B2 0 0 A 0 0 0 A A	1	A 0 0 A A 0 A E 0 D 0 0 A	1
A A 0 A A A 0 A 0 0 0 A A	2	A A 0 D D D D 0 0 0 0 A A	1
A A 0 A A 0 A A 0 0 0 A A	1	A A 0 A A A 0 A 0 0 0 A A	1
A A B1 B1 B1 0 A A 0 0 0 A A	1	A A 0 A A A 0 A A 0 0 0 A A	3
A A B2 B2 B2 0 A A 0 0 0 A A	2	A 0 B2 B2 B2 0 A A 0 0 0 A A	1
A A 0 A A A A A 0 0 0 A A	5	A A B2 B2 B2 0 A A 0 0 0 A A	2
A A 0 C 0 D D E A 0 0 A A	1	A 0 0 A A A A 0 0 0 A A	1
A A 0 D D D D D 0 0 D A A	1	A A 0 A A A A A 0 0 0 A A	5
A A 0 D D D D D 0 D D A A	1	A A 0 D D D D 0 0 0 D A A	1
Total released (R_k)	208		211

Appendix Table 3.2. Parameter constraints applied under the full model for each release, representing the minimum estimable model with the maximum number of parameters. Parameters not shown below were estimable by iteratively maximizing the likelihood of the multinomial model. Constraints include parameters that had to be fixed to a constant value or set equal to other parameters because they could not be estimated from the data set of detection histories.

R_1: December 2007		R_2: January 2008	
Parameter	Constraint	Parameter	Constraint
S_{A3}	$= S_{A2}$	Ψ_{C2}	$= 0$
$S_{D7, Sac}$	$= 1$	$\phi_{D4,E1,Sac}$	$= 0$
$S_{E1,D5}$	$= 1$	S_{A3}	$= S_{A2}$
P_{A3}	$= 0$	S_{B12}	$= 1$
P_{A5}	$= 1$	S_{B22}	$= 1$
$P_{E1,Sac}$	$= 1$	S_{C1}	$= 0$
P_{B11}	$= 1$	$S_{D7,Sac}$	$= 1$
P_{B21}	$= 1$	$S_{E1,D5}$	$= \phi_{D4,D5,Geo}$
P_{B22}	$= 1$	$S_{E1,A8,Sac}$	$= 0$
P_{B13}	$= 1$	P_{A3}	$= 0$
P_{B23}	$= 1$	P_{A4}	$= 1$
P_{C1}	$= 1$	P_{A5}	$= 1$
P_{D1}	$= 1$	P_{B11}	$= 1$
$P_{D2,Sac}$	$= 1$	P_{B12}	$= 1$
$P_{D3,Sac}$	$= 1$	P_{B13}	$= 1$
$P_{D4,Sac}$	$= 1$	P_{B21}	$= 1$
$P_{D7,Sac}$	$= 1$	P_{B22}	$= 1$
$S_{D7,Geo}$	$= 1$	P_{B23}	$= 1$
$P_{D2,Geo}$	$= 1$	P_{C1}	$= 0$
$P_{D3,Geo}$	$= 1$	P_{D1}	$= 1$
$P_{D4,Geo}$	$= 1$	$P_{D2,Sac}$	$= 1$
$P_{D5,Geo}$	$= 1$	$P_{D3,Sac}$	$= 1$
$P_{D7,Geo}$	$= 1$	$P_{D4,Sac}$	$= 1$
$P_{A8,Geo}$	$= 1$	$P_{E1,Sac}$	$= 1$
$P_{A9,Geo}$	$= 1$	$P_{D2,Geo}$	$= 1$
$P_{E1,Geo}$	$= 1$	$P_{D3,Geo}$	$= 1$
$S_{A8,Geo}$	$= 1$	$P_{A8,Geo}$	$= 1$
		$P_{E1,Geo}$	$= 1$
		$S_{A8,Geo}$	$= 1$

Appendix Table 3.3. Parameter estimates under the reduced model for releases of acoustically tagged late-fall juvenile Chinook salmon in December, 2007 (R_1) and January, 2008 (R_2). Parameters not estimated are indicated by an "NA" in the estimate column, and parameters fixed at a constant value are noted by an "NA" in the profile likelihood column.

Parameter	R_1: December 2007		R_2: January 2008	
	Estimate ($\widehat{SE}$)	95% Profile likelihood interval	Estimate ($\widehat{SE}$)	95% Profile likelihood interval
S_{A1}	0.951 (0.019)	0.907, 0.981	0.975 (0.020)	0.927, 1.000
S_{A2}	0.919 (0.019)	0.877, 0.951	0.915 (0.020)	0.869, 0.949
S_{A3}	0.919 (0.019)	0.877, 0.951	0.915 (0.020)	0.869, 0.949
S_{A4}	0.841 (0.055)	0.715, 0.928	0.942 (0.032)	0.857, 0.985
S_{A5}	0.874 (0.062)	0.734, 0.984	0.914 (0.061)	0.785, 1.000
S_{A6}	0.843 (0.075)	0.671, 0.963	0.728 (0.078)	0.563, 0.864
S_{A7}	0.886 (0.068)	0.733, 1.000	0.890 (0.058)	0.758, 1.000
S_{A8}	0.618 (0.090)	0.441, 0.789	0.548 (0.087)	0.380, 0.716
S_{B11}	0.715 (0.087)	0.534, 0.876	0.600 (0.155)	0.299, 0.855
S_{B12}	0.692 (0.128)	0.423, 0.893	1.000	NA
S_{B13}	0.308 (0.149)	0.087, 0.623	0.765 (0.221)	0.282, 1.000
S_{B21}	0.800 (0.103)	0.560, 0.946	0.923 (0.074)	0.702, 0.995
S_{B22}	0.790 (0.094)	0.576, 0.929	1.000	NA
S_{B23}	0.616 (0.130)	0.360, 0.841	0.728 (0.123)	0.464, 0.921
S_{C1}	0.286 (0.121)	0.099, 0.545	NA	
$S_{D1,Sac}$	0.667 (0.111)	0.437, 0.852	0.818 (0.067)	0.665, 0.923
$S_{D1,Geo}$	0.814 (0.051)	0.702, 0.898	0.938 (0.027)	0.872, 0.977
S_{D2}	0.900 (0.039)	0.808, 0.959	0.932 (0.025)	0.873, 0.970
S_{D3}	0.862 (0.045)	0.758, 0.934	0.772 (0.051)	0.672, 0.885
S_{D4}	0.491 (0.073)	0.352, 0.635	0.395 (0.080)	0.262, 0.604
S_{D5}	0.658 (0.129)	0.411, 0.946	0.733 (0.180)	0.415, 1.000
S_{D6}	0.700 (0.145)	0.393, 0.915	0.709 (0.181)	0.155, 1.000
S_{D7}	1.000	NA	0.866 (0.159)	0.463, 1.000
$S_{E1,D5}$	1.000	NA	0.750 (0.288)	0.245, 1.000
$S_{E1,A8}$	0.433 (0.189)	0.130, 0.780	0.683 (0.279)	0.165, 1.000
Ψ_{A1}	0.655 (0.042)	0.570, 0.733	0.802 (0.037)	0.722, 0.868
Ψ_{B11}	0.230 (0.037)	0.163, 0.308	0.086 (0.026)	0.044, 0.147
Ψ_{B21}	0.115 (0.028)	0.068, 0.178	0.112 (0.029)	0.063, 0.178
Ψ_{A2}	0.592 (0.056)	0.481, 0.696	0.612 (0.053)	0.506, 0.711
Ψ_{C2}	0.179 (0.043)	0.105, 0.273	0.000	NA
Ψ_{D2}	0.230 (0.048)	0.146, 0.331	0.388 (0.053)	0.289, 0.494
$\phi_{B11,B12}$	0.482 (0.096)	0.305, 0.674	0.400 (0.155)	0.146, 0.700
$\phi_{B11,B22}$	0.233 (0.077)	0.108, 0.403	0.200 (0.127)	0.036, 0.499
$\phi_{A7,A8}$	0.837 (0.074)	0.679, 0.978	0.781 (0.07)	0.634, 0.914

Appendix Table 3.3. Continued.

$\phi_{A7,E1}$	0.049 (0.034)	0.008, 0.143	0.109 (0.046)	0.040, 0.220
$\phi_{D4,D5}$	0.351 (0.070)	0.225, 0.497	0.354 (0.079)	0.225, 0.564
$\phi_{D4,E1}$	0.140 (0.049)	0.063, 0.253	0.041 (0.023)	0.010, 0.102
P_{A2}	0.959 (0.018)	0.915, 0.985	0.852 (0.034)	0.777, 0.910
P_{A3}	0	NA	0.000	NA
P_{A4}	0.949 (0.035)	0.850, 0.991	1.000	NA
P_{A5}	1.000	NA	1.000	NA
P_{A6}	0.821 (0.072)	0.655, 0.932	0.781 (0.073)	0.620, 0.899
P_{A7}	0.829 (0.064)	0.683, 0.928	0.850 (0.057)	0.719, 0.937
$P_{A8,Sac}$	0.905 (0.064)	0.734, 0.983	0.950 (0.049)	0.798, 0.997
$P_{A8,Geo}$	1.000	NA	0.950 (0.049)	0.798, 0.997
$P_{A9,Sac}$	0.812 (0.084)	0.618, 0.937	0.846 (0.071)	0.678, 0.949
$P_{A9,Geo}$	1.000	NA	0.846 (0.071)	0.678, 0.949
P_{B11}	1.000	NA	1.000	NA
P_{B12}	0.900 (0.095)	0.628, 0.994	1.000	NA
P_{B21}	1.000	NA	1.000	NA
P_{B22}	1.000	NA	1.000	NA
P_{B13}	1.000	NA	1.000	NA
P_{B23}	1.000	NA	1.000	NA
P_{C1}	1.000	NA	NA	
P_{D1}	1.000	NA	1.000	NA
P_{D2}	1.000	NA	1.000	NA
P_{D3}	1.000	NA	1.000	NA
P_{D4}	1.000	NA	0.958 (0.041)	0.829, 0.998
P_{D5}	0.922 (0.075)	0.699, 0.995	0.500 (0.118)	0.133, 0.872
P_{D6}	0.778 (0.139)	0.458, 0.959	0.500 (0.134)	0.255, 0.745
P_{D7}	1.000	NA	0.385 (0.135)	0.046, 0.848
P_{E1}	1.000	NA	1.000	NA
λ	0.748 (0.082)	0.570, 0.883	0.759 (0.080)	0.585, 0.888

Appendix 4

ADDITIONAL FIGURES AND TABLES FOR CHAPTER 5
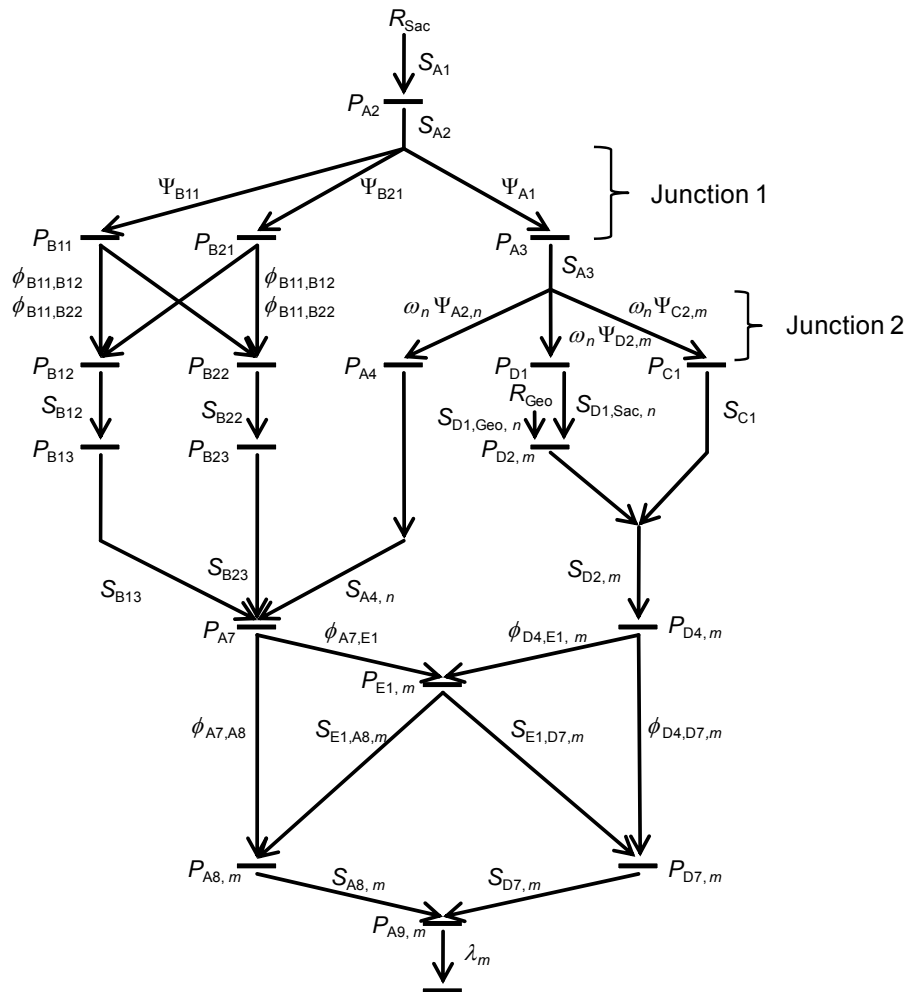
 Appendix Figure 4.1. Schematic of the mark-recapture model used to estimate survival (S_{hi}), detection (P_{hi}), route entrainment (Ψ_{hl}), and joint survival-entrainment ($\phi_{hi,jk}$) probabilities of juvenile late-fall Chinook salmon migrating through the Sacramento–San Joaquin River Delta for releases made in December 2008 and January 2009. Release sites are denoted by R_m (m = Sac (Sacramento) and Geo (Georgiana Slough)), parameters subscripted by n are conditional on the position of the Delta Cross Channel gate, and m denote parameters which can be estimated separately for each release site.

Appendix Table 4.1. Counts of detection histories for the model shown in Figure 4.2 for a release of R_1 = 208 fish on 4 December 2007 and R_2 = 211 fish on 16 January 2008. Counts for all other detection histories were zero and are not shown here. Each digit of the detection history indicates detection at telemetry stations within each of four migration routes (labeled A–D) and Three Mile Slough (E). A "0" indicating either a fish was not detected or a telemetry station within that route was not implemented at that position in the capture history (since some routes had more telemetry stations than others). Detection histories beginning with "0 0 0 D" indicate fish released in Georgiana Slough whereas those beginning with "A" are fish released into the Sacramento River.

R_1: December 2006		R_2: January 2007	
Detection history	Frequency	Detection history	Frequency
0 0 0 D 0 0 0 0 0 0	67	0 0 0 D 0 0 0 0 0 0	42
0 0 0 D D 0 0 0 0 0	7	0 0 0 D D 0 0 0 0 0	19
0 0 0 D D 0 D 0 0 0	1	0 0 0 D D D 0 0 0 0	17
0 0 0 D D D 0 0 0 0	11	0 0 0 D D D 0 0 0 A	1
0 0 0 D D D 0 0 A A	1	0 0 0 D D D 0 0 A A	4
0 0 0 D D D D 0 0 0	2	0 0 0 D D D D 0 A 0	2
0 0 0 D D D D 0 0 A	4	0 0 0 D D D D 0 A A	11
0 0 0 D D D D 0 A A	4	0 0 0 D D D DE 0 0 0	1
0 0 0 D D D DE 0 0 0	1	0 0 0 D D D DE EA 0 0	1
0 0 0 D D D DE EA A A	2	0 0 0 D D D DE EA A A	2
A 0 0 0 0 0 0 0 0 0	21	A 0 0 0 0 0 0 0 0 0	23
A 0 A a 0 0 0 0 A A	1	A 0 A d D D 0 0 A A	1
A 0 A a 0 0 A 0 0 0	1	A 0 B2 0 0 0 0 0 0 0	1
A 0 A a 0 0 A 0 A A	1	A 0 B2 B2 0 0 0 0 0 0	1
A 0 A a 0 A 0 0 0 A	1	A A 0 0 0 0 0 0 0 0	23
A 0 A a 0 A 0 0 A 0	1	A A A 0 0 0 0 0 0 0	13
A 0 B1 0 B2 A AE 0 0 0	1	A A A a 0 0 0 0 0 0	24
A A 0 0 0 0 0 0 0 0	14	A A A a 0 0 0 0 0 A	3
A A 0 0 B2 A A 0 A 0	1	A A A a 0 0 0 0 A 0	1
A A 0 d D D 0 0 0 0	1	A A A a 0 0 0 0 A A	1
A A 0 B2 0 0 A 0 0 0	1	A A A a 0 0 A 0 0 A	2
A A A 0 0 0 0 0 0 0	8	A A A a 0 0 A 0 A A	10
A A A 0 0 0 A 0 0 0	1	A A A a 0 A 0 0 0 0	1
A A A A 0 0 0 0 0 0	11	A A A a 0 A 0 0 0 A	3
A A A A 0 0 A 0 A A	4	A A A a 0 A A 0 0 0	2
A A A A 0 A 0 0 0 0	3	A A A a 0 A A 0 A 0	1
A A A A 0 A A 0 0 0	2	A A A a 0 A A 0 A A	11
A A A A 0 A A 0 0 A	1	A A A d 0 0 0 0 0 0	13
A A A A 0 A A 0 A 0	2	A A A d D 0 0 0 0 0	4
A A A A 0 A A 0 A A	3	A A A d D D 0 0 0 0	12
A A A C 0 0 0 0 0 0	13	A A A d D D D 0 0 0	2
A A A C 0 D 0 0 0 0	2	A A A d D D D 0 A A	4
A A A C 0 D D 0 0 A	1	A A A d D D DE EA 0 0	1
A A A C 0 D D 0 A 0	1	A A B1 0 0 0 0 0 0 0	3

Appendix Table 4.1. Continued

A A A C 0 D D 0 A A	1		A A B1 B1 0 0 0 0 0 0	1
A A A D 0 0 0 0 0 0	1		A A B1 B1 B1 0 0 0 0 0	1
A A A D D 0 0 0 0 0	1		A A B1 B1 B1 0 A 0 0 A	1
A A A D D D 0 0 0 0	4		A A B1 B1 B1 A 0 0 0 A	1
A A A D D D D 0 A A	3		A A B1 B1 B1 A 0 0 A A	1
A A A D D D DE 0 A A	1		A A B1 B1 B1 A A 0 A A	2
A A A a 0 0 0 0 0 0	4		A A B1 B2 0 0 0 0 0 0	1
A A A a 0 0 0 0 A 0	2		A A B1 B2 B2 0 A 0 A A	1
A A A a 0 0 A 0 0 A	1		A A B1 B2 B2 A 0 0 0 0	1
A A A a 0 0 A 0 A 0	1		A A B1 B2 B2 A A 0 A A	1
A A A a 0 0 A 0 A A	1		A A B2 0 0 0 0 0 0 0	3
A A A a 0 0 AE 0 0 0	1		A A B2 B1 0 0 0 0 0 0	1
A A A a 0 0 AE 0 A A	1		A A B2 B1 B1 0 0 0 A A	1
A A A a 0 A 0 0 0 0	3		A A B2 B1 B1 A 0 0 0 0	1
A A A a 0 A 0 0 A A	3		A A B2 B1 B1 A A 0 A A	1
A A A a 0 A A 0 0 0	2		A A B2 B2 0 0 0 0 0 0	2
A A A a 0 A A 0 A 0	1		A A B2 B2 B2 0 0 0 0 0	2
A A A a 0 A A 0 A A	5		A A B2 B2 B2 0 A 0 A A	2
A A A d 0 0 0 0 0 0	1		A A B2 B2 B2 A 0 0 0 A	2
A A A d D 0 0 0 0 0	2		A A B2 B2 B2 A 0 0 A A	1
A A A d D 0 D 0 A A	1		A A B2 B2 B2 A A 0 0 0	1
A A A d D D 0 0 0 0	3		A A B2 B2 B2 A A 0 A 0	2
A A A d D D 0 0 A A	1		A A B2 B2 B2 A A 0 A A	2
A A A d D D D 0 A A	4			
A A A d D D DE EA 0 0	1			
A A B1 0 0 0 0 0 0 0	12			
A A B1 0 B1 A A 0 A A	1			
A A B1 B1 0 0 0 0 0 0	2			
A A B1 B1 B1 0 0 0 0 0	5			
A A B1 B1 B1 0 A 0 0 0	1			
A A B1 B1 B1 0 AE ED A A	1			
A A B1 B1 B1 A A 0 0 A	1			
A A B1 B1 B1 A A 0 A A	2			
A A B1 B1 B1 A AE 0 A 0	1			
A A B1 B2 0 A A 0 A A	1			
A A B1 B2 B2 A A 0 0 0	3			
A A B1 B2 B2 A A 0 A 0	1			
A A B1 B2 B2 A A 0 A A	1			
A A B2 B2 0 0 0 0 0 0	1			
A A B2 B2 0 A A 0 0 A	1			
A A B2 B2 B2 0 0 0 A A	2			
A A B2 B2 B2 0 A 0 0 A	1			
A A B2 B2 B2 A 0 0 0 0	1			
A A B2 B2 B2 A 0 0 A A	1			

Appendix Table 4.1. Continued

A A B2 B2 B2 A A 0 A 0	1
A A B2 B2 B2 A A 0 A A	6
A A B2 B2 B2 A AE ED 0 0	1
Total released (R_k)	292

Total released (R_k)	292	292

Appendix Table 4.2. Parameter constraints applied under the full model for each release, representing the minimum estimable model with the maximum number of parameters. Parameters not shown below were estimable by iteratively maximizing the likelihood of the multinomial model. Constraints include parameters that had to be fixed to a constant value or set equal to other parameters because they could not be estimated from the data set of detection histories.

R_1: December 2007		R_2: January 2008	
Parameter	Constraint	Parameter	Constraint
$\phi_{B21,B12}$	$= 0$	Ψ_{C2}	$= 0$
$\phi_{B21,B22}$	$= 1$	$\Psi_{A2,open}$	$= 0$
S_{B23}	$=1$	ω_{open}	$= 0$
$S_{D1,open}$	$= S_{D1,closed}$	$S_{D1,open}$	$= 0$
$P_{E1,Sac}$	$= 1$	$S_{A4,open}$	$= 0$
$P_{E1,Geo}$	$= 1$	S_{C1}	$= 0$
P_{B21}	$= P_{B11}$	$S_{E1,D7}$	$= 0$
P_{B13}	$= 1$	$\phi_{A7,E1}$	$= 0$
P_{C1}	$= 1$	P_{A3}	$= 0$
P_{D1}	$= 1$	P_{A4}	$= 1$
$P_{D2,Sac}$	$= 1$	P_{B11}	$= 1$
$P_{D2,Geo}$	$= 1$	P_{B12}	$= 1$
		P_{B13}	$= 1$
		P_{B21}	$= 1$
		P_{B22}	$= 1$
		P_{B23}	$= 1$
		P_{C1}	$= 0$
		P_{D1}	$= 1$
		$P_{D2,Sac}$	$= 1$
		$P_{D3,Sac}$	$= 1$
		$P_{D4,Sac}$	$= 1$
		$P_{E1,Sac}$	$= 1$
		$P_{D2,Geo}$	$= 1$
		$P_{D4,Geo}$	$= 1$
		$P_{A8,Geo}$	$= 1$
		$P_{E1,Geo}$	$= 1$

Appendix Table 4.3. Parameter estimates under the reduced model for releases of acoustically tagged late-fall juvenile Chinook salmon in December, 2008 (R_1) and January, 2009 (R_2). For both release dates, survival in the interior Delta was set equal between release sites (Sacramento, Georgiana Slough) based on lack of significance of likelihood ratios tests. Parameters not estimated are indicated by an "NA" in the estimate column, and parameters fixed at a constant value are noted by an "NA" in the profile likelihood column.

| Parameter | R_1: December 2008 | | R_2: January 2009 | |
	Estimate ($\widehat{SE}$)	95% Profile likelihood interval	Estimate ($\widehat{SE}$)	95% Profile likelihood interval
S_{A1}	0.894 (0.023)	0.844, 0.933	0.883 (0.024)	0.832, 0.924
S_{A2}	0.920 (0.022)	0.870, 0.957	0.861 (0.027)	0.804, 0.908
S_{A3}	0.928 (0.026)	0.867, 0.970	0.881 (0.031)	0.811, 0.933
$S_{A4, open}$	0.600 (0.101)	0.401, 0.785	NA	
$S_{A4, closed}$	0.901 (0.066)	0.744, 1.005	0.616 (0.068)	0.482, 0.746
S_{A7}	0.924 (0.049)	0.815, 1.016	0.944 (0.053)	0.812, 1.030
S_{A8}	0.791 (0.062)	0.658, 0.900	0.902 (0.050)	0.783, 0.979
S_{B11}	0.413 (0.086)	0.256, 0.586	0.674 (0.155)	0.390, 0.980
S_{B12}	0.846 (0.100)	0.596, 0.964	0.818 (0.116)	0.537, 0.967
S_{B13}	0.606 (0.148)	0.321, 0.860	0.923 (0.111)	0.616, 1.063
S_{B21}	1.000	NA	0.826 (0.079)	0.641, 0.942
S_{B22}	0.962 (0.042)	0.829, 1.006	0.789 (0.094)	0.576, 0.929
S_{B23}	1.000	NA	0.900 (0.093)	0.665, 1.037
S_{C1}	0.286 (0.109)	0.113, 0.522	NA	
$S_{D1,Sac}$	0.917 (0.056)	0.764, 0.986	0.649 (0.078)	0.489, 0.789
$S_{D1,Geo}$	0.330 (0.047)	0.243, 0.426	0.580 (0.049)	0.482, 0.674
S_{D2}	0.844 (0.057)	0.722, 0.952	0.720 (0.050)	0.617, 0.809
S_{D4}	0.576 (0.074)	0.431, 0.716	0.518 (0.067)	0.389, 0.648
S_{D7}	0.862 (0.080)	0.676, 0.983	0.919 (0.071)	0.731, 1.014
$S_{E1,D7}$	0.686 (0.198)	0.289, 0.968	0.000	NA
$S_{E1,A8}$	0.847 (0.190)	0.393, 1.065	0.800 (0.179)	0.372, 0.987
ω_{open}	0.550 (0.05)	0.451, 0.646		
Ψ_{A1}	0.679 (0.037)	0.603, 0.749	0.747 (0.036)	0.672, 0.812
Ψ_{B11}	0.217 (0.033)	0.157, 0.288	0.096 (0.024)	0.055, 0.151
Ψ_{B21}	0.104 (0.025)	0.062, 0.158	0.158 (0.030)	0.105, 0.222
$\Psi_{A2,open}$	0.488 (0.068)	0.357, 0.619	0.000	NA
$\Psi_{A2,closed}$	0.687 (0.069)	0.543, 0.810	0.615 (0.050)	0.515, 0.708
Ψ_{C2}	0.329 (0.064)	0.214, 0.460	0.000	NA
$\Psi_{D2,open}$	0.183 (0.052)	0.096, 0.299	0.000	NA
$\Psi_{D2,closed}$	0.313 (0.069)	0.190, 0.455	0.385 (0.050)	0.292, 0.485
$\phi_{B21,B12}$	0.000	NA	0.174 (0.079)	0.058, 0.359
$\phi_{B21,B22}$	1.000	NA	0.652 (0.099)	0.449, 0.823

Appendix Table 4.3. Continued.

$\phi_{B11,B12}$	0.413 (0.086)	0.256, 0.586	0.500 (0.134)	0.255, 0.745
$\phi_{B11,B22}$	0.223 (0.073)	0.104, 0.384	0.286 (0.121)	0.099, 0.545
$\phi_{A7,A8}$	0.843 (0.057)	0.724, 0.950	0.944 (0.053)	0.812, 1.030
$\phi_{A7,E1}$	0.081 (0.032)	0.033, 0.158	0.000	NA
$\phi_{D4,D7}$	0.479 (0.074)	0.339, 0.624	0.433 (0.066)	0.309, 0.566
$\phi_{D4,E1}$	0.097 (0.041)	0.037, 0.198	0.085 (0.036)	0.031, 0.173
P_{A2}	0.962 (0.015)	0.924, 0.974	0.979 (0.012)	0.948, 1.000
P_{A3}	0.990 (0.010)	0.956, 0.999	1.000	NA
P_{A4}	0.976 (0.024)	0.899, 0.999	1.000	NA
P_{A7}	0.689 (0.056)	0.573, 0.790	0.585 (0.068)	0.451, 0.711
$P_{A8,Sac}$	0.765 (0.059)	0.637, 0.866	0.716 (0.064)	0.582, 0.829
$P_{A8,Geo}$	0.765 (0.059)	0.637, 0.866	1.000	NA
$P_{A9,Sac}$	0.825 (0.048)	0.720, 0.905	0.761 (0.060)	0.633, 0.864
$P_{A9,Geo}$	0.825 (0.048)	0.720, 0.905	0.947 (0.052)	0.787, 1.000
P_{B11}	0.947 (0.036)	0.846, 0.991	1.000	NA
P_{B12}	0.917 (0.080)	0.681, 0.995	1.000	NA
P_{B21}	0.947 (0.036)	0.846, 0.991	1.000	NA
P_{B22}	0.915 (0.057)	0.761, 0.985	1.000	NA
P_{B13}	1.000	NA	1.000	NA
P_{B23}	0.865 (0.072)	0.687, 0.962	1.000	NA
P_{C1}	1.000	NA	NA	
P_{D1}	1.000	NA	1.000	NA
P_{D2}	1.000	NA	1.000	NA
$P_{D4,Geo}$	0.931 (0.047)	0.802, 0.978	1.000	NA
$P_{D4,Sac}$	0.931 (0.047)	0.802, 0.978	1.000	NA
$P_{D7,Geo}$	0.833 (0.076)	0.654, 0.945	0.707 (0.110)	0.475, 0.883
$P_{D7,Sac}$	0.833 (0.076)	0.654, 0.945	0.836 (0.149)	0.462, 1.000
P_{E1}	1.000	NA	1.000	NA
λ	0.813 (0.049)	0.706, 0.895	0.901 (0.038)	0.810, 0.959

Appendix Table 4.4. Parameter estimates on the logit scale for the effect Release Group and Route:Release Group on survival for the best-fit individual covariate model.

Coefficient	$\hat{\beta}$ (SE)	95% Confidence interval (±1.96 SE)
Release 1	-1.24 (0.75)	-2.71, 0.23
Release 2,3	0.15 (0.63)	-1.08, 1.39
Release 4	-0.71 (0.61)	-1.90, 0.49
Release 6	-0.84 (0.58)	-1.98, 0.30
Release 7	-0.76 (0.69)	-2.10, 0.58
Release 8	0.39 (0.59)	-0.76, 1.54
Release 9	0.15 (0.61)	-1.04, 1.34
Release 10	-0.11 (0.70)	-1.48, 1.26
Release 11	0.46 (0.58)	-0.68, 1.60
I_{SS}:Release 1	0.43 (1.14)	-1.81, 2.67
I_{SS}:Release 2,3	-0.18 (0.98)	-2.11, 1.75
I_{SS}:Release 4	-0.96 (0.98)	-2.87, 0.96
I_{SS}:Release 6	-1.19 (1.07)	-3.28, 0.90
I_{SS}:Release 7	1.31 (1.40)	-1.44, 4.06
I_{SS}:Release 8	-0.27 (0.91)	-2.04, 1.51
I_{SS}:Release 9	0.39 (1.00)	-1.57, 2.34
I_{SS}:Release 10	0.24 (1.09)	-1.90, 2.37
I_{SS}:Release 11	-0.21 (0.92)	-2.01, 1.59
I_{ID}:Release 1	1.27 (1.35)	-1.39, 3.92
I_{ID}:Release 4	-0.22 (1.04)	-2.26, 1.82
I_{ID}:Release 6	-0.31 (1.01)	-2.29, 1.67
I_{ID}:Release 7	0.63 (1.20)	-1.72, 2.98
I_{ID}:Release 8	0.19 (1.00)	-1.78, 2.15
I_{ID}:Release 9	0.33 (1.09)	-1.81, 2.47
I_{ID}:Release 10	2.35 (1.60)	-0.77, 5.48
I_{ID}:Release 11	-0.21 (0.99)	-2.16, 1.74

Appendix 5

ADDITIONAL FIGURES AND TABLES FOR CHAPTER 6

Appendix Table 5.1. Results of reverse model selection for water velocity variables (V_j) showing the likelihood ratio test and associated statistics for the model with the given variable dropped relative to the preceding model with one additional variable.

Variable dropped	Linear predictor	Number of parameters	AIC	–Log-likelihood	Likelihood Ratio	*P*-value
None (full model)		16	800.8	384.4		
D (time of day)	$g(\pi_G)$	15	798.8	384.4	0.00	1.000
T (temperature)	$g(\pi_D)$	14	796.8	384.4	0.02	0.890
L (fork length)	$g(\pi_G)$	13	794.8	384.4	0.04	0.841
D (time of day)	$g(\pi_D)$	12	793.1	384.5	0.17	0.680
U (upstream flow)	$g(\pi_D)$	11	791.4	384.7	0.42	0.517
V_G	$g(\pi_D)$	10	790.0	385.0	0.58	0.446
T (temperature)	$g(\pi_G)$	9	788.8	385.3	0.86	0.354
ΔV_S	$g(\pi_G)$	8	787.7	385.8	0.83	0.362
L (fork length)	$g(\pi_D)$	7	786.8	386.4	1.15	0.284
None (all interactions)[*]		10	787.6	383.8		
$V_G \times U$	$g(\pi_G)$	9	786.1	384.1	0.49	0.484
$V_S \times V_G$	$g(\pi_G)$	8	785.9	385.0	1.79	0.181
$Q_S \times \Delta Q_S$	$g(\pi_D)$	7	786.8	386.4	2.91	0.088

[*] The interaction $V_S \times U$ was excluded from $g(\pi_G)$ due to high variance inflation factors caused by this term.

Appendix Table 5.2. Likelihood ratio tests when each variable is dropped from the best fit V_j model.

| Variable dropped	Number of parameters	Linear predictor	–Log-likelihood	Likelihood Ratio	AIC	P-value
None (best fit)	7		386.4		786.1	
Q_S	6	$g(\pi_G)$	415.1	57.4	842.2	<0.001
Q_G	6	$g(\pi_G)$	418.9	65.0	849.9	<0.001
U	6	$g(\pi_G)$	392.3	11.8	796.7	<0.001
Q_S	6	$g(\pi_D)$	447.5	122.1	906.9	<0.001
ΔQ_S	6	$g(\pi_D)$	392.7	12.6	797.4	<0.001

Appendix Table 5.3. Results of reverse model selection for discharge proportion variables (p_{Q_j}) showing the likelihood ratio test and associated statistics for the model with the given variable dropped relative to the preceding model with one additional variable.

| Variable dropped[*]	Linear predictor	Number of parameters	AIC	–Log-likelihood	Likelihood Ratio	P-value
None (full model)		15	809.4	389.7		
T (temperature)	$g(\pi_D)$	14	807.5	389.7	0.01	0.920
L (fork length)	$g(\pi_D)$	13	805.5	389.7	0.03	0.863
T (temperature)	$g(\pi_G)$	12	803.7	389.8	0.16	0.690
D (time of day)	$g(\pi_G)$	11	801.8	389.9	0.20	0.655
L (fork length)	$g(\pi_G)$	10	800.4	390.2	0.56	0.454
D (time of day)	$g(\pi_D)$	9	799.1	390.6	0.71	0.399
ΔQ_S	$g(\pi_D)$	8	798.0	391.0	0.91	0.340
p_{Q_S}	$g(\pi_D)$	7	797.1	391.6	1.08	0.299
None (all interactions)		10	801.1	390.6		
$\Delta Q_S \times p_{Q_G}$	$g(\pi_G)$	9	799.3	390.7	0.22	0.639
$\Delta Q_S \times U$	$g(\pi_G)$	8	797.1	391.6	1.25	0.264
$U \times p_{Q_G}$	$g(\pi_G)$	7	786.8	386.4	2.91	0.088

[*] The terms U and $p_{Q_S} \times p_{Q_G}$ was excluded $g(\pi_D)$ due to high variance inflation factors caused by these terms.

Appendix Table 5.4. Likelihood ratio tests when each variable is dropped from the best fit p_{Q_j} model.

Variable dropped	Number of parameters	Linear predictor	–Log-likelihood	Likelihood Ratio	AIC	P-value
None (best fit)	7		391.6		797.1	
p_{Q_S}	6	$g(\pi_G)$	419.9	56.7	851.8	<0.001
ΔQ_S	6	$g(\pi_G)$	414.2	45.2	840.3	<0.001
U	6	$g(\pi_G)$	396.0	8.9	804.0	0.003
p_{Q_S}	6	$g(\pi_D)$	404.8	26.6	821.7	<0.001
p_{Q_G}	6	$g(\pi_D)$	394.6	6.1	801.3	0.013
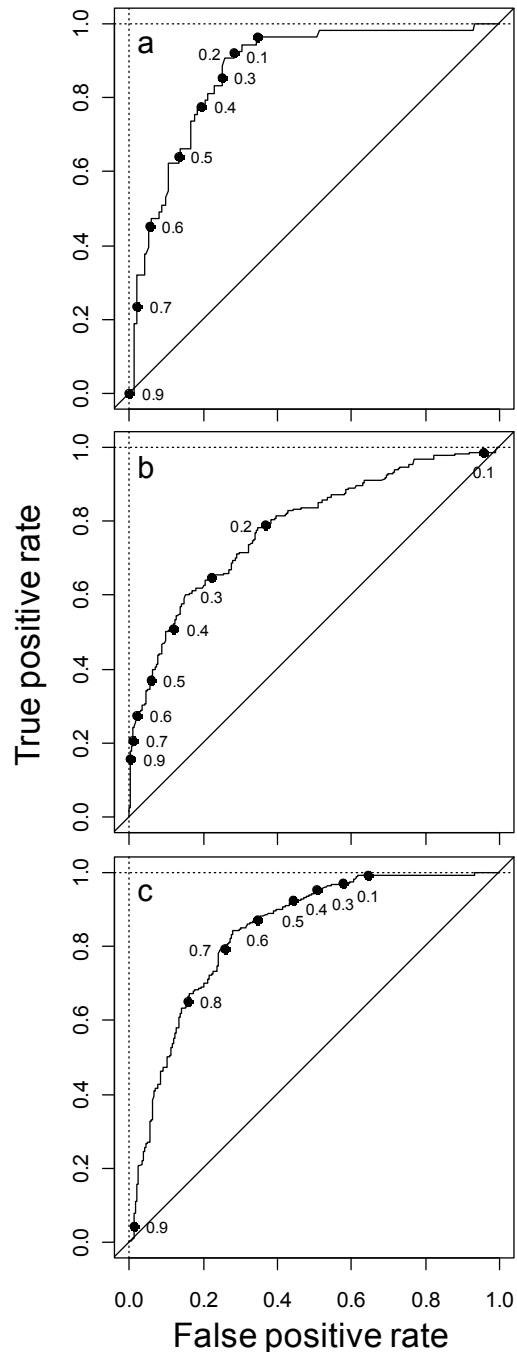
Appendix Figure 5.1. Reciever operating curve (ROC) showing the true and false positive rates for classifying fish to a) the Delta Cross Channel, b) Georgiana Slough, and c) the Sacramento River based on cutoff values of π_j ranging from zero to one (shown as labeled points). The 45° reference line shows the performance of a model with no ability to predict whether fish enter a particular route.
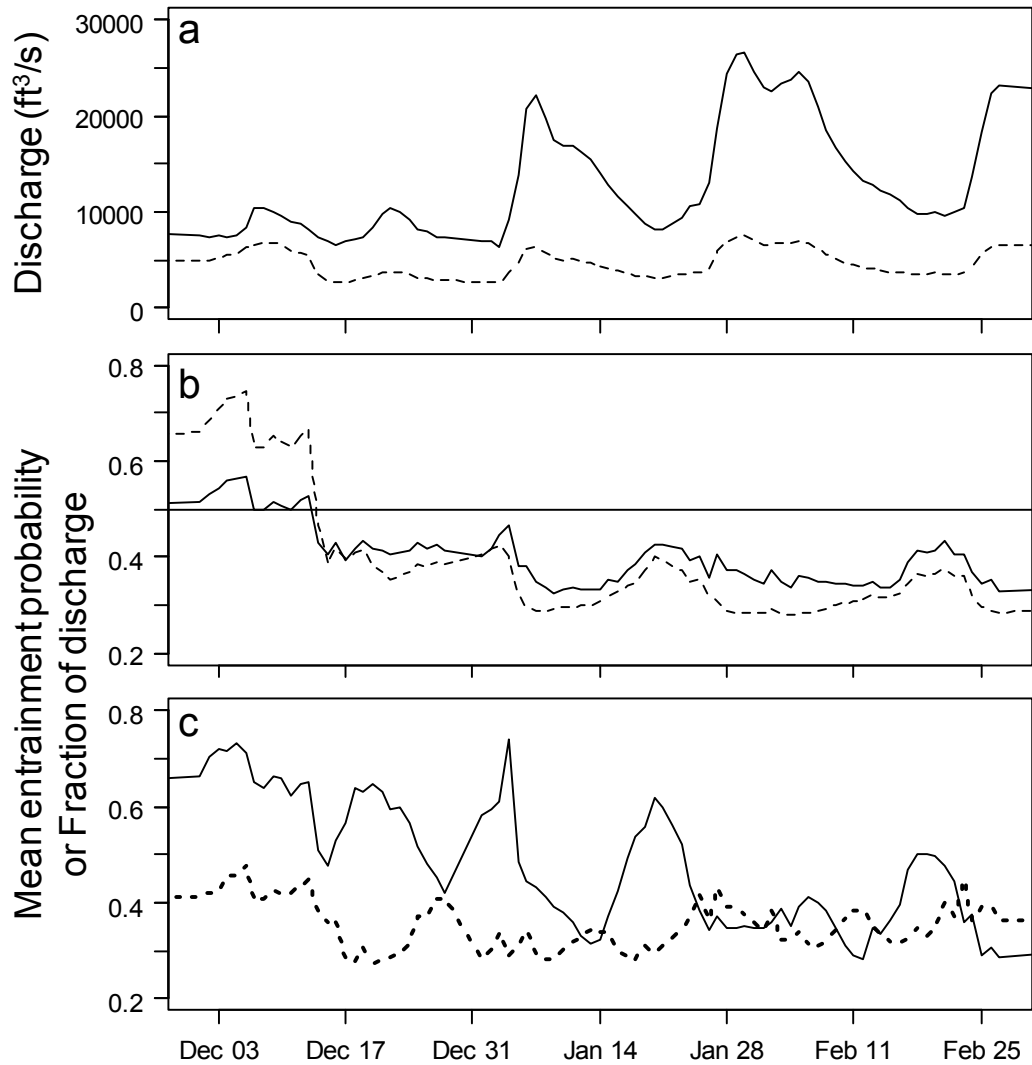
 Appendix Figure 5.2. Mean daily river flow (a) and mean predicted probability of entrainment into the interior Delta (b and c) during winter 2007/2008. The top panel (a) shows mean daily discharge entering the river junction ($Q_{\text{inflow,}}$ solid line) and mean daily discharge entering the interior Delta through both the Delta Cross Channel and Georgiana Slough (dotted line). Panel b shows the mean daily probability of entering the interior Delta ($\bar{\pi}_{\text{ID},d}$, solid line) and the

fraction of mean daily discharge entering the interior Delta ($p_{\bar{Q}_{\text{ID},d}}$, dashed line). Panel c shows

the mean entrainment probability for day (solid line) and night (heavy dotted line) diel periods. The Delta Cross Channel was open prior to December 15, 2007 and closed thereafter.
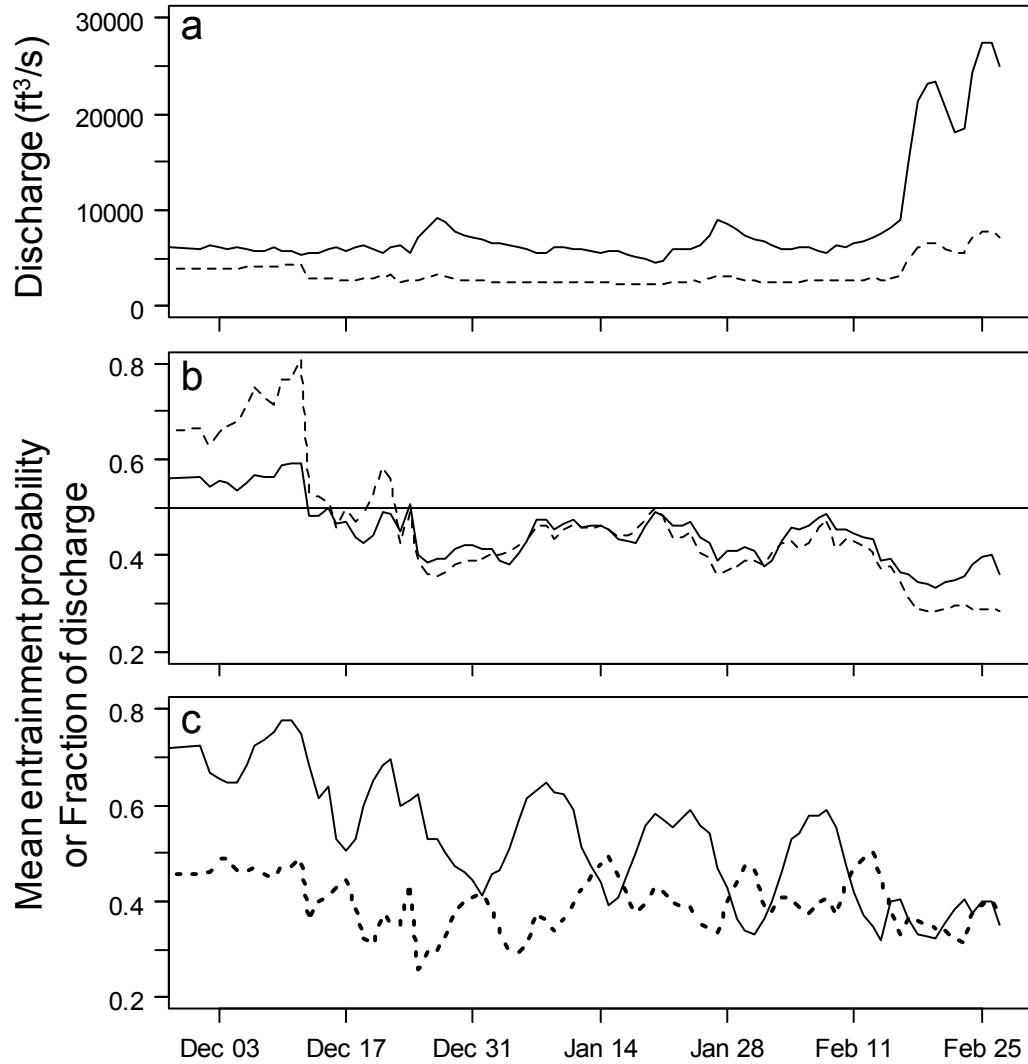
 Appendix Figure 5.3. Mean daily river flow (a) and mean predicted probability of entrainment into the interior Delta (b and c) during winter 2008/2009. The top panel (a) shows mean daily discharge entering the river junction (Q_{inflow}, solid line) and mean daily discharge entering the interior Delta through both the Delta Cross Channel and Georgiana Slough (dotted line). Panel b shows the mean daily probability of entering the interior Delta ($\bar{\pi}_{\text{ID},d}$, solid line) and the

fraction of mean daily discharge entering the interior Delta ($p_{\bar{Q}_{\text{ID},d}}$, dashed line). Panel c shows

the mean entrainment probability for day (solid line) and night (heavy dotted line) diel periods. Operation of the Delta Cross Channel followed a variable schedule but closed after December 22, 2008.

VITA

Russell W. Perry was born in Pawtucket, Rhode Island. For the first twenty years of his life, he survived city life by fishing local parks and snorkeling the waters of Narragansett Bay. In his most recent twenty years, he has lived west of the Great Divide, residing in Utah, Idaho, Alaska, British Columbia, and Washington. He received a Bachelor of Science degree in Fisheries and Wildlife Management at Utah State University, and received his Master of Resource Management degree in 2001 from Simon Fraser University. In 2010 he earned his Doctor of Philosophy from the School of Aquatic and Fishery Sciences at the University of Washington.